

**Stratigraphy, tectonics and subsurface petroleum geology of the Ocoa, Azua, and Enriquillo basins,  
Dominican Republic**

**2-day, pre-meeting field excursion**

**18th Caribbean Geological Conference**

**Santo Domingo, Dominican Republic**

**March 23-24, 2008**

**Field trip leaders:**

**Paul Mann, University of Texas at Austin**

**Pedro Pablo Hernaiz, INYPSA, Madrid, Spain**

**Wilson Ramirez, University of Puerto Rico at Mayaguez**

**Field trip schedule:**

**Day One (Santo Domingo to Barahona):** Depart Jaragua Hotel at 8 am (please be ready to go in the lobby at this time; we will need to leave promptly at 8 am). Most stops will be on or near the main highway connecting Santo Domingo and Barahona. We will take the morning to view the Eocene Peralta-Ocoa basin and visit the Higuerito oil field discovered in 1908. After lunch in Azua we will make multiple stops through the classic late Miocene-Pliocene shallowing-upward section that is well exposed at outcrops along the highway and in the valley of the Rio Yaque del Sur. See if you can recognize the main formations and their main contacts as we drive through this unvegetated area. In the afternoon, we will provide an overview of the subsurface geology of the valley that we will cross as we enter Barahona on the southern edge of the basin.

**Evening of Day One (meeting room at the Hotel Costa Larimar, Barahona):** After dinner at the hotel, we will have a powerpoint overview of the history of petroleum exploration in the Azua-Enriquillo basins; this will be a good time for questions about what we have seen on Day One and an overview of what we will see on Day Two. For those of you looking for research projects, thesis projects, or petroleum exploration opportunities, this would be a good time for questions and discussion.

**Day Two: (Barahona to Santo Domingo):** Depart Barahona hotel at 7 am (please be in the lobby with your bags packed and ready to load on the bus). We will drive from Barahona to the Salt and Gypsum mine localized in a thrusted diapir along the southern edge of the valley and then along the mini fold-thrust belt bounding the southern edge of Lake Enriquillo to the town of Jimani at the western end of the valley at the Haitian border (literary note: Jimani is featured in Graham Greene's novel, *The Comedians*). From there we go along the western lake edge to the town of La Descubierta for lunch. Keep your eyes peeled for flamingos, crocodiles and prehistoric petroglyphs on the cliffs near Descubierta. After lunch we will visit localities showing the faulted valley edges, folds and thrusts in the Sierra de Neiba and the unique occurrence of a subaerially exposed Holocene coral reef along the southern edge of the lake. Much of the western part of the valley is below sea level; see if you can follow the natural datum that marks modern sea level as we drive through this spectacular area. We will return to Jaragua Hotel by 7 pm.

**What to expect:**

**Weather.** It's going to be hot! It's the height of the dry season in the Dominican Republic, so imagine west Texas or the Imperial Valley of California in the summertime and you will be close to the conditions we will experience. Especially if you are coming from a winter climate, please take extra

precautions against spending two long days in a strong tropical sun. There will be several short hikes away from the bus.

To prepare for this, please bring a broad brimmed hat, sunscreen, sunglasses, hiking boots with stiff soles that will resist the penetration of cactus spines; long pants, personal water bottle containing purified water, hand lens, camera and charger, sufficient clothes and personal supplies for one night stayover only (to facilitate transfers, please leave the bulk of your luggage at your hotel in Santo Domingo).

In case your bags are late arriving at the airport, please pack what you need for this trip in your carryon bag. If your bags don't arrive on your plane, make arrangements for them to be delivered later to the hotel you are staying at in Santo Domingo.

To keep hydrated, drink plenty of water and avoid excessive alcohol and soft drinks. We will provide a cooler of purified water and cups on the bus but please bring several smaller water bottles in your backpack to help us out (you can purchase these in the hotel or at our lunch stops). You will be able to buy cold drinks and snacks at our breaks and lunchstops so bring some Dominican currency (you can change currency at the airport, at the hotel or at ATMs around both hotels using your credit or debit card – to do this you need your pin information).

We will provide you with boxed lunches prepared by the hotel on both days and dinner on the first night in Barahona. We will also provide the group with a few geologic hammers for common use. If you would like to bring your own hammer, make sure you put it in your checked baggage. You are welcome to collect rock samples with the exception of the Holocene reef stop which is in a national park.

**Languages:** we will conduct the trip mainly in English although Spanish will be provided as necessary.

**Safety precautions:** The meeting organizers have arranged for us a single, 50 passenger bus that is equipped with air conditioning and a restroom. We will also have one 4WD vehicle made available to us by Pedro Hernaiz and INYPSA that will follow the bus and can run errands as needed.

Please keep seated while the bus is moving – the roads are sometimes bumpy and the traffic can be stop and go. Some of our stops will be at roadcuts along the busy Santo Domingo-Azua-Barahona highway. There will be high speed truck and car traffic so please do not attempt to cross the highway unless instructed by the trip leaders. Please do not climb up on the faces of outcrops to prevent painful falls and/or dislodging loose rocks on those below.

Most of the areas we visit will have several types of long-spined cactus. Wear stout, ankle high hiking boots with thick, Vibram-type soles to protect your feet from “hypodermic-like” spine punctures while walking and avoid touching the spines with your hands or sitting down on them; the cacti branches will easily segment when brushed against and will lightly cling to your clothes and boots. If you are not aware of these “passengers” on your clothes or boots, you can inadvertently jam the spines deep into your skin. If this happens, remove the broken off spines carefully and treat with Neosporin to avoid infections at the punctured area.

Keep all your belongings centralized in a daypack or beltpack and keep that pack with you at all times. Remove all items from the bus on Sunday night.

There are bees, wasps and scorpions around so please let us know if you have a history of allergic reactions to stings and bring Benadryl or whatever treatment you require. There is dust and pollen in the dry, windy air so please bring any medications you might need to ward off allergies.

To prevent stomach problems, avoid drinking tap water in the hotels in Santo Domingo or Barahona or in restaurants. Prior and during this trip, also avoid drinks with ice cubes since you can never be sure if that water has been purified.

**Your cooperation.** With this large group of 40, we need your cooperation at each stop and to depart on time in the mornings. Please exit the bus quickly behind the leaders and gather around them in a compact, semi-circular group - so we can make ourselves heard at the back. We will be bringing a bullhorn to make ourselves heard especially with traffic noises at the highway stops. If you have questions, please wait til we finish the presentations.

Please do not wander off from the main group to look for outcrops, for shopping, etc., and return promptly to the bus with the main group. We will do a head count after each stop but if you notice that someone is missing, please let us know before the bus departs.

**Logistics.** On both mornings, be packed and ready to go at the scheduled departure times (8 am on Sunday and 7 am on Monday). If you have problems waking up early, make arrangements with both hotels for a wakeup call and set a personal travel alarm clock or watch alarm as a backup. Please drink alcohol in moderation and get to bed early on Sunday night, as our departure from the hotel on Monday morning will be very early (7 am). This early departure will allow us a long day in the field and a return time at a reasonable hour to Santo Domingo.

**Where we will be staying the night of Sunday, March 23;** The meeting organizers have reserved a block of rooms our entire group of 40 at the Hotel Costa Larimar in Barahona. Due to the large size of our group, we will have to share 20 double rooms, so please expect to share a double room on Sunday evening. If you are a light sleeper, you might bring some ear plugs as the ambient late night noise levels can be higher than you are used to.

**Hotel web site at:** <http://www.hotelcostalarimar.com/>

**Address:** Avenida Enriquillo no. 6, Barahona, Dominican Republic

**Phone:** 809-524-5111

**Fax:** 809-524-7063

**Hotel reviews at:** [http://travel.yahoo.com/p-hotel-361461-barcelo\\_bahoruco\\_beach\\_resort-i](http://travel.yahoo.com/p-hotel-361461-barcelo_bahoruco_beach_resort-i)

**Suggested readings:** The more you know about the geology, the more you will get out of the trip.

The bus will have a microphone that we will use to review some of the regional background information before we reach the outcrop. Since this is an arid area, you can see a lot of geology from the bus window so we will point out features of interest as we drive along.

The field guide is a compendium of published papers. Its main sources include these published papers:

### **Hispaniola tectonic setting and geologic history:**

Mann, P., 1999, Caribbean sedimentary basins: Classification and tectonic setting from Jurassic to present, *Caribbean Sedimentary Basins*, Elsevier Sedimentary Basins of the World Series, Series Editor, K. Hsu, p. 3-31.

Mann, P., Calais, E., Ruegg, J. C., DeMets, C., Dixon, T., Jansma, P., and Mattioli, G., 2002, Oblique collision in the northeastern Caribbean from GPS measurements and geological observations, *Tectonics*, v. 21, no. 6, 1057, doi:10.1029/2001TC001304.

Perez Estaun, A., et al., 2007, Geologia de Republica Dominicana: de la construccion de arcos-isla a la collision arco-continente, Boletin Geologico y Minero, v. 118, no. 2, p. 157-173.

### **Structure and stratigraphy of Peralta-Ocoa belt (outcrops seen on Day One):**

Dolan, J., Mann, P., de Zoeten, R., Heubeck, C., Shiroma, J., and Monechi, S., 1991, Sedimentologic, stratigraphic, and tectonic synthesis of Eocene-Miocene sedimentary basins, Hispaniola and Puerto Rico, in Mann, P., Draper, G., and Lewis, J. F., eds., *Geologic and Tectonic Development of the North America-Caribbean Plate Boundary in Hispaniola*, GSA Special Paper 262, p. 217-264.

Heubeck, C., Mann, P., Dolan, J., and Monechi, S., 1991, Diachronous uplift and recycling of sedimentary basins during Cenozoic tectonic transpression, northeastern Caribbean plate margin: Sedimentary Geology, v. 70, p. 1-32.

Hernaiz Huerta, P., and Perez-Estaun, A., 2002, Estructura del cinturon de pliegues y cabalagamientos de Peralta, Republica Dominicana, Acta Geologica Hispanica, v. 37, p. 183-205  
(also available online at: <http://www.geologica-acta.com:8080/geoacta/MostrarArticlesAGHAC.do?article=aghv3702>)

### **Structure, stratigraphy and petroleum geology of the Azua-Enriquillo basin (outcrops seen on Days One and Two):**

Mann, P., and Lawrence, S., 1991, Petroleum potential of southern Hispaniola: Journal of Petroleum Geology, v. 14, p. 291-308.

Mann, P., McLaughlin, P., van den Bold, W., Lawrence, S., and Lamar, M., 1999, Tectonic and eustatic controls on Neogene evaporitic and clastic deposition in the Enriquillo Basin, Dominican Republic, *Caribbean Sedimentary Basins*, Elsevier Sedimentary Basins of the World Series, Series Editor, K. Hsu, p. 287-342.

### **Structure and stratigraphy of the Sierra de Neiba and Enriquillo basin (outcrops seen on Day Two):**

Hernaiz Huerta, P., et al., 2007, La estratigrafia de la Sierra de Neiba (Republica Dominicana): Boletin Geologico y Minero, v. 118, no. 2, p. 313-336.

Hernaiz Huerta, P., et al., 2007, La estructura del suroeste de la Republica Dominicana: un ejemplo de deformacion en regime transpresivo: Boletin Geologico y Minero, v. 118, no. 2, p. 337-358.

### **Geology of the Enriquillo Holocene coral reef (outcrops seen on Day Two):**

Taylor, F., Mann, P., Valastro, S., and Burke, K., 1985, Stratigraphy and radioisotopic chronology of a subaerially exposed Holocene coral reef, Dominican Republic, Journal of Geology, v. 93, p. 311-332.

Stemann, T.A. and Johnson, K.G., 1992, Coral assemblages, biofacies and ecological zones in the mid-Holocene reef deposits of the Enriquillo Valley, Dominican Republic: Lethaia, v. 25, p. 231-241.

Torres, R., Chiappone, M., Geraldes, F., Rodríguez, Y., and Vega, M., 2001, Sedimentation as an important environmental influence on Dominican Republic Reefs: Bulletin of Marine Science, v. 69, no. 2, p. 805-818.

I have put the pdfs I have of the above papers in my outgoing ftp site if you would like to download them and print them out. Check later in the week for us to add the pdfs that we are still missing. To access them:

ftp: <ftp://ig.utexas.edu>

username: anonymous

password: your email address

Using an ftp ("FILE TRANSFER PROTOCOL") program (WS-FTP is what we use);

Login utig.ig.utexas.edu as user "anonymous" and give your email address as the password;

Then change directory ("CD" is the usual command) to /outgoing/paulm

The folder containing the papers is called: "Articles for Caribbean conf trip"

If you have any problems with downloading them, please contact Lisa Bingham at:  
[lisaw@ig.utexas.edu](mailto:lisaw@ig.utexas.edu)

**Hydrocarbon symposium:** This pre-trip meeting is thematically linked to a hydrocarbon session at the Caribbean conference that will be held all day on Wednesday. This session will provide an overview of active exploration activities in the northern and southern Caribbean.

**Cancellations and registration:** If you are on the attached participant list and have decided not to attend this trip for any reason, can you send me a note ([paulm@ig.utexas.edu](mailto:paulm@ig.utexas.edu)) along with the conference organizers: Hugo Dominguez ([hdominguez@yahoo.com](mailto:hdominguez@yahoo.com)) and Marilyn Tenreyo ([caribgeolconf2008@sodogeo.org](mailto:caribgeolconf2008@sodogeo.org)). If you have questions about your meeting or field trip registration or any other meeting logistics, please contact Marilyn Tenreyo by email or by phone (809-540-4888) or by fax (809-540-5591).

## Field Trip Participants

Name	Company	E-MAIL
Manuel Abad de los Santos	Consorcio Igme/ BRGM/ Inypsa (D. R.)	manuel.abad@dgyp.uhu.es
Michael Martinez	University of south Florida	martinez@marine.usf.edu
Jose Luis Granja Bruña	Universidad Complutense de Madrid	lgranbru@geo.ucm.es
Klaus Stanek	TU Bergakademie Freiberg (Alemania)	stanek@geo.tu-freiberg.de
Octavio Lopez	Dirección General de Mineria	n/a
Vera Cedeño	Dirección General de Mineria	n/a
Santiago Muñoz	Dirección General de Mineria	yuboa@hotmail.com
Luis Torres	Dirección General de Mineria	n/a
Wilton Khoury	Dirección General de Mineria	n/a
Melaneo Aquino	Dirección General de Mineria	n/a
Ramon Morrobel	Dirección General de Mineria	n/a
Jose Angel Rodriguez	Dirección General de Mineria	n/a
Armin Schafhauser	Neftex Petroleum Consultants LTD	Armin.Schafhauser@neftex.com
Rick Roberson	PGS MARINE	Rick.Roberson@pgs.com
Betonus Pierre	Marien Mining Company S.A	bpierre72@yahoo.es
Dr. Pete Emmet	Brazos Valley Services	pete-emmet@yahoo.com
Wilson Ramirez Martinez( guia)	Universidad de Puerto Rico	n/a
James Joyce	Universidad de Puerto Rico	n/a
Lisa Chismadia	Universidad de Puerto Rico	n/a
Viaviana Diaz (estudiante)	Universidad de Puerto Rico	n/a
Osvaldo Amaro L. (estud.)	Universidad de Puerto Rico	n/a
Carla Roig Silva (estud.)	Universidad de Puerto Rico	n/a
Elson Core (estud.)	Universidad de Puerto Rico	n/a
Ailec D. Soto Feliciano (estud.)	Universidad de Puerto Rico	n/a
Almin A. Rivera (estud.)	Universidad de Puerto Rico	n/a
Marianela Mercado(estud.)	Universidad de Puerto Rico	n/a
Kevián Augusto Perez(estud.)	Universidad de Puerto Rico	n/a
Fernando Perez Varela	IGME	fertriasico@hotmail.com
Paul Mann (guia)	University of Texas Institute for Geophysics	paulm@ig.utexas.edu
Pedro Pablo Hernaiz (guia)	INYPSA	phernaiz@inypsa.es
Manuel Caprile		mcaprile@cne.gov.do
Abrams Lewis	University of North of Carolina	grindlayn@uncw.edu
Nancy Grindlay	University of North of Carolina	abramsl@uncw.edu

## **Part I (stops 1-8 led by Paul Mann):**

**How to use this guide:** Part I of the guide by Paul Mann combines figures from published papers, text, and descriptions of the seven outcrop stops I will lead on Day One and the first stop of Day Two. **Figure 1** of this guide is intended to provide you with an overview of the two-day field trip route and the general geology of the island based on the USGS digital geologic map by French and Schenck (2004).

Note the most recent set of GPS vectors - kindly provided by Eric Calais (Purdue University) - have been plotted onto this map. The frame of reference for these vectors is a fixed or stationary Caribbean plate (hence the vectors in the south show progressively less motion as the Caribbean plate is approached). This “velocity field” of a moving crust shows the diffuse nature of the active plate boundary through Hispaniola and is the reason that the geomorphology and geologic structures that we will see on this trip are continuing to deform. You will get more out of the outcrop stops if you read the background text sections in the bus and before we arrive at the outcrop. This suggestion would also apply to the other two parts of the guide: **Part II by Pedro Hernaiz** and **Part III by Wilson Ramirez** that will cover stops 9-13 on Day Two.

When we reach these outcrops, we will give a quick presentation and make some suggestions concerning geologic features that you should try to locate on your own. Please hold your questions till after the leaders have finished their presentations and then focus your energies on looking at the rocks independently. After that, begin integrating your field observations with the regional information you have just read. Let us know if you need a geologic hammer or hand lens. If you hammer, please wear eye protection and be conscious of people around you.

Feel free to look around the outcrops but please don't attempt to cross the highway, step on cactus, or wander off!

## **Tectonics and sedimentation in the Paleogene Peralta-Ocoa basin (stops 1 and 2 on Day One)**

**Tectonic development of the Caribbean (Figures 2A-D).** The tectonic history of the Caribbean can be subdivided into several major phases that include:

- **Late Jurassic rift phase** occurred when North and South America rifted apart to create an oceanic area known as the proto-Caribbean Sea (**Fig. 2A**). This was the time of the formation of rifts in the Gulf of Mexico, the Yucatan Peninsula, and northern South America. Rich hydrocarbon source rocks were deposited during this phase in the Gulf of Mexico. Since the rocks of Hispaniola formed as part of the younger Caribbean arc , there are no Jurassic rifts (or source rocks) in Hispaniola.
- **Cretaceous passive margin phase** occurred following the cessation of rifting in the earliest Cretaceous (**Fig. 2B**). The post-rift passive margin section composed mainly of carbonate rocks blanketed the rifted topography in continental crust in the southeastern Gulf of Mexico, the Bahamas platform, and northern South America. These passive margins enjoyed open oceanic circulation in the wide proto-Caribbean seaway that was several hundred kilometers wide. These rocks host the rich source rocks of northern South America. Since the rocks in Hispaniola formed as part of the younger Caribbean arc, there are no passive margin rocks (or related source rocks) in Hispaniola.
- **Late Cretaceous to recent, arc-passive margin collisional phase** occurred when the Great Arc of the Caribbean and its adjacent oceanic plateau moved over the area of the proto-Caribbean seaway and collided with the passive margins that fringed the circum-Caribbean area (**Fig. 2B, 2C**). The Caribbean oceanic plateau formed in late Cretaceous time (Santonian) in the eastern Pacific Ocean. The Great Arc of the Caribbean extends formed in the early Cretaceous. By early Eocene, arc-continent collision was complete in western Cuba and proceeded in a diachronous manner along the edge of the Bahamas platform. This diachronous collision accompanied transfer of microplates from the Caribbean plate to the North America

plate in a clockwise fashion as forward progress of the Great Arc was halted by its collision with the Bahamas Platform (**Fig. 2C**). Foreland basins mark the collision between the arc and the continent and are especially important for providing high quality reservoir rocks to the thick and hydrocarbon-rich foreland basins of northern South America. Foreland basins in Cuba and Hispaniola are much smaller and sediment-starved since these intra-oceanic areas were distant from continental fluvial systems. Initiation of oceanic spreading in the Cayman trough in Middle Eocene time may be the result of a change in the direction of the Great Arc from a northeastward to an eastward direction. This course correction in the path of the Great Arc allowed it to move around a salient formed by the southeastern Bahamas platform (**Fig. 2C**).

- **Late Cenozoic strike-slip phase** occurred when the arc-continent collision zones converted into east-west-trending strike-slip faults along the northern and southern edges of the Caribbean plate (**Fig. 2D**). By late Miocene, localized convergence between the east-moving Caribbean plate and the southeastern extension of the Bahama platform led to thrusting and topographic uplift in Hispaniola. Uplift exhumed the early Cretaceous-Eocene section of the Great Arc in the Cordillera Central and the late Cretaceous Caribbean oceanic plateau in southern Hispaniola.

**Tectonic setting of Paleogene rocks in the circum-Caribbean (Figure 3).** The collisional phase left inactive segments of the Great Arc juxtaposed against continental margins. The single segment of the Great Arc that remains active today is the Lesser Antilles volcanic arc formed by continuing subduction of Atlantic oceanic crust (Fig. 3). Back-arc extension affected the Great Arc in Paleocene and Eocene time, split the Great Arc into two parallel chains, and produced thick sedimentary accumulations of mainly marine sedimentary and volcanic rocks in the intervening Yucatan, Grenada and Falcon basins (Fig. 3). Back-arc basin rocks in the circum-Caribbean area have been strongly affected and disrupted by post-Eocene strike-slip faulting associated with eastward displacement of the Caribbean plate (Fig. 2C, D). This post-Eocene deformation has led to a very thin belt of highly deformed rocks in central Hispaniola and a narrowing of the basinal areas of the Yucatan, Grenada and Falcon basins in areas that have experienced the greatest shortening (Fig. 4).

#### **Regional stratigraphy and structure of the Peralta-Ocoa belts (Figures 4-7).**

Differential northwest to southeast shortening across the Hispaniola segment of the Paleogene backarc belt is summarized on the cross sections in **Figure 4**. The areas that have experienced greatest shortening in central Hispaniola are characterized by high topography, vertical beds, local cleavage and low-grade metamorphism (sections A and B in Fig. 4). **Stop 1** will be in the area of intermediate shortening of the Peralta and Ocoa belts near the southern coast of Hispaniola (**section C in Fig. 4**). The belt continues offshore into the active Muertos trench and San Pedro “forearc basin” (**section D in Fig. 4**). In this offshore area, shortening is accommodated by subduction rather than sub-horizontal shortening of the upper crust as seen in central Hispaniola.

The Peralta belt consists of as much as 11.5 km of Early Eocene to early Late Eocene pelagic limestone, mudstone, sandstone, and siltstone of the Peralta Group (**Fig. 5C**) that was deposited in an elongate backarc basin (Dolan et al., 1991) (**Fig. 5A**). Sources for this basin include Campanian to Paleocene sedimentary rocks to the northwest (**Fig. 5B**). Syn-deformational features in Eocene sedimentary rocks in the Peralta basin seen at **stop 2** indicate that convergent deformation accompanied sedimentation (Witschard and Dolan, 1990). The basin has been deformed into a fold-thrust belt with thrusts dipping to the northeast beneath the higher topography of the Cordillera Central (Heubeck et al., 1991; Hernaiz-Huerta and Perez-Estaun, 2002) (**Fig. 6**). The overlying Ocoa belt consists of up to 8.6 km of Middle Eocene to Early Oligocene turbidites, debris flows, and olistostromes of the Rio Ocoa Group (**Fig. 5C**). These rocks were deposited in an elongate basin derived from Middle Eocene to Early Miocene closure, uplift, and erosion of the Peralta Group to the north and northwest (**Fig. 4**). Turbidites contain reworked Eocene faunas and lithologies similar to those of the underlying Peralta Group and exhibit northwest to southeast paleocurrents. Erosion of late Cretaceous rocks

of the Great Arc and overlying Paleocene carbonate rocks of the Cordillera Central provide additional belt-perpendicular sources of coarser-grained conglomerate and olistostromes. Following deposition of the Rio Ocoa Group, both the Peralta and Rio Ocoa Group were deformed in a southwest-verging, fold-thrust belt during the early Miocene.

Up to 1.5 km of Middle Miocene to Pleistocene sandstone, conglomerate, and reefal limestone of the Ingenio Caei Group were deposited in an elongate basin above a pronounced angular unconformity developed in the older rocks of the Rio Ocoa Group (**Fig. 5C**). Sediments of the Ingenio Caei Group were derived from Middle Miocene to Recent closure, uplift and erosion of the Rio Ocoa and Peralta Groups to the northwest.

### Olistolith blocks of the Rio Ocoa belt and their tectonic significance (Figs. 6, 7, 8) (stop 1)

At stop 1 near the small settlement of El Galeon we will park the bus on the highway shoulder and make a short walk to the bluff north of the highway where we will examine a large, fine-grained limestone block of Middle Eocene age that is enclosed within Eocene conglomerate and finer grained sandstone. The olistoliths are well exposed over an arid and extensive area of low hills in the rain shadow of the Cordillera Central (Fig. 6).

Heubeck et al. (1991) and Heubeck (1992) mapped a total of 502 olistoliths in the basal 1.4 km thick section of the Eocene deepwater Rio Ocoa Formation (total thickness of 2.5 km) in the field and using aerial photographs (Fig. 7A). Regional mapping shows that the olistoliths are concentrated in seven major stratigraphic horizons that have not been repeated by thrust faulting.

The olistoliths are composed of various facies of packstones and wacke-mudstone (Fig. 8A) of a shallow-water bank margin association (Fig. 8C) and are generally conformable to bedding as are most olistoliths reported in the classic localities of the Apennines. The largest olistoliths are up to 6 km in length and are found closest to the margin of the Cordillera Central (Fig. 8B). The decrease in size of the olistoliths away from the margin of the Cordillera Central suggests a provenance from that uplift (Fig. 8D). The olistoliths occur evenly along a 35-km length of the mountain front suggesting that they were derived from a line source rather than a point source (Fig. 6).

The olistoliths show internal folding by gentle to isoclinal folding or bedding-plane slip. The folds are interpreted as slump folds because of their random orientations and disharmonic style.

24 age determinations of the benthic and pelagic foraminifera in the carbonate olistolith blocks reported by Heubeck (1992) show an age range from late Paleocene to middle Eocene. The age range of the olistoliths is older than or coeval with the early Middle Eocene or Late Eocene age of the enclosing Rio Ocoa Formation. Lithologies of the Rio Ocoa Formation that enclose the olistoliths are either gravelly or unsorted deposits, or shaly, fine-grained, well-sorted sedimentary rocks. Enclosing sandstone is generally poorly represented. Water depths from benthic foraminifera of the Rio Ocoa Formation indicate deep bathyal to abyssal depths. Paleocurrent measurements on turbiditic sandstone from the Rio Ocoa Formation indicate that the dominant paralleled the northwest-trending margin of the Cordillera Central (Fig. 8E). Measurements on conglomerate, in contrast, exhibit an additional northerly component, suggesting a source of coarse input from the flanks of the Cordillera Central. Such an inference is also suggested by the logarithmically decreasing size of the olistoliths with increasing distance from the margin (Fig. 8D).

The close spatial association of the olistoliths with unsorted, coarse gravel units, their conformity with the matrix bedding, and sheared mud matrix at the base of some blocks suggests that the olistoliths were transported by large gravity flows. The widespread nature of the olistoliths and their repetitive occurrence in seven major horizons indicates that earthquakes may have provided a triggering mechanism. Thrusting and oversteepening of the Cordillera Central may have also contributed to the gravity flows.

What to examine at this outcrop:

- **Examine olistolith:** facies, fossils, deformation, bedding, other interbedded lithologies, orientation of block relative to surrounding beds, marginal shearing, depositional mechanism.
- **Examine matrix:** facies present, fossils, clast types, deformation, paleocurrents, depositional mechanism.

- **Integrate observations with regional tectonics:** what regional tectonic event might be recorded by the formation of the Ocoa basin and the deposition of the olistoliths?

## Deformed rocks of the Peralta Group and their relation to the overlying Rio Ocoa Group (Fig. 9) (stop 2)

Stop 2 will be at a highway road cut through the Sierra El Numero, which has a normally faulted, steep western escarpment and an unfaulted eastern edge that slopes gently eastward into the valley of the Rio Ocoa (**Fig. 9**). Dolan et al. (1991) and Heubeck et al. (1991) identified three main lithologic units: 1) **Ventura Formation**, composed of thin- to medium-bedded, grey and olive, fine-grained siliciclastic turbidites with rare sandstone and conglomerate; 2) **Jura Formation**, composed of shallow-water derived calcarenite, calcilutite and siliceous pelagic limestone; and 3) **El Numero Formation**, thick-bedded, bioturbated maroon marl and calcareous mudstone with abundant planktonic foraminifers and radiolarians (**Fig. 5C, 9**).

Weathering differences between the three units allow them to be mapped in the field and on aerial photographs. The thinner limestone units of the Jura Formation form narrow, resistant ridges, whereas the thicker clastic rocks of the other two formations are less resistant and form wider valleys between the limestone ridges (**Figure 9, cross section**). Mapping of the entire Sierra el Numero revealed 21 resistant ridges of El Numero Formation separated by the intervening valley-forming units. Limestone and mudstone units range from 50 to 300 m in thickness. Siliciclastic turbidites of the Ventura Formation were identified only in three horizons and range in thickness from 200 to 250 m. Sandstone of the Ventura Formation exhibit 35-140 m-thick, thinning and fining-upward sequences.

The typical lithologic sequence of the Peralta Group in the Sierra el Numero is, from base to top: turbidites-limestone-maroon mudstone-marl. While many of the contacts between formations is gradational, some contacts may represent structural repetitions along thrust faults can be observed.

Sandstone of the Ventura Formation is a lithic arkose and feldspathic litharenite with a large component of volcanic rock fragments. Maroon marl and mudstone of the El Numero Formation is interpreted as being deposited by turbidity currents and in situ pelagic deposition. Sedimentary structures in limestone of the Jura Formation indicate it was deposited by turbidity currents. The finer units of the Jura Formation contain reworked, shallow water benthic foraminifers, red algae and echinoid fragments.

Age dating of nanoplankton and planktonic foraminifera in turbiditic rocks of the Ventura Formation show early to middle Eocene ages for these rocks. Foraminifers of the Jura Formation show an age of middle Eocene while those in the mudstone of the El Numero formation show a late Middle Eocene to early Late Eocene age. Reworked Cretaceous and Paleocene faunas are common.

North-northwest-striking beds of the Peralta Group are abruptly truncated by the north-south-striking contact of the basal beds of the overlying Rio Ocoa Group (**Fig. 9**). Although dips on either side of the contact are indistinguishable, the contact appears to be a slight angular unconformity, separating units of different strike, but nearly equal dip. In map view, the older rocks of the Peralta Group strike into the base of the younger rocks of the Rio Ocoa Group (**Fig. 9**). Shearing along this contact suggests that the contact was deformed by later, probably early Miocene convergence (Heubeck and Mann, 1991).

At this stop we will examine rocks on either side of the contact. The road cut in the late 1980s showed a 1 m wide fault with a north-south strike and dipping 45° to the east that Heubeck and Mann (1991) interpreted as an early Miocene reverse fault because of its parallelism to the trend of axial traces of major early Miocene folds in the area.

As we drive through the area and look at the rocks near the contact at **Stop 2**, try to observe the major differences on either side of this contact and speculate on its tectonic control:

- **Examine the rocks on either side of the contact:** the Peralta Group rocks are fine-grained rocks that are virtually devoid of conglomerate and other coarse-grained rocks. Compare these rocks to the Rio Ocoa Group east of the contact that are coarse-grained to shaly with olistolith horizons. Olistoliths of maroon mudstone and marl identical to those of the El Numero Formation are found in olistostrome horizons near the base of

the Rio Ocoa Formation. 15 ages from nanoplankton and foraminifera from the basal section of the Rio Ocoa Group yield ages of Middle to Late Eocene. These ages partially overlap with early Eocene to early late Eocene ages from samples from the underlying Peralta Group.

- **Examine the differences in structural style on either side of the contact:** Witschard and Dolan (1990) document soft-sediment deformational features in the Peralta Group including isoclinal folding and stratal disruption. Similar deformational features are absent in the finer-grained rocks of the Rio Ocoa Group.

Rocks of the Rio Ocoa Group are characterized by brittle, post-depositional faulting and large-scale folding.

- **Integrate observations with regional tectonics:** what regional tectonic event might be recorded by the unconformity and abrupt change in lithology and structure across this contact?

## Tectonic setting, geology and hydrocarbons in the Neogene Azua-Enriquillo basin (stops 3, 4, 5, 6, and 7 on Day Two and stop 8 on Day Two).

### Tectonic transpression in Hispaniola: Variations in structural styles along the North America-Caribbean plate boundary (Fig. 10)

As we leave the Sierra el Numero and drive into the Azua and Enriquillo basins we enter an area of very young anticlinal mountains and synclinal valleys. This geomorphology reflects active transpression that is affecting the Hispaniola segment of the North America-Caribbean plate boundary zone.

GPS-determined motion of the Caribbean plate relative to North America predicts significant along-strike variations in the style of deformation along the 3100-km-long plate boundary (DeMets et al., 2000) (Fig. 10). The plate boundary extends from the Motagua Valley of Guatemala to the Lesser Antilles arc and has a GPS-derived rate of mainly left-lateral displacement of 21 mm/yr. The direction of plate motion known from GPS and the trend of the plate boundary faults allows predictions to be made about the progressive changes in structural styles along the length of the plate boundary from:

- **Transtension** in northwestern Central America and the western Cayman trough where the plate vector and the trend of the plate boundary diverge over a wide area.
- **Pure strike-slip faulting** in the central Cayman trough where the Caribbean plate vector and the trend of the plate boundary faults are parallel with the strike-slip faults.
- **Transpression and oblique underthrusting** in the eastern Cayman trough and southern Cuba where there is convergence between the plate vector and the plate-bounding faults.
- **Even greater amounts of transpression in the Hispaniola region** in the Hispaniola region, particularly in the zone of contact between arc rocks of the Caribbean plate and thinned continental rocks of the southeastern Bahamas platform (Fig. 11). Hispaniola exhibits a complex pattern of earthquakes and geologic structures with evidence for both crustal strike-slip and thrust faulting and shallow subduction of Atlantic and Caribbean crust. This pattern of transpression suggests strain partitioning in which part of the deformation is accommodated by north-south shortening and part is accommodated by east-west-striking left-lateral strike-slip faults (Mann et al., 2002; Calais et al., 2002).
- **Oblique subduction of Atlantic oceanic crust** beneath the northeastern edge of the Caribbean plate in Puerto Rico and the Virgin Islands.

### Regional structural effects of tectonic transpression in Hispaniola (Fig. 11)

There are three main geologic elements deformed in the Hispaniola oblique collisional zone (Fig. 11A). In the north is the 20-25-km-thick transitional crust of the southeastern Bahamas capped by 1-5.5 km-high carbonate banks (Dolan et al., 1998). The southeastern Bahamas are presently converging on Hispaniola in a west-southwesterly direction at a rate of about 20 mm/yr (Fig. 11A). The ~22-km-thick core of the island of Hispaniola and the neighboring islands of Cuba and Puerto Rico is composed of crystalline island arc-related rocks of Cretaceous and early Cenozoic age deformed in the Cretaceous, the Eocene, and by the ongoing phase of Bahama convergence. The third and final geologic element of Hispaniola is a 10-20-km-

thick oceanic plateau known from marine geophysical studies in the Caribbean Sea and from onland exposures in southern Hispaniola (Fig. 11).

Late Neogene to active oblique convergence between the Bahamas platform and Caribbean oceanic plateau has resulted in greater Miocene and younger convergent deformational features and higher topography in Hispaniola than observed either to the east in Puerto Rico or to the west in Cuba (Fig. 11A). This preferential shortening in the Hispaniola area because of oblique collision with the southeastern Bahama Platform is consistent with GPS results by Mann et al. (2002) and Manaker et al. (in revision) showing greater relative motion of central Hispaniola than Puerto Rico relative to a fixed Caribbean plate (Figs. 1, 11A). Relative motion between the southwestwardly moving Hispaniola block and the more stationary Puerto Rico block is accommodating by rifting in the Mona Passage between the two islands (Dolan et al., 1998; van Gestel et al., 1998; Jansma et al., 2000) (Fig 11A).

A regional, unbalanced cross section modified from Mann et al. (1991) and shown in Figure 11B illustrates several important features about the Cenozoic structural history of Hispaniola:

- A prominent folding and thrusting event in central Hispaniola is late Miocene and younger in age and verges southward to southwestward, consistent with the current GPS-based direction of Hispaniola tectonic transport shown in Figure 11A.
- Late Miocene and younger reverse and oblique-slip faulting is responsible for the present pattern of morphotectonic units in central Hispaniola, including the distribution of the three major ramp, or thrust-bound, basins – the Cibao, San Juan-Azua, and Enriquillo (Fig. 11B).
- Cretaceous-Eocene island-arc terranes of the northern and central part of the island are topographically high-standing and deeply eroded. The Cretaceous oceanic plateau in the southern part of the island is relatively low-standing and less deeply eroded. The lower elevation of the oceanic plateau in the south may reflect its footwall position relative to the higher-standing hanging wall block represented by the island-arc terranes in the north.

### **A short history of hydrocarbon exploration in Hispaniola (1904-present) (Fig. 12A)**

**Compilation of exploration wells.** Hydrocarbon exploration in Hispaniola has been concentrated in elongate, northwest- to west-northwest-trending, thrust- and strike-slip-fault-bounded “ramp” basins: the Cibao, San Juan-Azua, and Enriquillo (Figure 12B). In Haiti - which occupies the western one-third of the island - the San Juan-Azua basin of the Dominican Republic is known as the Plateau Central basin and the Enriquillo basin is known as the Cul-de-Sac basin (Fig. 12A). The Cibao basin of the northern Dominican Republic does not extend into Haiti, nor does the Artibonite basin of western Haiti extend into the Dominican Republic. 59 previous petroleum exploration wells have been drilled in the Dominican Republic during the period of 1904-2001 and 8 wells were drilled in Haiti during the period from 1944 to 1977. To date, there have been only two offshore wells drilled in Hispaniola (both at shelfal depths in Port-au-Prince Bay, Haiti) (Fig. 12A).

**Early exploration efforts.** Natural oil seeps were known from Spanish colonial times in the Azua basin (Fig. 12A). Petroleum was first reported in 1862 in the province of Azua by the American consul in the Dominican Republic who represented the administration of Abraham Lincoln (Nelson, 1862). The natural oil seeps at Higuerito hill along the mountain front of the Cordillera Central northwest of the provincial capital of Azua were first documented in a geologic report by the American geologist William Gabb, who conducted systematic geologic field studies in the Dominican Republic from 1869 to 1871 (Gabb, 1872).

Oil replaced gold as the major impetus for geologic exploration in Hispaniola during the early part of the 20<sup>th</sup> century. During the period 1915-1923, the U.S. government occupied both Haiti and the Dominican Republic and commissioned the United States Geological Survey to carry out a systematic reconnaissance of the oil, gas, and mineral potential of the country. The effort by the survey was headed up by the distinguished American stratigraphers, Thomas Wayland Vaughan and Wendell P. Woodring. The results of these studies were published in two volumes on both the geology of the Dominican Republic (Vaughan et al., 1921) and

Haiti (Woodring et al., 1924). These studies established the basic stratigraphy of the late Neogene siliciclastic basins of both the Dominican Republic and Haiti with many of their proposed formation names still in use today.

Exploration drilling commenced in the early twentieth century in the Azua basin which had the greatest concentration of natural oil and gas seeps (Fig. 12A). Eight wells were drilled amongst the dense concentration of seeps at Higuerito (**Stop 3**) by the Lancaster & Kreider Company between 1904 and 1907 (Table 1A). Abandoned well heads plugged by concrete with L&K stamped in the concrete were still visible in the 1980's. Outcrops are poor near Higuerito because the crest of the hill is mantled by Quaternary gravel and weathered, massive siltstone and consequently the geologic structure of the hill and the relation of this structure to the natural seeps were never clear to early geologic mappers. As a result, drilling was mainly guided by the location of natural seeps. The total depths of early Higuerito wells averaged 900 ft (274 m) with the deepest well (L&K-5) penetrating 1085 ft (331 m). Their first well, L&K-1, reportedly blew out between 400 and 500 barrels of oil for a period of approximately one week. Lancaster & Kreider abandoned the Higuerito concession in 1904 after their continued failure to contain high volumes of saltwater from entering the borehole.

Dominican Investment Company continued exploration at Higuerito between 1920 and 1923. Their first two wells, Intercean-1 and Intercean-2, were drilled near the seeps to depths of 2166 ft (660 m) and 2677 ft (816 m), respectively. Although both these wells reported "good" shows of oil, Dominican Investment Company abandoned their effort at Higuerito in 1923 and drilled a third well, Intercean-3, 4.5 miles (7 km) to the west on the Maleno anticline where natural seeps were also present (Fig. 3). In the Maleno area, outcrops are better than Higuerito and a large doubly-plunging anticline was identified by surface mapping.

Intercean-3 was drilled to a depth of 2,937 ft (895 m) near the crest of the Maleno anticline and encountered many oil shows. However, no production was established and the drilling concession to Dominican Investment Company lapsed in 1923. The casing was removed from the Intercean-3 borehole creating an anthropomorphic seep of water, flammable methane gas, and oil stains that remains active today.

The Texas Company acquired the concession to the Maleno area and drilled the Texas Company-1 well in 1924 near the Maleno seeps to a depth of 2,893 ft (882 m). The well is reported to have produced 3 to 5 BBO/day.

**Exploration program by Dominican Seaboard from 1939-1947.** Dominican Seaboard Company, a subsidiary of Standard Oil of New Jersey, renewed exploration in both the Higuerito and Maleno areas, carried out additional geologic mapping (Dohm, 1941a, b, c) and geophysical surveys (Tucker, 1945). Seaboard drilled a series of holes between 1939 and 1947. The Seaboard wells included two wells at Higuerito, seven wells with one offset at the Maleno anticline, and an additional well each on two anticlines west of Maleno at El Mogote (1940) and Las Hormigas (1944) (Fig. 12A). Most of the Seaboard efforts during this period focused on the Maleno anticline where most wells produced small amounts of oil. Although little geophysical data has survived to the present, Seaboard was able to acquire gravity and seismic data from the Maleno anticline in addition to extensive air photo and surface geologic studies. Maleno-1, drilled in 1939 to a depth of 1197 ft (365 m), produced 200 BOPD of 20° API oil from the Trinchera Formation at a depth of 410 ft (125 m). After producing some 25,000 BBLO, production at Maleno-1 eventually tapered off and the well produced only water. Today, oil with no water-cut drips slowly from the abandoned but functioning wellhead. The Maleno 1-A well, offset 270 ft (90 m) from the Maleno-1 well, produced 4554 BBO from the sand that produced in Maleno-1 (Anonymous, 1939).

Wells drilled by Seaboard at greater distances from the Maleno anticline in the western Azua basin all proved to be unsuccessful. Although Hormigas-1 exhibited promising shows of gas, the well was abandoned at 5070 ft (1545 m) because of mechanical problems (Fig. 3). The Quita Coraza-1 well, which was drilled in 1940 to a depth of 4300 ft (1300 m) in the core of a large doubly-plunging anticline in the far west of the basin, was also a dry hole. Seaboard ventured out of the Azua basin in 1945 to drill the Comendador-1 well (TD 5896 ft, 1797 m) on an anticline in the far western part of the San Juan basin near the border with Haiti.

In 1946, Seaboard drilled the Mella-1 well on a structural high largely defined by gravity studies in the deep, central part of the Enriquillo basin (TD 8759 ft, 2670 m).

The deepest and final well drilled in 1947 by Seaboard is Maleno-7, which tested the carbonate section of the Sombrerito Formation underlying siliciclastic rocks of the Trinchera Formation. This well demonstrated the reservoir potential of the Sombrerito Formation when an uncontrolled blowout of hot sulfurous water occurred on June 17, 1947, and flowed at an estimated 50,000 barrels of water per day. According to Boardman (1947), Seaboard abandoned its interests in the Dominican Republic “in view of the magnificent prospects offered by Arabia”.

**Efforts by Atlantic Refining Company (Arco) in Haiti from 1944-1947.** Arco drilled two wells in the Central Plateau basin, one well in the Cul-de-Sac basin, and one well in the Artibonite basin at about the same time efforts by Seaboard were concluding in the Dominican Republic (Fig. 12A). These wells were not documented, but appear to have been mainly drilled in the core of large domes or doubly-plunging anticlines in the Neogene sedimentary fill of these three basins.

**Efforts by Petrolera Dominicana, C por A, from 1956-1958.** This company and its affiliate, Petrolera Azuana, initiated an exploration program in the Azua basin by carrying out a review of all geological and geophysical data collected by Seaboard. Their drilling activity began with three shallow wells drilled near the previous Seaboard Maleno-1 and 1A wells at the crest of the Maleno anticline in 1958: Maleno-1 (358 ft, 109 m), Maleno-2 (907 ft, 276 m), Maleno-3 (423 ft, 129 m), and Maleno 4-A (500 ft, 152 m). During October and November of 1958, Petrolera Dominicana reentered the Seaboard Maleno-1 well and renamed it Maleno-4. In addition, the Petrolera Azuana-1 well was spudded at Higuerito in 1958 to a depth of 3030 ft (924 m). Although oil and gas shows were recorded in all of these wells, none were productive.

Surface mapping indicated the presence of a surface anticline west of the Maleno anticline. This new structure was tested by the 2814-ft-(858 m)-deep Km-19-1 well drilled on the so-called Km 19 anticline because of its proximity to that roadside km marker marking the distance from Azua on the Azua-San Juan road. The Km-19 anticline was identified using the results of earlier mapping by Seaboard. In 1959-60, the Km-19 anticline was tested by the deepest well ever drilled in the Azua basin, the 10,004 ft-(3049 m)-deep Km-19-2 well. Oil and gas shows were recorded from 2820 ft (860 m) to 6500 ft (1980 m). The second deepest well in the Azua basin, DT-1, was drilled in 1960 to a depth of 9920 m (3024 m) on the west flank of the Maleno anticline (Anonymous, 1960). The well was sited on an upthrown block in the anticlinal crest by reevaluation of existing seismic data collected earlier by Seaboard. This well has the best and most complete electric log in existence for the Azua basin. Gas shows were observed in the upper 3500 ft (1067 m) of the DT-1 well, an oil show was noted at 4172 ft (1272 m) in the Trinchera Formation, and oil and gas shows were noted from 4740 to 4788 ft (1445 to 1459 m). An additional well, Arroyo Blanco-1, was drilled on the Km-19 anticline but no records of this borehole have survived. Palo Alto-1 was spudded in late 1960 on a seismically-explored gravity anomaly in the eastern end of the Enriquillo basin but the well was abandoned as a dry hole (Llinas, 1972). Further seismic surveys and mapping identified structures in the Enriquillo basin which were tested by the Mella-2 well in the central part of the basin and the Cabritos-1 well in the western part of the basin (Llinas, 1972). Apart from traces of asphaltic material in the Cabritos well and nearby surface seeps of oil and gas near the village of Boca Cachon close to the Dominican-Haiti border (Guerra Pena, 1956), no hydrocarbons were found in the central or western parts of the Enriquillo basin.

**Efforts by Gas y Petrolera Dominicana (GASPOM) and International Resources, Ltd., from 1964-1970.** These companies reviewed Seaboard and previous well results and acquired new gravity and 117 km of seismic data. During the period of 1969-1970, they drilled seven wells in the Higuerito and Maleno areas. Three wells concentrated on the Higuerito structure: GPD Higuerito-1 was drilled to 2487 ft (758 m), GPD-Leon-1 to 3078 ft (938 m), and GPD-Leon-2 to 2802 ft (854 m). The GPD DT-1A well was drilled on the far western flank of the Maleno anticline to a depth of 4353 ft (1327 m). There is no surviving information on the GPD-Maleno-1 and 2 wells or the GPD Pyramid-1 well but all three are thought to have been drilled in 1969. GPD spudded one well in 1964, Dominicanos-1, outside of the Azua basin area in an area of deformed Eocene rocks near Baní. Drilling ceased at a depth of 2260 ft (689 m) because of political

unrest related to the Dominican civil war, but resumed in 1967 to a depth of 3440 ft (1049 m), at which depth the hole was abandoned as a dry hole. Gas shows were reported during drilling but were untested above 3350 ft (1021 m). GPD relinquished its acreage in the early 1970s.

**Efforts by Tenneco from 1969-1974.** Tenneco acquired offshore acreage in shallow shelf areas of Ocoa Bay adjacent to the Azua basin and Samana Bay adjacent to the Cibao basin of northern Dominican Republic (Fig. 3). Tenneco obtained 174 miles (281 km) of multi-channel seismic data from Ocoa Bay in 1969 and additional seismic data in Samana Bay, the eastern offshore extension of the Cibao basin. Some of the Tenneco lines from Samana Bay were subsequently interpreted by Edgar (1991).

**Efforts by Petrolera Las Mercedes, S. A., from 1979-1984.** This company was awarded a concession for the Azua basin in 1979 but was only able to collect some poor quality gravity and seismic reflection data without drilling any wells. They relinquished their concession to the Azua area in 1984. A grant by Petrolera Las Mercedes to the University of Texas Marine Science Institute (now University of Texas Institute for Geophysics) allowed 1100 km of offshore seismic reflection data to be collected across the San Pedro basin. These data were later interpreted by Ladd et al. (1981) and Heubeck et al. (1991). An additional 790 km of onshore seismic lines were collected from the edges of the San Pedro basin, along with gravity and surface mapping. The company drilled three wells in the eastern San Pedro basin south of Santo Domingo and reported oil shows in the San Pedro-1 well, which was drilled to a depth of 6064 ft (1848 m). However, samples were found to contain traces of Venezuelan crude oil apparently placed on the cuttings to create the false hope of an in situ oil show (Walters, 1991).

**Efforts by Canadian Superior Oil Corporation from 1979-1981.** This company obtained the concession to the Enriquillo basin in 1979 and collected 1043 km of seismic reflection data that were used to site the Charco Largo-1 well in the central part of the basin near the sites of the Mella-1 and 2 wells drilled in the 1960s (Mann et al., 1999). The Charco Largo-1 well was drilled to a depth of 15,847 ft (4830 m), but was abandoned as a dry hole in 1981.

**Efforts by Mobil Oil Company from 1991-1993.** Mobil was awarded the concession to the Azua and San Pedro basins in 1991 and carried out field studies, gravity surveys, and geochemical studies of the Azua oils. They also acquired 1500 km of multi-channel seismic reflection data from the southern coast of the Dominican Republic. One third of these data were focused on the shelf area of Ocoa Bay adjacent to the Azua basin (Fig. 3). In 1993, Mobil awarded its concession to Murfin Dominicana, Inc. (Murfin Drilling Company and Partners). The farm-in was contingent upon Murfin Dominicana, Inc. (MDI) drilling a Mobil-proposed onland well, Punta Salinas-1, on the southeastern edge of Ocoa Bay. This well was drilled in 1995-1996 to a depth of 5170 ft (1576 m) and abandoned as a dry hole.

As part of this drilling effort, S. Pierce and J. Munthe (formerly with Mobil) carried out a regional sampling program in the Dominican Republic for Mobil during 1988 and 1992 to locate areas of mature source rocks (Pierce, 1989; Munthe, 1989). Sedimentary samples ranged from lower Cretaceous to lower Pliocene limestone, evaporite, shale, siltstone, sandstone, and volcaniclastic sandstone. The majority of the samples yielded total organic carbon (TOC) values that were below the generative potential of 0.3% for carbonate lithologies and 0.5% for shale (Tissot and Welte, 1984). Siliciclastic units with TOC values within the lower end of petroleum generative capacity included lower Pliocene shale units of the Angostura Formation that are interbedded with salt deposits in the central Enriquillo basin (TOC of 0.5-1.86) (**Stop 8**), and late Miocene turbiditic sandstone of the Trinchera Formation in the Azua basin (TOC of 0.01-0.52) (**Stops 5, 6, 7**). Limestone units with TOC values within the lower end of petroleum generative capacity included the Sombrerito Formation in the Azua, San Juan, and Enriquillo basins (TOC upper range values from 0.26 to 0.55). Highest TOC values in the Sombrerito Formation (**Stop 3**) occur in the San Juan and Azua basins.

For comparison, TOC values determined by Mobil from upper Cretaceous claystone and limestone cuttings from DSDP site 146/149, Leg 15, in the Caribbean Sea south of Hispaniola (DSDP, 1971; Moiola, 1989) exhibited considerably higher TOC (range of 1.06 to 6.81%). The only other area of rich source rocks described from the Caribbean plate is from late Cretaceous Pacific forearc basinal settings in Costa Rica

where total organic carbon contents of late Cenomanian-Campanian shale range from 15-33%. These high carbon values are believed to relate to an upwelling near the Middle America trench (Erlich et al., 1996).

**Efforts by Murfin Dominicana, Inc. (MDI), from 1993 to 2002.** Currently, MDI holds a concession for 2.8 million acres covering the coastal areas of the San Pedro and Azua basins. MDI activity to date includes the acquisition of 42 km of seismic data over the Maleno, Higuerito, and Las Hormigas areas. In addition, MDI obtained geochemical data on the warm springs in the Azua area. In 2002, S. Pierce oversaw the drilling of two new wells at the Maleno field for MDI: Maleno East 1 and 2. At this time, they opened the wellhead on Seaboard Maleno-6 which flowed gas then oil. Oil also continued to flow from the wellheads of Maleno 1 and Maleno 1-A in 2002.

### **Regional seismic line across the San Juan ramp basins showing Neogene shortening and Cordillera Central Neogene uplift event (Fig. 13)**

Two main basin trends are present in south-central Hispaniola: the west-northwest trending San Juan basin and the east-west-trending Azua basin (Fig. 1, 12A). The two basins merge to the east in the Azua basin, which contains both west-northwest and east-west late Neogene structural elements. The main fault bounding the northern edge of the San Juan-Azua basin is the San Juan-Los Pozos fault zone, a 200-km-long fault lineament (Fig. 1, 12A) of northwest-side-up reverse faulting separating Eocene sedimentary rocks from Neogene rocks of the San Juan and Azua basins (Dolan et al., 1991). This fault locally juxtaposes Eocene rocks against Miocene carbonate rocks of the Sombrerito Formation along the northern edge of the San Juan basin (Harms, 1989). Another important sub-parallel thrust to the north, the San Juan-Restauración fault zone, juxtaposes arc basement rocks with Eocene rocks of the Peralta belt of Eocene turbiditic rocks (Dolan et al., 1991). The southern edge of the San Juan basin is defined by several imbricate, south-dipping thrust faults that place older Cenozoic carbonate rocks of the Sierra de Neiba over Neogene basinal sedimentary rocks of the San Juan basin (Nemec, 1980) (Fig. 5). A Plio-Pleistocene belt of shallow intrusions and volcanic cones crops out orthogonal to the trend of reverse faults and forms a physiographic and possibly structural boundary between the San Juan and Azua basins (Vespucci, 1980) (Fig. 4).

A Vibroseis seismic line collected in the western part of the San Juan basin by Western Geophysical for Weeks Petroleum shows the main elements of the southern faulted edge of the San Juan ramp basin and its stratigraphic succession (Fig. 13A). The arc inferred Cretaceous to Eocene arc basement is overlain by a carbonate interval correlated to outcrops of the Eocene-Miocene Neiba-Sombrerito section in the Sierra de Neiba (cf. Part II of this guide). Overlying the carbonates is a slightly asymmetrical clastic wedge derived from erosion of the Cordillera Central to the north.

The late Miocene clastic wedge was diverted by the northeast-trending ramp structure of the San Juan basin into the Azua basin at its southeastern end (Fig. 13B). Uplift of the Sierra de Neiba blocked clastics from entering the central part of the Enriquillo ramp basin; this sheltered environment allowed massive evaporites to form in early Pliocene time (Fig. 13B).

### **Stratigraphy of the Azua and Enriquillo basins (Fig. 14) (stops 3-12 on Days One and Two)**

The Neogene litho- and biostratigraphy of the Enriquillo and Azua basins has been documented in detail by McLaughlin (1989), McLaughlin et al. (1991), McLaughlin et al. (1991), and McLaughlin and Sen Gupta (1994). The characteristics of five Neogene units relative to hydrocarbon exploration in the region are briefly summarized here and are discussed further in Part II of this guide. For a historical perspective of stratigraphic nomenclature, Mann et al. (1991) provides a chart showing how the formation names used by McLaughlin et al. (1991) and in this paper evolved from prior usages proposed by previous workers, including exploration geologists with Seaboard. The equivalent formation names, age, thickness and facies of the five units are compared in three places where they are best known from either drilling or outcrops: the central Enriquillo basin (Charco Largo well), the northeast margin of the Enriquillo basin in the valley of the Río Yaque, and the northeast margin of the Azua basin in the valley of the Rio Via (comparison of the three areas shown in Figure 14). These five Neogene stratigraphic units are similar in thickness but younger in age

than the section encountered in the Comendador-1 well of the western San Juan basin shown on the regional seismic line in Figure 13B. The five units we will visit on this trip include:

• **Sombrerito Formation (Stop 3):** This formation is a 250-500-m-thick section of pelagic and shallow-water limestone, marl, and shallow-marine-carbonate debris flows that record a middle Miocene period of carbonate deposition through central and southern Hispaniola. The formation crops out mainly around the flanks of the Sierra de Neiba and forms a carbonate “basement” beneath the thick siliciclastic sequences of both the Enriquillo and Azua basins (Fig. 13A). The type locality of the formation was proposed to be in the Arroyo Sombrerito at the eastern end of the Sierra de Neiba and has been described by McLaughlin et al. (1991). At the type locality, the formation is characterized by buff marl and pelagic limestone. At other localities in the southern San Juan basin, the formation consists of blue-gray marls interbedded with pink, indurated calcareous sandstone or buff marl interbedded with thin beds of dark shale. Marls are rich in fragments of calcareous plankton and deep-water benthic foraminifera. Sandstone beds contain convolutions indicating rapid deposition from suspension and shallow-water carbonate debris.

Calcareous plankton indicate that the formation ranges in age from late early Miocene in the San Juan-eastern Enriquillo basin and into the earliest part of the late Miocene in the Azua basin. Benthic forams described by McLaughlin from these outcrops indicate deposition in middle bathyal or greater depths and these data combined with lithofacies indicate a lower slope setting open to the sea (McLaughlin et al., 1991).

Coeval shallow-water facies of the Sombrerito Formation have been described on the north flank of the San Juan basin (Bold, 1983) and in the area of Ocoa Bay, where Pierce observed shallow-marine red algal grainstones with excellent inter- and intragranular porosity in the Loma de Vigia directly to the west of Ocoa Bay. These Sombrerito grainstone outcrops tend to be poorly bedded with thin shale partings. Pervasive fracturing of the unit in the easternmost Azua basin appears related to movements along the northeast-striking Beata fault zone (Fig. 1). Reefal sections of Sombrerito Formation have also been encountered at depths of several thousand feet in wells in the Azua basin (Boardman, 1947). The middle Miocene age of the Sombrerito Formation indicates it was deposited during a time of high eustatic sea level (Fig. 14). High sea level and drowning of siliciclastic source areas may be one explanation for the low amount of siliciclastic sediment interbedded in the Sombrerito Formation (**Stop 3**). The Sombrerito Formation is proposed to act as the main potential source rock and reservoir for hydrocarbons in the Azua basin.

• **Trinchera Formation:** The Trinchera Formation consists of an approximately 1,000-2,650-m-thick section of mudstone, siltstone, sandstone, and conglomerate that records the onset of siliciclastic sedimentation in the San Juan, Azua and Enriquillo basins (Fig. 13A, B). The Trinchera Formation is widespread over the San Juan and Azua basins but pinches out to the southwest in the central Enriquillo basin, where the formation is only 322 m thick at the base of the Charco Largo well (Mann et al., 1999) (Fig. 14). The type locality of the Trinchera formation is the Trinchera bluffs along the banks of the Río Yaque del Sur near the boundary between the Azua and San Juan basins. Although faulted in most localities, the contact between the Sombrerito and Trinchera Formations is a gradational carbonate to siliciclastic transition (**Stop 7**).

Facies of the Trinchera Formation are typical of those deposited in a submarine fan setting. Lithofacies and benthic foraminiferal biofacies described by McLaughlin (1991) and McLaughlin et al. (1991) indicate deposition in a prograding, shoaling slope setting. Paleocurrent studies and paleowater depth variations indicate that the shelf-slope siliciclastic section progrades southward in the late Miocene and early Pliocene by the growth of a laterally confined submarine fan. Large-scale clinoforms present on the seismic lines shown in Figure 13A from the San Juan basin illustrate the southward progradation of the formation in this area from source areas in the Cordillera Central during late Miocene time. Lithofacies include middle fan facies deposited in outer neritic water depths (**Stop 6**) and more proximal conglomerate and massive sandstone beds deposited at inner neritic depths and capping the formation (**Stop 5**). More conglomerate of the Trinchera Formation is exposed in the eastern Azua basin than in other areas to the west in the Azua and Enriquillo basins. This is consistent with an interpretation of this area as one of the confining, proximal edges of the more distal submarine fan in areas to the west.

The infilling of the Azua basin caused shoaling of the basin in some areas (**Stop 5**). Benthic foraminifera indicate a change from middle bathyal depths of nearly 1,000 m in the lower part of the formation to upper bathyal depths of approximately 200 m at the top. The Río Via section in the eastern Azua basin exhibits more abundant conglomerate and reworked shallow-water faunas supporting the concept that this area was the shallow eastern basin margin that confined the thicker and more fine-grained fan to the west in the Azua and Enriquillo basins. Sandstone petrography and conglomerate clast types match closely with igneous, metamorphic and sedimentary rock types presently exposed in the Cordillera Central. The late Miocene age of the Trinchera Formation indicates that it was deposited during a time of low eustatic sea level (Fig. 14). In addition to late Miocene tectonic activity discussed below, low sea level may have expanded onland siliciclastic source areas and the narrow shelf feeding the submarine fan.

• **Angostura and Quita Coraza Formations:** The Angostura Formation in the Charco Largo well in the central Enriquillo basin consists of 1562 m of clear to milky, anhedral halite interbedded in greenish-gray indurated, silty, slightly calcareous shale (Mann et al., 1999). The Angostura Formation is seen to unconformably overlie the Trinchera Formation on well and on seismic data. The formation also crops out in the core of thrust-faulted anticlines along the southern edge of the basin (**Stop 8**). In these outcrops, the formation is about 300 m thick and consists of both halite and gypsum. Litho- and biofacies indicates deposition in a restricted, shallow lagoon with brackish to hypersaline conditions. A poor ostracode fauna indicates an age near the Mio-Pliocene boundary.

In the eastern part of the Enriquillo basin and in the Azua basin, the age-equivalent unit to the Angostura Formation is the Quita Coraza Formation, a 200- to 700-m-thick siltstone horizon that separates the deep-marine Trinchera and shallow-marine Arroyo Blanco Formations (Fig. 1). This easily erodible shale unit controls the course of the Río Yaque del Sur and forms a prominent marker bed useful for mapping major anticlines and synclines on aerial photographs and in the field.

The contact with the underlying Trinchera Formation is conformable and gradational as is its upper contact with the Arroyo Blanco Formation, where a prominent color and grain sized contrast is observed between the blue siltstone of the Quita Coraza Formation and the overlying pale brown sand and conglomerate of the Arroyo Blanco Formation (**Stop 5**). Foraminifera from the formation indicate an age range from latest Miocene to Pliocene. Lithofacies and biofacies studied by McLaughlin (1991) and McLaughlin et al. (1991) indicate transition from outer to inner neritic settings.

• **Las Salinas and Arroyo Blanco Formations:** The Las Salinas Formation is a 2,000-m-thick section of shallow-marine and marginal-marine siliciclastic rocks that conformably overlie the Angostura Formation in the Charco Largo well but are overthrust by the Angostura Formation along the edges of the Enriquillo basin (**Stop 8**). Ostracodes indicate a shallow embayment with variations from brackish, to marine to hypersaline (McLaughlin, 1991; McLaughlin et al., 1991). The presence of gypsum beds of 1-2 m in thickness formed in tidal pool settings support the brackish setting (Mann et al., 1999). The Las Salinas Formation is equivalent to the 700-m-thick Arroyo Blanco Formation found in the eastern Enriquillo and Azua basins (Fig. 14). These two formations, composed mainly of conglomerate, sandstone, siltstone, oolitic limestone, and gypsum include the stratigraphically highest marine sedimentary rocks of the Azua basin. The Arroyo Blanco Formation is best exposed in the eastern part of the Enriquillo basin where post-early Pliocene tectonic tilting exposes a natural cross section of an early Pliocene margin gently sloped towards the central Enriquillo basin (Mann et al., 1999). The formation forms a coarsening-upwards regressive sequence that includes a prominent marker horizon of in-situ or reworked coral at its base and sandstone and conglomerate at its top. Conglomerate clast types in the Las Salinas and Arroyo Blanco Formations match those igneous, metamorphic and sedimentary rock types presently exposed in the Cordillera Central.

The upper 500 m of the Arroyo Blanco Formation in the Azua basin consist of 90 or more fining- and thinning-upward cycles composed of conglomerate, sandstone, and siltstone that form prominent, erosionally resistant, strike-parallel ridges on aerial photographs (**Stop 5**). These cycles range in thickness from 2 to 14 m, have erosive bases, and are lenticular on the scale of tens of meters (Fig. 22). Medium-grained sandstone and pebbly sandstone bodies exhibit planar and trough cross beds and contain shell fragments. McLaughlin

(1991) and McLaughlin et al. (1991) interpret the lower part of the Arroyo Blanco Formation as deposition in a shallow-marine offshore setting adjacent to scattered patch reefs. The numerous thinning- and fining-upwards cycles of the upper Arroyo Blanco Formation are interpreted as delta or tidal channel deposits that transported coarser-grained sediments from source areas in the adjacent highlands to the submarine fan at the slope-break. As the channels became choked with sediment or migrated laterally, the channel axis and overbank areas became infilled by fine-grained sediments characteristic of the upper part of the fining-upward cycle.

• **Jimani and Arroyo Seco-Via Formations:** The Jimani Formation is an approximately 125-m-thick section of fossiliferous limestone, sandstone, and mudstone that lies unconformably on slightly folded rocks of the Las Salinas Formation in the central and western part of the Enriquillo basin. Ostracode faunas of the Jimani Formation indicate a Pleistocene age for at least part of this formation; biofacies reflect environmental variation between nearly fresh-water and shallow-marine conditions. The litho- and biofacies indicate a Pleistocene depositional setting similar to that observed in the Holocene: a lagoonal to lacustrine setting with intermittent connections to the Caribbean Sea. The Via Formation is a 500-600-m-thick proximal alluvial fan conglomerate facies found only in the easternmost Azua basin adjacent to the San Juan-Los Pozos reverse fault zone (Fig. 1). The 1000-m-thick Arroyo Seco Formation is composed of non-marine sandstone and conglomerate deposited in fluvial or braidplain environments. We have no direct age control on either the Via Formation or Arroyo Seco Formation other than the fact that both conformably overlie the Arroyo Blanco Formation and are therefore post-early Pliocene in age. We make no attempt to distinguish Quaternary sand and gravel from underlying sand and gravel of the Arroyo Seco Formation. Rocks of the Arroyo Seco and Via Formation can be distinguished from overlying horizontal Quaternary deposits on the basis of the former's tectonically-induced dips of 30-45°.

### Neogene paleogeography of the Azua and Enriquillo basins (Fig. 15).

Figure 15 is modified from McLaughlin et al. (1991) and presents an interpretation of depositional events, eustatic seal level, and paleogeography of the southern San Juan, Azua and Enriquillo basins based on our knowledge of the lithofacies and biofacies of formations reviewed above. The middle Miocene was a time of deep-water, normal marine conditions recorded by the deposition of the pelagic limestone and marl of the Sombrerito Formation (**Fig. 15A, B, C; Stop 3**). A paucity of terrigenous siliciclastic material in the Sombrerito Formation indicates source areas of the Cordillera Central had not yet undergone significant uplift and erosion or had been uplifted but remained in a submarine setting. Local shallow water, reefal conditions prevailed in the Sombrerito Formation in the eastern Azua basin.

Lower stands of eustatic sea level in the early late Miocene through earliest Pliocene (Fig. 14) and coincident tectonic uplift of the Cordillera Central induced submarine siliciclastic deposition of the Trinchera Formation (Fig. 15C-E). Coincident uplift of the Cordillera Central and Sierra de Neiba and formation of the San Juan and Enriquillo ramp basins (Fig. 13B) focused the main depocenter of the submarine fan into the Azua basin and easternmost Enriquillo basin (Fig. 15D, E). Rising eustatic sea level in the early Pliocene (Fig. 14) flooded the area and ended siliciclastic sedimentation of the Trinchera Formation. This transgression is marked by siltstone of the Quita Coraza Formation, and seems to have been the flooding event with which the following cycle of flooding and desiccation of the central Enriquillo basin began. The latter part of the early Pliocene saw the deposition of a massive, 1.5-km-thick halite section in the center of the Enriquillo basin during this series of marine influx and evaporation events (Fig. 15F). Later regressions are recorded by thin gypsum beds deposited in the Arroyo Blanco Formation along the northeastern edge of the main evaporite depocenter. The last event in the basin history is the progradation of a non-marine siliciclastic wedge deposited under fluvial and braid-plain conditions as the Arroyo Seco Formation (Fig. 15F, G). The Via Formation is a coarser fan facies reflecting erosion of the mountain front of the Cordillera Central in the eastern Azua basin (Fig. 15F). Continued folding in a transpressional setting culminated in the present pattern of deep basins separated by high mountain ranges (Fig. 15H).

## Petroleum geology of the Azua basin (stop 4)

Pierce and Mobil geologists used about 500 km of seismic data to make a map to the top of the Sombrerito Formation carbonate rocks, which forms a seismically prominent “basement horizon” beneath the less-consolidated siliciclastic sedimentary rocks of the Azua and Enriquillo basin (Fig. 16B). This map reveals a major depocenter directly east of Ocoa Bay that reaches depths of 15,000 feet. To the northeast, the depth of basement rises rapidly to depths of 7,500-10,000 feet in the area of the Maleno oil field and eastern end of the Sierra de Neiba (Fig. 16B). The depocenter is aligned roughly northeast-southwest and is parallel to the Beata fault zone. The depocenter may be long-lived because of its association with the area of thickest accumulations of late Miocene Trinchera Formation and early Pliocene Arroyo Blanco Formation (Fig. 15F, G).

An anticline-syncline pair, also oriented parallel to the Beata fault zone, occurs within this depocenter. The depocenter corresponds to a major –300 nannotesla low on the aeromagnetic map although these data only constrain the onland areas and do not extend into Ocoa Bay (Fig. 16A). One interpretation is that the depocenter has formed as a left-stepping pull-apart basin on the left-lateral Beata fault zone because the northern edge of the magnetic low/depocenter coincides with the Azua fault, a very prominent northeast-striking surface fault described below.

Mapping of the top of the Sombrerito Formation in Ocoa Bay revealed the Ocoa Bay fault zone defined along the axis of a large, elongate anticlinal dome in the carbonate rocks (Fig. 16B). This fault is a splay off the Beata fault zone and defines the present-day shelf-slope break in Ocoa Bay. The convergent nature of the fault and associated anticline is consistent with left-lateral shear along the Beata fault zone.

The outcrop pattern, topographic expression, and aeromagnetic pattern of the northeast-trending belt of Plio-Pleistocene intrusions and volcanic eruptions exhibits two internal trends of cones and shallow plugs: a northeast trend parallel to the overall belt and a northwest trend (Vespucci, 1980; Electroconsult, 1984). There is an excellent correlation between mapped plugs and volcanic cones and point source magnetic highs on the aeromagnetic map (Fig. 16A). Elongate aeromagnetic highs suggest that two northwest-trending belts of intrusions extend to the southeast beyond the mapped outcrop limit of the volcanic belt (Fig. 16A). The northern high extends into an area of the Peralta belt, an Eocene-aged accretionary wedge with an otherwise remarkably flat magnetic signature consistent with the estimated 10-km structural thickness of the belt (Dolan et al., 1991). The great stratigraphic thickness of the Peralta belt is supported by the penetration of 3 km of Eocene sedimentary rocks at the Punta Salinas 1 and 2 exploration wells on the east side of Ocoa Bay (Fig. 12A).

The southern high extends along a thrust-faulted structural high containing the Maleno and Higuerito oilfields (Fig. 16A). Alternatively, these elongate magnetic highs could represent older Cretaceous basement highs uplifted by northwest-southeast directed folding and thrusting. However, the lack of Cretaceous outcrops, the isolated nature of the highs in an area of flat magnetic signature, and the similarity of the magnetic highs to known outcrop areas of the volcanic belt suggest that their source is likely controlled by a buried extension of the Plio-Pleistocene volcanic/intrusive belt (Fig. 16A). It's possible that localized maturation of oil in the Maleno and Higuerito region is attributed to the presence of the volcanic plugs intruded into the young sedimentary rocks.

## Reevaluating a century of exploration at the Higuerito oil field (Stop 4)

The structure of the Higuerito field has remained obscure since the first drilling in 1904 for several reasons: 1) the structure is complex and not well exposed in deeply incised valleys as at Río Via to the southeast; 2) some of the bedrock units of the area are covered by a gravel terrace related to the mountain front alluvial fan of the Río Peralta found east of the oilfield (Fig. 17); and 3) much of the bedrock exposure in the oil field at the crest of the anticline is massive gray siltstone inferred to be part of the Quita Coraza Formation (Fig. 18A). We present a new cross section of the faulted anticline of the Higuerito field based on interpretation of aerial photographs and correlation to the Río Via monocline; detailed surface mapping of all

accessible outcrops (Fig. 17); and interpretation of a dip seismic line kindly provided by Murfin Drilling Company for use in this study (Fig. 18A).

Direct correlation between the Río Via section and units cropping out at the Higuerito field is difficult because the prominent stratigraphic units seen on aerial photographs are obscured by Quaternary deposits in the area northwest of Rio Via. However, the prominent shale valley of the Quita Coraza Formation cropping out in the Rio Via monocline can be traced for about 10 km to the northwest to the area to the north of the Higuerito field.

A major difference between Higuerito and Rio Via is the presence of southwestward basinward dips indicative of folding of the Neogene stratigraphic section as shown on the cross section in Figure 18A. Dips range on the order of 20-30° over much of the anticline but the steepest dip value of 60° suggests the possibility of a more steeply-dipping southwest limb giving the structure a southwestward asymmetry. We interpret the massive gray shale cropping out in the field itself to be the Quita Coraza Formation based on correlation of the well logs. The Higuerito-2 well intersected a major shear zone, which we interpret to be one of three, low-displacement forelimb thrust faults that have developed during the later of the thrusting. All three thrust faults are inferred from bedding measurements and the depth of the shear zone in the Higuerito-2 well to be sub-vertical and not restricted to a certain stratigraphic horizon. A problem in our section is the difference in thickness of the Quita Coraza Formation on the two limbs of the fold (Fig. 18A). It's possible that this mismatch is stratigraphic or that it reflects our failure to correctly distinguish shale units of the Trinchera Formation and the Quita Coraza Formation. Detailed paleontologic sampling of this unit would be one test to distinguish the deeper-water and older Trinchera shale from the shallow-water and younger shale of the Arroyo Blanco Formation.

Seismic reflection line 101 in Figure 13 crosses the Higuerito oil field at an oblique angle to its strike (Fig. 17). The intersection of the line with Higuerito-1 compares well with the interpretation based on surface data in Figure 18A despite the differences in vertical exaggeration and orientation: an asymmetric fold axis framed by two thrust faults and a third thrust in a more basinward position. Line 101 indicates that a similar style of thrust imbrication extends for 3 km north of the oilfield. This deformational pattern contrasts with the undeformed formation boundaries observed in Rio Via and suggested by air photos in the area between Rio Via and Higuerito. It is possible that the degree of shortening increases dramatically over the 8 km distance from Rio Via to Higuerito as the mountain front fault swings from the dominantly northeast-trending strike-slip lateral ramp position to dominantly northwest-trending thrust fault orientation.

**Post-mortem of drilling efforts at Higuerito oilfield.** In light of our cross section in Figure 12B, it is interesting to compare the brief production history of the Higuerito field to the observed and interpreted structures. Higuerito-1, the first well drilled in Hispaniola in 1904, is perfectly sited at the crest of the anticline and within the structural compartment bounded by thrust faults B and C on Figure 18B. This well, located on natural seeps and drilled into the Trinchera Formation and upper Sombrerito Formation, blew out between 400 to 500 BBO for approximately one week in 1904. According to unpublished well reports, the primary reservoir rock in the Higuerito wells is marine sandstone of the Trinchera Formation from 910 ft. to 1,400 ft (277 m to 427 m) and underlying alternating marine sandstone and shale from 1,400 to 2,014 ft (427 to 614 m). Subsequent wells drilled off the crest of the anticline and outside of the structural compartment between faults B and C were unsuccessful or yielded trace amounts of oil and gas. We propose that faults B and C are lateral sealing faults to an upper Sombrerito Formation carbonate-hosted source, a Trinchera Formation-hosted reservoir, and that shale of the overlying Quita Coraza Formation provides the upper seal of the trap. Natural oil and gas seeps indicate that the upper seal of the trap has been partially breached by faults B and C and/or other smaller faults not recognized in the field or on the existing well logs.

**Structure of Maleno oil field, Azua basin.** The Maleno oilfield, like the Higuerito oil field 10 km to the east, is located at the crest of a large, asymmetric (steep limb to the southwest) anticline deforming the four major Neogene formations of the Azua basin (Fig. 18B). We present a new cross section of the anticline of the Maleno field based on interpretation of aerial photographs (Fig. 17) and correlation with Azua basin

stratigraphy reviewed above; detailed surface mapping of all accessible outcrops; and interpretation of a dip seismic reflection line kindly provided by Murfin Drilling Company for use in this study.

Direct correlation between the stratigraphy cropping out at the Maleno field and the adjacent Higuerito oilfield to the east is difficult because the prominent stratigraphic units seen on aerial photographs are obscured by Quaternary deposits to the east and west (Fig. 17). All of the prominent hogbacks seen framing the Maleno, Las Hormigas and Km-19/2 anticlines are part of the Arroyo Blanco Formation. Dips range on the order of 30° on the more gently dipping northeast limb of the Maleno fold and on the order of 30-40° on the steeper dipping southwest limb of the fold (Fig. 18B). Most Maleno wells cluster on the axis of the fold although the Maleno-DT or “deep test” well is drilled off axis on the south flank of the fold (Fig. 18B). Most wells penetrated to the top of the Sombrerito Formation where production was attained. Our surface mapping revealed no surface faulting although unpublished surface and seismic reflection mapping by Seaboard revealed a high-angle fault along the fold axis (cf. several faults seen on seismic line in Figure 19 across the fold axis). This observation of surface faults is supported by the observation that several Seaboard wells in the Maleno anticline reported slickensides and fractured lithologies in all formations penetrated: Seaboard Maleno no. 3, Seaboard Maleno no. 6, and Maleno no. 7 (Boardman, 1947). Seaboard subsurface data also show the steeper southwestern limb of the fold.

Subsurface mapping to the top of the Sombrerito Formation by Pierce has shown that the Maleno anticline extends as a fault-bounded ridge for approximately 15 km in a west-northwest direction (Fig. 16B). Seismic line 103 (Fig. 19) provided by Murfin Drilling Company reveals a listric thrust fault defining the steeper, southwest limb of the Maleno fold and a zone of backthrusts bounding the northeast flank of the fold. Both sets of thrust faults may root on a thrust fault that has propagated southwestward into the sedimentary rocks of the Azua basin from a position beneath the present-day mountain front of the Cordillera Central (Fig. 16B). The level to which these faults penetrate upwards in the section is not clear due to the low quality of the upper part of the seismic record. Onlap can be observed by the Trinchera Formation onto the underlying Sombrerito Formation indicating fold activity was occurring during late Miocene (early Trinchera Formation) time. This onlap would represent the late Miocene southward progradation of the Trinchera submarine fan from source areas in the Cordillera Central (Fig. 13B) as also observed on Line LM-1 in the western San Juan basin (Fig. 13A).

**Reevaluation of drilling efforts at Maleno oilfield.** In light of our cross section in Figure 18B, seismic line 103 in Figure 19, and the well log of the second deepest well (Maleno-DT-1, TD 9,930 ft (3027 m) – Fig. 18) drilled into the Maleno anticline and the entire Azua basin, it is interesting to compare the brief production history of the Maleno field to the observed structures.

Oil shows in both the Maleno DT-1 and the Km-19/2 wells are confined to the Sombrerito Formation in a depth range of 4,000-10,000 ft (1219-3048 m). The confinement of shows to the Sombrerito Formation supports the observation that Middle Miocene carbonate rocks of the Sombrerito Formation are the likely source for most of the oil production. The major reservoir units of the Maleno field are two sandstone bodies named informally by Seaboard geologists as the A and B sands. These sandstones are gray, calcareous, fine to medium grained with fossil leaf prints. Pebble conglomerate is also present as described in detail at the Interocean no. 3 well by Bermudez (1943). The A sand varies from a gross thickness of 60 ft. to 163 ft. (18-50 m) and occurs at depths ranging from 187 ft. to 500 ft. (57-152 m) below the surface. Although no values of porosity or permeability are available, the Petrolera Azuana Maleno-2 well drilled in 1958 (T.D. 907 ft. – 276 m) flowed at a rate of 240 bbw/day for in the A sand (Fenoglio, 1958). At a depth of 400 ft. (122 m), the B sand flowed 300 barrels per day in the Seaboard Maleno no. 1 well. The nearby Seaboard Maleno 1-A well produced 600 barrels per day. Both wells began producing salt water before commercial production could be realized. It was estimated that between 23,000 and 45,000 barrels could have been produced from both wells. To put the size of this field in perspective, the Ghawar supergiant field of Saudi Arabia is estimated to produce over 5 million barrels of oil per day or about 6.25% of global daily production.

An oil show in sandstone beds of the Trinchera Formation in the Km-19/2 well supports the idea that submarine fan sandstone has reservoir potential in the area of this well also. The 4,000-10,000 ft (1219-3048

m) production zone at Maleno is much deeper than the 1,500-1,800 ft. (457-549 m) production zone at Higuerito, where basin-edge thrust tectonics has elevated the Sombrerito Formation much closer to the surface. The possible presence of a west-northwest-oriented, subsurface Plio-Pleistocene shallow intrusion at Maleno and Higuerito may be another factor in the local maturation of the Sombrerito Formation in some but not all folds of the Azua basin (e.g., no shows were reported in the well as the Las Hormigas anticline). Surface mapping indicates that the Km-19/2 fold is a minor, parasitic fold on the southwest flank of the main Las Hormigas anticline with little closure (Fig. 17). This observation may explain the failure of this well.

### **Lunch in Azua**

#### **Prograding and shallowing upward clastic wedge in the Azua and Enriquillo basins (stops 5, 6, and 7).**

From Higuerito we will proceed to the west along the main highway to Barahona. The lowlands of the Rio Yaque Valley exhibit some classic stratigraphic sections that have been studied since the U.S. occupation of the island almost a century ago. We will travel down section with stop 5 near the shallow-water contact between the Quita Coraza and Arroyo Blanco Formations and stops 6 and 7 in the deep-water Trinchera submarine fan section. At stop 7 we will run out of outcrop as we enter the Enriquillo basin proper and will take that opportunity to review the subsurface geology of the Enriquillo basin which will also be discussed at stop 8 on Day Two.

#### **Structure of the Quita Coraza-Los Guiros anticline-syncline pair (stop 5).**

This anticline-syncline pair, which is well exposed in this desert-like area in the western Azua basin, were originally mapped by geologists from Seaboard (Dohm, 1941b, c) (Fig. 20). The highway follows an eroded strike valley in the less resistant blue shales of the Quita Coraza Formation. We present a new cross section of these structures (Fig. 21) based on interpretation of aerial photographs and detailed surface mapping of all accessible outcrops (McLaughlin et al., 1991; Mann et al., 1991; Mann et al., 1999).

The biostratigraphy of the cross section in Figure 21 has been studied in detail by McLaughlin et al. (1991a). No seismic reflection data have been collected in this area. The folds are broad, open structures with dips ranging from 20-30°. The main difference in structure in this area in comparison to the Maleno and Higuerito areas to the east is the lack of asymmetry in the folding. The lack of asymmetry of these folds is probably related to their positions well within the center of the eastern Azua basin and removed from basin-edge thrust tectonics.

In light of our cross section in Figure 21, the Quita Coraza well, a dry hole with no shows, was poorly sited well off the axis of the anticline. Moreover, there is no evidence for surface seeps in this area nor is there any evidence from the aeromagnetic map in Figure 16A for subsurface intrusions which might help promote local maturation, as in the Maleno and Higuerito areas.

#### **Stratigraphy of the Quita Coraza-Arroyo Blanco transition zone area at stop 5**

The map in Figure 23 summarizes the outcrop patterns, water depths and paleocurrents of the three main units exposed in this area: submarine fan rocks of the Trinchera Formation, neritic blue shale of the Quita Coraza Formation, and shallow water clastic rocks of the Arroyo Blanco Formation. Note how the outcrop patterns of all three belts widen to the southeast in the direction of the Enriquillo basin. The highway we travel on across the uplifted Sierra Martin Garcia cuts obliquely across section and passes downward in section in the Trinchera Formation. We eventually come out on the carbonate basement of the “Sombrerito Formation” after passing through about 3 km of Trinchera Formation. The widening outcrop belts represent the filling of this part of the Azua-Enriquillo ramp basin by the major clastic wedge that originated by uplift of the Cordillera Central (Fig. 13B). An enigma is that the Charco Largo well drilled in the center of the Enriquillo basin only contains a few hundred meters of Trinchera Formation but a greatly expanded section of overlying clastic rocks and evaporites (Fig. 12A).

**Quita Coraza Formation.** This formation consists of 200 to 700 m of massive siltstones with rare interbeds of very thinly bedded turbiditic sandstone. The contact with the underlying Trinchera Formation is conformable and gradational and is placed at the highest thick-bedded turbiditic sandstone. Foraminifera show the Quita Coraza marks a brief 1 m.y. long transition from an outer to inner neritic setting of early Pliocene age (Fig. 22).

**Arroyo Blanco Formation.** This formation is about 700 m thick, conformably overlies the Quita Coraza Formation, and includes the stratigraphically highest rocks of the Azua basin (Fig. 22). The Arroyo Blanco Formation is a coarsening upward sequence that includes a growth position coral reef at its base and a shallow marine sandstone and conglomerate section near its top. Its transition to the overlying Arroyo Seco and Rio Via Formations is placed at the transition into non-marine sedimentation. Facies of the Arroyo Blanco Formation indicate conditions at its base was a clastic-dominated shelf with scattered coral reefs to an overlying coastal deltaic complex with thick, coarsening upward sequences made up of many individual, fining-upward cycles. Benthic foraminifera of the Arroyo Blanco Formation are typically inner shelf forms with water depths of less than 100 m and containing eel grass environments.

As we drive through the area and look at the rocks near the contact at **Stop 5**, try to identify the three major formations on both sides of the highway and where their contacts are found:

- **Examine the rocks on either side of the Quita Coraza-Arroyo Blanco contact:** what water depth and environmental changes are occurring and what are the possible tectonic and eustatic controls (cf. Fig. 14).
- **Examine the cyclic sedimentation in the lower Arroyo Blanco Formation:** What are some possible controls that could explain the vertical cycles and color changes?
- **Integrate observations with regional tectonics:** what regional tectonic event might be recorded by this vertical change in facies? Compare the vertical section seen in this outcrop with the paleogeographic map shown in Figure 15.

### Stratigraphy of the Trinchera Formation at Stop 6

As we drive south to Stop 6 we will pass very coarse deposits that represent inner submarine fan deposits formed by the filling of large submarine valleys. Look for truncations at the base of channels and composite channels formed by several nested channels. Foraminifera show that these rocks were deposited in the upper bathyal zone (about 200 m water depth). Rapid filling of the basin by this confined fan system (as suggested by paleocurrents that are uniform to the southwest) likely led to rapid infilling of the basin. Continuing southward and down section, we will pass into the inner fan environment characterized by more distal, parallel-sided and much thinner turbidites with occasional channel-fill turbidites. These rocks were deposited in the middle bathyal zone (about 1000 m water depth).

At stop 6, we will examine a channelized sandstone cut into finer grained turbidites.

- **Use a hand lens to identify grain types:** what can you say about the source area for the fan (Fig. 24B).
- **Examine the base of the coarser grained sandstone beds:** What is the paleocurrent direction (Fig. 23).
- **Integrate observations with regional tectonics:** what regional tectonic event might be recorded by this vertical change in facies? Compare the vertical section seen in this outcrop with the paleogeographic map shown in Figure 15.

### Stratigraphy of the Sombrerito-Trinchera transition at stop 7

We will continue to drive south and deeper into the late Miocene submarine fan. The facies change to very thinly bedded turbidites with an increasing shale component. This area would correspond to the basin plain that was deposited across the existing carbonate basin of the Sombrerito Formation. This same transition is recorded in the Charco Largo well to the west in the Enriquillo basin (Fig. 25A). Notice the thickening and coarsening upward cycles in this section that are common in outer fan environments (Fig. 24A). At this stop, focus on the following:

- **Use a hand lens to identify grain types:** what can you say about the source area for the fan; has it changed from Stops 5 and 6? (Fig. 24B).

- **Examine the base of the coarser grained sandstone beds:** What is the paleocurrent direction; has it changed from the previous stops? (Fig. 23).
- **Integrate observations with regional tectonics:** what regional tectonic event might be recorded by this vertical change in facies? Compare the vertical section seen in this outcrop with the paleogeographic map shown in Figure 15.

### **Homework assignment: Understanding the subsurface geology of the Enriquillo basin**

As we approach the hotel in Barahona, we will pause to view the low-lying entry to the Enriquillo Valley. This is the sill area that prevents the Caribbean Sea from transgressing into the sub-sea level valley. The well cross section in Figure 25A summarizes the abrupt thickness and facies changes seen in an east-west direction from the area of stop 7 to the west end of the Cul-de-Sac Valley of Haiti. The most remarkable change is the presence of 1.5 km of halite and gypsum in the Charco Largo well.

Your homework assignment for the first stop on Day Two is to present a plausible sequence of events to explain the relationships seen on the cross section of Figure 25A.

- **Hint:** Figure 25B provides three possible scenarios for the filling of the basin? What environmental conditions are needed to form the giant evaporite deposit?
- **Hint:** What is the paleocurrent direction; has it changed from the previous stops? (Fig. 23).
- **Hint:** Use the subsurface structural contour map of the Sombrerito “basement” unit to speculate on what is created the immense space that is filled by sediment and water in the Enriquillo Valley. Compare the seismic section in Figure 26B with the structure map in 26A. Speculate on what the play concept was for drilling the dry holes in the center of the basin. Give some possible reasons why these holes failed.
- **Hint:** Compare the subsidence curve in Figure 27C to the Charco Largo well in Figure 27A upon which it is based. What is the possible control on the rise and fall of subsidence from about 6 to 2 Ma?
- **Integrate observations with regional tectonics:** Compare the vertical section seen in Charco Largo well with the paleogeographic map shown in Figure 15. Why did over 3 km of submarine fan deposits never reach the Charco Largo area?

### ***Overnight in Barahona***

#### **Exposed evaporites along the southern margin of the Enriquillo basin (stop 8).**

Loma Sal y Yeso (“Salt and Gypsum Hill”) forms a low range of hills elevated by a combination of thrust faulting and salt diapirism between the Sierra de Bahoruco and the topographic depression of the Enriquillo basin (Fig. 28A, B, C). Loma Sal y Yeso is the only exposed salt-cored fold in the fold belt that runs along the mountain front and supports subsurface data showing that evaporites are restricted to a small area in the eastern Enriquillo basin.

At stop 8 we will examine the three major units that make up the hill and their deformational features. Unit 1 is a 200 m-thick strip of massive halite of the Angostura Formation (Fig. 14) that occurs as an elongate strip at the edge of the hill. Examine outcrops of the halite to identify fabrics, flow bands, small scale folds and interbedded mudstones. Unit 2 makes up most of the hill and is composed of about 350 m of massive bedded gypsum and interbedded siltstone of the Angostura Formation. Identify textures and deformation in this unit and speculate on how its environment might differ from that of the halite. Unit 3 is a 30 m thick section of “paper shale” and thin interbeds of siltstone. The paper shale is faulted against the halite. The paper shale contains rare fish fossils imprinted on bedding planes and is interpreted as an anoxic lake deposit. The basinward edge of the hill is marked by Razorback Ridge, a 3 m thick vertical bed of highly resistant limestone that marks the base of the Las Salinas Formation (Fig. 14). This limestone marks a marine transgression into the valley that terminated evaporate deposition. Overlying the limestone are ripple-marked sandstone beds recording low energy, near shore conditions in a shallow marine or lacustrine environment. Paleowave direction was ENE to WSW. Vertical worm burrows characteristic of intertidal or beach

environments are found in the rippled units. Higher in the section are fining upward sandstone bodies that record higher energy and deeper water conditions than the underlying rippled units.

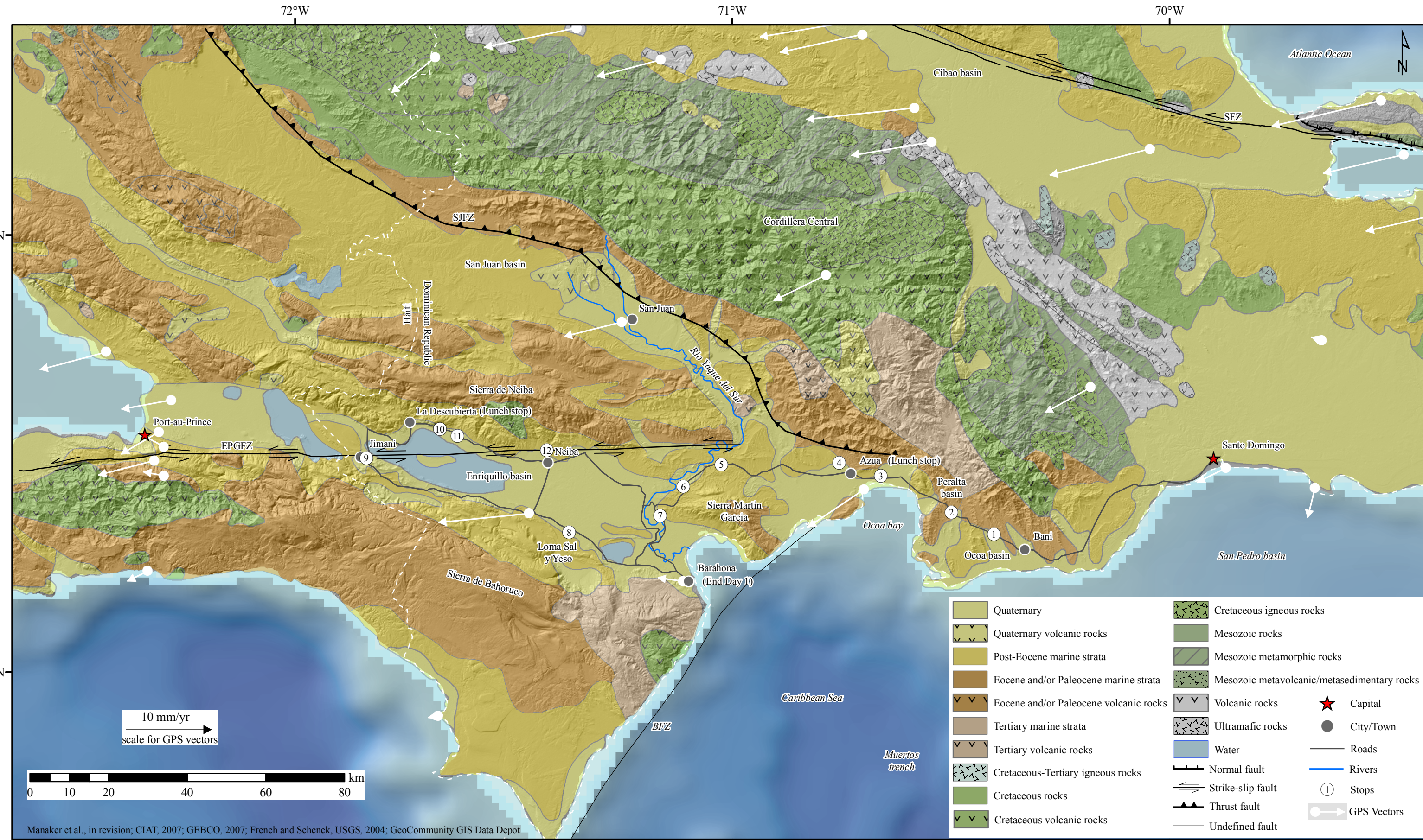
- **Use a hand lens to identify grain types:** what can you say about the source area for the fan; has it changed from the older Trinchera Formation?
- **Examine the base of the coarser grained sandstone beds:** How has the paleocurrent direction changed from the Trinchera Formation?
- **Summarize the vertical facies changes and compare to the paleogeographic map in Figure 15.** How can this information be used to distinguish the three basin-filling models shown on Figure 25B?
- **Integrate observations with regional tectonics:** what regional tectonic event might be recorded by this vertical change in facies? Compare the vertical section seen in this outcrop with the paleogeographic map shown in Figure 15.

## REFERENCES CITED

- Bermudez, P. J., 1943, Bermudez' report no. 32, Intercean no. 3 well, Azua province, unpublished report.
- Boardman, L. R., 1947, Geological report on Maleno well no. 7, Azua basin, Dominican Republic, unpublished report to Dominican Seaboard Oil Company, Ciudad Trujillo, Dominican Republic.
- Buitrago, J., 1994, Petroleum systems of the Neiva area, Upper Magdalena Valley, Colombia, in Magoon, L., and Dow, W., eds., *The Petroleum System – From Source to Trap*, AAPG Memoir 60, p. 483-497.
- DeMets, C., P. Jansma, G. Mattioli, T. Dixon, F. Farina, R. Bilham, E. Calais, and P. Mann, 2000, GPS geodetic constraints on Caribbean-North America plate motion, *Geophysical Research Letters*, v. 27, p. 437-440.
- Dohm, C. F., September 20, 1941a, The Comendador anticline, Republica Dominicana (unpublished Seaboard Dominicana office report no. 14), 10 p.
- Dohm, C. F., October, 1941b, Geologic map of aerial mosaic no. 15, Quita Coraza, Dominican Republic (unpublished Seaboard Dominicana map, approximate scale 1:20,000).
- Dohm, C. F., 1941c, Geologic map of aerial mosaic no. 14, El Mogote, Dominican Republic (unpublished Seaboard Dominicana map, approximate scale 1:20,000).
- Dolan, J. F., Mann, P., de Zoeten, R., Heubeck, C., Shiroma, J., and Monechi, S., 1991, Sedimentologic, stratigraphic, and tectonic synthesis of Eocene-Miocene sedimentary basins, Hispaniola and Puerto Rico, in Mann, P., Draper, G., and Lewis, J., eds., *Geologic and Tectonic Development of the North America-Caribbean Plate Boundary*, Geological Society of America Special Publication 262, p. 217-263.
- Dolan, J. F., Mullins, H., and Wald, D., 1998, Active tectonics of the north-central Caribbean region: Oblique collision, strain partitioning, and opposing slabs, in Dolan, J., and Mann, P., eds., *Active Strike-slip and Collisional Tectonics of the Northern Caribbean Plate Boundary Zone*, Geological Society of America Special Paper 326, p. 1-61.
- Eicher, D. B., 1943a, Maleno well no. 3, Azua province, Dominican Republic, unpublished well log, Dominican Seaboard Company.
- Eicher, D. B., 1943b, Maleno well no. 6, Azua province, Dominican Republic, unpublished well log, Dominican Seaboard Company.
- Electroconsult, 1984, Unpublished report for the Yayas-Constanza Project, Dirección General de Minería, 27 p.
- Fenoglio, A. F., 1958, Petrolera Azuana, C. por A. (Maleno-2), unpublished well report, Petrolera Azuana, Ciudad Trujillo (Santo Domingo), Dominican Republic.
- Gabb, W. M., 1872, On the occurrence of petroleum on the island of Santo Domingo: American Journal of Science and Arts, v. 3, no. 18, New Haven, Connecticut.
- Guerra Peña, F., 1956, Las principales cuencas sedimentarias de la Republica Dominicana y sus posibilidades petroliferas: Symposium sobre Yacimientos de Petroleo y Gas, Tomo IV, XX Congreso Geológico International, Mexico City, Mexico.

- Harms, F. J., 1989, Konglomeratisches Jungtertiär im Valle de San Juan (südwestliche Dominikanische Republik, Grosse Antillen): Zusammensetzung, Herkunft, und Alter der Gerölle, Fazies [unpublished Ph.D. thesis]: Hanover, West Germany, University of Hannover, 141 p.
- Haq, B., Hardenbol, J., and Vail, P., 1987, Chronology of fluctuating sea levels since the Triassic: Science, v. 235, p. 1156-1167.
- Heubeck, C., Mann, P., Dolan, J., and Monechi, S., 1991, Diachronous uplift and recycling of sedimentary basins during Cenozoic tectonic transpression, northeastern Caribbean plate boundary: Sedimentary Geology, v. 70, p. 1-32.
- Heubeck, C., and Mann, P., 1991, Structural geology and Cenozoic tectonic history of the southeastern termination of the Cordillera Central, Dominican Republic, in Mann, P., Draper, G., and Lewis, J. F., *Geologic and tectonic development of the North America-Caribbean plate boundary in Hispaniola*, Geological Society of America Special Paper, p. 315-336.
- Heubeck, C., 1992, Sedimentology of large olistoliths, southern Cordillera Central, Hispaniola, Sedimentology, v. 67, p. 474-482.
- Jansma, P., Lopez, A., Mattioli, G., DeMets, C., Dixon, T., Mann, P., and Calais, E., 2000, Neotectonics of Puerto Rico and the Virgin Islands, northeastern Caribbean from GPS geodesy: Tectonics, v. 19, p. 1021-1037.
- Ladd, J., Shih, T., and Tsai, C., 1981, Cenozoic tectonics of central Hispaniola and adjacent Caribbean Sea: AAPG Bulletin, v. 65, p. 466-489.
- Llinas, R.A., 1972, Geología del área Polo-Duverge, Cuenca de Enriquillo, Codia: Publication of Colegio Dominicano de Ingenieros, Arquitectos, y Agrimensores (Santo Domingo, Dominican Republic, Part 1 in No. 31, p. 55-65, and Part 2 in No. 32, p. 40-53.
- Mann, P., McLaughlin, P. P., Jr., and Cooper, J. C., 1991a, Geology of the Enriquillo-Azua basins, Dominican Republic, 2: Structure and tectonics, in Mann, P., Draper, G., and Lewis, J. F., *Geologic and tectonic development of the North America-Caribbean plate boundary in Hispaniola*, Geological Society of America Special Paper, p. 367-389.
- Mann, P., Draper, G., and Lewis, J. F., 1991b, An overview of the geologic and tectonic development of Hispaniola, in Mann, P., Draper, G., and Lewis, J. F., *Geologic and tectonic development of the North America-Caribbean plate boundary in Hispaniola*, Geological Society of America Special Paper, p. 1-28.
- Mann, P., and Lawrence, S., 1991, Petroleum potential of southern Hispaniola: Journal of Petroleum Geology, v. 14, p. 291-308.
- Mann, P., 1999a, Caribbean sedimentary basins: Classification and tectonic setting from Jurassic to Present: in Mann, P., ed., *Caribbean Basins, Sedimentary Basins of the World* (series editor, K. Hsu), Elsevier, p. 3-31.
- Mann, P., McLaughlin, P., van den Bold, W., Lawrence, S., and Lamar, M., 1999b, Tectonic and eustatic controls on Neogene evaporitic and siliciclastic deposition in the Enriquillo basin, Dominican Republic: in Mann, P., ed., *Caribbean Basins, Sedimentary Basins of the World* (series editor, K. Hsu), Elsevier, p. 287-342.
- Mann, P., Calais, E., Ruegg, J-C., DeMets, C., Jansma, P., and Mattioli, G., 2002, Oblique collision in the northeastern Caribbean from GPS measurements and geological observations: Tectonics.
- McLaughlin, P. P., Jr., 1989, Neogene planktonic foraminiferal biostratigraphy of the southwestern Dominican Republic: Journal of Foraminiferal Research, v. 19, p. 294-310.
- McLaughlin, P. P., Jr., 1991, Migration of Neogene marine environments, southwestern Dominican Republic: Geology, v. 19, p. 222-225.
- McLaughlin, P. P., Jr., van den Bold, W. A., and Mann, P., 1991, Geology of the Enriquillo-Azua basins, Dominican Republic, 2: Foraminiferal/ ostracode biostratigraphy and depositional history in Mann, P., Draper, G., and Lewis, J. F., *Geologic and tectonic development of the North America-Caribbean plate boundary in Hispaniola*, Geological Society of America Special Paper, p. 337-366.
- McLaughlin, P. P., Jr., and Sen Gutpa, B. K., 1994, Benthic foraminiferal record in the Miocene-Pliocene sequence of the Azua basin, Dominican Republic: Journal of Foraminiferal Research, v. 24, p. 75-109.

- Moiola, R. J., 1989, Technical service job no. 506-7996, Geochemical analysis of DSDP cores, Leg 15, and outcrop samples, Dominican Republic, unpublished report, Mobil.
- Nelson, P. H., 1862, A report on the oil prospects of the Dominican Republic, Western Natural Gas Company, Houston, Texas (unpublished report).
- Nemec, M., 1980, A two-phase model for the tectonic evolution of the Caribbean, Transactions of the 9<sup>th</sup> Caribbean Geological Conference, Santo Domingo, Dominican Republic, p. 23-38.
- Norconsult, 1983, Dominican Republic Petroleum Exploration Appraisal (volume 1), Norconsult internal report, Sandvika, Norway, 79 p.
- Tissot, B., and Welte, D., 1984, *Petroleum Formation and Occurrence*, Springer-Verlag, Berlin.
- Tucker, P. M., September, 1945, Results of the gravity meter and vertical magnetometer survey of the San Juan and Azua basins, Dominican Republic (Santo Domingo office report no. 40), 8 p.
- Vaughan, T. W., and five others, 1921, *A geological reconnaissance of the Dominican Republic*: Washington, D. C., Gibson Brothers, 267 p.
- Vespucci, P., 1980, Preliminary account of the petrology of the late Cenozoic volcanic province of Hispaniola, Transactions of the 9<sup>th</sup> Caribbean Geological Conference, Santo Domingo, Dominican Republic, p. 379-389.
- Woodring, W., Brown, J., and Burbank, W., 1924, *Geology of the Republic of Haiti*: Baltimore, Maryland, The Lord Baltimore Press, 631 p.



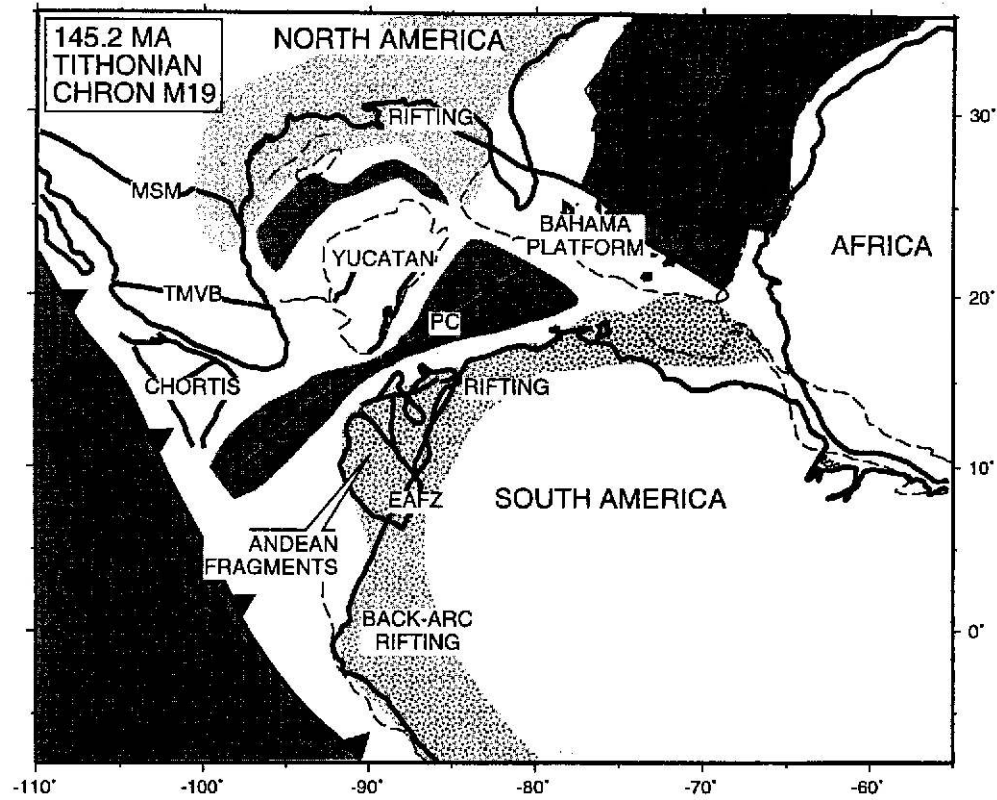


Figure 2A. Reconstruction of the Caribbean region at 45 Ma (Tithonian, magnetic anomaly M19). Dots in Atlantic Ocean represent magnetic anomaly and fracture zone picks by Müller et al. (1999) based on interpretation of Geosat gravity images. Key to abbreviations: PC=proto-Caribbean oceanic crust (dark line represents speculative position of spreading ridge); MSM=Mohave-Sonora megashear; TMVB=Trans-Mexican volcanic belt; EAFZ=Eastern Andean fault zone.

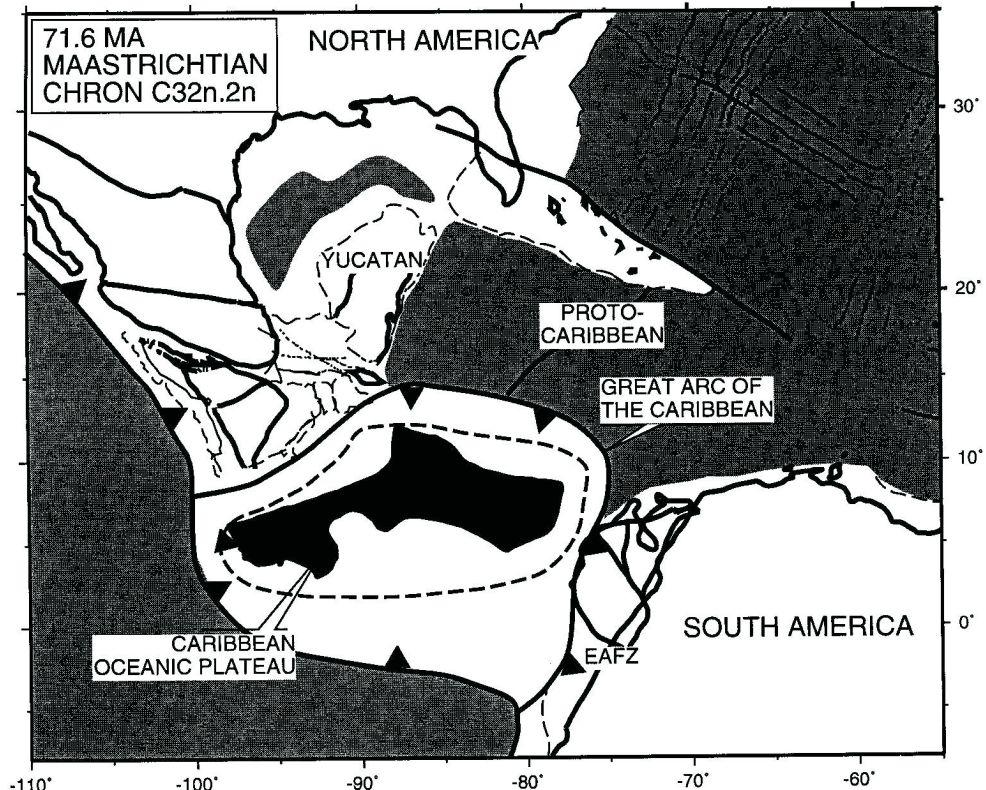


Figure 2B. Reconstruction of the Caribbean region at 71 Ma (Maastrichtian, magnetic anomaly C32n.2n). Key to abbreviation: EAFZ=Eastern Andean fault zone.

From Mann (1999)

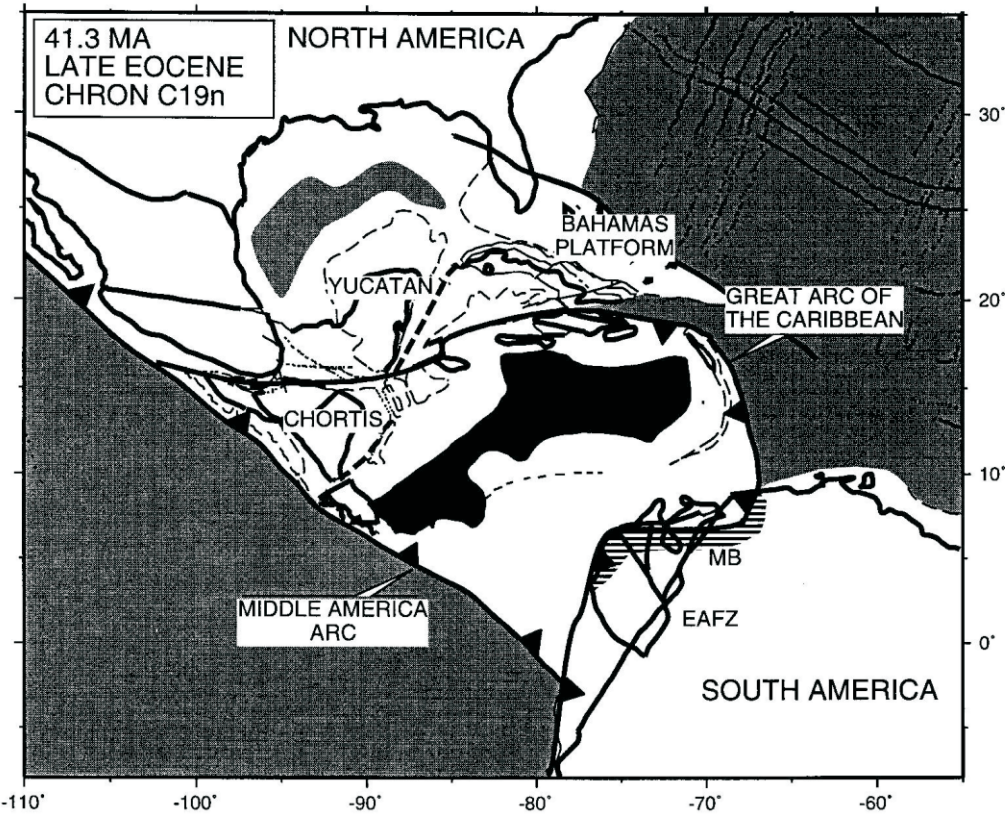


Figure 2C. Reconstruction of the Caribbean region at 41.3 Ma (Middle Eocene, magnetic anomaly C19n). Key to abbreviations: MB=Maracaibo foreland basin; EAFZ=Eastern Andean fault zone.

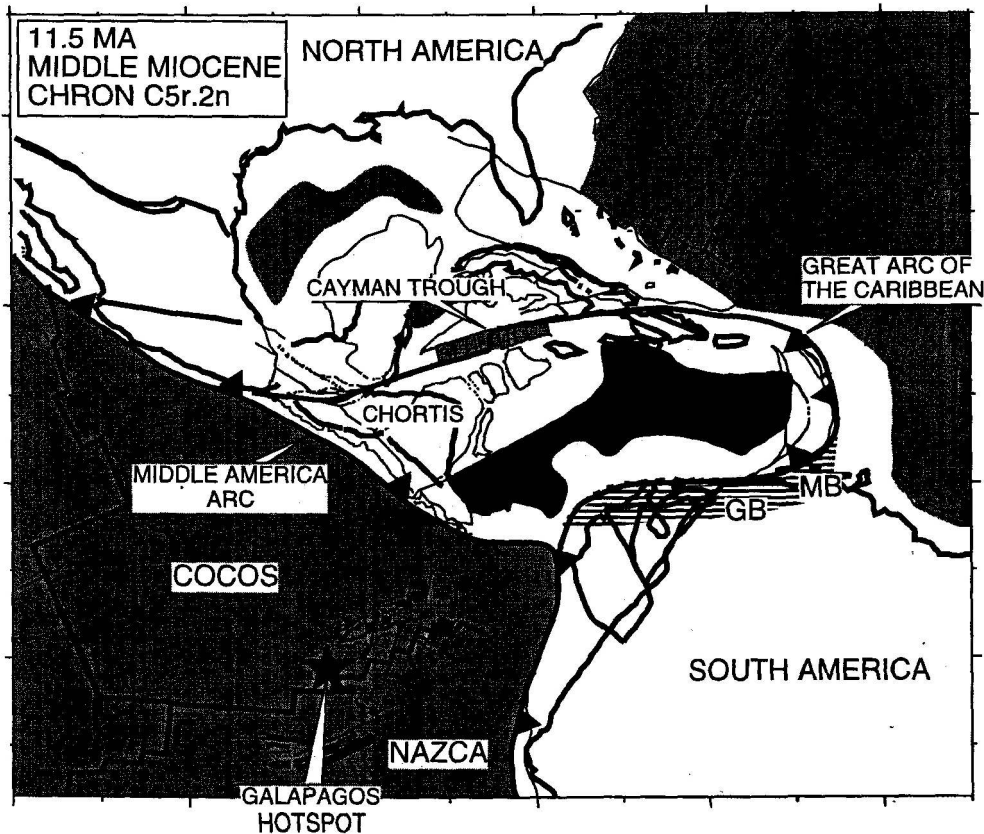


Figure 2D. Reconstruction of the Caribbean region at 11.5 Ma (latest Middle Miocene, magnetic anomaly C5r.2n). Key to abbreviations: GB=Guárico foreland basin; MB=Maturín foreland basin.

From Mann (1999)

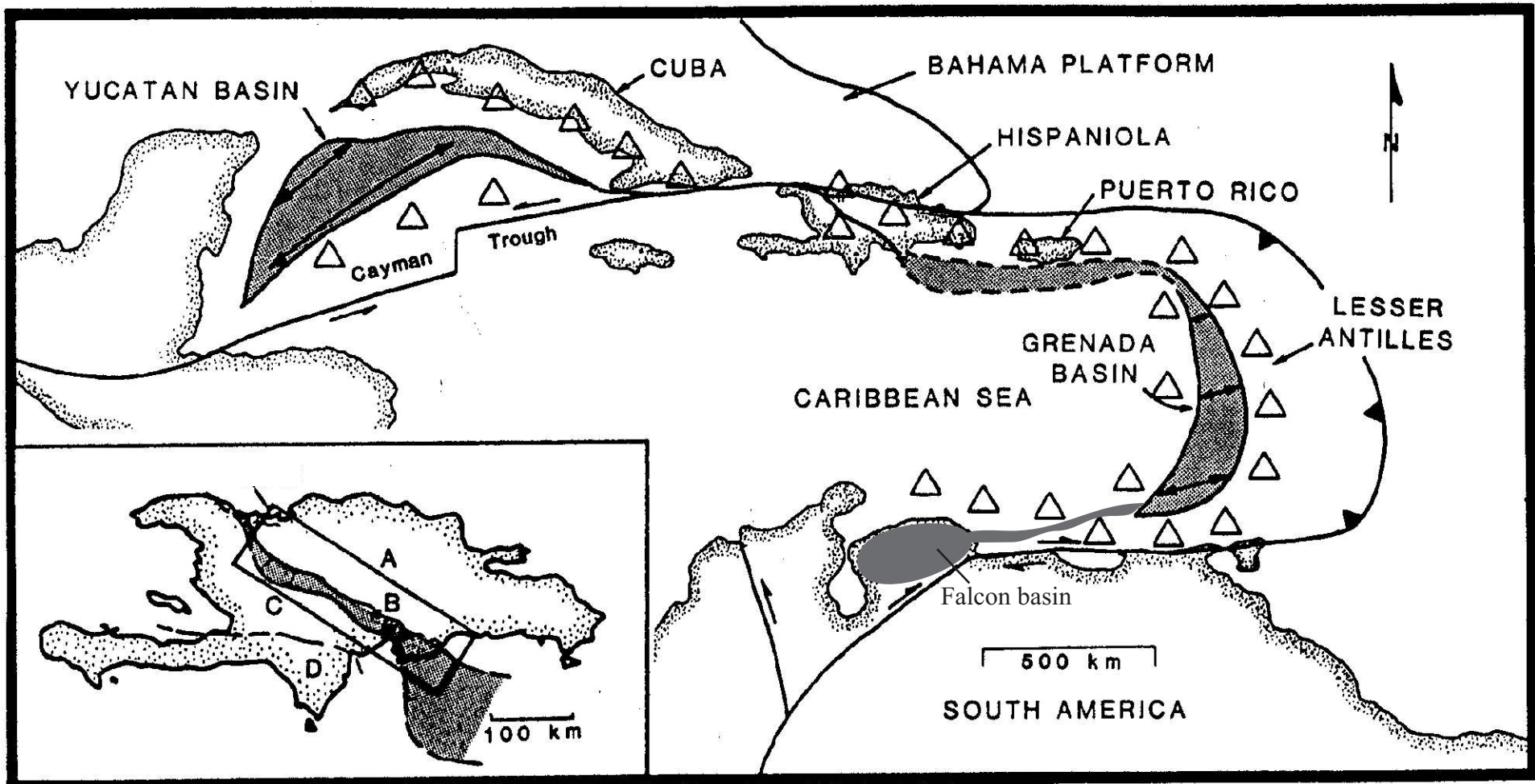


Figure 3. The basement of much of Hispaniola is composed of Cretaceous-Eocene island arc rocks formed along the “Great Caribbean Arc” (marked by triangles). Back-arc rifting in the Yucatan and Grenada basins (shaded in grey) split the arc along much of its length during Paleogene (?) time (arrows show interpreted direction of opening). We propose that the Peralta-Rio Ocoa belt in central Hispaniola is the shortened and uplifted remnant of a once continuous back-arc basin which connected the Yucatan and Grenada basins. The dashed continuation of the back-arc basin to the south of Puerto Rico and eastern Hispaniola is speculative. Eocene-Recent oblique closure of the Hispaniola segment of the back-arc basin is contemporaneous with the opening of the Cayman Trough, a pull-apart basin formed at a left step in the strike-slip fault separating the North America and Caribbean plates. Inset map shows four geologic provinces of Hispaniola: A=Cretaceous island arc basement of central and northeastern Hispaniola; B=Late Cretaceous-Pleistocene Peralta-Rio Ocoa belt and projected offshore extension (shaded in grey); C=Eocene remnant arc of Hispaniola; D=Late Cretaceous-Eocene oceanic plateau of southwestern Hispaniola.

From Huebeck et al. (1991)

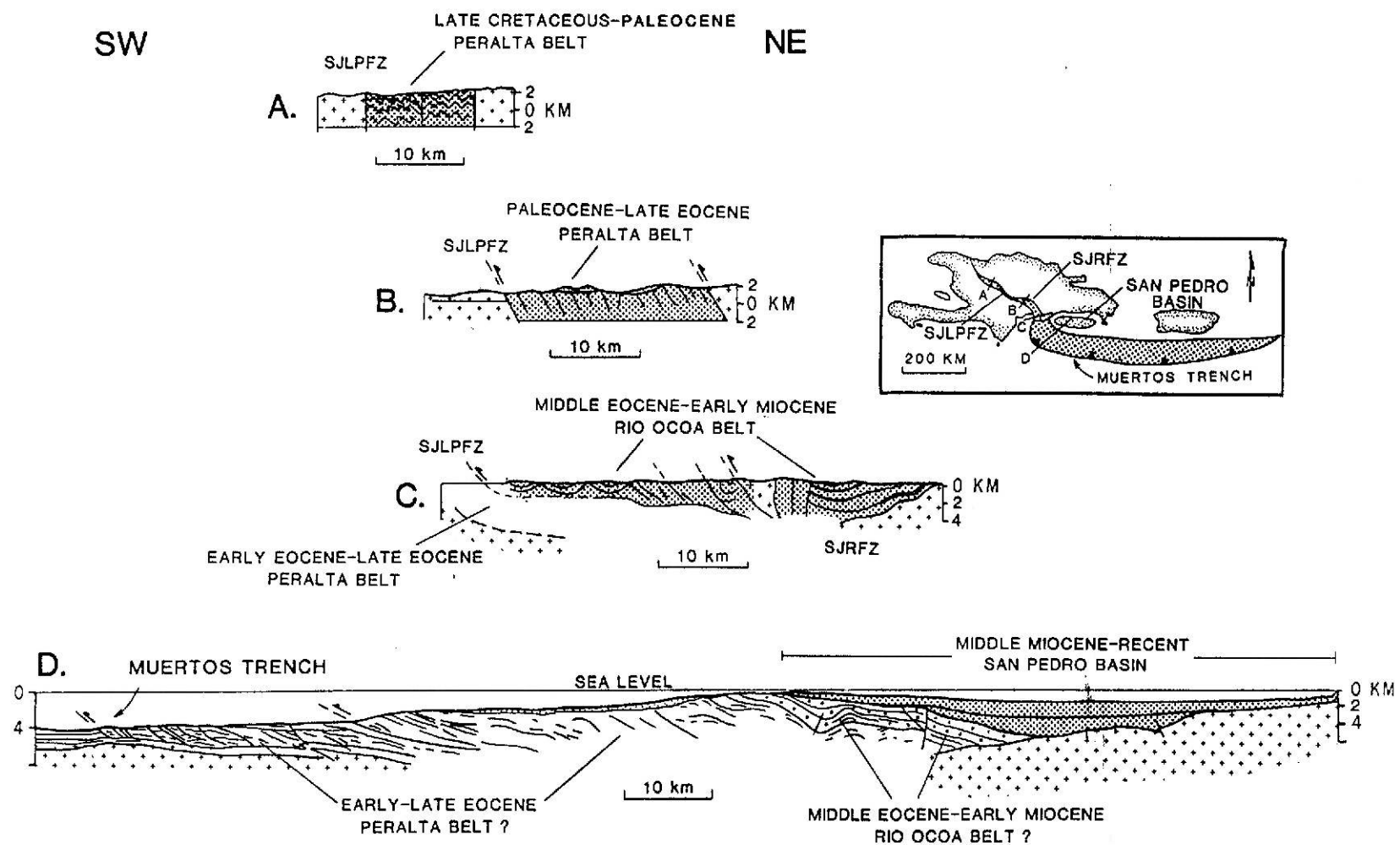


Figure 4. Regional cross-sections across the Peralta-Rio Ocoa belt. Sources of data are as follows: section A from Boisson (1987); section B from Lewis et al. (1983); section C from Huebeck (1988) and Huebeck and Mann (1991); section D from Biju-Duval et al. (1983). In the uncollided southeastern part of the belt, adjacent to the offshore Muertos trench, we speculate on the subsurface position of older, buried basin generations known from onland studies in the Peralta-Rio Ocoa belt.

From Huebeck et al. (1991)



Figure 5A. Location map of Hispaniola and Puerto Rico with the four major Paleogene sedimentary belts discussed shown in black.

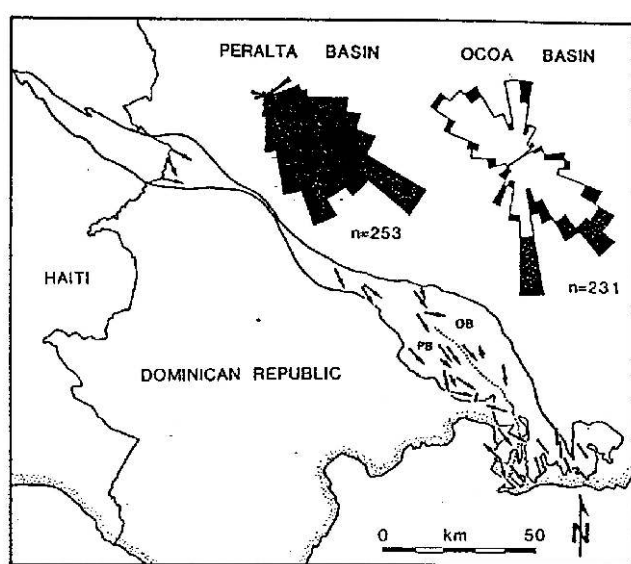


Figure 5B. Schematic map of the Peralta belt showing paleocurrent site means and rose diagrams from both the Peralta and Ocoa basins. In rose diagrams unidirectional indicators are shown in black; bidirectional indicators are unpatterned.

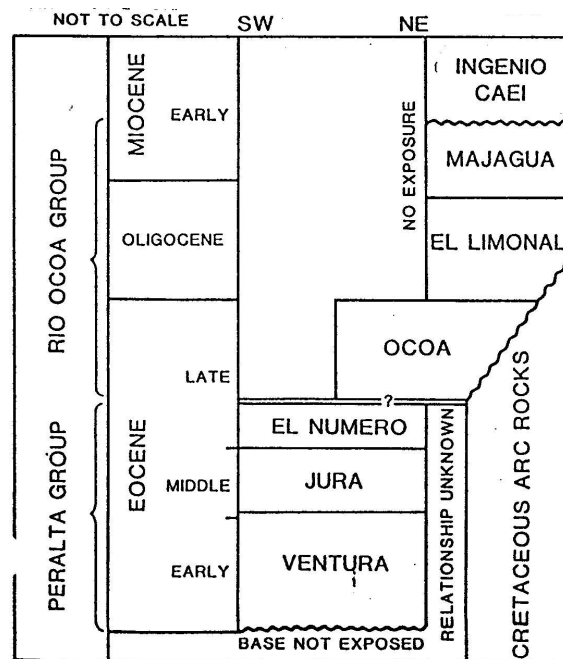


Figure 5C. Schematic stratigraphic correlation chart for the Peralta belt.

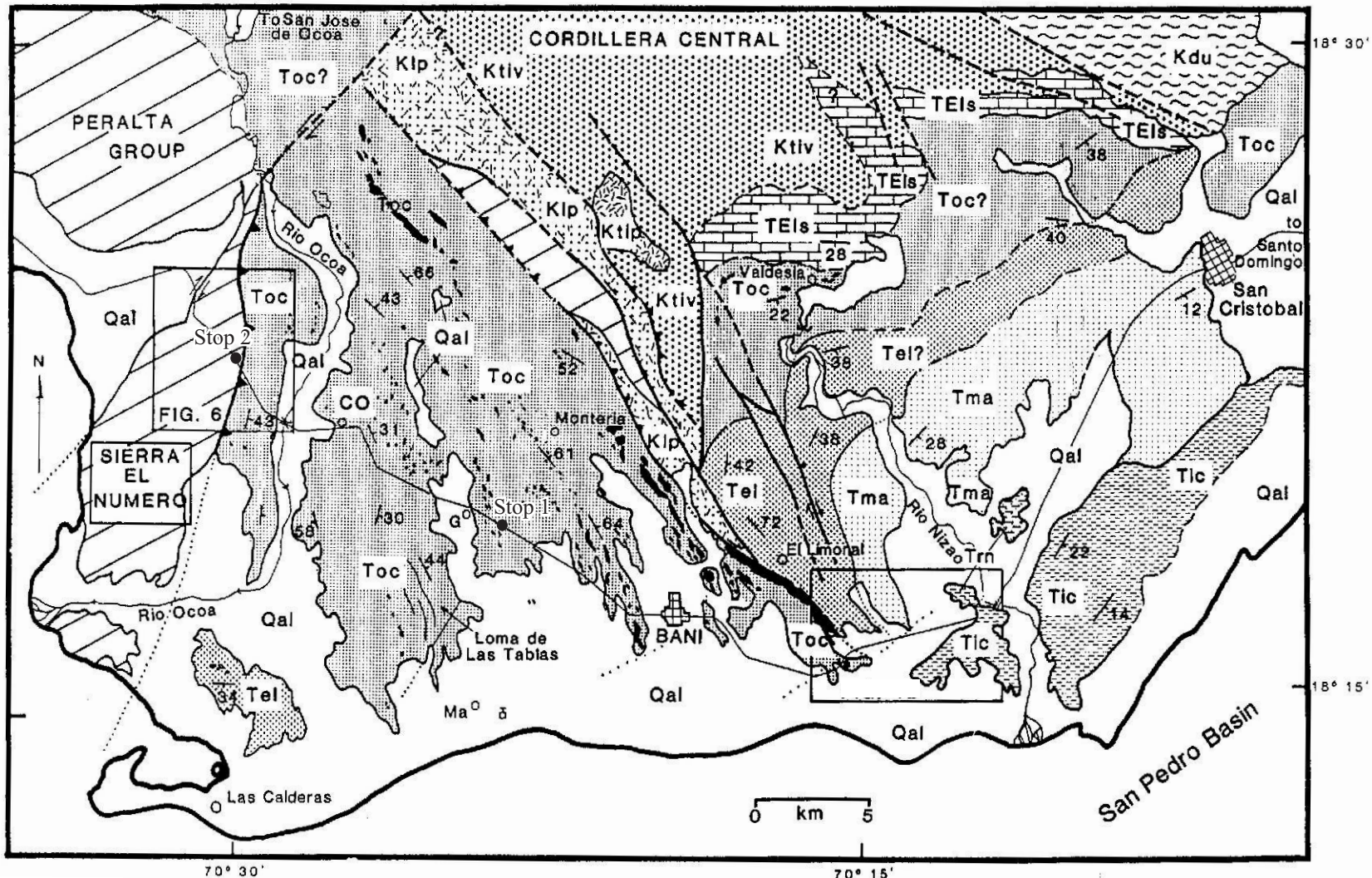


Figure 6. Geologic compilation of the southeastern Peralta-Rio Ocoa belt, Dominican Republic, based on detailed 1:25,000 scale map of Heubeck (1988), published maps by Bijuduval et al. (1983), Dominguez (1987) and Bowein (1966), and unpublished mapping by Mann. Location of map area in relation to the rest of the Peralta-Rio Ocoa belt is shown in Figure 2. Three superimposed, unconformity-bounded sedimentary sequences (Peralta, Rio Ocoa, and Ingenio Caei Groups) of Late Cretaceous to Recent age fringe the Cretaceous-Eocene island arc basement exposed at the southeastern termination of the cordillera Central. Boxes indicate the location of detailed maps of basal unconformities separating the Peralta and Rio Ocoa Groups (Figure 6) and the Rio Ocoa and Ingenio Caei Groups (Figure 12). Large, mostly limestone olistoliths within the Rio Ocoa Formation are shown in black. Key to abbreviations of villages: Ma=Matanzas, G=Galeón, CO=Crucé de Ocoa.

From Huebeck et al. (1991)

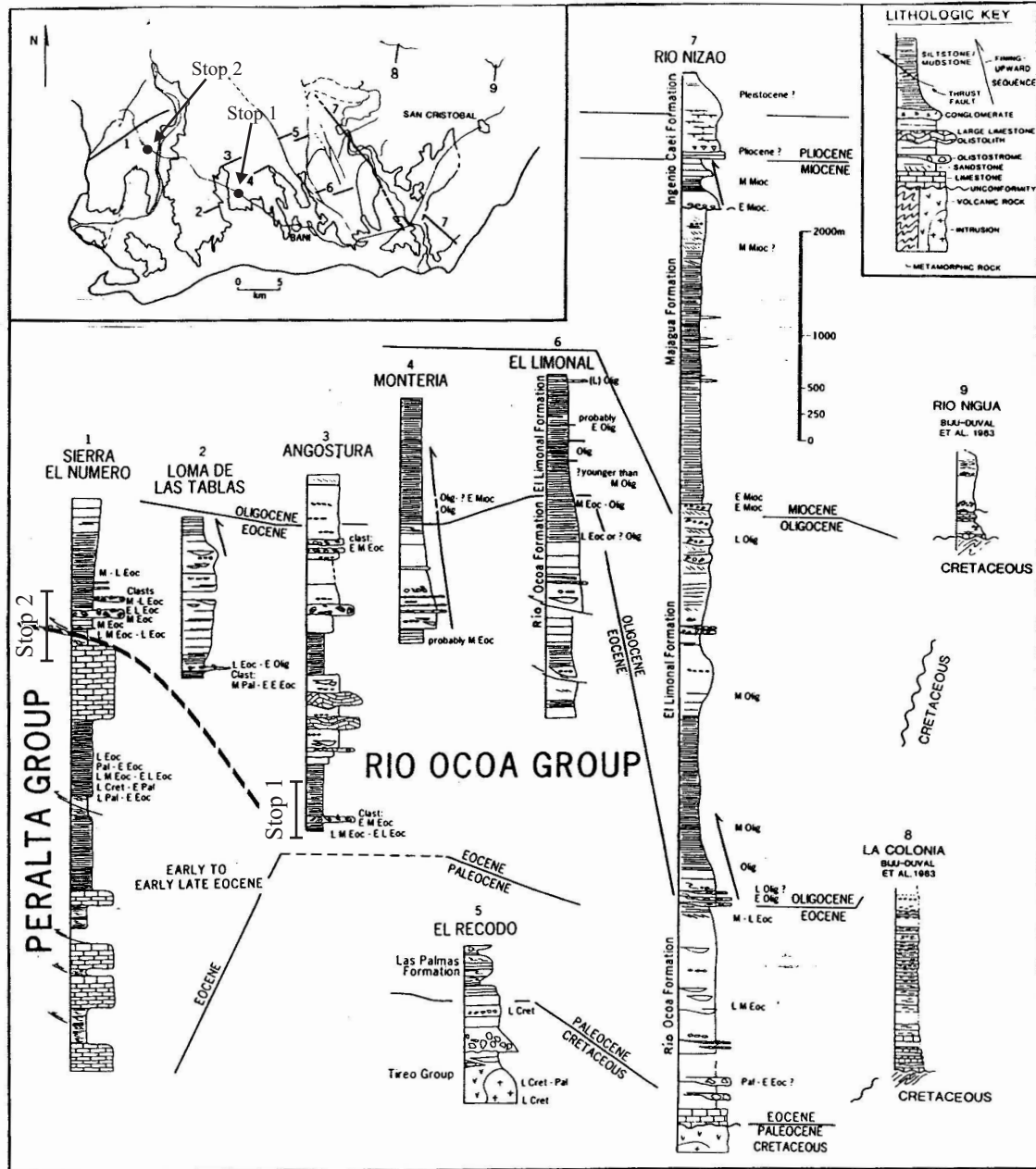


Figure 7A. Stratigraphic columns from the southeastern Peralta-Rio Ocoa belt from the Sierra El Numero in the west to the San Cristobal area in the east. Location of sections and lithologic key are shown in inset maps. Location of time lines is based on micropaleontological data discussed in text and shown to right of columns. Sections 1-7 are from Heubeck (1988) and Mann (unpublished data); sections 8 and 9 are from Biju-Duval et al. (1983).

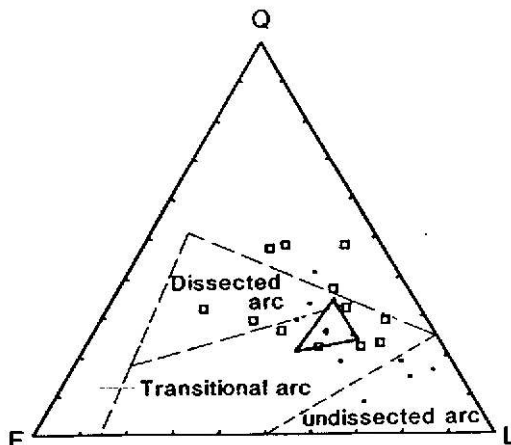


Figure 7B. Triangular diagram showing quartz-feldspar-lithic (QFL) composition of 19 sandstones from the Rio Ocoa Formation. Outline of tectonic provinces from Dickinson et al. (1983). Open squares and dots represent samples from measured sections near the village of Montería and Loma de Las Tablas (see Figure 4 for place localities; see Heubeck, 1988, for precise locations of sandstone samples). Small, solid triangle represents 2-sigma confidence limits of the mean sample composition, following the procedure of van der Plas and Tobi (1965).

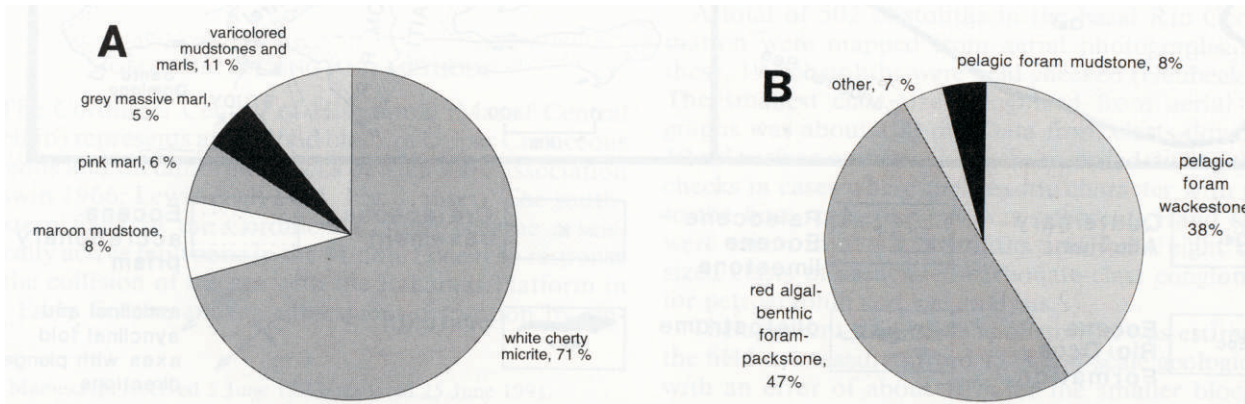


Figure 8A. Pie diagrams of olistolith lithology. A) Outcrop lithology of 181 olistoliths. B) Thin section lithology of 40 olistoliths. Note the strong bimodality, defined by a packstone and by a wacke-/mudstone.

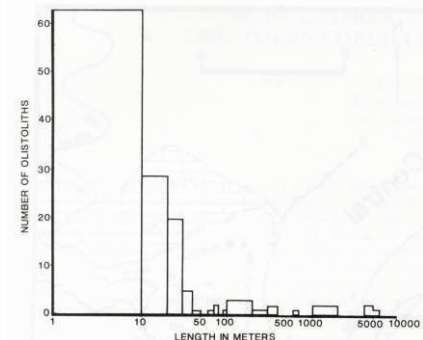


Figure 8B. Log-normal histogram showing the apparent maximum length of 1356 olistoliths. Six slide blocks exceed 1 km in length. Blocks with lengths between 10 and 50 m are common.

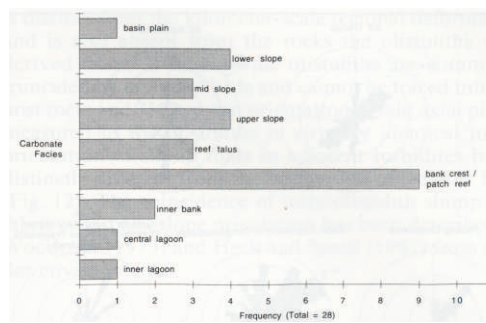


Figure 8C. Carbonate facies histogram of 28 olistoliths. The facies distribution is dominated by a shallow-water bank margin association. Slope and basin plain deposits are common; inner platform deposits (bank and lagoon) are rare.

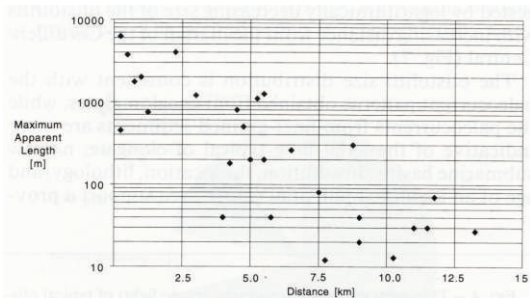


Figure 8D. Log-normal scatter-plot of olistolith size plotted against distance from the margin of the Cordillera Central. The well-defined logarithmic decrease in size with increase in distance strongly suggests a provenance from the Cordillera Central. Distance measurements are not corrected for an estimated 25% shortening perpendicular to strike because other, potentially more significant factors (paleotopography, slope steepness, clast shape) cannot be adequately accounted for.

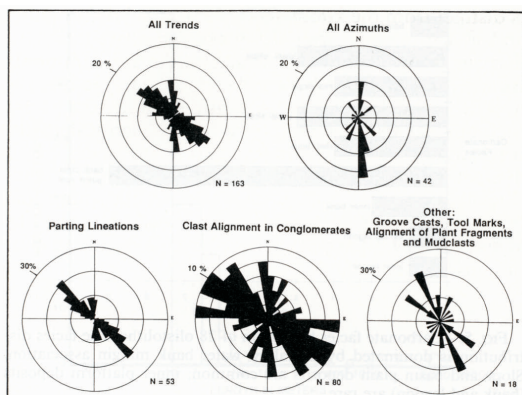


Figure 8E. Paleocurrent rose diagrams from the turbidites and debris flows of the Rio Ocoa Formation, host rock to the olistoliths. The coarse clastic deposits show, in contrast to the paleocurrents of the finer-grained deposits, a well-developed bimodality, supporting a partial derivation of the conglomerates and olistoliths from the Cordillera Central (from Heubeck et al. 1991).

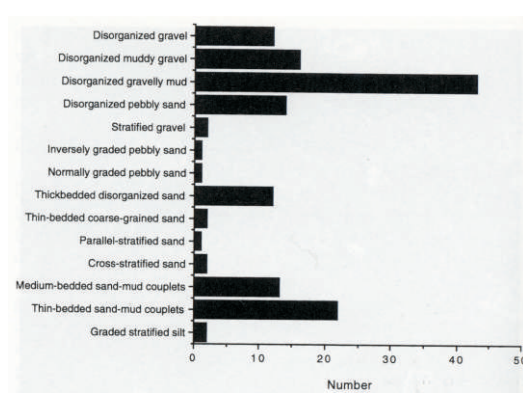


Figure 8F. Host rock lithology adjacent to 142 olistoliths. Classification of clastic sediment type after Pickering et al. (1986). The slide blocks are preferentially associated with gravelly muds, interpreted as products of debris flows or with thin-bedded sand-mud couplets, interpreted as mid-fan turbidites. Most likely, olistoliths were transported by debris flows of varying thickness; their protruding tops were later covered by turbidites.

From Huebeck (1992)

## GEOLOGY OF THE NORTHERN SIERRA EL NUMERO

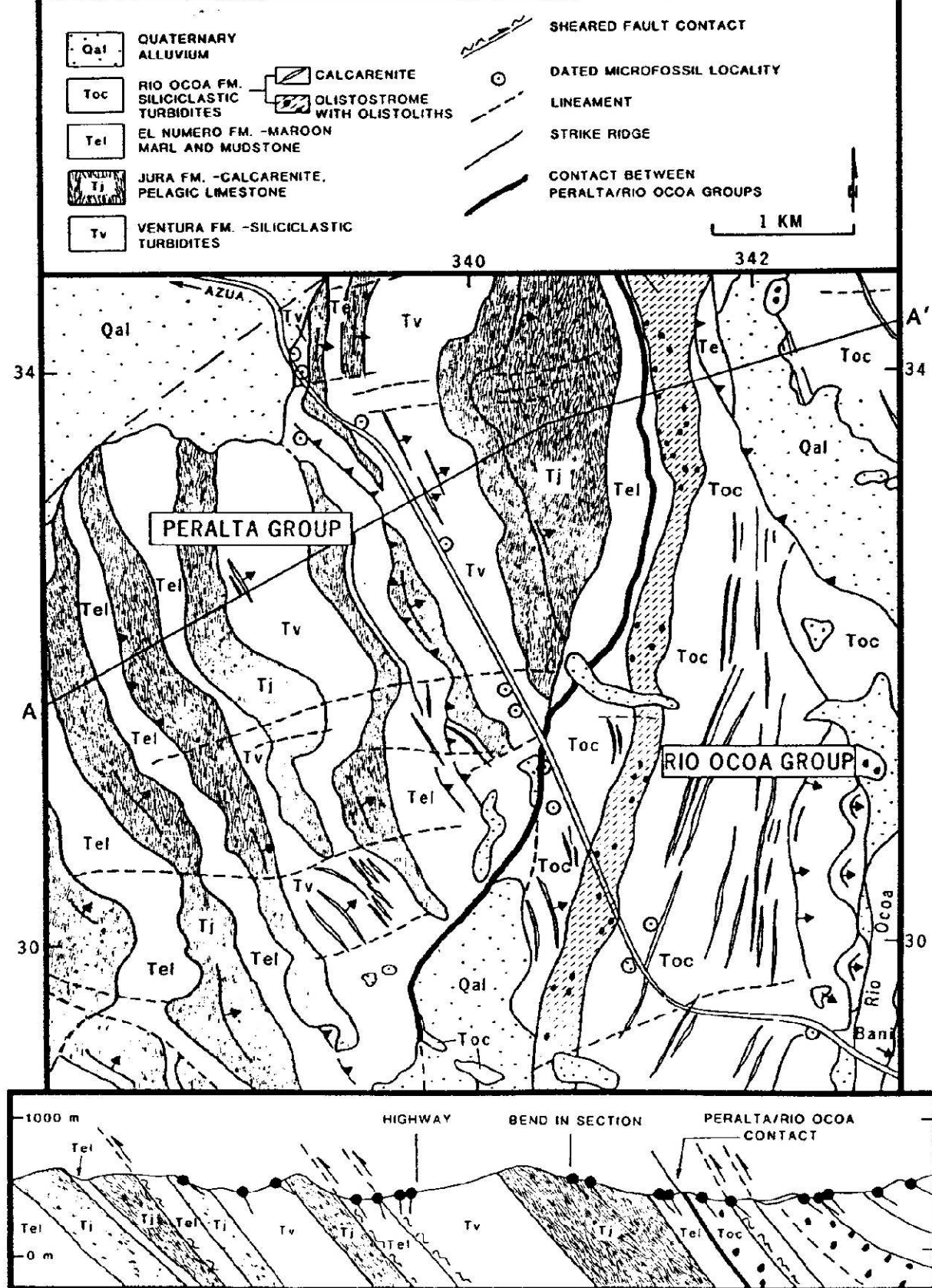


Figure 9. Geologic map of the faulted unconformity separating the Peralta and Rio Ocoa Groups in the Sierra El Numero based on unpublished 1:25,000 scale mapping by Mann. Location of map area is indicated on Figure 6.

From Huebeck et al. (1991)

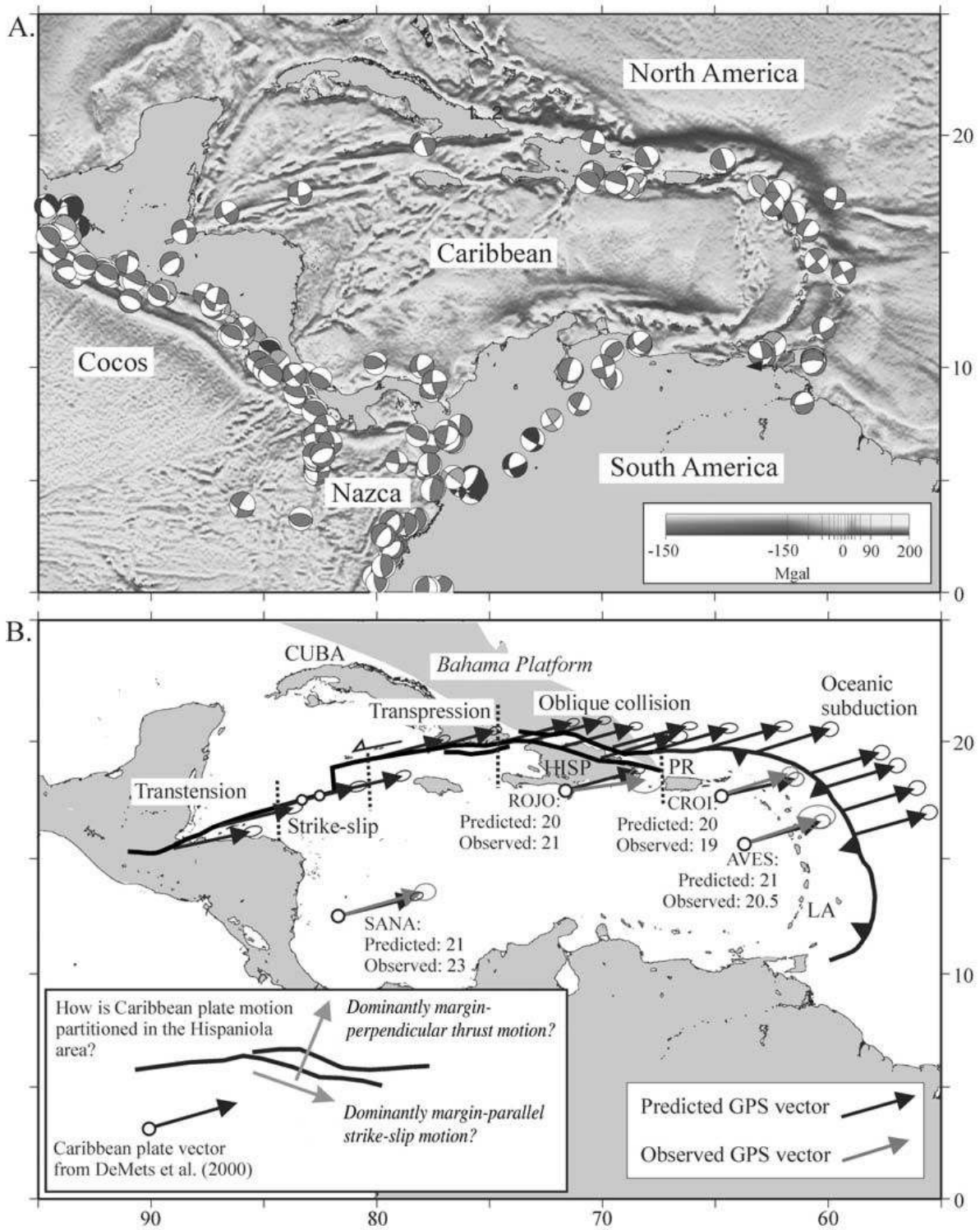


Figure 10A. Major plates of the Caribbean region and compilation of earthquake focal mechanisms showing present-day plate kinematics. Base map is a satellite-derived gravity map of the Caribbean compiled by Sandwell and Smith (1997). B. Caribbean-North America velocity predictions of DeMets et al. (2000) (black arrows) based on GPS velocities at four sites in the stable interior of the plate (light grey vectors) and two fault strike measurements in the strike-slip segment of the North America-Caribbean boundary (open circles). The predicted velocities are consistent with the along-strike transition in structural styles from transtension in the northwestern corner of the plate to oblique collision between the Caribbean plate in the Hispaniola (HISP) and Puerto Rico (PR) region and the Bahama Platform. One of the main objectives of GPS-based geodesy is to determine how this motion is partitioned into margin-parallel strike-slip and margin-perpendicular thrust motions as shown in the inset diagram.

From Mann et al. (2002)

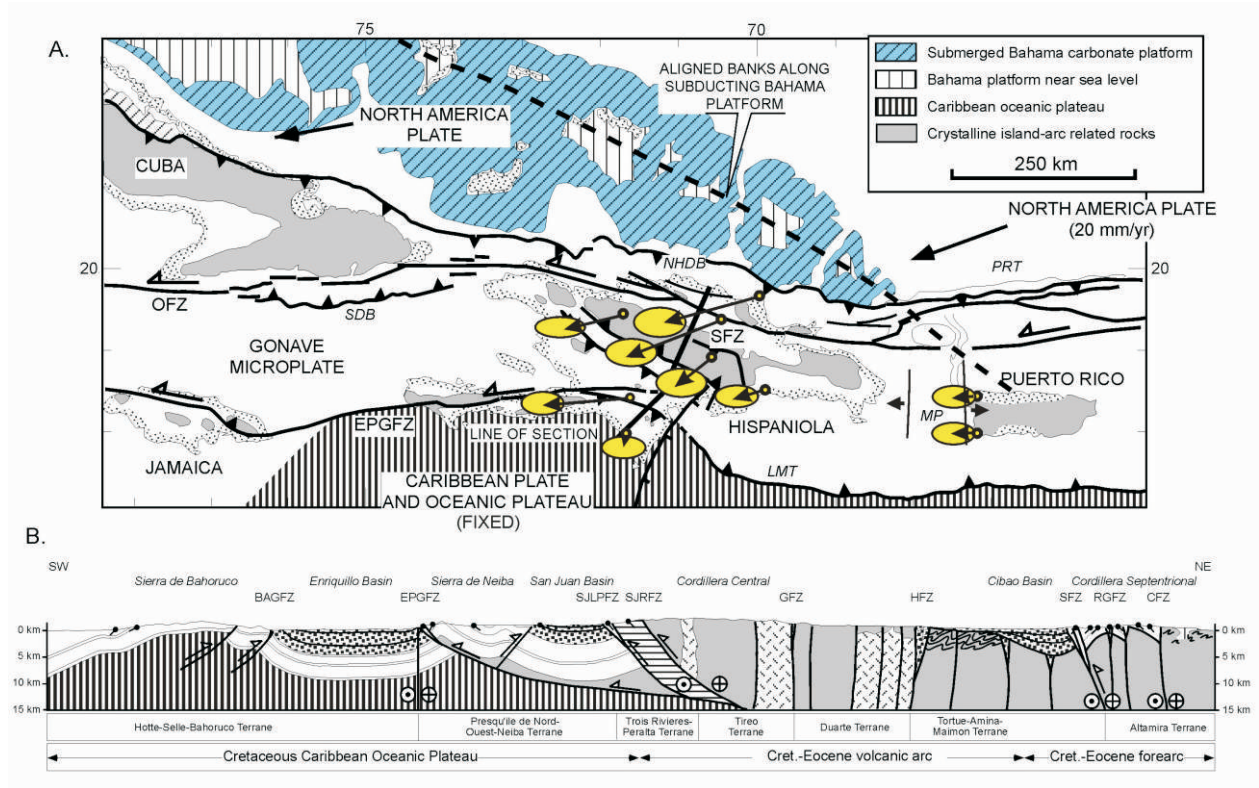


Figure 11. A. Map of the northeastern Caribbean plate margin modified from Dolan et al. (1998). Crystalline basement rocks represent the exhumed core of the Caribbean island arc that became inactive in Eocene to Oligocene time in this area. Rocks of the Bahamas carbonate platform on the North America plate north of Hispaniola are part of a passive-margin sequence formed following the Mesozoic rifting of North and South America. Rocks of the Caribbean plate mainly formed as part of a Pacific-derived oceanic plateau in Late Cretaceous time. Arrows with yellow ellipses represent observed GPS velocities for sites in Hispaniola relative to the Caribbean plate (modified from Mann et al., 2002). Convergence and southwestward-directed backthrusting of Hispaniola over the Caribbean plate is related to the local impedance of the eastward migration of the Caribbean plate by the salient of the Bahamas platform. The crustal thickness of the Caribbean oceanic plateau south of Hispaniola varies significantly in an east-west direction adjacent to Hispaniola and probably plays an important role in the deformation of the obliquely convergent deformation of Hispaniola. Key to abbreviations: LMT = Los Muertos trench; EPGFZ = Enriquillo-Plantain Garden fault zone; PRT = Puerto Rico trench; SFZ = Septentrional fault zone; NHDB = North Hispaniola deformed belt; OFZ = Oriente fault zone; SDB = Santiago de los Caballeros de la Sierra fault zone; MP = Mona Passage. B. Regional cross section across Hispaniola modified from Mann et al. (1991b). Convergence between the Bahamas Platform and the Caribbean oceanic plateau across the island of Hispaniola has led to extreme topographic uplift, erosion of the extinct arc core, and formation of three Neogene thrust-bound ramp basins: the Enriquillo, San Juan and Cibao. Vectors with error ellipses show motion of areas in Hispaniola relative to a fixed Caribbean plate (from Mann et al., 2002). Southwestward motion of Hispaniola is an expression of backthrusting of the area as a result of oblique collision with the Bahama Platform. Puerto Rico is not colliding with the Bahama Platform and shows no significant relative motion with the Caribbean plate. Rifting in the Mona Passage (MP) allows Hispaniola to respond independently of Puerto Rico. The hydrocarbon-bearing Azua basin discussed in this paper is the southeastern extension of the San Juan basin in south-central Dominican Republic and has undergone late Neogene southwestward-directed thrust faulting.

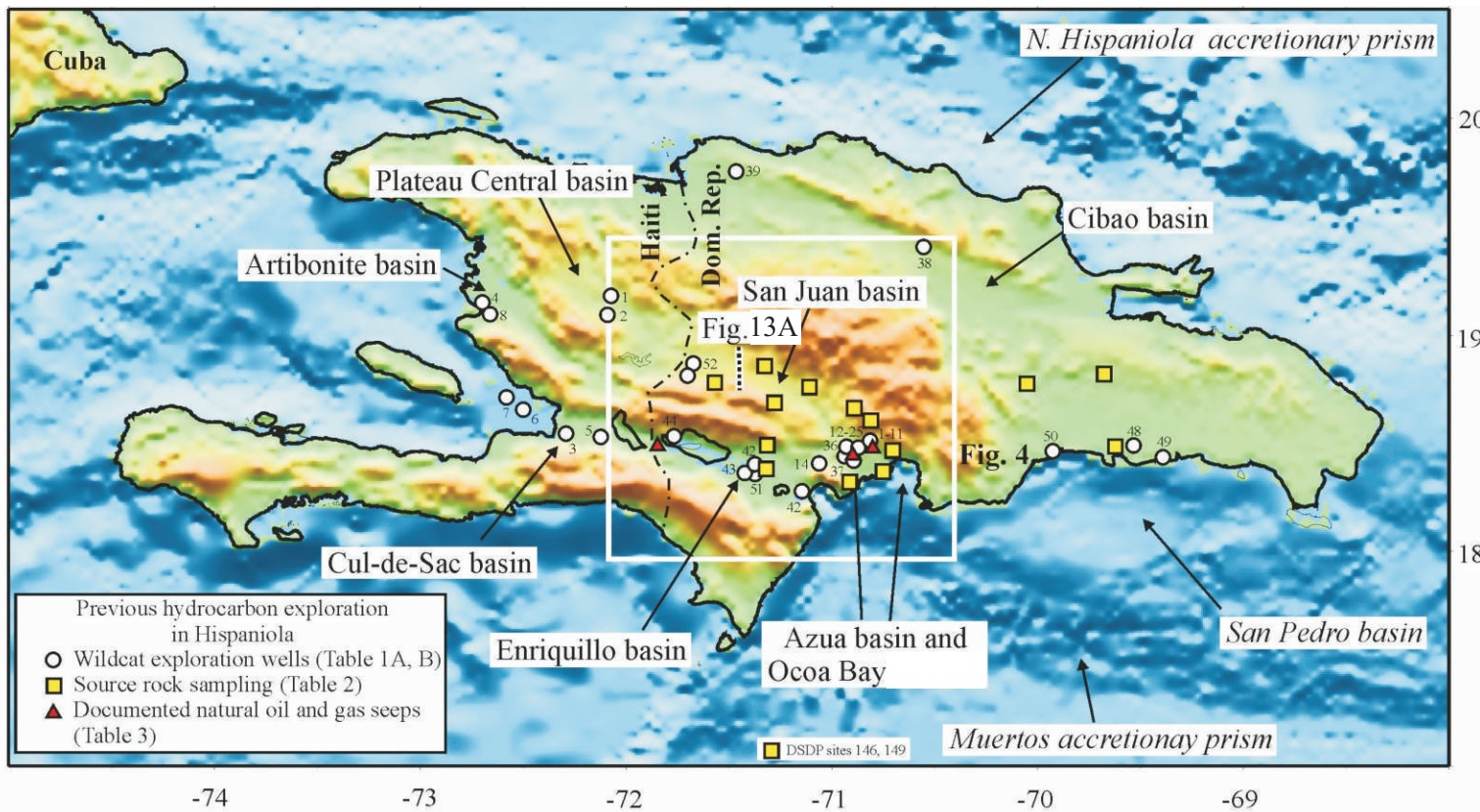


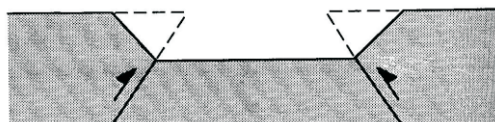
Figure 12 A. Topographic and bathymetric map of the Hispaniola region showing the major basins on the island and all previously drilled wildcat exploration wells in the Dominican Republic, Haiti, samples analyzed for source rock geochemistry, and documented natural oil and gas seeps. There have been only two offshore wells drilled to date in Port-au-Prince Bay, Haiti (Cul-de-Sac-1, Arcadines-1).

A. RIFT VALLEY (J.W. GREGORY, 1896)



Figure 12B. Comparison of cross-sectional profiles of rift valleys and ramp valleys. Both structures produce similar topographic basins and can be distinguished only by careful mapping of basin structure.

B. RAMP VALLEY (B. WILLIS, 1928)



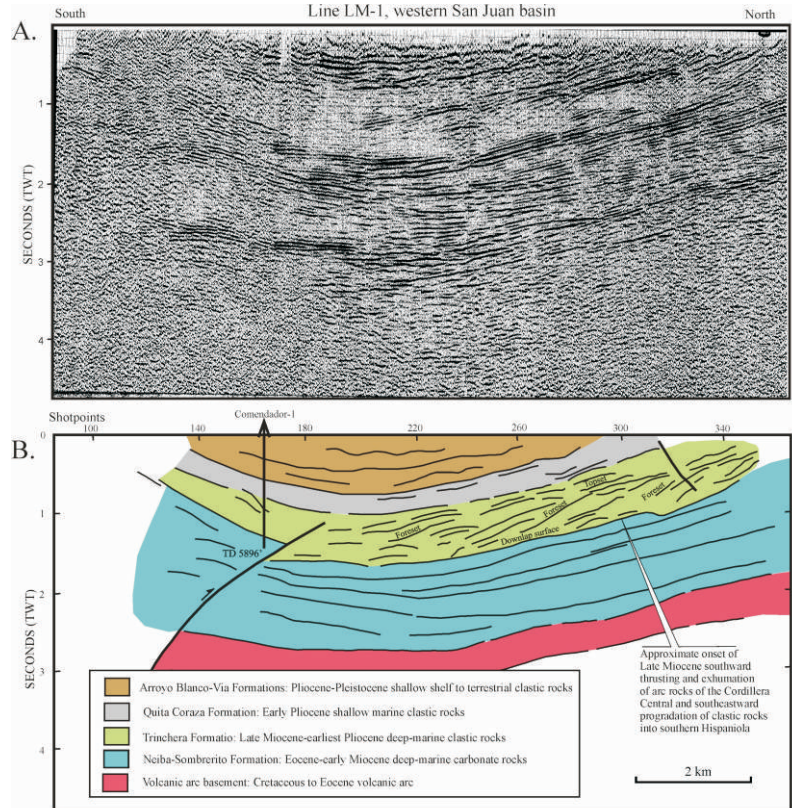


Figure 13A. North-south Vibroseis onland seismic reflection, dip line LM-1 across the central part of the San Juan basin (cf. Figure 4 for location). The data in A was published by Nemec (1980) and the interpretation in B is slightly modified from his interpretation. Data acquisition was performed by Western Geophysical and was recorded along a road extending sixteen kilometers north and five kilometers south of the Dominican town of Las Matas de Farfan. The energy source consisted of four vibrators recording through a 48-trace cable. The data was processed 24-fold with crooked line corrections. Interpretation of subsurface units in B is based on the seismic character of the units, correlation to updip outcrops, and the Comendador 1 well drilled by the Dominican Seaboard Oil Company in 1945.

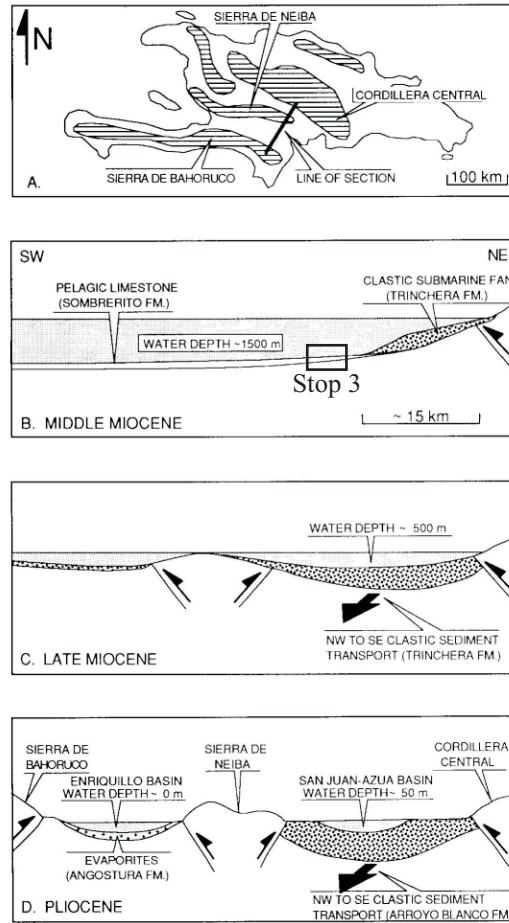


Figure 13B. Schematic cross sections showing middle Miocene to Pliocene structural control on clastic sedimentation in the Enriquillo and Azua basins. A, Major present-day mountain ranges of Hispaniola (horizontal ruled areas) and line of cross section for B, C, and D through the eastern San Juan-Azua and Enriquillo basins. B, Initial middle Miocene emergence and erosion of the Cordillera Central; C, Continued late Miocene emergence and erosion of the Cordillera Central; initial uplift of the sierra de Neiba produces northwest to southeast clastic sediment transport in the San Juan and Azua basins. D, Pliocene uplift of the Cordillera Central, Sierra de Neiba, and Sierra de Bahoruco isolates the San Juan-Azua and Enriquillo basins. Elevation of the Sierra de Neiba shields the Enriquillo basin from clastic sediment and allows the precipitation of massive evaporite deposits in the central part of the basin during early Pliocene time. From Mann et al. (1991)

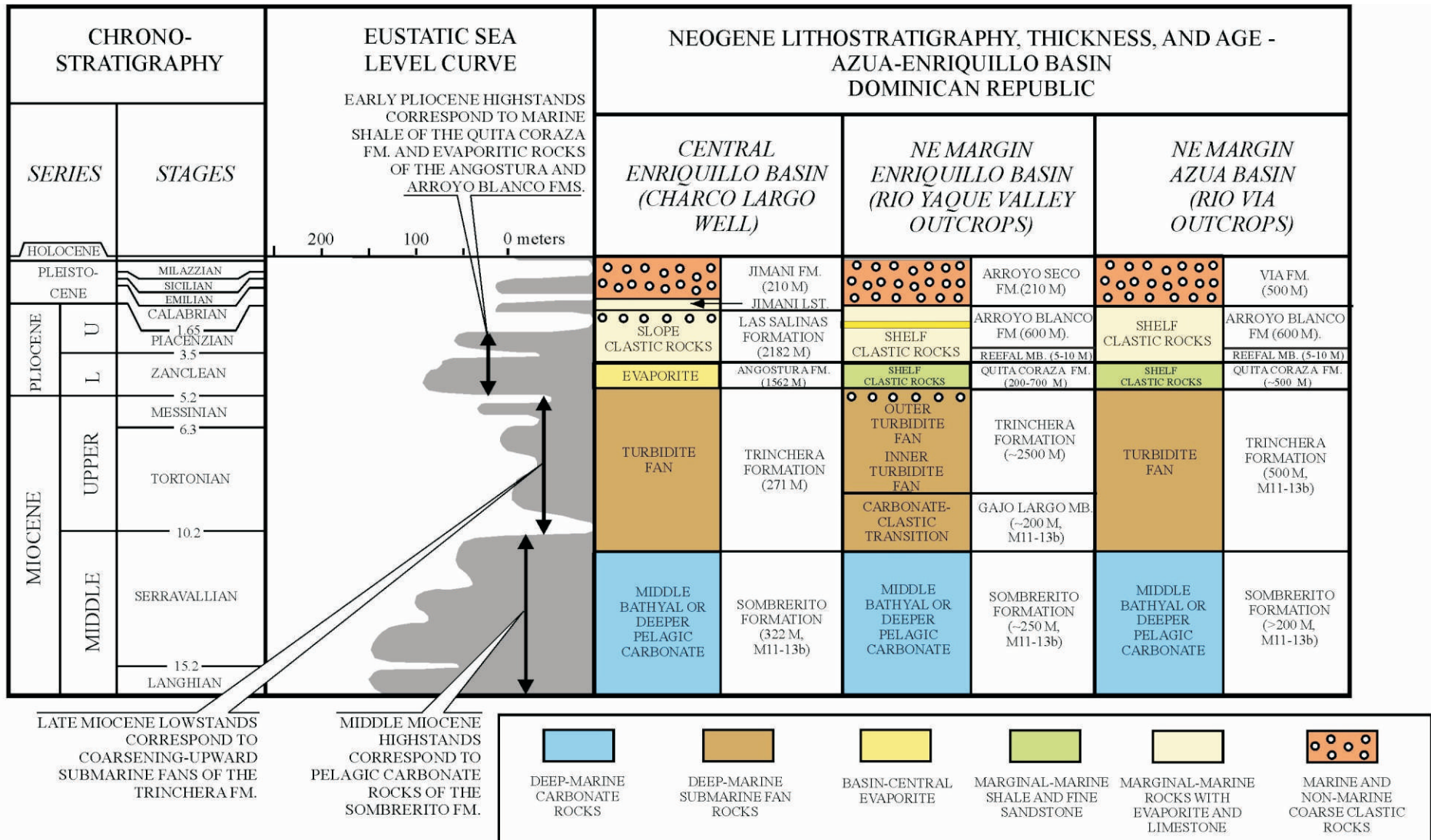


Figure 14. Comparison of sea-level curve of Haq et al. (1987) to stratigraphy of the central Enriquillo basin as recorded in the Charco Largo-1 well in the central Enriquillo basin, along the northeast margin (Rio Yaque area and Rio Via area outcrops – cf. Figure 21 for location). Micropaleontologic ages are based on McLaughlin et al. (1991), McLaughlin and Sen Gupta (1994), and Mann et al. (1999).

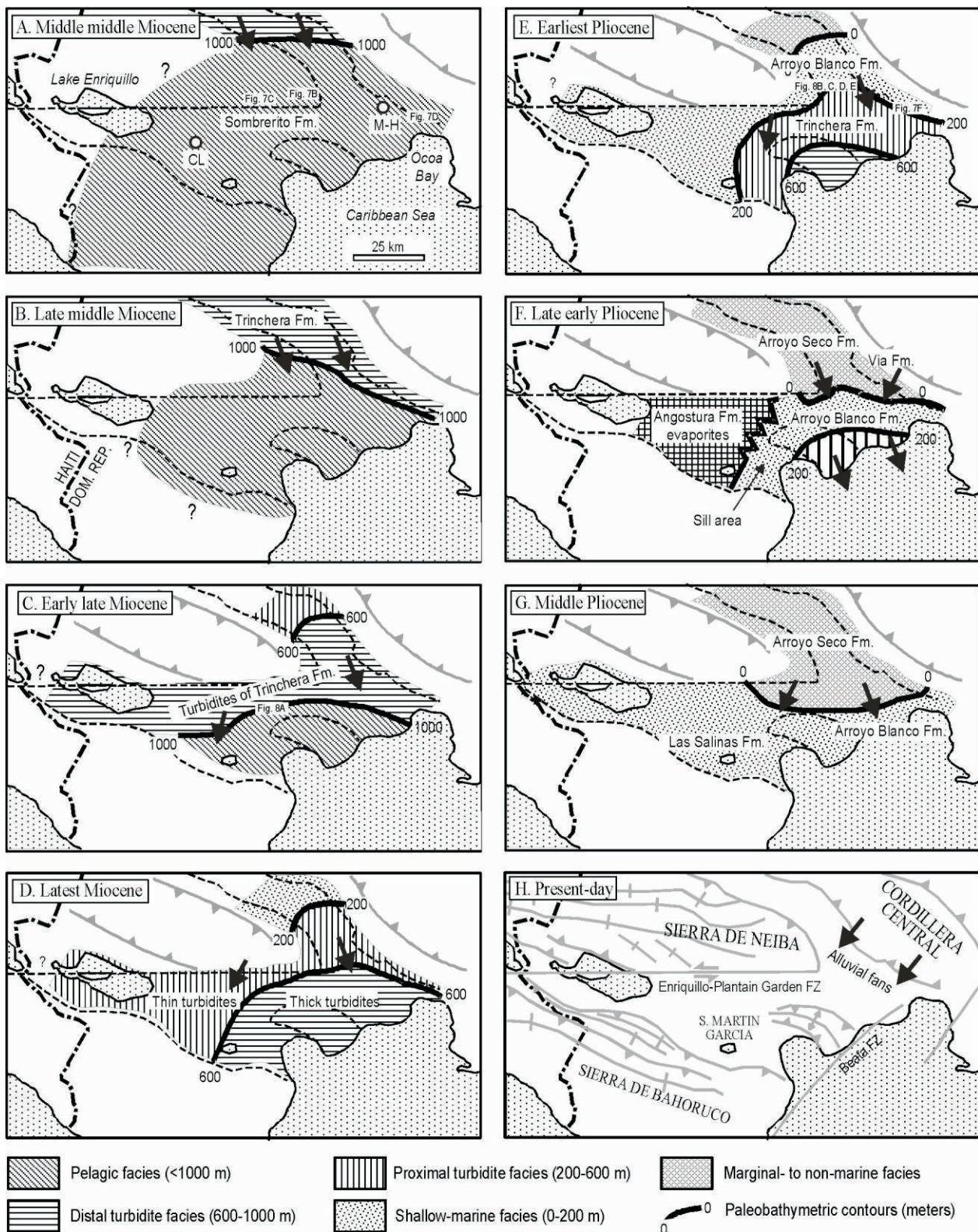


Figure 15. Schematic diagram of paleoenvironments in Miocene and Pliocene time of the Enriquillo, Azua and eastern San Juan basins based on McLaughlin et al. (1991) and Mann et al. (1999). A. Middle Middle Miocene. B. Late Middle Miocene. C. Early Late Miocene. D. Latest Miocene. E. Earliest Pliocene. F. Late Early Pliocene. G. Middle Pliocene. H. Present-day. Arrows indicate approximate paleocurrent directions.

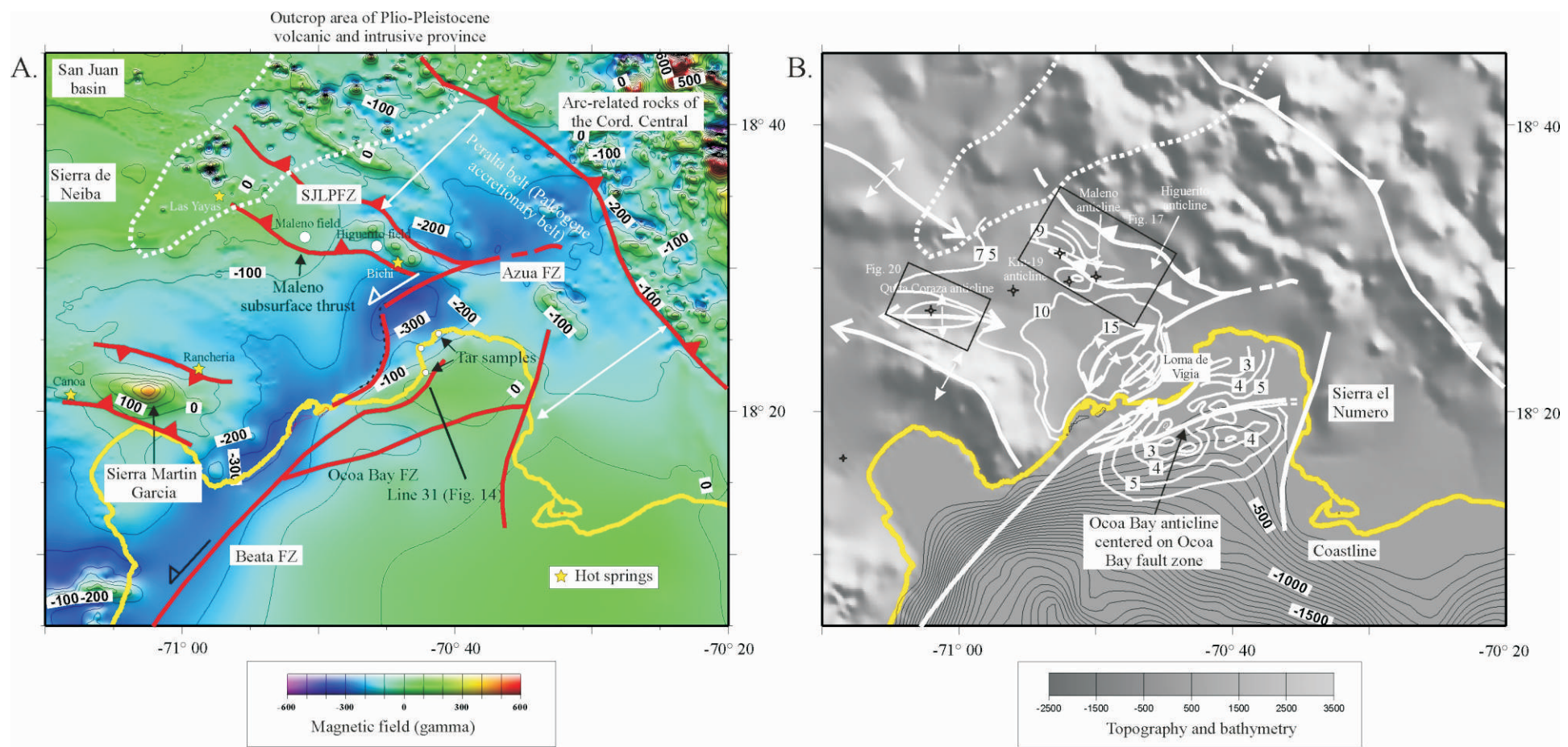


Figure 16. A. Aeromagnetic map of land areas within the intersection area of the Enriquillo, Azua, and San Juan basins (data provided by Direccion General de Mineria and used with permission) (yellow line represents present-day coastline of Hispaniola). Areas of high relief anomalies include Cretaceous-Eocene plutonic and arc rocks of the Cordillera Central and the Plio-Pleistocene volcanic province of mafic cones and shallow plugs erupted from 1.9 to 2.7 Ma. The Beata-Azua fault zone forms a magnetic low formed by a trough of thick sedimentary rocks of Miocene to Recent age. Isolated, northwest-trending magnetic highs may represent Cretaceous basement slivers uplifted along northeast-dipping thrust faults and/or Plio-Pleistocene mafic cones and shallow plugs at depth. B. 15-second resolution digital elevation map of the area with illumination from the northeast. Offshore bathymetry is predicted using Smith and Sandwell (1998) satellite-based gravity map. Depth to top of Sombrerito Formation carbonate rocks was done by Pierce using about 500 km of seismic data collected by Mobil and Murfin Petroleum. The Azua basin is the only area of the Dominican Republic and Haiti where hydrocarbons have been produced in the Maleno and Higuemite faulted anticlines and therefore has the highest concentration of oil exploration wells on the island (cf. Figure 12A).

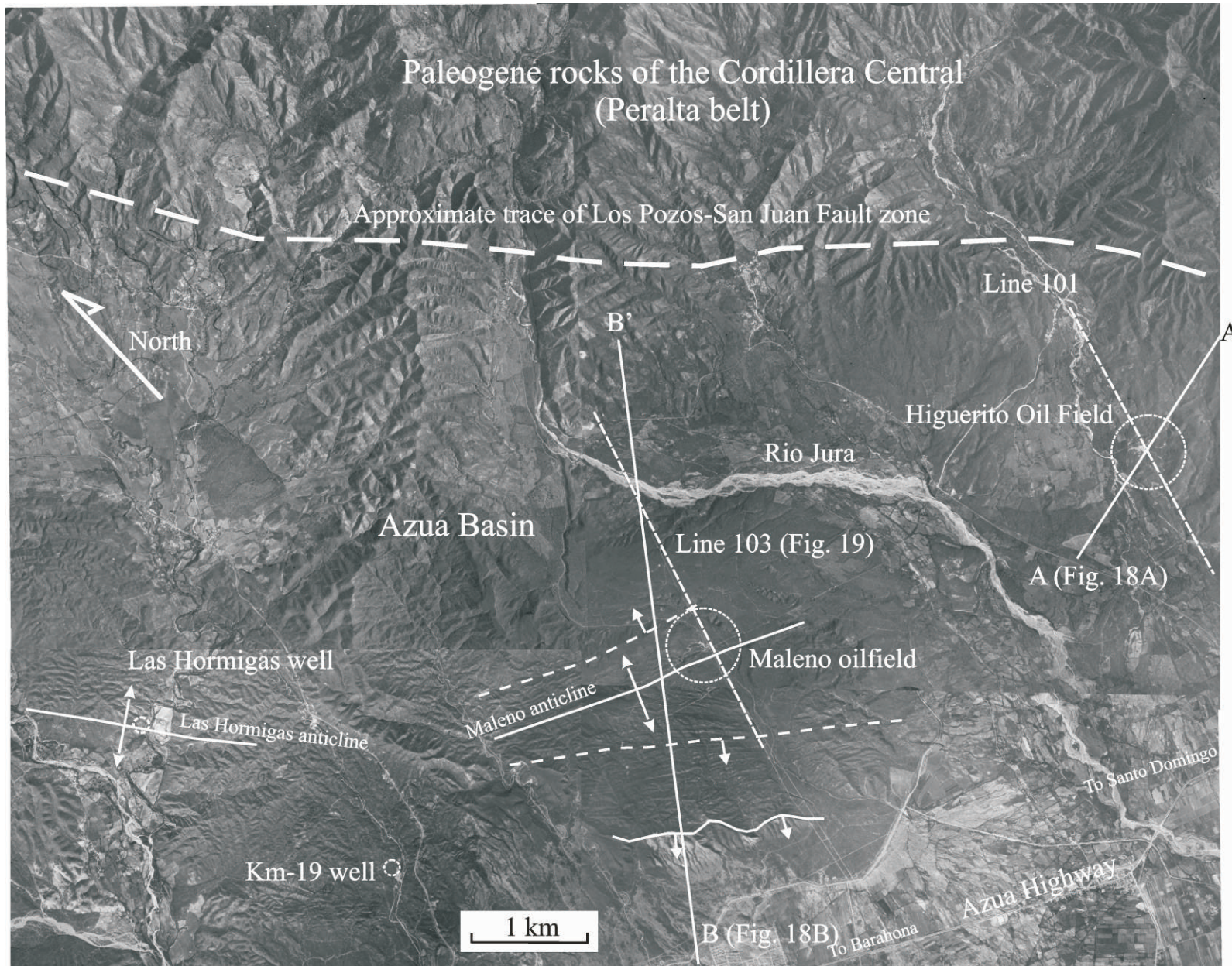


Figure 17. Mosaic of four aerial photographs showing location of Higuerito and Maleno oil fields in relation to surface anticlines and the San Juan-Los Pozos thrust fault defining the mountain front of the Cordillera Central. Maleno wells 1, 1A, 2, DT, and 3 are clustered in the circled area marked “Maleno oilfield”. Prominent strike ridges are mostly composed of sandstone and conglomerate of the Arroyo Blanco Formation.

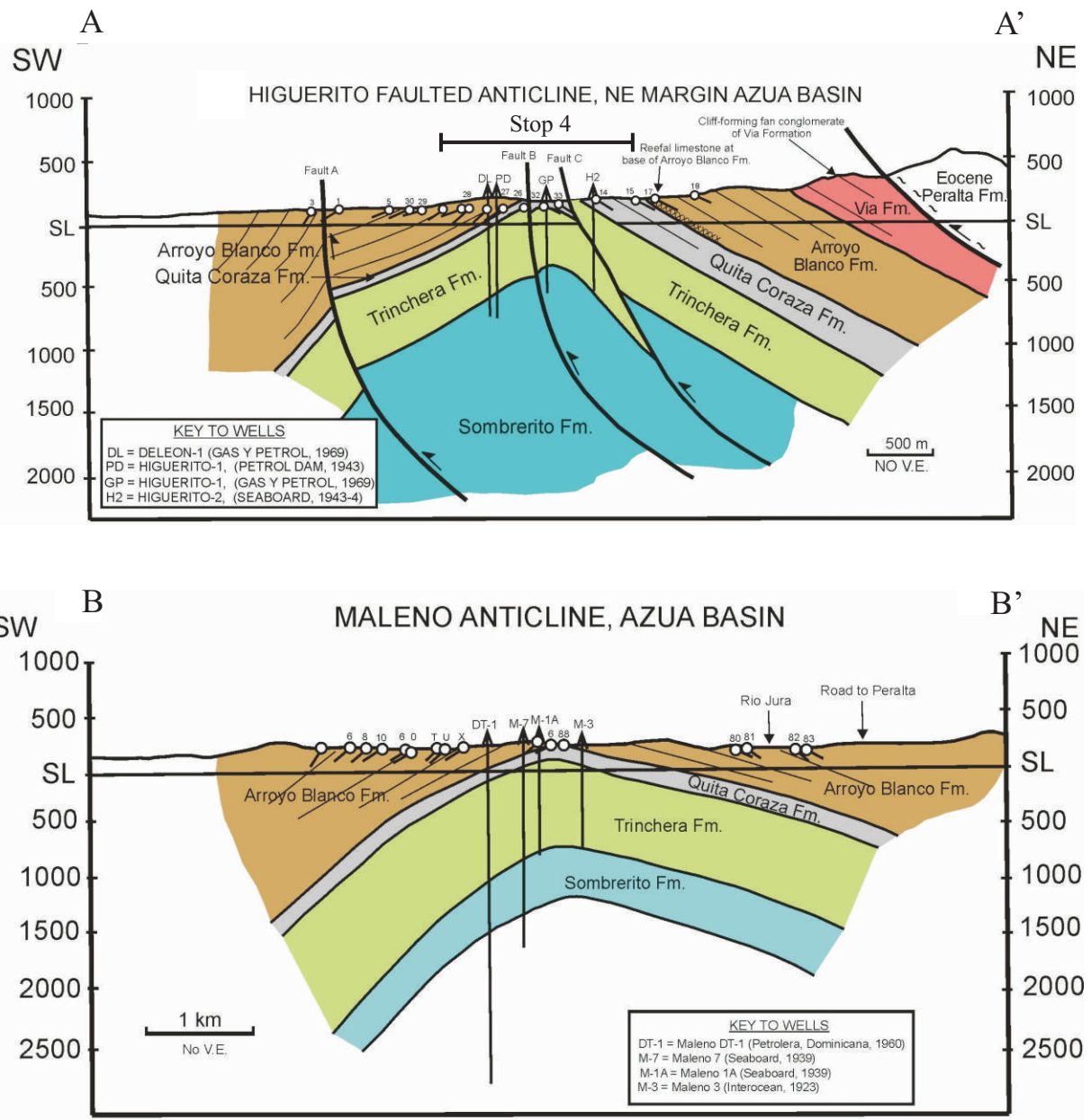


Figure 18. Cross sections of oil and gas-bearing anticlines in the Azua basin based on surface mapping. A.. Higuerito faulted anticline (area of STOP 4 is located) which acts as the structural trap for the Higuerito oil field. This is the most complex surface structure in the Azua basin because of its proximity to the overthrusting mountain front of the Cordillera Central. B. Cross section of the Maleno anticline based on surface mapping and well correlation (line of section shown on map in Figure 17). The anticline is asymmetric with a steeper southwestern flank. This geometry is consistent with a southwestward thrusting of the Cordillera Central over the Azua basin as also observed at the Higuerito faulted anticline.

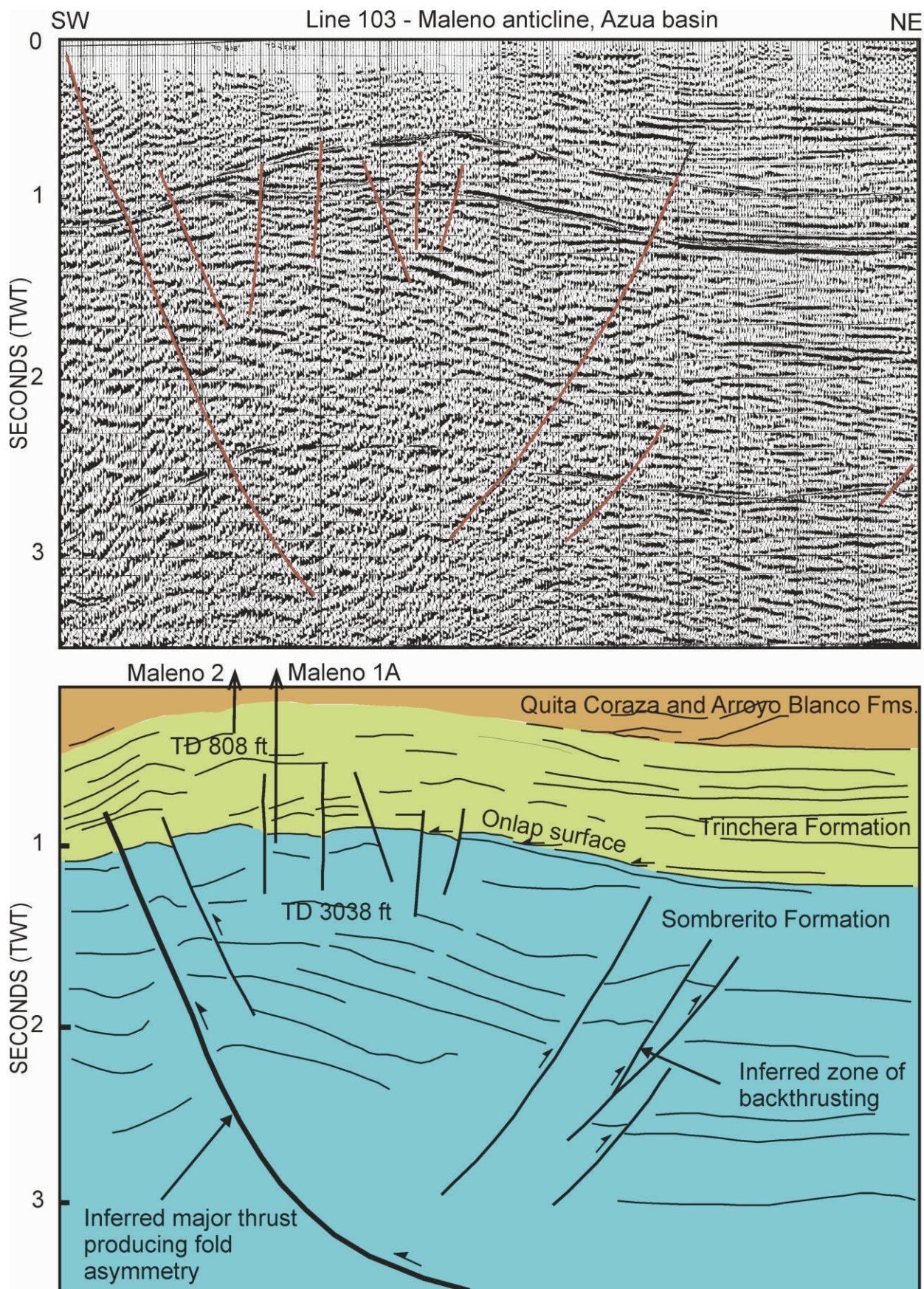


Figure 19. Seismic line 103 through the Maleno oil field (line of section shown on map in Figure 17). The asymmetric anticline at depth is controlled by a northeast-dipping thrust fault formed along the mountain front separating the Azua basin and the Cordillera Central (see map in Figure 16). Data provided courtesy of Murfin Petroleum.

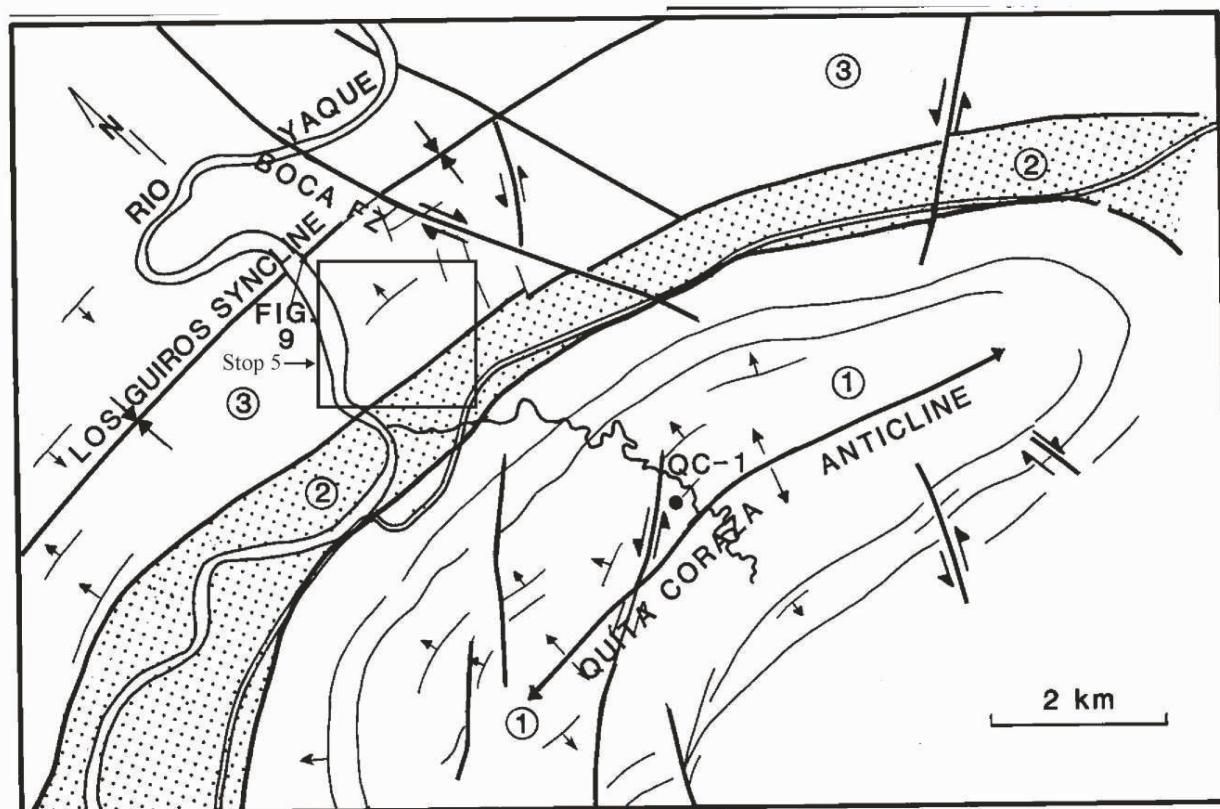
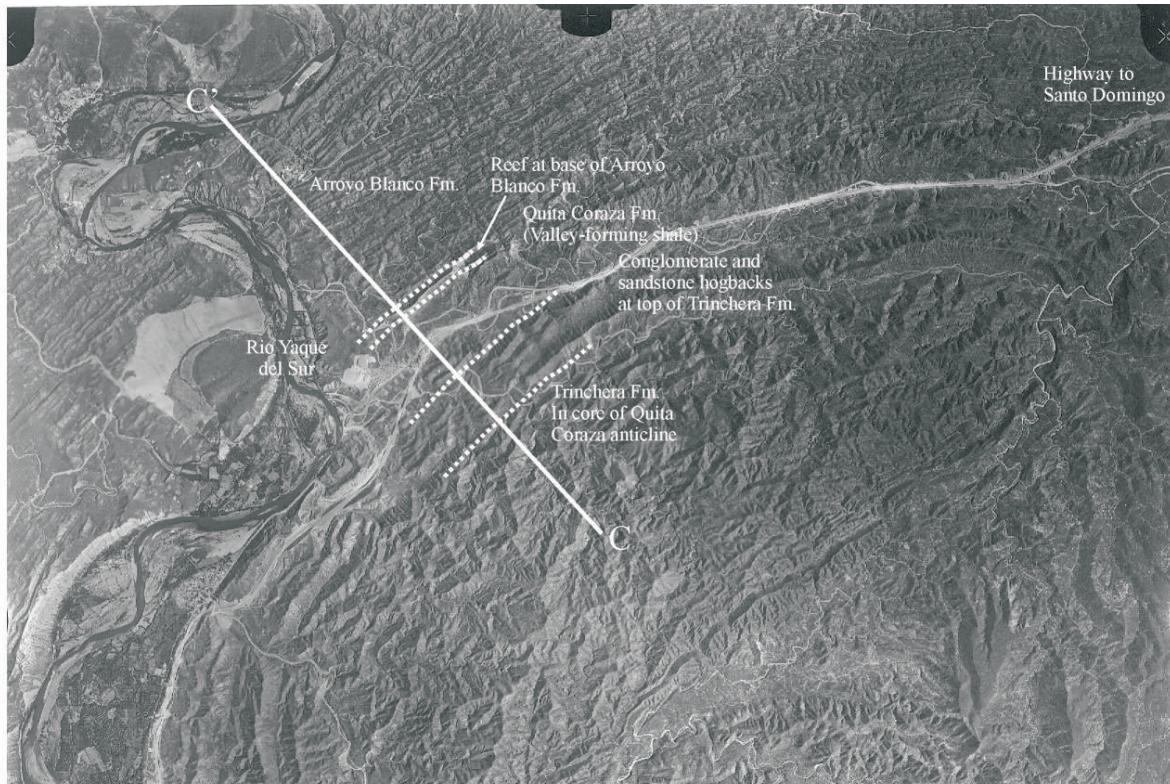


Figure 20. Geologic map and aerial photograph mosaic of the Quita Coraza anticline and Los Guiros syncline pair in the western Azua basin (location of map shown in Figure 16B). Outcrops along dry stream beds along the approximate line of cross section shown provide a section of the Trinchera Formation penetrated by exploration wells of the Azua basin. Key to numbered stratigraphic units: 1 = upper Miocene-lower Pliocene Trinchera Formation; 3 = lower Pliocene Quita Coraza Formation (shaded pattern); 4 = lower-upper Pliocene Arroyo Blanco Formation. QC-1 indicates approximate location of Quita Coraza well. The large kidney-shaped anticline is the Quita Coraza anticline, while the syncline is the Los Guiros syncline. Prominent strike ridges are resistant sandstone and conglomerate beds within the Trinchera and Arroyo Blanco Formations. The Azua-Barahona highway and the course of the Rio Yaque del Sur follow the outcrop of easily erodible shales of the Quita Coraza Formation.

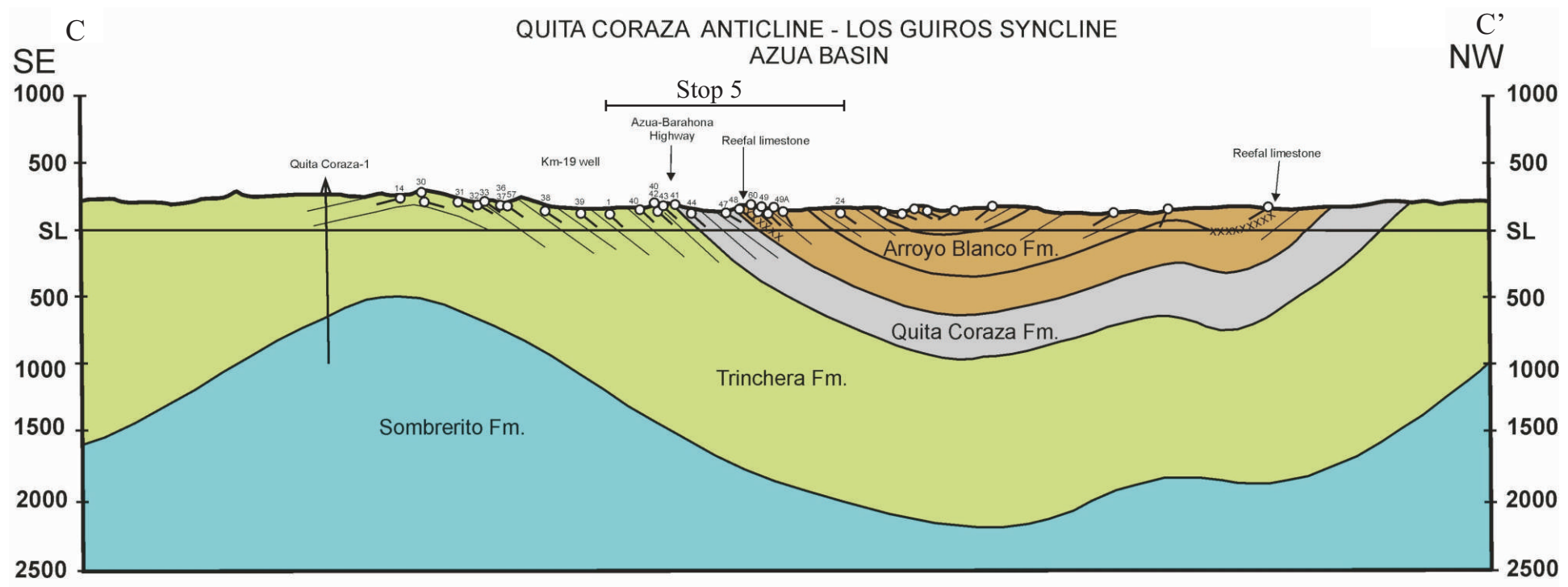


Figure 21. Cross section of the Quita Coraza-Los Guiros anticline-syncline pair based on surface mapping and correlation to the Quita Coraza-1 well. Location of section to be seen at STOP 5 is indicated.

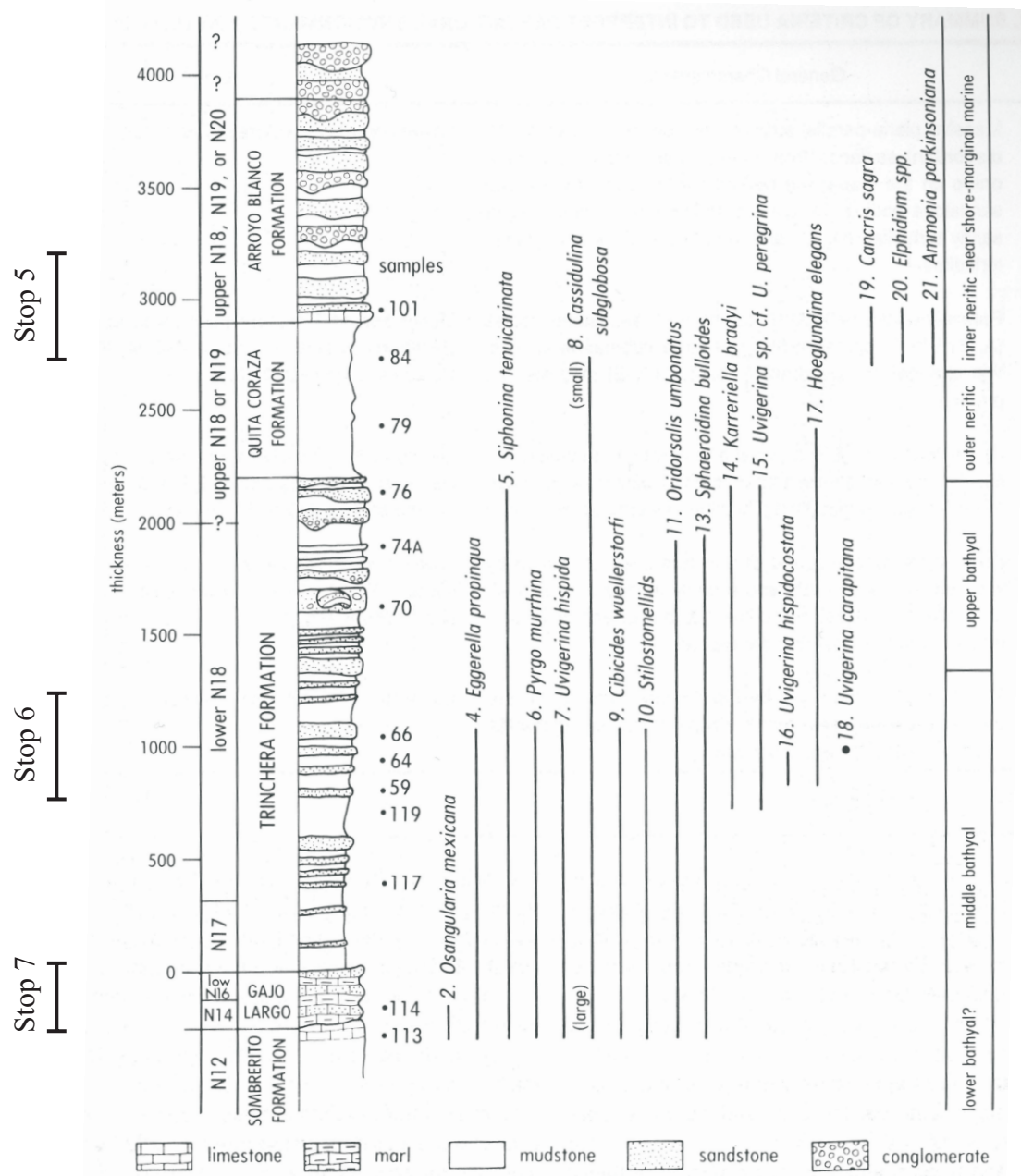


Figure 22. Composite stratigraphic section for the lower Rio Yaque del Sur Valley area of the Azua basin showing the range of bathymetrically useful species of benthic foraminifera and an interpretation of their paleobathymetry. The numbers before each species name are keyed to references that document their paleobathymetric significance. From McLaughlin et al. (1991)

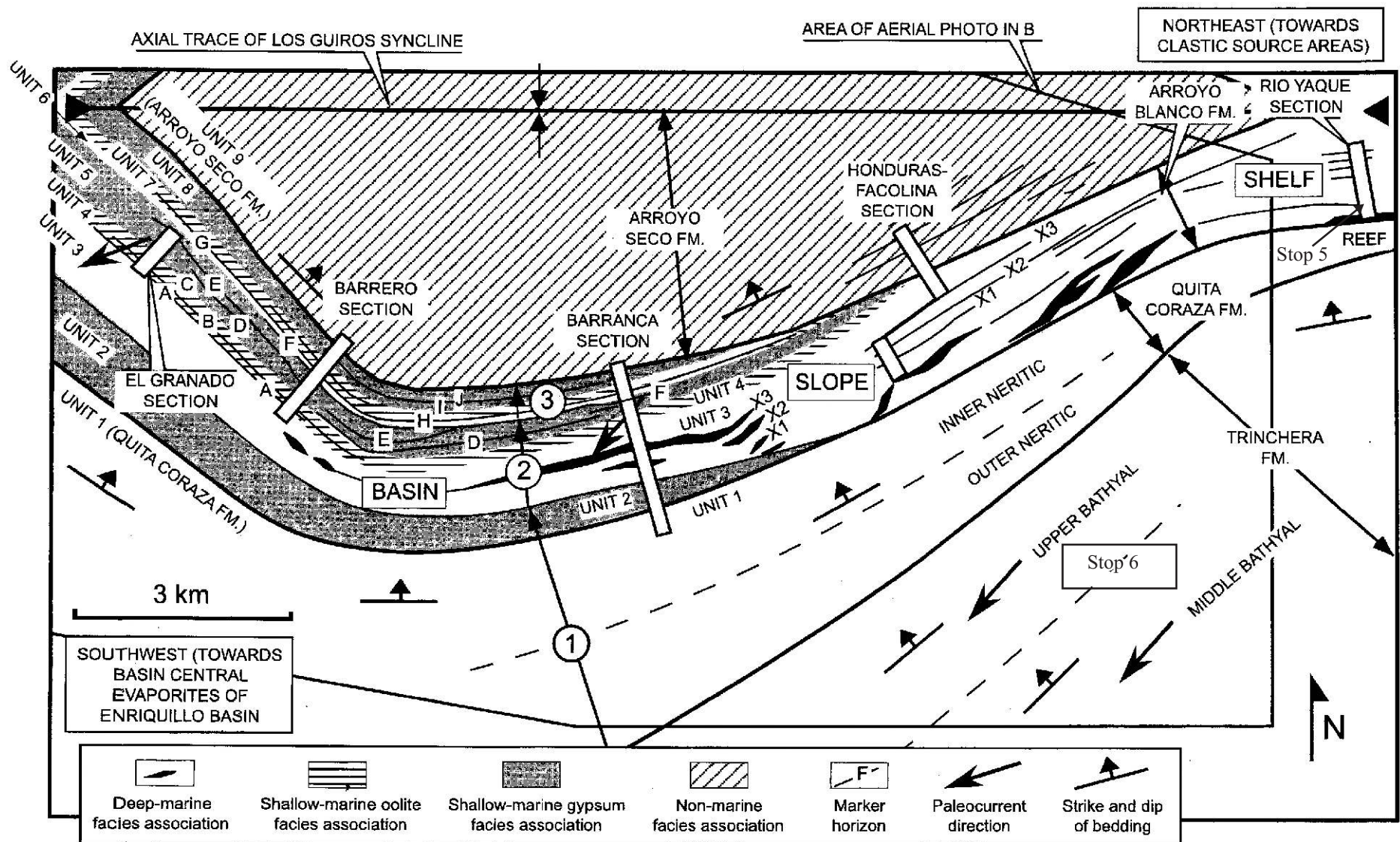


Figure 23. Schematic map of major groups of sedimentary facies along the eastern margin of the Enriquillo basin based on aerial photograph interpretation and field mapping. Key to number facies groups: unit 1=massive marine siltstone of Lower Pliocene Quita Coraza Formation; unit 2-8-shallow-marine oolite and gypsum facies associations of the Lower Pliocene Arroyo Blanco Formation; unit 9=non-marine facies association of the Upper Pliocene-Pleistocene (?) Arroyo Seco Formation. Letters identify resistant ridge of gypsum, oolitic limestone, or calcarenous-debris flows that are used to correlate the measured sections which are identified by name.

From Mann et al. (1999)

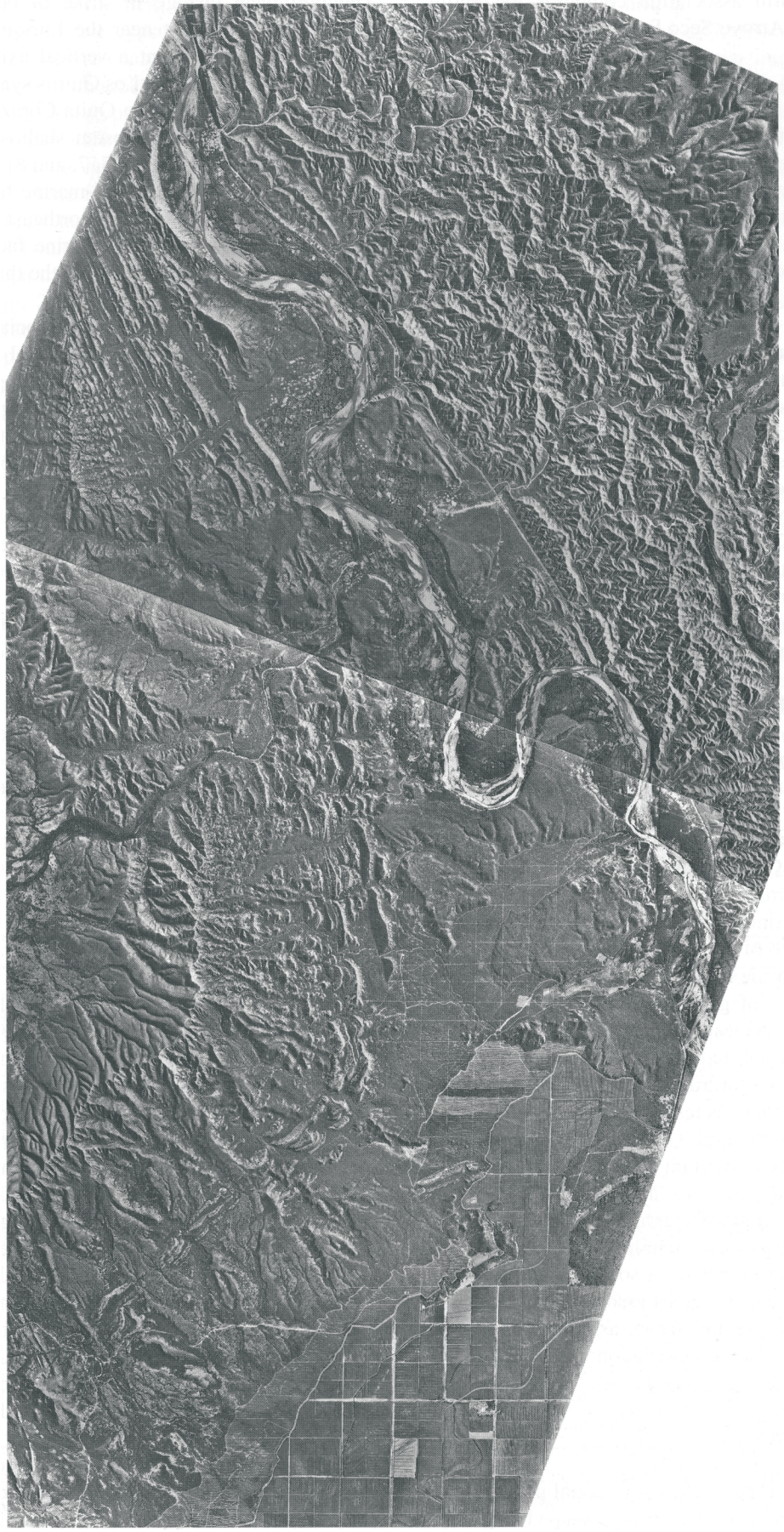


Figure 23b. Example of aerial photograph used as a basemap for the map shown in (A) (photograph number 721, ICM-I(58)-13-V-14 12-29 December 1958, original scale 1:60,000).

From Mann et al., (1999)

**SUMMARY OF CRITERIA USED TO INTERPRET DEPOSITIONAL ENVIRONMENTS FOR TURBIDITE FACIES\***

Environment	General Characteristics	Example
Stop 5 Slope	Massive plane-parallel stratified pelites (G) in places with discordant surfaces from slump scars and/or sediment onlap on the slope; the pelites can include channelized sandstone bodies (A), chaotic horizons (F), thin shaly or sandy turbidites (D, E), and more rarely thick and graded turbidites	Lower part of Quita Coraza Formation
	Inner fan	Parallel-bedded pelites (G) cut by thick sandstone bodies (A, B) which represent filling of large submarine valleys; thin channel and overbank turbidites (D, E) may also be present
Stop 6 Middle fan	Characterized by thin channel and overbank turbidites (D, E) with coarser, lenticular channel-fill turbidites (A, B); positive megasequences (fining/thinning-upward) are evident	Middle part of Trinchera Formation; middle parts of highway section , middle part of Arroyo Salado section
	Outer fan	Predominantly composed of thin turbidites deposited by low-density currents (D) and broadly lenticular "classical" channel turbidites; negative megasequences (thickening/coarsening-upward) are typical
Stop 7 Basin plain	Thin turbidites deposited by low-density currents (D) are usually dominant, with thin horizons of hemipelagites (G) often present and rarely dominant	Lower part of Trinchera Formation (transitional to outer fan)

\*After Mutti and Ricci Lucchi, 1972

Figure 24A.

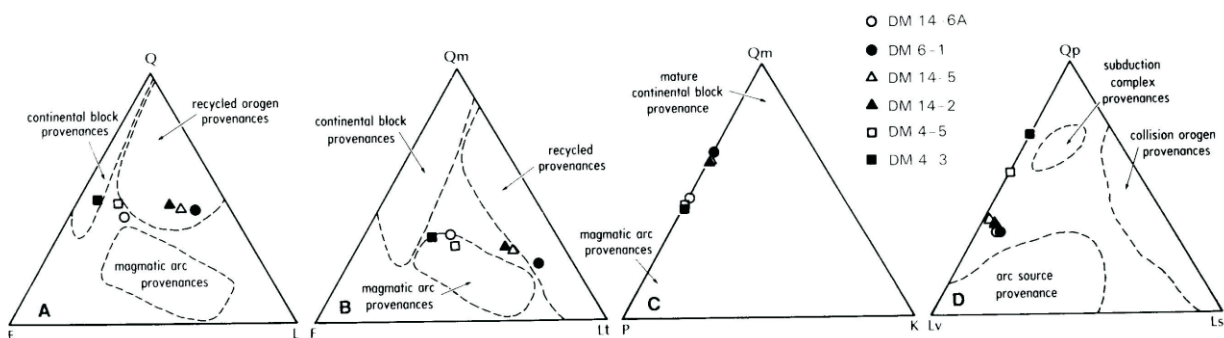


Figure 24B. Ternary diagrams showing sandstone compositions of the Trinchera Formation. Six sandstone samples were collected from measured sections along the Azua-Barahona Highway.

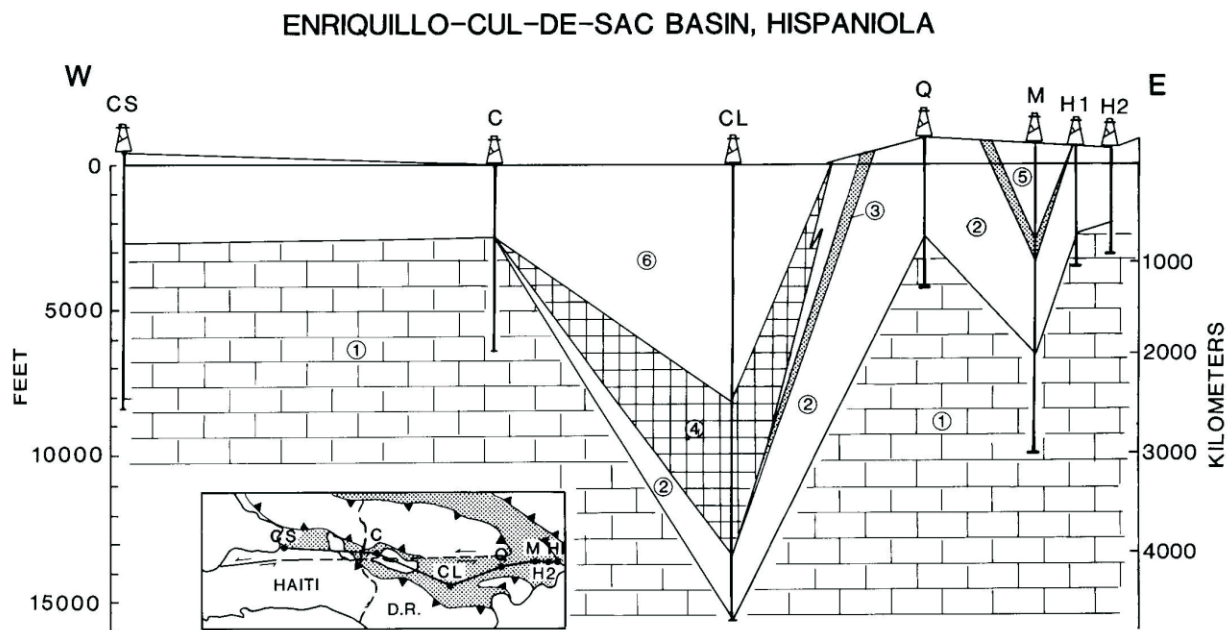


Figure 25A. East-west longitudinal cross section of the Enriquillo-Cul-de-Sac basin constructed using published data from petroleum exploration wells drilled from 1943 to 1980 (modified from Figure 6 of Bowin, 1975). Inset map provides lines of sections. Key to well abbreviations: CS: Cul-de-Sac No. 1; C=Cabritos No. 1; CL=Charco Largo; Q=Quita Coraza No. 1; M=Maleno No. 1; H1=Higuerito No. 1; H2=Higuerito No. 2. All data are from Bowin (1975) except for Charco Largo well, which is from de Leon (1983). Key to numbered lithologies: 1 indicates Paleocene-middle Miocene carbonate rocks (upper part is Sombrerito Formation); 2 indicates middle Miocene-lowest Pliocene, deep-marine clastic rocks (Trinchera Formation); 3 indicates lower Pliocene marine rocks (Quita Coraza Formation), transitional between units 2 and 5 and possibly between units 2 and 4 in the subsurface; 4 indicates lower to middle Pliocene (?) halite and gypsum (Angostura Formation); 5 indicates lower to upper Pliocene shallow-marine and fluvial clastic rocks (Arroyo Blanco Formation); 6 indicates lower to upper Pliocene shallow-marine and fluvial clastic rocks (Las Salinas Formation) and Quaternary alluvium. Note the across-strike cross section A-B of Figure 3, which is based on surface structural data, crosses this along-strike section near the Quita Coraza well. From Mann et al. (1991)

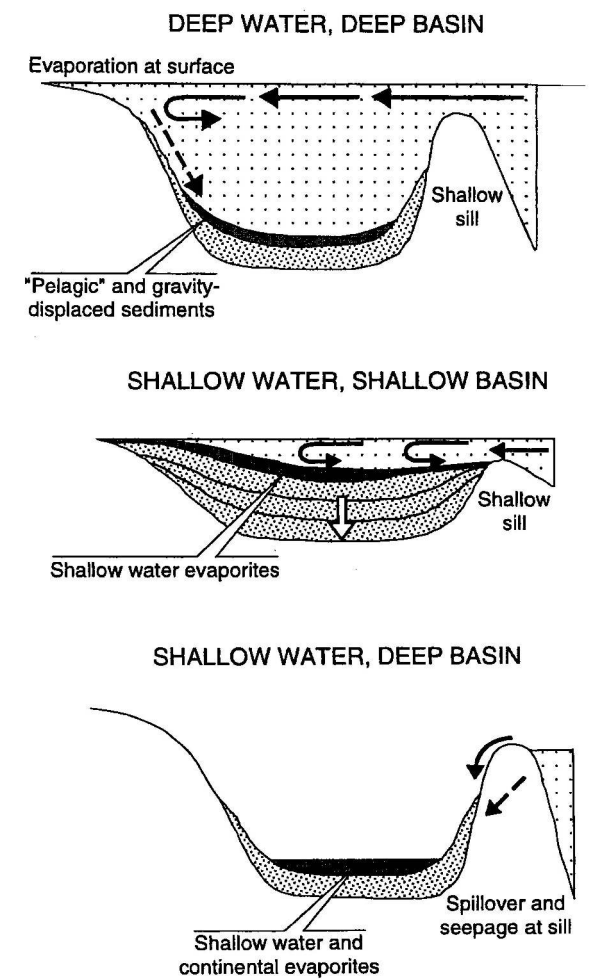


Figure 25B. Three models for the deposition of massive evaporite deposits like the one present in the Enriquillo basin (modified from Kendall, 1984). Because it is presently about 50 m below sea level, the Enriquillo basin is a likely shallow-water, deep-basin setting for evaporites.

From Mann et al. (1999)

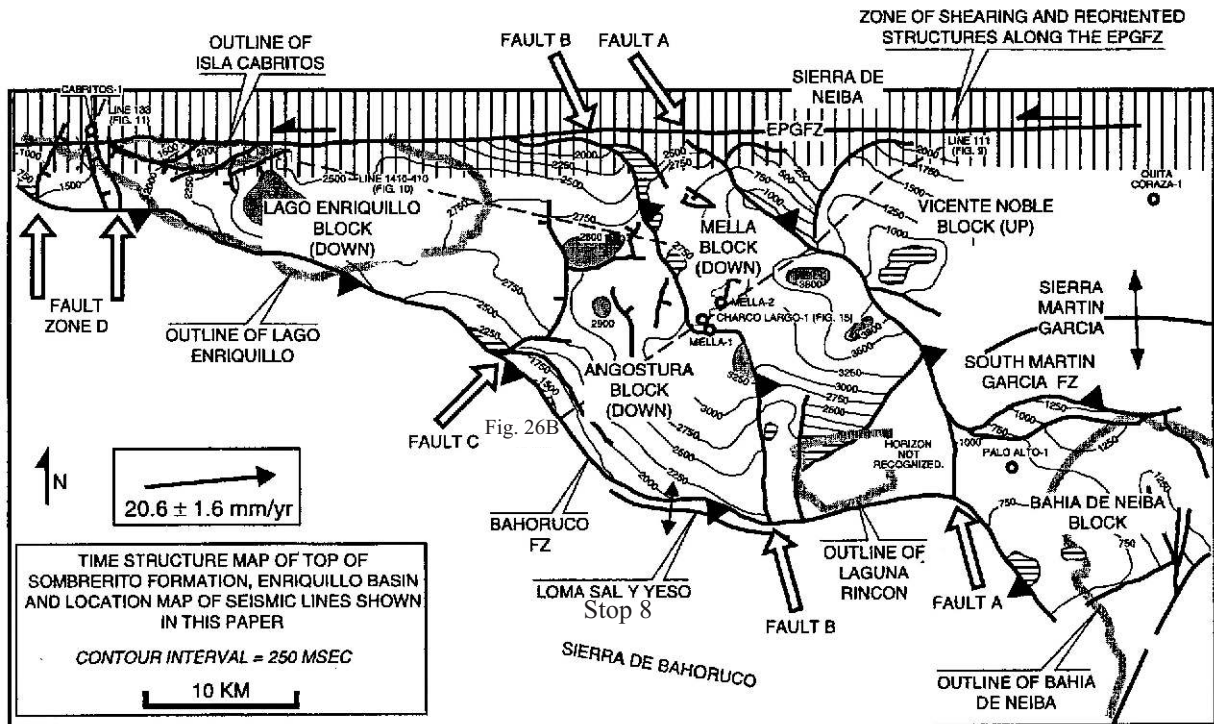


Figure 26A. Time structural map (contour interval 50 ms) of the reflector interpreted as the top of the earliest-Late Miocene Sombrerito Formation. Major faults subdivide the subsurface of the basin into several major structural blocks. The two central blocks have undergone the greatest amount of subsidence in post-Miocene time because they are being dynamically depressed by thrust or strike-slip faults at their margins. Much of the present-day surface of the Lago Enriquillo block is about 50 m below sea level and is isolated from the Caribbean Sea by a low sill about 10 m above sea level at the Bahía de Neiba and Mella blocks. The lined pattern at the top of the map indicates the zone of recent left-lateral shearing along the Enriquillo-Plantain Garden fault zone of Mann et al. (1995). The inset box shows the GPS-derived rate and direction of Caribbean plate motion relative to a fixed point on the North America plate (Dixon et al., 1998).

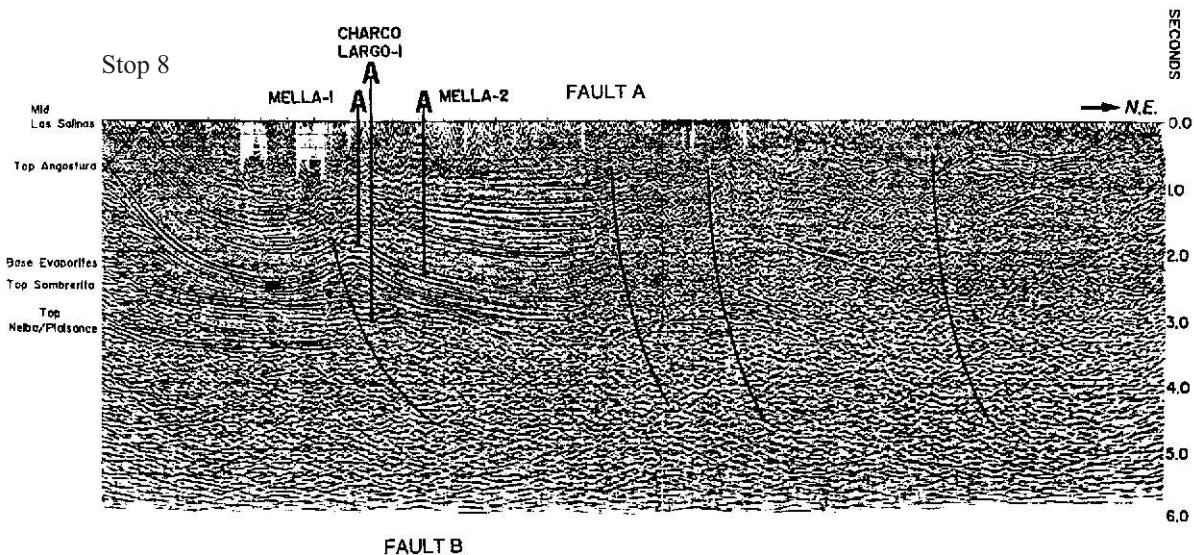


Figure 26B. Regional migrated multi-channel seismic line 111 from the central part of the Enriquillo basin (location on Figure 26A). The line crosses the deepest three blocks of the central part of the basin (Angostura, Mella, Vicenta Noble). Prominent reflectors are indicated in the left margin.

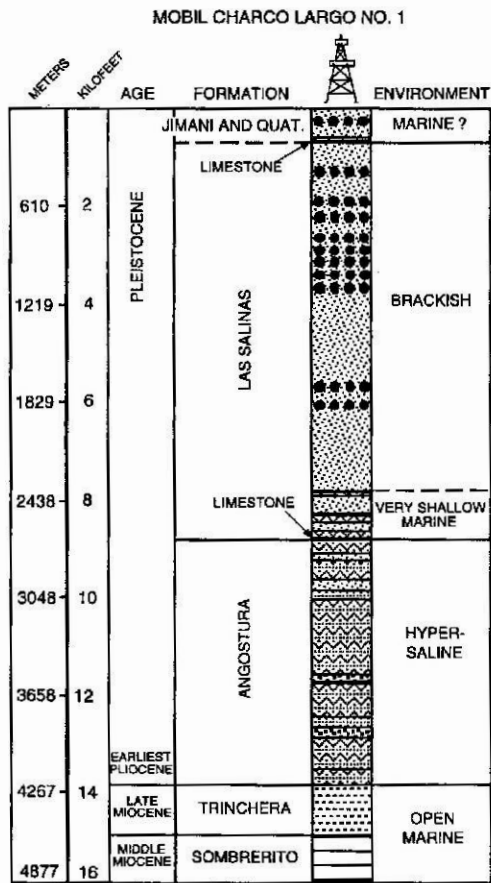


Figure 27A. General stratigraphic section of the Largo-1 well of the central Enriquillo basin. Lithologies are based on a detailed well log and an accompanying report provided to us by Mobil; ages and environments of deposition are based on micropaleontologic work by McLaughlin and Bold using sample material taken from well cuttings. Key to symbols: brick pattern=deep-water limestone; dashed pattern=shale; v pattern=massive halite; stipple=sandstone and shale; heavy black dots=conglomerate. From Mann et al. (1999)

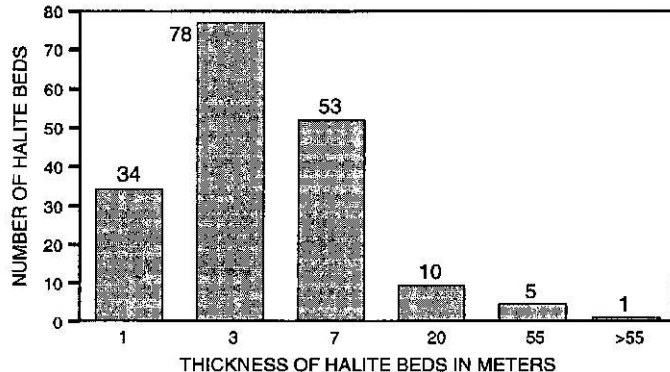


Figure 27B. Histogram showing thickness of halite beds in the Charco Largo-1 well as reported on the detailed well log.

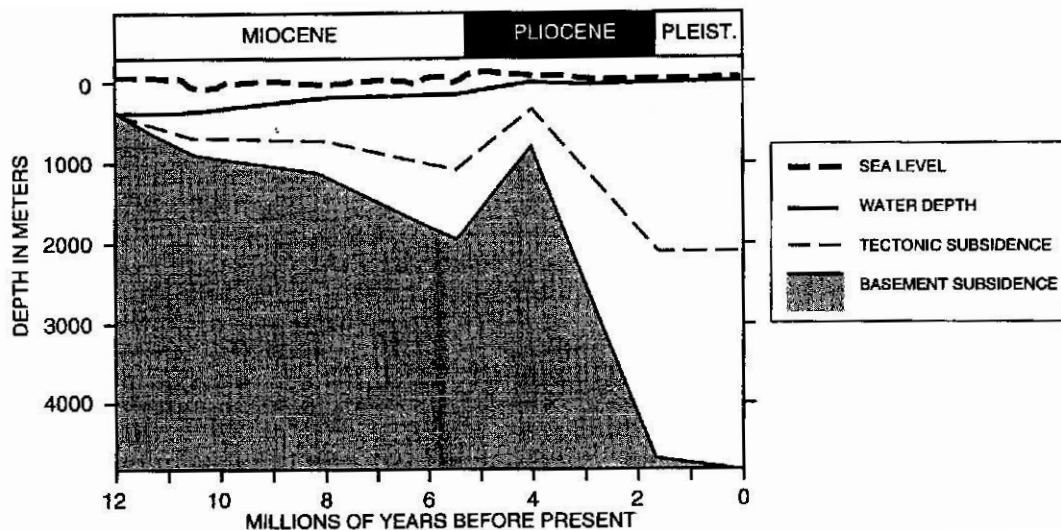


Figure 27C. Subsidence history of the Charco Largo-1 well. From Mann et al. (1999)

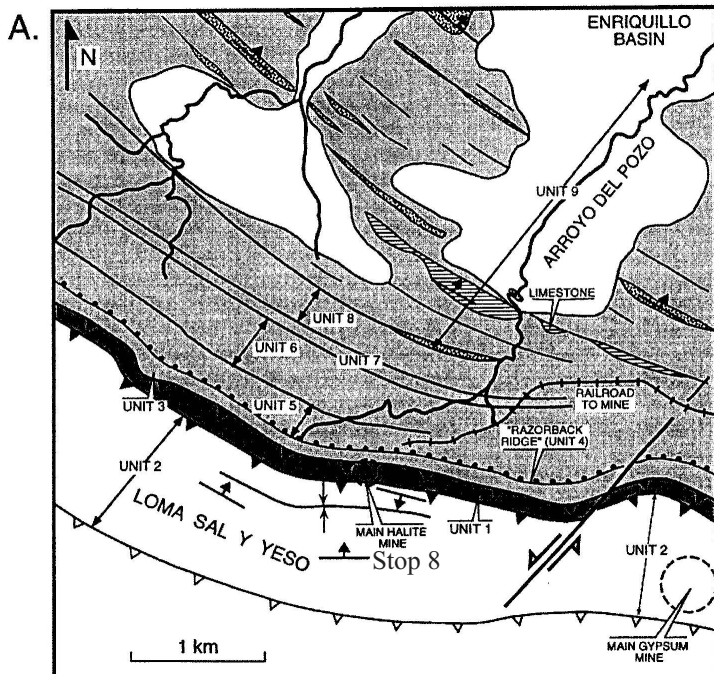


Figure 28A. Geologic map of Loma Sal y Yeso in the area of the open-pit salt mine and measured section in Arroyo del Pozo. Key to numbered horizons: 1=recrystallized, flow-banded halite and overlying shale of the Angostura Formation; 2=recrystallized massive to thinly bedded gypsum and interbedded shale of the Angostura Formation; 3=finely laminated gypsum and unfossiliferous, massive, gray silty mudstone overthrust by halite of the Angostura Formation; 4="Razorback Ridge", a resistant bed of shallow-marine grainstone taken as the base of the Las Salinas Formation; 5=ripple-marked sandstone and interbedded siltstone; 6=trough-cross bedded sandstone and interbedded siltstone; 7=coquina beds interbedded in siltstone; 8=growth position coral reefs and reworked coral debris interbedded in siltstone; 9=recrystallized micrite and calcarenite interbedded in siltstone.

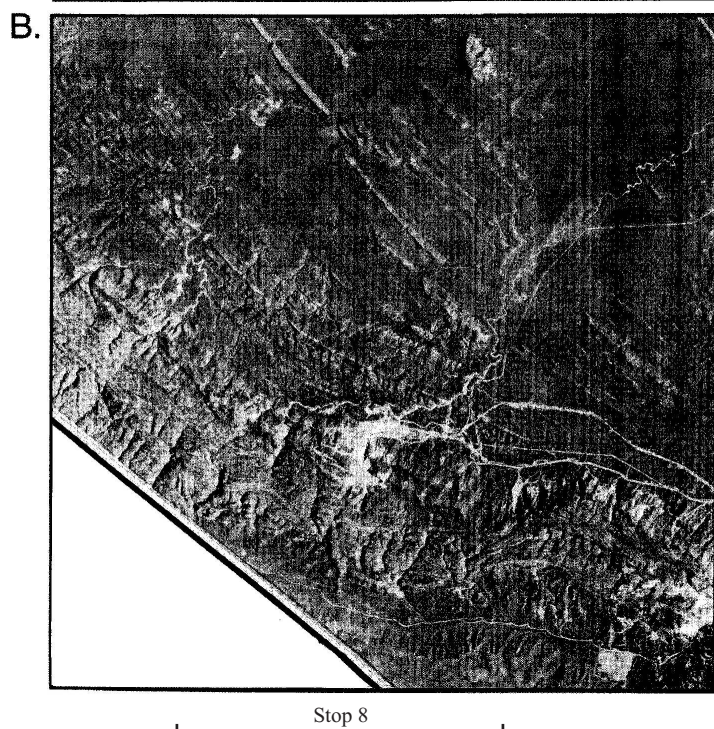


Figure 28B. Aerial photograph is Marena series (1983), roll 43, flight 21, no. 212 (original scale 1:40,000).

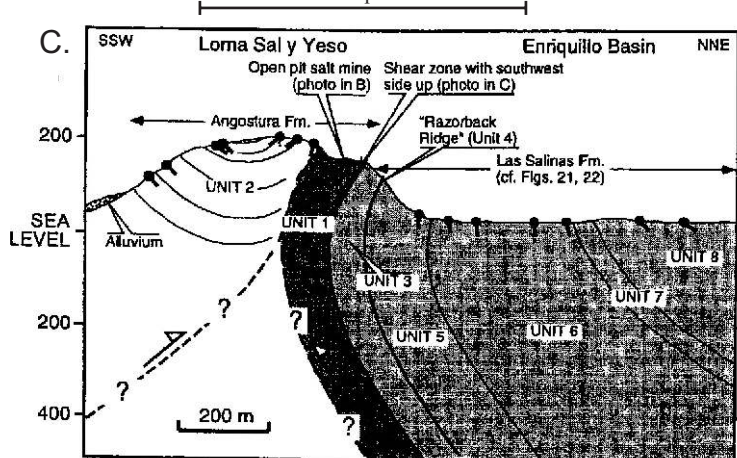


Figure 28C. Cross-section of the Loma Sal y Yeso in the area of the open-pit salt mine. Tadpoles indicate measured dips of bedding. Numbered horizons are the same as Figure 28A. The downdip extension of the halite and thrust faults is speculative but consistent with the geometry of halite seen on seismic line 111 north of Loma Sal y Yeso (compare to line in Figure 26B).

## **Part II (stops 9, 10, 12, and 13 led by Pedro Hernaiz):**

### **Geología general y estratigrafía de las cuencas de Enriquillo y Azua y su entorno regional General geology and stratigraphy of the Enriquillo and Azua basins and environs**

Las cuencas de Enriquillo y Azua, conjuntamente con la de San Juan, se localizan en el sector SO de la República Dominicana (Fig. 1) y tienen una evolución más o menos conjunta, aunque no simultánea, controlada por el levantamiento de sus relieves limítrofes, de norte a sur: el Cinturón de Peralta del margen meridional de la Cordillera Central, formado mayoritariamente por series turbidíticas de edad Paleógena; y las sierras de Neiba, de Martín García y de Bahoruco, formadas fundamentalmente por rocas carbonatadas del Eoceno-Mioceno (Fig. 1). En este capítulo se describen los rasgos geológicos básicos de estos dominios y se presenta una síntesis de la estratigrafía de las cuencas de Enriquillo y Azua y de las partes colindantes de las sierras mencionadas.

### **Características geológicas generales de los Dominios de la región SO de La República Dominicana General geologic patterns of the domains in the SW Dominican Republic**

La cuenca de San Juan se localiza entre la Cordillera Central y la sierra de Neiba. Tiene un perfil geométrico siniforme relativamente simple y está rellena por más de 7.000 m de materiales terciarios y cuaternarios correspondientes a ambientes marinos en la base y continentales a techo (Fig. 2) (Norconsult 1983; García y Harms 1988; Mann *et al.* 1991 b y d.). Esta cuenca se sitúa en el antepaís del cinturón de Peralta y tanto su relleno como su estructura interna han sido controladas principalmente por la evolución estructural de éste (Mann *et al.*, 1991 b y d). Su límite norte con este cinturón consiste en una falla inversa o cabalgamiento; regionalmente algunos autores atribuyen a esta falla (falla San Juan-Los Pozos-Fig. 1) grandes desplazamientos sienestrales durante el Oligoceno-Mioceno (Pindell y Barrett, 1990; Dolan *et al.*, 1991). El límite sur o sureste con la sierra de Neiba es, sin embargo, menos neto y se resuelve por medio de un sistema escalonado de fallas de alto ángulo con saltos menores en la vertical y también en dirección.

En su extremo SE, donde se produce el enlace con la cuenca de Enriquillo, la cuenca de San Juan adquiere el nombre de cuenca de Azua. Este cambio topográfico responde también a un cambio cierto en la geometría de la cuenca que justifica su individualización: a) sustrato elevado respecto a la de San Juan, b) consecuentemente, menor espesor de relleno (inferior a los 3.000 m); y c) mayor complejidad estructural; todos ellos, efectos adicionales producidos fundamentalmente por la acción localizada del indenter de Beata. La estructura de la cuenca de Azua se ha definido como del tipo domos y cubetas, la cual consiste en una serie de cubetas sinclinales de dirección NO-SE a ONO-ESE, separadas por domos anticlinales, cuyos márgenes suelen ser cabalgantes sobre las cubetas (Mann *et al.*, 1991 d). Las cubetas están llenas por los mismos materiales que la cuenca de San Juan, respecto a los cuales son algo más modernos (Mioceno Medio-Cuaternario) como consecuencia de la progradación de su depósito hacia el sur.

La cuenca de Enriquillo se extiende con una dirección ONO-ESE entre las sierras de Neiba y Bahoruco, desde la frontera con Haití hasta la bahía de Neiba al sur de la Sierra de Martín García (Fig. 1). Su geometría en planta aproximadamente romboidal ya sugiere que su estructura tiene una mayor control de la tectónica de desgarre que las cuencas anteriores. Está rellena por materiales del Mioceno al Cuaternario que forman una secuencia somerizante de más de 4.000 de espesor, muy similar a las de las cuencas de San Juan (sector meridional) y Azua (Fig. 2). La característica distintiva de la cuenca de Enriquillo respecto a éstas, es la presencia de formaciones evaporíticas que alcanzan espesores notables.

Se denomina Cinturón de Peralta al segmento dominicano del *terreno de Trois-Rivieres-Peralta* (Dolan *et al.*, 1991). Consiste en un potente secuencia de rocas sedimentarias (localmente metasedimentarias

en Haití) del Cretácico Superior- Pleistoceno, que con una dirección general NO-SE discurre a lo largo del flanco meridional de la Cordillera Central (Mann *et al.*, 1991 b). Este dominio se identifica con la cuenca trasera del arco de isla Circum-Caribeño y se ha sugerido que posteriormente sufrió una modificación a prisma acrecional como consecuencia de la traslación del frente de subducción al margen meridional de la isla (Biju Duval *et al.*, 1983; Witchard y Dolan, 1990). En ella, el régimen de depósito fue eminentemente turbidítico y a veces caótico; los estudios de paleocorrientes indican que su relleno se produjo subparalelamente a su eje (NO-SE) y con un sentido de progradación de las facies hacia el SE (Dolan *et al.*, 1991; Heubeck *et al.*, 1991). En su sector SO, Heubeck (1988), Heubeck *et al* (1991) y Dolan *et al.* (1991), han subdividido la estratigrafía del cinturón en tres grandes grupos deposicionales, separados entre sí por discordancias mayores: El Grupo Peralta, de edad Paleoceno-Eoceno, el Grupo Río Ocoa, de edad Eoceno Medio-Mioceno Inferior, y el Grupo Ingenio Caei, del Mioceno Inferior-Pleistoceno (Fig. 5.2). La estructura interna del cinturón de Peralta está definida por un sistema de pliegues y cabalgamientos con vergencia al SO, algunos de los cuales, los más internos, llegan a involucrar al basamento (Heubeck y Mann, 1991; Hernaiz Huerta, 2000 a y b; Hernaiz Huerta y Pérez Estaún 2002).

La Sierra de Neiba forma parte del denominado terreno de Presqu'île du Nord-Ouest-Neiba, unidad definida con poca precisión y que en su descripción original también incluye la cuenca de San Juan (Mann *et al.*, 1991a) (Fig. 1). Con orientaciones variables de ONO-ESE, NO-SE y E-O, determinadas por el relevo de pliegues de gran radio, esta sierra se compone casi enteramente de calizas de edad Eoceno-Mioceno Inferior (Fm Neiba y equivalentes) y por margocalizas de edad Mioceno (Fm Sombrerito y equivalentes) cabalgantes sobre la cuenca de Enriquillo. En las descripciones bibliográficas (p.e. Mann *et al.*, 1991a), se cita la presencia de rocas volcanosedimentarias ocupando supuestamente el núcleo de los anticlinales. La nueva cartografía ha permitido comprobar que estas rocas, además de tener gran extensión y continuidad, se hallan intercaladas entre las formaciones calcáreas del Eoceno-Mioceno Inferior(Fig. 1). Adicionalmente, el descubrimiento de un pequeño afloramiento de materiales calcáreos con intercalaciones de basaltos con signatura N-Morb, datados como Cretácico Superior, lo sitúa como probable sustrato de esta sierra (Hernaiz Huerta *et al.*, 2007a).

La Sierra de Martín García (Fig. 1) se ha adscrito al mismo dominio paleogeográfico que la Sierra de Bahoruco (Cooper, 1983), sin embargo, nuevas observaciones indican que comparte facies con la parte oriental de la Sierra de Neiba y con la vertiente norte de la Sierra de Bahoruco. En contraste con las sierras paralelas de Neiba y de Bahoruco, la Sierra de Martín García describe un cambio de dirección desde NO-SE en su mitad oriental a E-O o incluso NE-SO en su tercio occidental. Sus márgenes coinciden con fallas inversas de alto ángulo y vergencias opuestas.

La denominación del terreno Hotte-Selle-Bahoruco (Mann *et al.*, 1991a) procede de los nombres de las tres sierras contiguas, las dos primeras en Haití y la tercera en la República Dominicana que con directrices generales ONO-ESE se extienden de oeste a este por el sector meridional de La Española (Fig. 1). La formación más representativa es la Fm Dumisseau (Maurrasse *et al.*, 1979) del macizo de La Selle, con más de 1.500 m de una alternancia de basaltos masivos y basaltos almohadillados no metamórficos, doleritas, calizas pelágicas, cherts, limolitas silíceas y areniscas volcanogénicas, en la que las dataciones paleontológicas (Maurrase *et al.*, 1979) y radiogénicas (Sayeed *et al.*, 1978; van der Berghe, 1983, Bellon *et al.*, 1985), le atribuyen un intervalo entre el Cretácico Inferior a principalmente el Cretácico Superior. En el macizo de la Hotte y en la Sierra de Bahoruco hay formaciones basálticas equivalentes a la Fm Dumisseau, con edades del Maastrichtiense-Paleoceno (Fm Macaya) y del Maastrichtiense, respectivamente. Las similitudes petrológicas y geoquímicas entre los basaltos de la Fm Dumisseau y los basaltos perforados en el DSDP en el mar del Caribe (p.e. “horizonte B”, de edad Coniaciense-Campaniense), permiten interpretar el terreno de Hotte-Selle-Bahoruco como un bloque emergido de la meseta o *plateau* oceánico del Caribe (Maurrase *et al.*, 1979; Sen *et al.*, 1988; Girard *et al.*, 1982). Por encima de la Fm Dumisseau y equivalentes, una importante discontinuidad marca el final del volcanismo basáltico y el comienzo de un régimen esencialmente sedimentario, con predominio de facies carbonatadas y ocurrencias volcánicas, que comprende

el intervalo del Cretácico terminal al Mioceno. Concretamente, en la Sierra de Bahoruco, Llinás (1971) y Mann *et al.*, (1991b) citan por encima de la citada discordancia, la Fm Río Arriba del Cretácico terminal (más de 500 m de espesor) y sobre ella, primero, una serie de calizas pelágicas del Eoceno, asimilable en términos generales a la Fm Neiba (1000-1500 m), y después, un conjunto de calizas masivas con abundantes facies someras que, por su atribución al Mioceno, se correlacionan con la Fm Sombrerito (Fig. 2).

## Síntesis estratigráfica del cinturón de Peralta

### Stratigraphic summary of Peralta belt

En el sector adyacente a la cuenca de Azua estudiado en los proyectos SYSMIN (hojas de San José de Ocoa, Azua, Yayas de Vjajama, Sabana Quéliz), sólo están representados los dos grupos inferiores de los tres regionalmente definidos en el sector SO de este dominio, el Grupo Peralta y el Grupo Río Ocoa, este último no del todo completo. Su depósito se produjo como relleno de una cuenca (de Trois Rivieres-Peralta) desarrollada en la parte trasera del arco de isla del Cretácico Superior, aquí caracterizado por las rocas volcanosedimentarias de la Fm Tireo.

La sedimentación del Grupo Peralta (Fig. 3) es marina y se relaciona con un surco subsidente abierto al SE en el que se depositaron más de 5000 m de serie (Dolan 1988, Heubeck, 1988, Dolan *et al.*, 1991). El contacto basal corresponde a una discordancia de la Fm Ventura o Jura sobre la Fm Tireo, bien visible en el sector al norte de la localidad de Padre las Casas (Díaz de Neira, 2000 a; Díaz de Neira y Hernaiz, 2000). La Fm Ventura, es una sucesión de más de 1000 m de espesor de areniscas, lutitas y margas, con dominio de las areniscas. En las areniscas se reconocen numerosos clastos de plagioclásas y fragmentos de rocas volcánicas y vulcanosedimentarias procedentes de la Fm Tireo. Se ha interpretado que estos sedimentos representan facies de lóbulo correspondientes a sistemas de abanicos submarinos (Hernaiz Huerta, 2000b; Díaz de Neira, 2000 a y b). La parte superior de la formación (últimos 50 m), en el tránsito a la Fm Jura, presenta capas centimétricas de areniscas y lutitas margosas.

Sobre la Formación Ventura, y mediante contacto concordante, la Fm Jura consiste en una sucesión de 200-300 m de espesor medio de calizas tableadas con algunos niveles de margas. El contenido paleontológico está formado por foraminíferos planctónicos y en menor medida bentónicos que datan el Eoceno Medio. Se interpretan como calizas correspondientes a una rampa carbonatada con eventual influencia de tormentas (Hernaiz, 2000b; Díaz de Neira, 2000 a y b). Normalmente presenta un intervalo intermedio más terrígeno (mayor proporción de niveles de calizas arenosas y areniscas, con estructuras tractivas más abundantes), con desarrollo local de brechas. En este tramo intermedio hay que destacar la presencia de intraclastos de calizas con fauna litoral que constituyen los únicos vestigios de las facies de plataforma somera, que no se encontrarían muy distantes. El tránsito a la Fm El Número se realiza por medio de una serie roja de unos 100 m de espesor, que se ha denominado “las Capas rojas del Jura” (Hernaiz Huerta, 2000b). En la Fm El Número hay un predominio de facies margosas y pelíticas que intercalan frecuentes niveles decimétricos de areniscas siliciclásticas y, en menor medida, calcáreas. Su espesor alcanza los 3000 m. Dentro de esta formación se han reconocido al menos 8 niveles de megaturbiditas que resedimentan materiales de las plataformas carbonatadas de la propia Fm El Número. Estas megacapas tienen espesor de orden decamétrico. En la parte superior de la formación se desarrollan hasta 4 intervalos de calizas tableadas y en bancos, de 50 a 100 m de espesor, ocasionalmente muy fosilíferas, que producen fuertes resalte. Su edad, acotada por las formaciones infra y suprayacentes, es Jurásico Superior.

El Grupo Río Ocoa sólo está representado en la zona de estudio por su unidad basal, la Fm Ocoa, que es claramente discordante y erosiva sobre Grupo Peralta (Fig. 4). En términos generales, esta formación se ha definido como un potente conjunto de naturaleza eminentemente pelítica que alberga numerosos olistolitos e intercala frecuentes intervalos olistostómicos y de conglomerados (Bourgois *et al.*, 1979b; Biju Duval *et al.*, 1983; Heubeck, 1988; Dolan *et al.*, 1991). La figura 4 muestra un esquema estratigráfico sintético de esta formación en la zona San José de Ocoa (Hernaiz Huerta, 2000b), donde su espesor supera los 8000 m. Su sedimentación se produjo en un surco muy subsidente y alargado, abierto al SSE (Heubeck, 1988; Dolan *et al.*,

1991). Este surco estaba delimitado al NE por un margen activo (cabalgamiento frontal del basamento) y al SO por un margen pasivo, posiblemente definido (al menos en parte) por las calizas tableadas de la Fm Neiba (aproximadamente equivalentes a la Fm. Jura en el sustrato de la Cuenca de Azua). Al N y NNE, en las zonas más proximales del sistema, se preservan las facies clásticas someras, representadas por depósitos conglomeráticos que hacia el S y SO pasan a términos fanglomeráticos y pelíticos con intercalaciones de materiales olistostómicos (Díaz de Neira y Hernaiz, 2000). En las posiciones más distales, al S y SO, se reduce la presencia de los niveles olistostómicos y predominan los términos turbidíticos (Díaz de Neira 2000b). Bourgois *et al.* (1979), identificaron en esta formación una asociación de fauna atribuida al Eoceno Superior, que es también la edad asignada por Heubeck (1988) y Dolan *et al.*, (1991). Sin embargo no se descarta que sus términos conglomeráticos superiores sean correlacionables con la Fm El Limonar de Heubeck (1988) en cuyo caso su edad se extendería hasta el Oligoceno.

### **Sintesis estratigrafica de las Sierras de Neiba, Martin Garcia y del margen norte de la Sierra de Bahoruco.**

### **Stratigraphic summary of the Sierras de Neiba, Martin Garcia, and northern margin Sierra de Bahoruco**

La nueva cartografía de la Sierra de Neiba identifica el Cretácico Superior en un bloque (Unidad de El Manguito) entre afloramientos de formaciones paleógenas (Hernaiz Huerta 2004a; Hernaiz Huerta 2006, Hernaiz Huerta *et al.*, 2007). La Unidad de El Manguito consiste en alternancias de calizas grises recristalizadas y lutitas negras que intercalan basaltos de afinidad oceánica (signatura N-Morb, Escuder Viruete, 2004), correlacionables con la sucesión cretácea de Bahoruco (p.e. Fm Río Arriba). Esta correlación permite interpretar la Unidad de El Manguito como el sustrato de las series paleógenas de la Sierra de Neiba, y ello permite prolongar al menos hasta esta sierra, la extensión del *plateau* oceánico del Caribe (Hernaiz Huerta 2004a, Hernaiz Huerta 2006, Hernaiz Huerta *et al.*, 2007).

Sobre este basamento, la Formación carbonatada de Neiba (*sensu lato*) comprende el intervalo Eoceno Inferior-Mioceno Inferior (Fig. 3). En la parte centro-oriental y septentrional de la sierra, la intercalación del Conjunto Volcanosedimentario de El Aguacate de Neiba ha permitido separar, por encima y por debajo de él, respectivamente, una Fm Neiba inferior y una Fm Neiba superior (Hernaiz Huerta 2004a, 2004b; Hernaiz Huerta *et al.*, 2007) (Fig. 5). Con espesores de más de 1.000m y de 300-1.000m respectivamente, ambas unidades están formadas por una sucesión monótona de calizas con sílex (tableadas y en bancos la primera, tableadas y con intercalaciones margosas en los términos superiores, la segunda), que corresponden a ambientes de plataforma externa. La Fm Neiba inferior incluye en su parte más alta un nivel de calizas con corales, que indica una somerización de la plataforma antes del depósito de las rocas vulcanosedimentarias del Complejo El Aguacate. La ausencia del conjunto volcanosedimentario en la parte meridional y occidental de la sierra, limita arealmente la subdivisión propuesta para la Fm Neiba, con la complicación adicional de que la Fm Neiba inferior y el tramo basal de la Fm Neiba superior están sustituidos por brechas calizas y carniolas, formando una nueva unidad cartográfica denominada informalmente Fm Neiba brechoide (Fig. 5). Los clastos de la brecha son mayoritariamente calizas arrecifales con macroforaminíferos de plataforma interna. El origen de la brechificación aparenta ser diagenético, al estar los clastos poco removidos y atravesar los contactos litológicos entre formaciones. En el margen norte de la Sierra de Bahoruco y en la vertiente sur de la Sierra de Martín García las facies de la Fm Neiba caracterizan a la Fm Neiba superior.

El Conjunto Volcanosedimentario de El Aguacate de Neiba (Figs. 5 y 6), está formado por 200-600m de rocas volcánicas y sedimentarias con gran continuidad cartográfica en la parte septentrional de la sierra. Son brechas y tufitas con intercalaciones de andesitas y basaltos, alternando con asociaciones de calcarenitas y margas; calizas, margocalizas y margas; conglomerados, brechas polimicticas grauvacas y calizas. El medio deposicional es una plataforma con cinturones de facies carbonatadas de someras a profundas, que incorpora productos piroclásticos y coladas. La signatura volcánica obtenida en el vulcanismo es similar a la de los

basaltos OIB intraplaca, y los relaciona, posiblemente, con el ascenso de una pluma mantélica (Escuder Viruete, 2004; Hernaiz Huerta *et al.*, 2007)

No se han precisado biozonas en la Fm Neiba, no obstante, las asociaciones de fauna y su posición estratigráfica, restringen la Fm Neiba inferior al Eoceno Inferior-Medio, la Fm Neiba superior, al Eoceno Superior-Mioceno Inferior y el Conjunto Volcanosedimentario de El Aguacate, al intervalo Eoceno Medio-Superior. La Fm Neiba brechoide comprende desde el Eoceno Inferior al Superior (Hernaiz Huerta 2004a, 2004b; Hernaiz Huerta *et al.*, 2007a). Dos dataciones absolutas obtenidas en el Conjunto Volcanosedimentario de El Aguacate por los métodos U/Pb y Ar/Ar dan resultados muy similares,  $51,7 \pm 0,5$  Ma y  $50,1 \pm 3,4$  Ma respectivamente (Friedman, 2004; Ullrich, 2004) y coinciden con una datación anterior por el método K/Ar, 52.7 Ma (Bellon *et al.*, 1985).

La Fm Sombrerito se superpone a la Fm Neiba por un contacto paraconforme, localmente marcado por un nivel de brechas volcánicas o brechas sedimentarias con cantos de rocas volcánicas, erosivas sobre el infrayacente, que sugieren una discontinuidad regional (Fig. 5). Consiste en más de 500 m de margas ocres con intercalaciones variables de calcarenitas, que forman tramos cartográficos. En la serie más completa del NE de la sierra se distinguen tres tramos, inferior, medio y superior, los dos últimos denominados respectivamente Mb Loma de La Patilla (75-100m de espesor) y Mb Gajo Largo (0-200m) (Díaz de Neira, 2004a). El medio de depósito se sitúa en el tránsito entre la llanura submarina y los sistemas turbidíticos carbonatados que la alimentan, e implica una profundización de la cuenca respecto a la formación infrayacente. En algunos sinclinales del sector oriental de la sierra, y en la ladera meridional, la Fm Sombrerito parece estar representada únicamente por su tramo inferior.

En el sector occidental de la sierra y en la ladera sur al oeste de La Descubierta, la Fm Sombrerito consiste en más de 250 m de calizas masivas, mayoritariamente arrecifales, de aspecto carniolar y pulverulento (Hernaiz Huerta, 2004b). En los afloramientos más occidentales de la hoja de Boca Cachón, incluye alternancias decimétricas de calcarenitas, margocalizas y margas de tonos ocres, o niveles de calizas bioclásticas con gasterópodos y corales retrabajados junto a tramos de lavas vesiculares, brechas, aglomerados y tobas (Deschamps, 2004). En la Sierra de Bahoruco las facies carniolares masivas con intervalos subordinados calcareníticos y margosos se han definido como Mb Barahona (Díaz de Neira, 2004b). Por lo tanto, de este a oeste a lo largo la Sierra de Neiba, y hacia el sur, la Fm Sombrerito presenta un cambio de facies no del todo bien caracterizado. La Unidad de Cortadero (Hernaiz Huerta, 2004 b), formada por calizas tableadas profundas y calizas arrecifales aflora a lo largo del flanco meridional de este sierra en su parte media y oriental y se piensa que puede representar una unidad de tránsito entre los dos tipos de facies citadas.

En la Sierra de Martín García, los términos inferiores de la Fm Sombrerito contienen facies arrecifales similares al Mb Barahona y facies de plataforma abierta. La serie culmina con el Mb Gajo Largo.

Finalmente la unidad del Majagual, es similar en litología y edad a la Unidad de Cortadero, pero por su posición cartográfica poco clara en mitad de la Fm Neiba brechoide y en parte cabalgada por ésta, se ha tratado como una unidad aparte.

## Síntesis estratigráfica de las cuencas de Herniquillo y Azua

### Stratigraphic summary of Erníquillo and Azua basins

El relleno de la cuenca de Enriquillo comienza con la Fm Trinchera (Figs. 2 y 7). Su corte más característico es el talud de la carretera de Azua a Barahona, al SO de la localidad de Fondo Negro, que a su vez coincide con su máximo espesor (McLaughlin *et al.*, 1991). Desde este corte la formación disminuye de espesor hacia el este y hacia el oeste, acuñándose en el subsuelo del lago Enriquillo. En el citado corte de la carretera, la Fm Trinchera es una sucesión rítmica de más de 1.500m de margas y areniscas siliciclásticas, interpretada como depósitos de un sistema deltaico-turbidítico progradante: facies turbidíticas con predominio margoso de *levee* distal en la parte inferior, facies areniscosas canalizadas y de margen de canal en la parte media, y secuencias negativas de barras deltaicas en la superior. En el sinclinal de Vallejuelo del interior de la

Sierra de Neiba, los términos superiores de la serie se asemejan a los descritos en la cuenca de Azua y en el sector meridional de la cuenca de San Juan (Hernaiz Huerta, 2004a), con intercalaciones de conglomerados y areniscas con laminación paralela, *hummocky ripples* de oleaje y un mayor grado de bioturbación, indicativo de medios más someros, posiblemente una llanura deltaica. En estas localidades la Fm Trinchera erosiona al Mb Gajo Largo y parcialmente al Mb Loma de la Patilla de la Fm Sombrerito. La Fm Trinchera es significativamente la primera que incorpora grandes volúmenes de materiales del arco de isla (Fm Tireo). Su edad se atribuye al intervalo Mioceno Superior-Plioceno Inferior (McLaughlin *et al.*, 1991).

La Fm Quita Coraza es de dominancia margosa con intercalaciones decimétricas de areniscas y calizas margosas (Figs. 2 y 7). El espesor máximo supera los 400m y se adelgaza hacia el centro de la cuenca de Enriquillo y hacia el extremo oriental de la cuenca de Azua. Su edad se atribuye sin demasiada precisión al Plioceno Inferior (McLaughlin *et al.*, 1991). Se interpreta como una bahía abierta progresivamente más somera.

La Fm Angostura es característica de la cuenca de Enriquillo (Figs. 2 y 7). Su base no aflora, pero según los datos del sondeo Charco Largo, se depositó directamente sobre una Fm Trinchera muy adelgazada (271m). Su espesor máximo (1.582m) en el centro de la cuenca de Enriquillo coincide aproximadamente con el sondeo Charco Largo y se acuña o cambia de facies rápidamente de forma centrífuga. Lateralmente equivale a parte de la Fm Quita Coraza y sus términos superiores a la parte inferior de la Fm Arroyo Blanco-Las Salinas. El sondeo Charco Largo atravesó halita con intercalaciones de arcillas verdes, más frecuentes a techo. El mejor corte en superficie es la Mina de Sal y Yeso con un tramo inferior halítico (200m), un tramo intermedio yesífero (300m) y un tramo superior de yesos y arcillas (50m). La Fm Angostura se sedimentó en una cuenca subcircular de tipo lagunar con un ambiente costero hipersalino (Mann *et al.*, 1999). Algunas asociaciones de ostrácodos datan el techo como Plioceno Inferior (McLaughlin *et al.*, 1991; Mann *et al.*, 1999).

Las formaciones Arroyo Blanco y Las Salinas constituyen el relleno de las cuencas de Azua y Enriquillo durante la parte media y alta del Plioceno (Figs. 2 y 7). Su similitud de facies, edad y posición estratigráfica permite agruparlas en una misma unidad heterolítica de lutitas con intercalaciones de orden métrico y decamétrico de areniscas y conglomerados, calizas arrecifales y yesos. Estos últimos son especialmente abundantes en el sector oriental de la cuenca de Enriquillo, al norte de Vicente Noble. En el margen meridional de la cuenca de Enriquillo (sector de La Salina) yace sobre la Fm Angostura con un nivel guía bioclástico de 2m de espesor en su base ("razorback ridge") (Mann *et al.*, 1999). Los espesores aflorantes en la cuenca de Enriquillo superan 1.000 m, y alcanza 2.182 m en el sondeo Charco Largo, que coincide aproximadamente con el depocentro. La Fm Arroyo Blanco-Las Salinas se depositó en un medio deltaico de tendencia progradante hacia el sur, con una paleogeografía compleja que integra variedad de subambientes: parches arrecifales y barras de desembocadura, llanura deltaica correspondientes a ambientes lagunares y de llanura mareal con canales, y canales distributarios de dominancia fluvial y lóbulos de *crevasse*. Las facies más distales (prodelta) se reconocen en el sector SO de la cuenca (Ardévol, 2004). Los conglomerados son más abundantes hacia los márgenes de la cuenca con área fuente en las sierras en curso de elevación; es el caso de los conglomerados que orlan la Sierra de Neiba en las hojas de Galván y La Descubierta con espesores próximos a 1.000 m. Forman ciclos métricos que culminan en margas y lutitas margosas interpretados como ciclos retrogradantes de abanicos aluviales. Por su fauna de ostrácodos y foraminíferos, la Fm Arroyo Blanco-Las Salinas se atribuye al Plioceno, pero su posición estratigráfica entre las formaciones de Quita Coraza y Angostura y de Arroyo Seco y Jimaní, se atribuye al Plioceno Medio-Superior (McLaughlin *et al.*, 1991; Mann *et al.*, 1999).

La Fm Arroyo Seco culmina el relleno de la cuenca de Enriquillo en su sector norte y noreste (Figs. 2 y 7). El corte más representativo es el del río Barrera (hoja de La Descubierta) con más de 800 m de conglomerados organizados en un mínimo de once ciclos granocrecientes formando cuñas rotadas que se abren hacia el sur (Ardévol, 2004). En cada ciclo se distingue un término inferior de lutitas, areniscas y conglomerados y un término superior conglomerático. Su edad se atribuye al Plioceno Superior y con incertidumbre al Pleistoceno Inferior (McLaughlin *et al.*, 1991; Hernaiz Huerta, 2004 a, 2004b)

La Fm Jimaní es característica del sector occidental de la cuenca de Enriquillo (Figs. 2 y 7). Su base es discordante sobre la Fm Arroyo Blanco, cambiando de facies de un corte a otro. En la serie de Los Cuarteles de la hoja de La Descubierta se han medido más de 600m de calizas tableadas con ostrácodos y gasterópodos en la base, un primer tramo de conglomerados continentales al que sucede una alternancia de margas y calcarenitas y un resalte de más de 100m de calizas arrecifales, y por último, un potente ( $>300$ m) paquete de conglomerados y brechas calcáreas de tonos rojizos. El medio de depósito es una bahía poco profunda con conexiones intermitentes con el mar Caribe, que evoluciona desde un ambiente perimareal confinado a un medio restringido, posteriormente a un ambiente periarrecifal y por último a abanicos aluviales-*fan deltas* que en su parte inferior se interdigitan con parches arrecifales. Las dataciones indican una edad Plioceno Superior-Pleistoceno (McLaughlin *et al.*, 1991; Deschamps, 2004).

Una ultima transgresión marina desde la bahía de Neiba, datada en 9020 BP, permitió el crecimiento de un sistema arrecifal expuesto en la periferia del lago Enriquillo (Mann *et al.*, 1984; Taylor *et al.*, 1985). En este sistema, formado sobre una pendiente deposicional, se reconoce un nivel basal de ostreidos, un cuerpo principal formado por corales masivos o ramosos y un término superior supra-arrecifal coetáneo o coronado por estromatolitos algales. La súbita irrupción por el este de los depósitos deltaicos del Río Yaque (5000 BP), provocó la desconexión con la bahía, la muerte de los arrecifes y el tránsito al sistema lacustre actual (Mann *et al.*, 1984; Taylor *et al.*, 1985; Díaz de Neira, 2004a, 2004b).

La estratigrafía de la Cuenca de Azua es muy similar, pero más sencilla que la de Enriquillo (Figs. 2 y 7). Se reconocen las siguientes formaciones de edad Mioceno-Pleistoceno Inferior (fig. 6): Trinchera, Quita Coraza, Arroyo Blanco y Arroyo Seco García y Harms (1988) McLaughlin *et al.* (1991), Díaz de Neira, 2000b; Díaz de Neira y Solé (2000). La Fm Trinchera alcanza, con sus facies turbidíticas habituales, un espesor de 1.000-2.700m. En el entorno de algunas estructuras anticlinales (p.e. de la Bahía de Ocoa), puede estar ausente y sus facies, pasan a ser más proximales (Díaz de Neira y Solé 2000). La Fm Quito Coraza está formada, igual que en la cuenca de Enriquillo por margas en las que se intercalan delgados niveles de areniscas, y su espesor puede alcanzar 700m. A nivel regional no siempre está presente entre las Fms. Trinchera y Arroyo Blanco Conforme a la tendencia regional, a partir del Plioceno Inferior en la cuenca de Azua los sistemas sedimentarios evolucionaron a ambientes progresivamente más someros y progradaron, de NO a SE y de NE a SO, completando el relleno de la cuenca en un régimen de transición a continental o netamente continental (McLaughlin *et al.*, 1991; Díaz de Neira, 2000b; Díaz de Neira y Solé, 2000). Al primero corresponden los más de 700 m de conglomerados, areniscas, lutitas y, eventualmente, calizas arrecifales, de la Fm Arroyo Blanco. Al segundo, los cerca de 800 m de conglomerados de la Fm Arroyo Seco, todos ellos generados en un amplio sistema de abanicos aluviales.

## Bibliografía

- Ardévol, Ll., 2004. Informe Sedimentológico de los Proyectos “L” y “K” de Cartografía Geotemática de la República Dominicana. Programa SYSMIN. Dirección General de Minería, Santo Domingo
- Bellon, H., Villa, J.M., Mercier De Lepinay, B., 1985. Chronologie  $^{40}\text{K}$ - $^{39}\text{Ar}$  et affinités geoquimiques des manifestations magnétiques au Crétace et au Paleogene dans L’ille d’Hispaniola. Geodynamique des Caraïbes, Editions Technip, 12-24
- Biju-Duval, B., Bizon, B., Mascle, A., Muller, C., 1983. Active margin processes; field observations in southern Hispaniola. En J.S. Watkins, C.L. Drake, (eds.). Studies in continental margin geology. American Association of Petroleum Geologist Memoir, 34, 325-346
- Cooper, C., 1983. Geology of the Fondo Negro region, Dominican Republic. MSc Thesis, State University of New York, Albany, 145 p
- Deschamps, I., 2004. Mapa Geológico de la hoja a E. 1:50.000 n° 5871-IV (Boca Cachón) y Memoria correspondiente. Proyecto “L” (Zona SO) de Cartografía Geotemática de la República Dominicana. Programa SYSMIN. Dirección General de Minería, Santo Domingo.

Díaz de Neira, J.A., 2000 a. Mapa Geológico de la Hoja a E. 1:50.000 nº 6072-III (Padre Las Casas) y Memoria correspondiente. Proyecto “C” de Cartografía Geotemática de la República Dominicana. Programa SYSMIN. Dirección General de Minería, Santo Domingo

Díaz de Neira, J.A., 2000 b. Mapa Geológico de la Hoja a E. 1:50.000 nº 6071-II (Azua) y Memoria correspondiente. Proyecto “C” de Cartografía Geotemática de la República Dominicana. Proyecto de Cartografía Geotemática de la República Dominicana. Programa SYSMIN. Dirección General de Minería, Santo Domingo

Díaz de Neira, J.A., 2004 a. Mapa Geológico de la Hoja a E. 1:50.000 nº 5971-I (Villarpando) y Memoria correspondiente. Proyecto “L” (Zona SO) de Cartografía Geotemática de la República Dominicana. Programa SYSMIN. Dirección General de Minería, Santo Domingo.

Díaz de Neira, J.A., Hernaiz Huerta, P.P., 2000. Mapa Geológico de la Hoja a E. 1:50.000 nº 6072-II (Sabana Quéliz) y Memoria correspondiente. Proyecto “C” de Cartografía Geotemática de la República Dominicana. Programa SYSMIN. Dirección General de Minería, Santo Domingo.

Díaz de Neira, J.A., Solé, F.J., 2002. Precisiones estratigráficas sobre el Neógeno de la Cuenca de Azua. Acta Geologica Hispanica. En A. Pérez-Estaún, I. Tavares, A. García Cortes, P.P. Hernaiz Huerta (eds.). Evolución geológica del margen norte de la Placa del Caribe, República Dominicana. Acta Geológica Hispánica, 37 163-181

Dolan, J.F., 1988. Paleogene sedimentary basin development in the eastern Greater Antilles; three studies in active-margin sedimentology. Ph.D. Thesis, University of California, Santa Cruz, 235 p.

Dolan, J.F., Mann, P., De Zoeten, R., Heubeck, C., Shiroma, J., Monechi, S., 1991. Sedimentologic, stratigraphic, and tectonic synthesis of Eocene-Miocene sedimentary basins, Hispaniola and Puerto Rico. En P. Mann, G. Draper, J.F. Lewis (eds.), Geologic and tectonic development of the North America-Caribbean plate boundary in Hispaniola. Geological Society of America Special Paper 262, 217-263

Escuder Viruete, J., 2004 a. Informe de Petrología y Geoquímica de las Rocas Ígneas y Metamórficas del Proyecto L (Zonas Este y Suroeste) de Cartografía Geotemática de la República Dominicana Programa SYSMIN. Dirección General de Minería, Santo Domingo

Garcia, E., Harms, F., 1988. Informe del Mapa Geológico de la Republica Dominicana escala 1:100.000, San Juan (4972). Santo Domingo, 97 p

Girard, D., Beck, C., Stephan, J.F., Blanchet, R., Maury, R., 1982. Pétrologie géochimie et signification géodynamique de quelques formations volcaniques crétacées péri-caraïbes. *Bulletin de la Société Géologique de France*, 24, 535-544

Hernaiz Huerta, P.P., 2000 a. Mapa Geológico de la Hoja a E. 1:50.000 nº 6172-III (Arroyo Caña) y Memoria correspondiente. Proyecto “C” de Cartografía Geotemática de la República Dominicana. Programa SYSMIN. Dirección General de Minería, Santo Domingo.

Hernaiz Huerta, P.P., 2000 b. Mapa Geológico de la Hoja a E. 1:50.000 nº 6071-I (San José de Ocoa) y Memoria correspondiente. Proyecto “C” de Cartografía Geotemática de la República Dominicana. Programa SYSMIN. Dirección General de Minería, Santo Domingo

Hernaiz Huerta, P.P., 2004 a. Mapa Geológico de la Hoja a E. 1:50.000 nº 5971-IV (Galván) y Memoria correspondiente. Proyecto “L” (Zona SO) de Cartografía Geotemática de la República Dominicana. Programa SYSMIN. Dirección General de Minería, Santo Domingo

Hernaiz Huerta, P.P., 2004 b. Mapa Geológico de la Hoja a E. 1:50.000 nº 5871-I (La Descubierta) y Memoria correspondiente. Proyecto “L” (Zona SO) de Cartografía Geotemática de la República Dominicana. Programa SYSMIN. Dirección General de Minería, Santo Domingo

Hernaiz Huerta, P.P., Pérez-Estaún, A., 2002. Estructura del cinturón de pliegues y cabalgamientos de Peralta, República Dominicana. En A. Pérez-Estaún, I. Tavares, A. García Cortes, P.P. Hernaiz Huerta (eds.). Evolución geológica del margen norte de la Placa del Caribe, República Dominicana. Acta Geológica Hispánica, 37, 183-205

- Heubeck, C., 1988. Geology of the southeastern termination of the Cordillera Central, Dominican Republic. M.A. Thesis. University of Texas, Austin, 333 p
- Heubeck, C., Mann, P., 1991. Structural Geology and Cenozoic Tectonic History of the Southeastern Termination of the Cordillera Central, Dominican Republic. En P. Mann, G. Draper, J.F. Lewis, (eds.), Geologic and tectonic development of the North America-Caribbean plate boundary in Hispaniola. Geological Society of America Special Paper 262, 315-336
- Heubeck, C., Mann, P., Dolan, J., Monechi, S., 1991. Diachronous uplift and recycling of sedimentary basins during Cenozoic tectonic transpression; northeastern Caribbean plate margin. *Sedimentary Geology*, 70, 1-32
- Llinas, R.A. 1971. Geología del área Polo-Duvergé, Cuenca de Enriquillo, República Dominicana. Tesis Doctoral. México City, México, Universidad Nacional Autónoma de México, Facultad de Ingeniería, 83 p
- Mann, P., Burke, K., Matsumoto, T., 1984 . Neotectonics of Hispaniola; Plate motion, sedimentation and seismicity at a restraining bend. *Earth and Planetary Science Letters*, 70, 311-324
- Mann, P., Draper, G., Lewis, J.F., 1991 b. An overview of the geologic and tectonic development of Hispaniola. En P. Mann, G. Draper, J.F. Lewis (eds.), Geologic and tectonic development of the North America-Caribbean plate boundary in Hispaniola. Geological Society of America Special Paper 262, 1-28
- Mann, P., McLaughlin, P.P., Cooper, C., 1991d. Geology of the Azua and Enriquillo basins, Dominican Republic; 2, Structure and tectonics. En P. Mann, G. Draper, J.F. Lewis (eds.), Geologic and tectonic development of the North America-Caribbean plate boundary in Hispaniola. Geological Society of America Special Paper 262, 367-390
- Mann, P., McLaughlin, P., Van den Bold, W.A., Lawrence, S.R., Lamar, M.E., 1999. Tectonic and Eustatic Controls on Neogene Evaporitic and Siliciclastic Deposition in the Enriquillo Basin, Dominican Republic. En P. Mann (ed.), Caribbean Basins. *Sedimentary Basins of the World*, 4 (Series
- Maurrasse, F.J.-M., G., Husler, J., Georges, G., Schmitt, R., Damond, P., 1979. Upraised Caribbean sea-floor below acoustic reflector B" and the Southern Peninsula of Haiti. *Geologie en Mijnbouw*, 8, 71-83
- McLaughlin, P.P., Van Den Bold, W.A., Mann, P., 1991. Geology of the Azua and Enriquillo basins. Dominican Republic; 1, Neogene lithofacies, biostratigraphy, biofacies, and paleogeography. En P. Mann, G. Draper, J.F. Lewis (eds.), Geologic and tectonic development of the North America-Caribbean plate boundary in Hispaniola. Geological Society of America Special Paper 262, 337-366.
- Norconsult, 1983. Dominican Republic. Petroleum Exploration Appraisal. Report for Dirección General de Minería. Santo Domingo, 81 p
- Pindell, J. L., Barrett, S. F., 1990. Geological evolution of the Caribbean region: a plate tectonic perspective. En G. Dengo, J.E. Case (eds.), The Caribbean, Volume H, Decade of North American Geology. Geological Society of America, Boulder, Colorado, 404-432
- Sayeed, U., Maurrasse, F., Keil, K., Husler, J., Smith, R., 1978. Geochemistry and petrology of some mafic rocks from Dumisseau, Haïti. *EOS Transactions of the American Geophysical Union*, 59, 403
- Sen, G.R., Hickey-Vargas, G., Waggoner, Marausse F., 1988. Geochemistry of basalts from the Dumisseau Formation, southern Haiti; Implications for the origin of the Caribbean crust. *Earth Planetary Science Letters*, 87, 423-437
- Taylor, F.W., Mann, P., Valastro, S., and Burke, K., 1985. Stratigraphy and radiocarbon chronology of a subaerially exposed Holocene coral reef, Dominican Republic. *Journal of Geology*, 93, 311-332
- van den Berghe, B. 1983. Evolution sédimentaire et structurale depuis le Paleocene de secteur "Massif de la Selle-Barouco-Nord de la Ride de Beata" dans l'orogenie nor Caraïbe (Hispaniola Grandes Antilles). These de doctorat, Universidad Marie y Pierre Curie, Paris, 205 p
- Witschard, M., Dolan, J.F., 1990. Contrasting structural styles in siliciclastic and carbonate rocks of an offscraped sequence; The Peralta accretionary prism, Hispaniola. *Geological Society of America Bulletin*, 102; 792-806

## Figures

Fig. 1. Mapa geológico simplificado del sector SO de la República Dominicana

Fig. 1. Simplified geological map of SW Dominican Republic

Fig. 2. Síntesis estratigráfica de sector SO de la República Dominicana

Fig. 2. Stratigraphic summary of SW Dominican Republic

Fig. 3. Columna estratigráfica sintética del Grupo Peralta en el sector de Ocoa. Según Solé, en Hernaiz Huerta (2000b)

Fig. 3. Simplified stratigraphic log of Peralta Group in Ocoa area. After Solé, in Hernaiz Huerta (2000b)

Fig. 4. (A) Columna estratigráfica sintética de la Fm Ocoa en la terminación SE del Cinturón de Peralta, según Solé, en Hernaiz Huerta (2000b); (B) Serie sintética de la Fm. Ocoa en el sector oriental de la hoja de San José de Ocoa, según Hernaiz Huerta (2000b)

Fig. 4. (A) Simplified stratigraphic log of Ocoa Fm in the SE end of Peralta Belt, after Solé, in Hernaiz Huerta (2000b); (B) Synthetic log of Ocoa Fm in eastern area of San José de Ocoa sheet, según Hernaiz Huerta (2000b)

Fig. 5. Correlación de columnas estratigráficas sintéticas de las formaciones de la sierra de Neiba en las hojas de Galván y La Descubierta. Según Hernaiz Huerta 2006

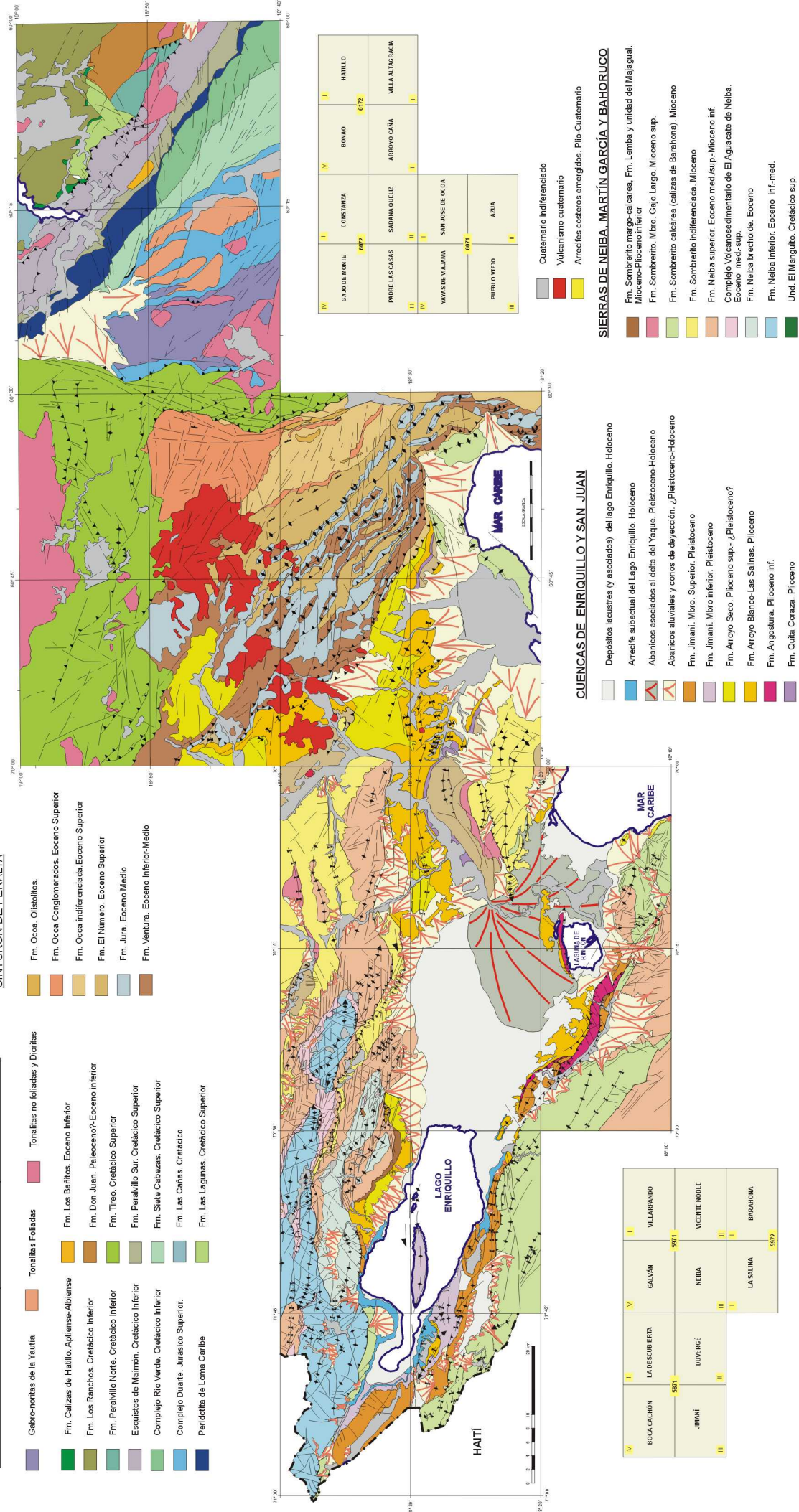
Fig. 5. Stratigraphic correlation of Sierra de Neiba formations simplified logs in Galván and La Descubierta sheets. Alter Hernaiz Huerta 2006

Fig. 6. Esquema de distribución de litologías y unidades del conjunto volcanosedimentario de El Aguacate en la sierra de Neiba. Según Hernaiz Huerta 2006.

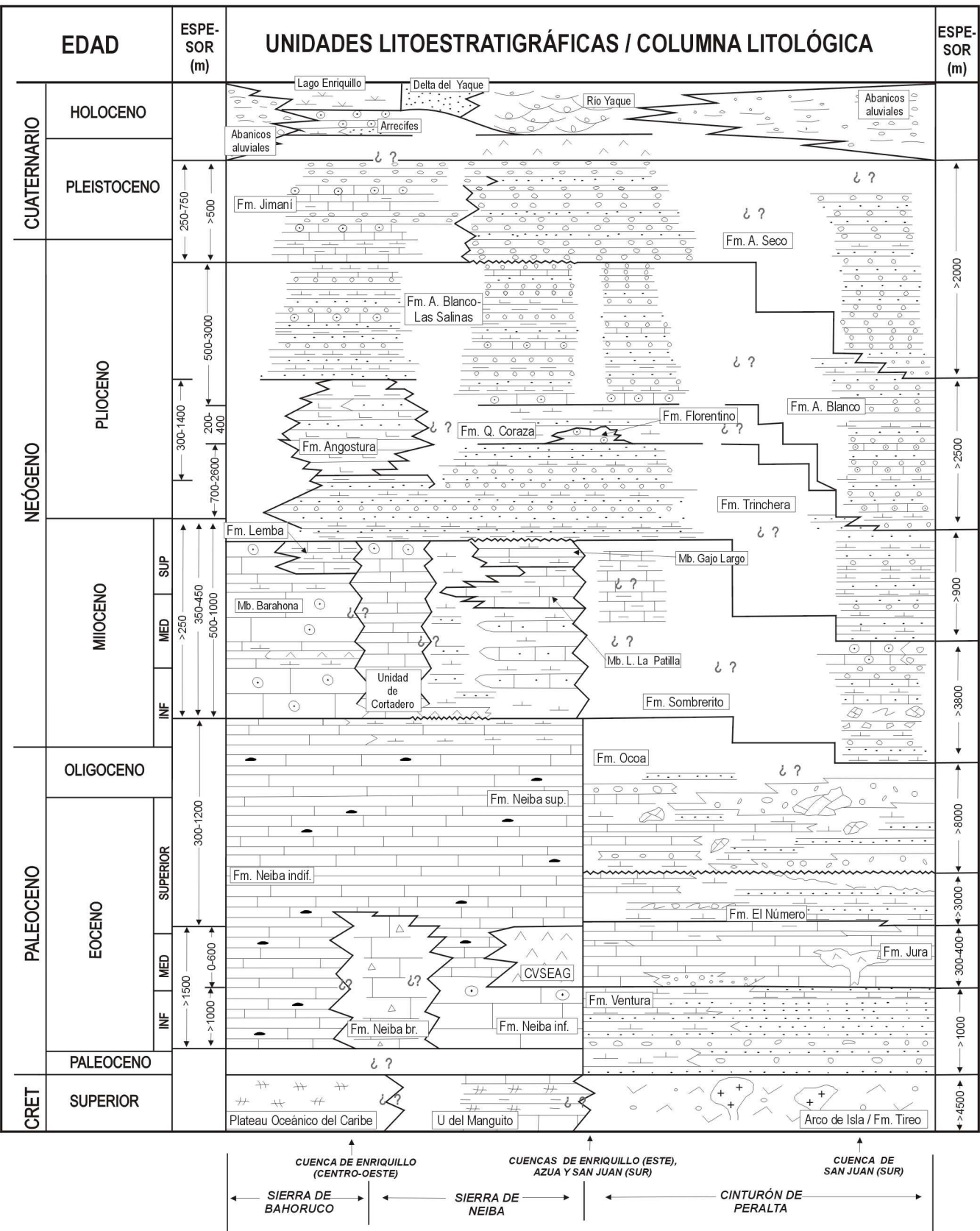
Fig. 6. Lithologies and units distribution of El Aguacate volcanosedimentary complex. After Hernaiz Huerta 2006.

Fig. 7. Columnas estratigráficas sintéticas de las cuencas de Enriquillo (elaborada a partir de la descripción y la columna del sondeo Charco Largo de Mann *et al.*, 1999) y Azua (según Solé, en Díaz de Neira, 2000 b)

Fig. 7 Simplified stratigraphic logs of Enriquillo (deduced from the description and the Charco largo oil exploration log of Mann *et al.*, 1999) and Azua basins (after Solé, in Díaz de Neira, 2000 b)



# SÍNTESIS ESTRATIGRÁFICA DEL SECTOR SO DE LA REPÚBLICA DOMINICANA

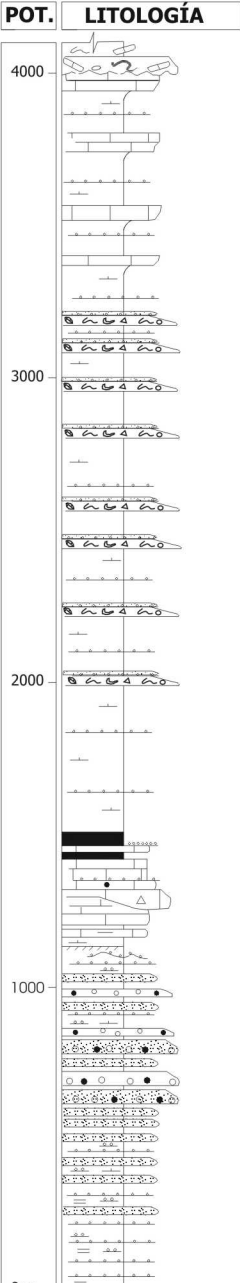


LEYENDA DE LITOLOGÍAS Y FACIES

	Caliza		Margocalizas		Marga		Arenisca		Olistolitos		Vulcanismo de arco de isla
	Caliza con Silex		Calcareita		Lutita		Depósito de debris flow		Conglomerado		Basalto oceánicos
	Caliza brechoide		Caliza arrecifal		Sales y Yesos		Slumps		Episodios volcánicos		Granitoides

# GRUPO PERALTA

EDAD	POT.	LITOLOGÍA
EOCENO		
SUPERIOR		
INFERIOR		

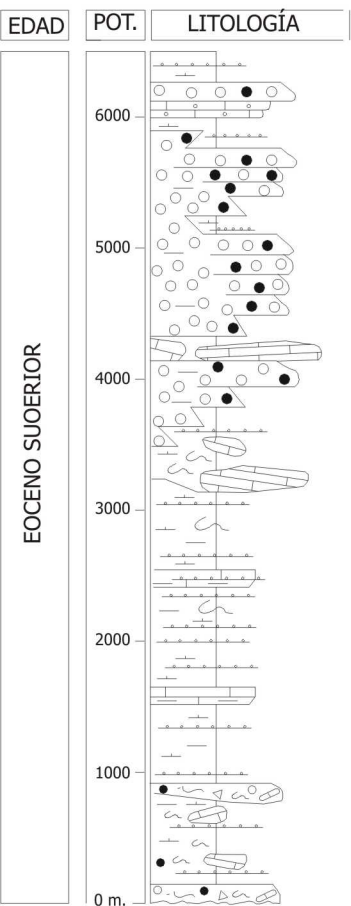
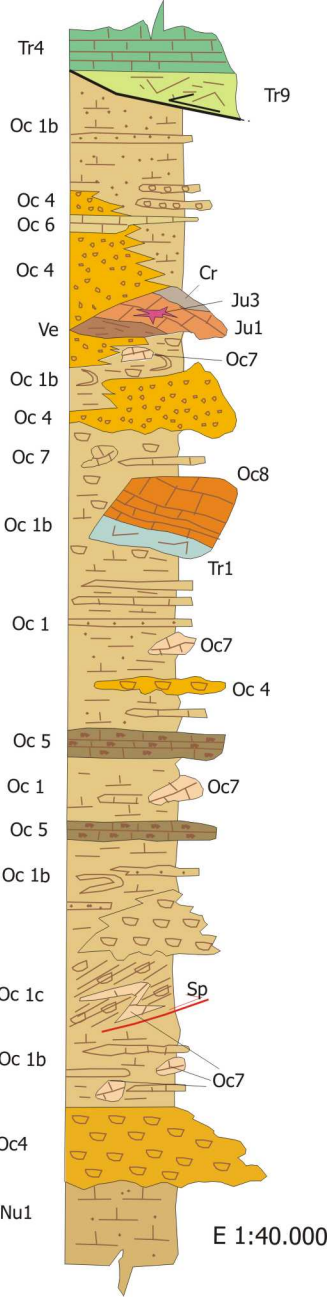


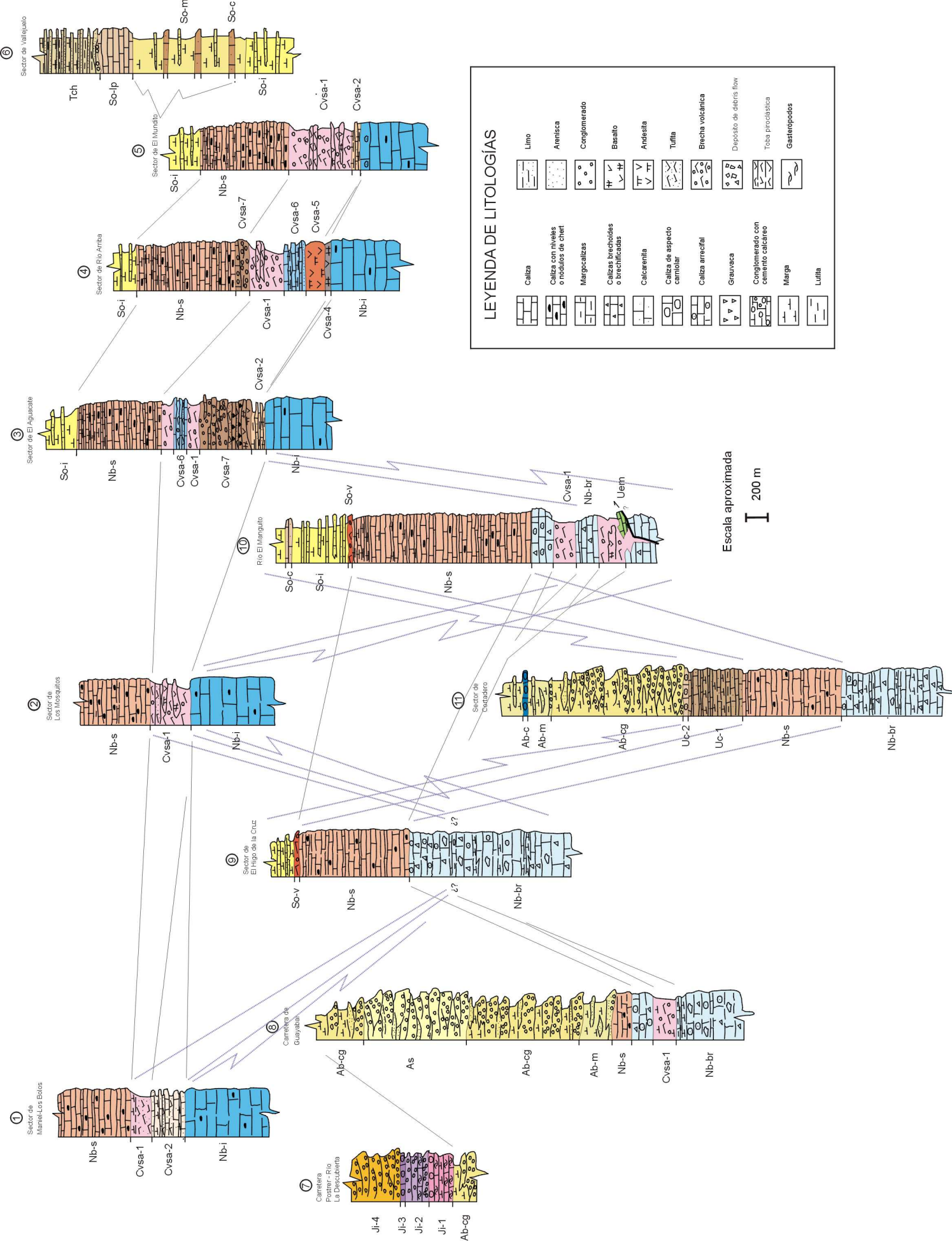
UNIDADES LITOESTRATIGRÁFICAS
GRUPO RÍO OCOA
Fm. EL NÚMERO
GRUPO PERALTA
CAPAS ROJAS DEL JURA
Fm. JURA
Fm. VENTURA

TR.  
SUP.

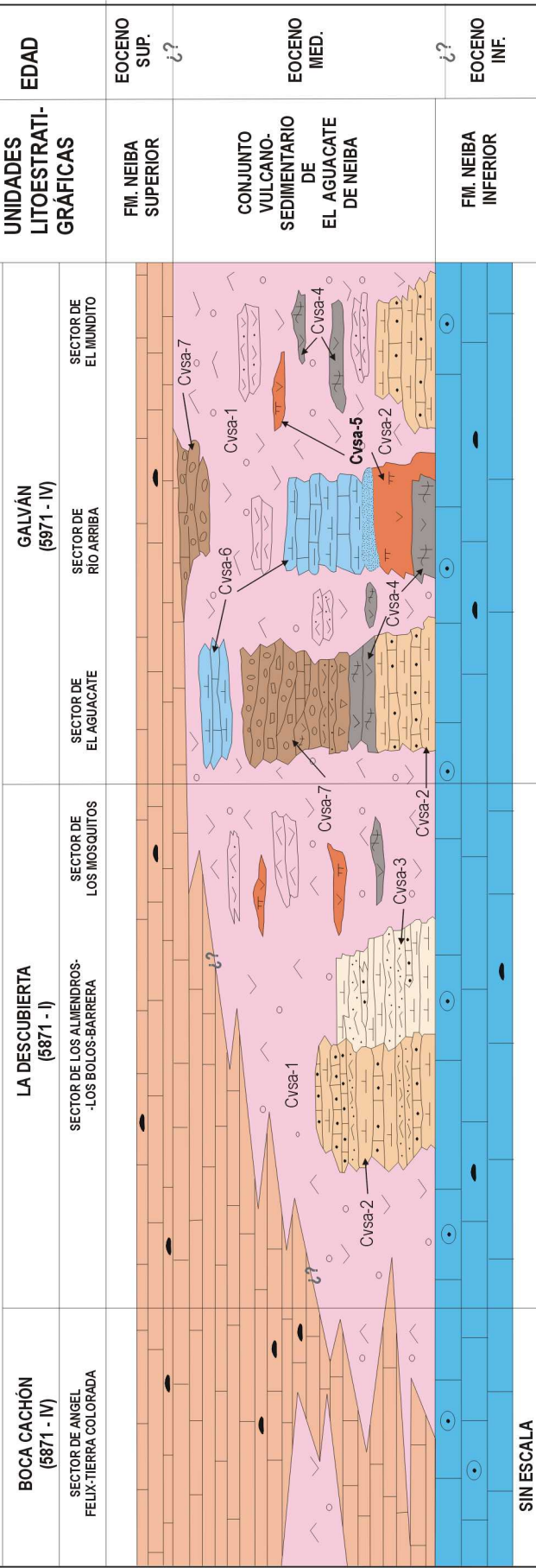
TR.  
MED.

TR.  
INF.

**A)****B)**

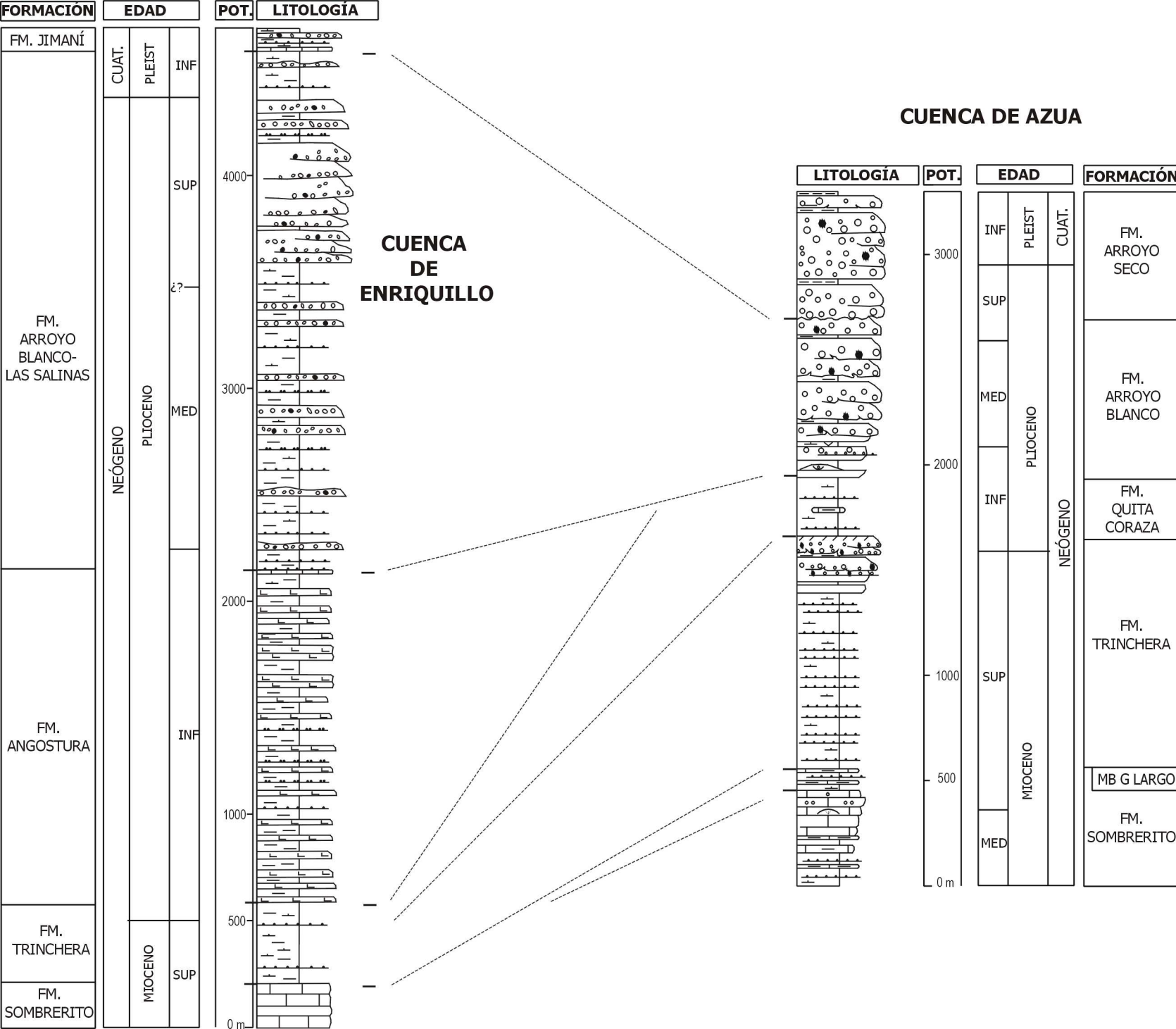


# HOJAS A ESCALA 1:50.000



## LEYENDA DE LITOLOGÍAS

	Caliza		Calcareita		Conglomerado con cemento calcáreo		Marga		Tufita
	Caliza con niveles o nódulos de chert		Basalto		Brecha volcánica		Andesita		Grauvacas
	Margocalizas		Depósito de debris flow		Arenisca				



## **Estructura de las cuencas de Enriquillo y Azua y de los dominios colindantes** **Structure of the Enriquillo-Azua basins and environs**

En este capítulo se describe la estructura de la región SO de la República Dominicana. Razones de proximidad entre los dominios, de simultaneidad y de relación en la génesis de sus estructuras, han aconsejado que esta descripción se realice por sectores. Así, se contempla un sector oriental, que agrupa la cuenca de Azua y el Cinturón de Peralta (Fig. 1); y un sector occidental, que agrupa la cuenca de Enriquillo, la sierra de Neiba y el margen septentrional de la sierra de Bahoruco (Fig. 2). La sierra de Martín García es común a ambos sectores pero se describe principalmente dentro del segundo.

### **La estructura del cinturón de Peralta**

#### **The structure of Peralta belt**

La estructura del cinturón de Peralta se caracteriza por el desarrollo de cabalgamientos de dirección NO-SE y pliegues asociados de vergencia hacia el SO (Figs. 1 y 3). La distribución de estas estructuras no es uniforme sino que sigue una marcada zonación de NE a SO (Fig. 4). Esta zonación se interpreta como la expresión en superficie de la estructura profunda del cinturón como consecuencia de su erosión y ha servido para la elaboración del corte sintético de la Fig. 3. en los niveles estructurales inferiores, situados al SO, predominan los cabalgamientos, en los niveles estructurales intermedios, predominan los pliegues, y más al NE, en los niveles estructurales más altos, la estructura consiste en una serie monoclinal con buzamiento general al NE (Figs. 3 y 4).

En el corte de la Fig. 3, se ha interpretado que la serie monoclinal debe marcar la posición en profundidad de una importante rampa en el bloque de muro o bloque cabalgado, la cuenca de Azua, que delimita la parte cobijada de esta cuenca bajo el cinturón de Peralta. Los niveles estructurales intermedios, con desarrollo predominante de pliegues, se interpreta que corresponden a aquellos sectores del cinturón que se sitúan inmediatamente encima de la rampa o sobre la culminación de ésta. Esta zona de pliegues está limitada en su frente por el cabalgamiento de El Naranjo (Figs. 3 y 4). Por problemas de espacio (geométricos), se ha interpretado que la fm Tireo esta involucrada en los pliegues del dominio intermedio (“zona de pliegues”, Fig. 4), como lo demuestra el que las formaciones Ventura y Jura se apoyen discordantemente sobre la Fm. Tireo en esta zona.

Como muestra el corte de la Fig. 3, la zona de cabalgamientos se supone localizada por encima de un rellano en el bloque cabalgado. Esta geometría se deduce de la posición, en sección, de las charnelas de las estructuras sinclinales. La profundidad del rellano se ha calculado, de forma estimativa, por el método de balance de área (Dahlstrom, 1969).

Los pliegues del cinturón de Peralta se pueden clasificar como pliegues de propagación de falla (Butler, 1982; McClay, 1992) desarrollados en el frente de cabalgamientos. Así lo confirma la común asociación anticlinal-sinclinal, este último frecuentemente roto por su flanco subvertical o inverso y parcialmente cobijado por el primero. Los ejes de los pliegues son subhorizontales, su dirección, NO-SE, y vergencia, hacia el SO, consecuentes con las de los cabalgamientos (Fig. 5)

La dirección de los ejes de los pliegues muestra un gran paralelismo en el conjunto del cinturón, incluso a lo largo de distancias considerables. Este hecho y la ausencia de trenes de pliegues dispuestos en escalón sugieren que la deformación se produjo bajo un predominio de la componente de cizalla pura, con una dirección de acortamiento aproximadamente ortogonal (o muy poco oblicua) a las directrices estructurales. La dirección del transporte tectónico deducida de los ejes de los pliegues, de las líneas de corte y de las líneas de bifurcación, es NE-SO y también viene apoyada por otros elementos como la orientación de algunas fallas transversales (*tear faults*) y rampas laterales. No obstante, la cartografía también recoge la presencia de numerosas fallas de dirección E-O que producen pequeños desplazamientos levógiros en las trazas de pliegues y cabalgamientos. Estas fallas, subparalelas a muchas de las generadas tanto en el cinturón Intermedio como en el sector SO de la sierra de Neiba y la cuenca de Enriquillo, de alguna forma denuncian que la componente

de cizalla pura, aunque dominante, no es exclusiva en el desarrollo del cinturón de Peralta y en él debió intervenir, fundamentalmente en sus estadios finales, una mínima componente de cizalla simple.

La restitución de la deformación (pliegues y cabalgamientos) del cinturón de Peralta en la transversal de la hoja de San José de Ocoa (Fig. 3 B) permite deducir un acortamiento interno aproximado de 12 km (40%). A esta cifra hay que sumar unos 10-15 km correspondientes al desplazamiento del cinturón por encima de la cuenca de Azua.

### 8.1.2. La estructura de la cuenca de Azua

#### 8.1.2. The structure of Azua basin

La estructura general de la cuenca de Azua se ha descrito como del tipo domos y cubetas, por cuanto consiste en anticlinales de dirección NO-SE a E-O y rango kilométrico que separan cubetas sinformes (Mann *et al.*, 1991 d). Los anticlinales suelen tener inmersiones opuestas a lo largo del eje, vergencias en ambos sentidos y generalmente son cabalgantes sobre las cubetas. Dentro de esta estructura general, se diferencian claramente dos sectores, un sector oriental localizado inmediatamente al norte de la bahía de Ocoa, y un sector occidental representado por el resto de la cuenca, cuyas estructuras guardan una continuidad con las del extremo oriental de la cuenca de Enriquillo.

Los pliegues de la cuenca de Azua están relacionados con los cabalgamientos. En términos generales corresponden a pliegues de propagación de falla, y es común la asociación <<anticlinal de bloque de techo / sinclinal en el bloque de muro>> (Figs. 6 y 8). Los pliegues son abiertos y sus curvaturas varían en la vertical, y muestran evidencias de un engrosamiento y adelgazamiento sedimentario simultáneo a su desarrollo, por lo que también se pueden definir como pliegues de crecimiento (McClay, 1992). Las frecuentes discordancias y discontinuidades internas, así como la tendencia somerizante general de la cuenca, evidencian unas relaciones tectónica-sedimentación intensas. La cuenca de Azua y su entorno representan la cuenca de antepaís del cinturón de Peralta, de tal forma que su estructura y relleno han sido controlados por el avance de la deformación de este cinturón hacia el SE. Sin embargo, este control no es exclusivo del cinturón de Peralta puesto que en la deformación también interviene el efecto del *indenter* de Beata, así como la tectónica de desgarres que afecta de lleno a los sectores contiguos al oeste de la cuenca de Enriquillo, sierra de Neiba y sierra de Martín García.

Hernaiz Huerta (2000) y Hernaiz Huerta y Pérez Estaún (2002) interpretaron la cuenca de Azua como una “zona triangular” (en sentido amplio) a gran escala y las estructuras de las sierras de Neiba y de Martín García, las asimilaron a geometrías de tipo *pop up* (McClay, 1992). En el mismo trabajo se indicaba que en el interior de la cuenca, los cabalgamientos debían enraizar en profundidad en una superficie de despegue cuya localización, deducida del radio de curvatura de los pliegues asociados a los cabalgamientos, se proponía a una profundidad mínima de 3,5 a 4 km (Fig. 8). No obstante, los mismos autores indicaron que el plegamiento de gran radio que caracteriza a estas sierras y las fuertes anomalías aeromagnéticas asociadas a los núcleos de estas estructuras (CGG, 1997) sugerían que el enraizamiento de los cabalgamientos podía ser, de manera alternativa, relativamente profundo llegando a involucrar al basamento. Los posteriores estudios realizados en los sectores contiguos de la cuenca de Enriquillo, y sierras de Neiba y de Martín García (ver más adelante), han aconsejado reinterpretar la estructura en el sentido indicado en los cortes de las figuras 6, 7, y 8, en los que tanto los cabalgamientos marginales de la sierra de Martín García como los internos de la cuenca de Azua se reinterpretan con un perfil subvertical y enraizados en profundidad.

El acortamiento medido en el interior de la cuenca según un plano perpendicular a las estructuras es escaso en comparación al calculado para el cinturón de Peralta y se estima en torno a los 3,5 km (9%). Este acortamiento, no obstante, es mínimo puesto que no considera los posibles desplazamientos ocurridos fuera de dicho plano como consecuencia de la componente en dirección de algunas estructuras.

En el sector oriental de la cuenca, la estructura está relacionada con la indentación de la cresta de Beata. La cresta de Beata (Heubeck y Mann, 1991), es un promontorio alargado con forma de cuña hacia el

norte que se dispone en el centro del *plateau* oceánico del Caribe con una dirección NNE-SSO transversalmente a los límites meridional de la isla La Española y septentrional de la placa Sudamericana (Mauffret y Leroy, 1997). Según Heubeck y Mann *et al.*, (1991 a) y Mann *et al.*, (1991 b), la cresta de Beata funcionó a partir del Plioceno Medio como un *indenter* de unos 50 km de ancho que, empujado desde el otro margen, colisionó con el sector central de La Española en sentido SSO-NNE, y se “incrustó” en una zona no del todo bien definida pero que más o menos coincide con la bahía de Ocoa.

Como ya describieran Heubeck y Mann (1991) y Mann *et al.*, (1991d), los efectos más evidentes de la colisión del *indenter* tienen que ver con las estructuras arqueadas que caracterizan el entorno de la bahía de Ocoa. Estas se refieren tanto al arco de estructuras anticlinales de la Fm. Sombrerito que orlan la Bahía, como al propio giro de más de 90° que en sentido horario realizan las estructuras del extremo SE del cinturón de Peralta (Fig. 1). Ambas estructuras se desarrollaron simultáneamente, como consecuencia de la penetración del *indenter* hacia el NNE y produjeron al mismo tiempo el cierre completo de la cuenca de Azua por el este.

Las sierras de La Vigía, los Cacheos y Loma Vieja que rodean la Bahía de Ocoa (Fig. 1) tienen la misma estructura braquianticinal alargada que la sierra de Martín García y se ha llegado a sugerir (Ramírez, 1995) que podrían representar la prolongación de ésta. Si esto fuera así, el arco que dibujan estas sierras implicaría un desplazamiento mínimo del centro del arco de unos 20 km respecto de su posición original. Según se desprende de la cartografía realizada en el Proyecto SYSMIN (Fig. 1) y de las previas de Heubeck y Mann (1991) y Mann *et al.* (1991 c), este arco está limitado por fallas NNE-SSO, con movimiento sinestral, en el margen occidental y fallas NNO-SSE y movimiento dextral en el oriental.

Como se ha mencionado anteriormente, una de las consecuencias principales de la indentación de la cresta de Beata fue el cierre por el este de la cuenca de Azua, de tal forma que al norte de la bahía de Ocoa, el cinturón de Peralta cabalga directamente sobre las sierras anticlinales de Los Cacheos y Loma Vieja, configurando una zona triangular prácticamente cerrada (Fig. 9).

Los efectos de la colisión del *indenter* de Beata rebasan ampliamente el ámbito de la bahía de Ocoa. Mann *et al.* (1991d) asocian el vulcanismo cuaternario de la región a este proceso, aunque esta asociación se hace con reservas puesto que el citado vulcanismo no se encuentra estrictamente alineado con la zona de influencia del *indenter* sino que tiene un desplazamiento de 20 a 40 km al este respecto de ella.

Por otra parte, unos kilómetros al norte de la bahía de Ocoa, la cartografía revela una cierta densidad de fallas de dirección submeridiana que se concentran en una banda de anchura kilométrica coincidente con la zona de influencia de la cresta de Beata (Figs. 1 y 10).

### **Sector occidental: Sierras de Neiba, Martin Garcia y margen septentrional de la Sierra de Bahoruco**

### **Western area: Sierras de Neiba, Martin Garcia, and northern margin of Sierra de Bahoruco**

#### **La estructura de la Sierra de Neiba**

La estructura de la Sierra de Neiba está definida por pliegues de longitud de onda kilométrica, limitados por cabalgamientos de alto ángulo y cortados por una intensa fracturación, configurando un domo elevado más de 2000 m sobre las cuencas adyacentes de San Juan y Enriquillo (Figs. 2; 11 y 12). Los pliegues presentan direcciones cambiantes de NO-SE a E-O e incluso ENE-OSO y una disposición escalonada en relevo izquierdo de sus trazas axiales (Figs. 2 y 13). Las estructuras más prominentes son grandes pliegues anticlinales, comúnmente con doble inmersión, que se relevan en escasos kilómetros. A gran escala existe una inmersión hacia el ESE que determina el afloramiento de las series más antiguas (Fm Neiba inferior y Neiba brechoide) en los sectores occidentales, mientras que las más modernas (Neiba superior, Sombrerito) lo hacen principalmente al este de la sierra. Los sinclinales son estrechos, cobijados por los flancos cabalgantes de los anticlinales, con el núcleo ocupado por la Fm Sombrerito en los sectores orientales y por la Fm Neiba superior o el Conjunto Volcanosedimentario en los occidentales.

La Sierra de Neiba se superpone a la cuenca de Enriquillo por un sistema de cabalgamientos de ángulo elevado, con sucesivos saltos en la vertical (Figs. 11 y 12). Un ejemplo es el cabalgamiento que limita por el sur anticlinal de La Descubierta, superponiendo la Fm Neiba brechoide sobre la Fm Jimaní, lo que implica un importante salto vertical (Fig. 2 y 11-corte II-II'). Hacia el oeste, en la hoja de Boca Cachón, este cabalgamiento se prolonga en un desgarre. Hacia el este su continuidad se pierde y la geometría del frente de la sierra en superficie es un flanco monoclinal sobre el que se apoyan discordantes las series que forman el relleno marginal de la cuenca (Figs. 2, 11 y 12). Finalmente, en la terminación oriental de la sierra, la disposición cartográfica escalonada en sentido izquierdo y asintótica de los pliegues (Fig. 2) sugiere su interrupción contra la falla de Enriquillo.

### **La estructura del margen septentrional de la Sierra de Bahoruco**

La estructura del margen norte de la Sierra de Bahoruco se caracteriza por: a) una disposición monoclinal hacia el N/NE o suavemente plegada de las series calcáreas de Neiba superior y Sombrerito; b) el desarrollo de un frente de deformación asociado a cabalgamientos sobre la cuenca de Enriquillo; y c) la presencia de fallas rectilíneas de dirección NO-SE con movimiento vertical inverso y en dirección que modifican este frente y producen la compartimentación del flanco en bloques progresivamente más elevados hacia en interior de la sierra y ligeramente cabalgantes hacia el exterior de la misma (Figs. 2 y 12).

La tendencia monoclinal hacia el N/NE o suavemente plegada de las series calcáreas de Neiba superior y Sombrerito es característica del Bahoruco central (hojas de Duvergé y Las Salinas). Los pliegues tienen orientación NO-SE con flancos entre 10° y 30° cortados por fallas inversas (Fig. 12). Hacia el NO, en la hoja de Jimaní, los pliegues presentan una disposición escalonada derecha con trazas axiales E-O que se interrumpen contra una falla situada en Haití.

El contacto entre la Sierra de Bahoruco y la cuenca de Enriquillo es un sistema de fallas con componente inversa (Fig. 2 y 12), que sumada al relieve estructural producido por el plegamiento, supera 3.000m en las transversales orientales (Las Salinas, Barahona), al que hay que añadir 2.000m de profundidad hasta el centro de la cuenca de Enriquillo (Norconsult 1983; Mann *et al.*, 1999). El desplazamiento en dirección, más difícil de estimar, no supera 1 o 2 km. El desplazamiento vertical es máximo en la transversal de Las Salinas, donde el cabalgamiento sobre la Fm Angostura (Fig. 12-corte C-C') forma un flanco fallado subvertical. Los contactos con algunas de las formaciones adyacentes (p.e. la Fm Jimaní) son sustractivos, sugiriendo movimientos halocinéticos de las evaporitas de la Fm Angostura (Llinás 1971). Hacia el SE, en la transversal de Barahona, la geometría del frente se ha interpretado como un cabalgamiento de plano subvertical enterrado bajo los depósitos cuaternarios, que superpone la Fm Neiba superior sobre la Fm Trinchera, con un salto superior a 3.000m. (Fig. 12-corte D-D')

Hacia el NO, en el sector occidental de la hoja de Duvergé y en la hoja de Jimaní, la Sierra de Bahoruco desciende de cota en escalones producidos por la componente inversa de las fallas en dirección (Fig. 2). La cartografía de la hoja de Jimaní y los cortes geológicos (García Senz, 2004) son consistentes con estos datos y muestran la disposición discordante y en onlap de las Fms. Arroyo Blanco-Las Salinas y Jimaní, con un buzamiento al sur, sobre el sustrato erosionado de la Fm Sombrerito (Fig. 2 y 12-corte A-A'), inclinada monoclinalmente hacia la cuenca. Los depósitos conglomeráticos más altos de la Fm Jimaní dispuestos a lo largo del frente de la sierra se relacionan con su elevación. En la hoja de Jimaní el frente de deformación de la sierra produce depresiones alargadas como la depresión de El Limón separadas por lomas anticlinales. El frente termina en una zona triangular que deforma las formaciones Arroyo Blanco-Las Salinas, Jimaní y también el arrecife plio-cuaternario (Fig. 12-corte A-A').

### **8.2.3. La estructura de la Sierra de Martín García**

La Sierra de Martín García es un anticlinorio con doble vergencia cabalgante sobre las cuencas de Enriquillo y Azua. Su trayectoria cambia de NO-SE en el extremo oriental de la sierra a E-O o ENE-OSO en el extremo occidental, con una acusada inmersión hacia el oeste (Figs. 2 y 12-corte D-D'). El margen

meridional es un cabalgamiento que superpone las Fms. Neiba y Sombrerito sobre las Fms. de Arroyo Blanco-Las Salinas con un salto vertical próximo a 3.000m (Fig. 12-corte D-D').

En la vertiente norte de la Sierra el límite con la cuenca de Enriquillo son varios cabalgamientos de trazado curvo que desplazan la Fm Sombrerito y el contacto de ésta y su miembro superior Gajo Largo (Fig. 12-corte D-D'). Lateralmente hacia el este, el salto es mayor, con superposición de la Fm Sombrerito sobre la Fm Trinchera. Hacia el norte, la estructura de la cuenca de Enriquillo es un sinclinal (Los Güiros, Mann *et al.*, 1991 c; 1999) de plano axial subvertical o ligeramente vergente tanto al norte como al sur y una traza axial E-O alabeada que se prolonga desde la cuenca de Azua. La continuidad del flanco se interrumpe por el anticlinal de Quita Coraza asociado a un cabalgamiento de vergencia sur (Fig. 12-corte D-D'). El flanco septentrional del sinclinal de los Güiros es cortado por el frente meridional de la Sierra de Neiba que coincide aproximadamente con la terminación oriental de la falla de Enriquillo. Los nuevos datos cartográficos de superficie combinados con los contornos estructurales del subsuelo de la cuenca (Fig. 2) sugieren la continuidad hacia en NO del sinclinal de los Güiros con el sinclinal de Apolinario Perdomo.

#### 8.2.4. La estructura de la cuenca de Enriquillo

La estructura interna de la cuenca de Enriquillo (Fig. 2) ha sido descrita en los informes de la Canadian Oil Superior Ltd. (resumidos en Norconsult, 1983) y en la revisión de Mann *et al.* (1999). Los dos trabajos muestran en el este de la cuenca dos cabalgamientos NNO-SSE oblicuos al resto de estructuras. Ambos cabalgamientos tienen vergencia oeste, el más oriental con un salto elevado ( $2800\text{mseg} = 4.500\text{m}$ , aprox.) mayor que el occidental ( $750\text{mseg} = 1.300\text{m}$ , aprox.). Estos dos cabalgamientos, junto con las estructuras del margen de la Sierra de Martín García dividen la cuenca en bloques de geometría anticlinal que fueron el objetivo de la exploración petrolífera (Fig. 8 de Mann *et al.*, 1999). La profundidad del techo de la Fm Sombrerito es máxima ( $3.800\text{mseg} = 6000-6500\text{m}$ , aprox.) cerca del contacto con el cabalgamiento oriental y se sitúa a cotas medias aproximadas de 3.500-4.000 en el resto de la cuenca. En los altos estructurales más elevados esta cota asciende hasta 1500-2000m (Fig. 2).

La única estructura intracuenca aflorante es el cabalgamiento E-O de la laguna de El Rincón, que eleva a la superficie a la Fm Angostura. Tiene vergencia sur, contrapuesta a la Sierra de Bahoruco. En el mapa aeromagnético (CGG, 1999) esta estructura y el doble cabalgamiento que limita por el sur la Sierra de Martín García producen una anomalía continua que sugiere su conexión. Los geólogos de la Canadian Oil Superior Ltd. interpretaron en líneas sísmicas los cabalgamientos del interior de la cuenca de Enriquillo entroncados en una superficie de despegue a techo de la Fm Sombrerito. En su reinterpretación, (Mann *et al.*, 1999, ver su Fig. 9) trazan planos de cabalgamiento subverticales que también afectan a la Fm Sombrerito y penetran al menos hasta la parte alta de la Fm Neiba superior. Las líneas sísmicas revelan así mismo una disarmonía en el plegamiento de las evaporitas de Angostura respecto a las infayantes Fms Trinchera (muy adelgazada) y Sombrerito, así como su acumulación diapírica en las charnelas anticlinales. Este modelo parece aplicable al cabalgamiento de la laguna del Rincón (Fig. 12-cortes C-C' y D-D').

#### 8.2.5. La falla de Enriquillo

Esta importante falla, con un desplazamiento izquierdo (Mann *et al.*, 1995) estimado en 30-50km (van der Berghe, 1983; Calmus, 1983), presenta a lo largo de la península meridional de Haití un trazado E-O con curvaturas restrictivas al movimiento, escarpes, desplazamientos de la red de drenaje y elevaciones de arrecifes subactuales. En la República Dominicana la superficie de la falla discurre bajo el Lago Enriquillo y es paralela al escarpe de la Sierra de Neiba. Más hacia el este comienzan las estructuras en relevo y los puentes hasta su desaparición en la cuenca de Azua. La isla Cabritos y las dos más pequeñas del Lago Enriquillo se interpretan como anticlinales escalonados en sentido izquierdo contra la falla (Mann, 1983 y Mann *et al.*, 1991b). El levantamiento topográfico del arrecife subactual a la altura de Las Clavellinas, medido por medios taquimétricos se relaciona con su movimiento (Taylor *et al.*, 1985). En el presente trabajo, se ha

podido comprobar en este mismo punto (hoja de la Descubierta, X: 0230800.; Y: 5047600), un basculamiento de 20-25° hacia el sur de la serie limo-arcillosa que acompaña al arrecife. Más al oeste, en la hoja de Jimaní, una terraza del abanico aluvial de Jimaní y limos con gasterópodos y corales del relleno del lago están basculados 17° hacia la falla (García Senz, 2004) (Fig. 14).

En el margen meridional de la Sierra de Neiba, Mann *et al.* (1995) identifican escarpes de terraza, contrastes de vegetación, desplazamientos en la red de drenaje y manantiales con travertinos, que asocian al movimiento de la falla de Enriquillo. Varias fallas E-O cartografiadas en este trabajo cortan y desplazan los abanicos aluviales más antiguos, sin que ninguna de ellas se pueda identificar con el trazado de la falla principal.

## La fracturación

Las calizas de la Sierra de Neiba presentan una intensa fracturación (Fig. 13). A fin de determinar su relación con las estructuras contractivas se han resaltado en color y por familias las fallas con relaciones de corte que permiten asignar un sentido de movimiento. El resto se ha dejado en blanco y negro y sin resaltar (Fig. 14).

Los sistemas NNO-SSE y ENE-OSO presentan, sentidos de movimiento en dirección, derechos e izquierdos respectivamente Ambos curvan y cortan las trazas de los pliegues y cabalgamientos, pero es el sistema ENE-OSO el que muestra una relación genética más clara delimitando las terminaciones de los grandes anticlinales. El sistema NNO-SSE tiene mayor desarrollo en el sector central de la Sierra de Neiba, con fallas de trazado neto y desplazamientos derechos. Algunas fallas producen en los pliegues y cabalgamientos efectos similares al descrito anteriormente, que evidencian su desarrollo simultáneo con ellos, aunque, mayoritariamente se sobre imponen a estructuras ya formadas. En cartografía, este sistema presenta un giro en planta y terminaciones asintóticas contra la falla de Enriquillo, consistentes con un movimiento izquierdo.

En la figura 14 se ha separado con distinto color, un sistema de dirección NE-SO a NNE-SSO, que corta casi perpendicularmente a las estructuras principales. Las fallas de este sistema tienen pautas de movimiento mal definidas: una parte muestra una componente normal y otra desgarres secundarios derechos e izquierdos. Incluye además numerosas fallas E-O a ONO-ESE con desplazamientos izquierdos de pequeña cuantía, subparalelas a la falla de Enriquillo que forman un amplio corredor coincidente en anchura con la Sierra de Neiba.

### 8.2.7. Correlación de la estructura con el mapa aeromagnético.

Como complemento a la descripción de la estructura, se ha procedido a una correlación con el mapa de gradiente magnético vertical que, en esta zona, ofrece una imagen más próxima a la superficie que el reducido al polo (Hernaiz Huerta 2004 a; 2004 b; 2006).

En la figura 15 se han superpuesto los contactos geológicos y las estructuras extraídas del esquema geológico regional de la zona (Fig. 2), al mapa de gradiente vertical, en el que se han dejado las etiquetas correspondientes a las principales anomalías descritas en un informe de elaborado por García Lobón (2004 a) para el Proyecto L de Cartografía Geotemática. Los números corresponden a las distintas anomalías, puntos o alineaciones que se enumeran a continuación y que, para este efecto, se han dividido en aquellas relacionadas con la litología y las que reflejan aspectos estructurales.

#### Anomalías relacionadas con la litología

- 1) Probablemente la correlación más obvia en toda la zona corresponde a las de anomalías N1 a N8 con el vulcanismo del complejo volcanosedimentario de El Aguacate. Esta correlación es tanto litológica como

estructural por cuanto estas anomalías reproducen la presencia de este vulcanismo y las estructuras anticlinales a las que está cartográficamente asociado, incluida su disposición escalonada.

2) Una anomalía similar a las anteriores coincide con el núcleo de la sierra de Martín García por lo que es de esperar que en niveles relativamente someros de la Fm. Neiba superior también haya intercalaciones volcánicas que, no obstante, no se ha reconocido en superficie.

3) Esta anomalía ocupa toda la zona central de la cuenca. Según García Lobón (2004), se puede interpretar originada por una “placa magmática” asentada a una profundidad entre 3.000 y 4.500 m y que pudiera corresponder a una lámina basáltica. Parece acertada esta interpretación puesto que el sondeo Charco Larco identifica dentro de la serie de la Fm. Angostura varias intercalaciones de dioritas hornbléndicas.

4) Las intercalaciones volcánicas que presenta la Fm. Sombrerito en la hoja de Boca Cachón producen anomalías puntuales muy netas. El tipo de anomalía es el mismo que reproducen los afloramientos de esta misma formación en el frente de la sierra de Bahoruco pese a que en ellos no se han identificado intercalaciones volcánicas en superficie.

5) Los afloramientos de la Fm. Trinchera dan lugar a anomalías que prácticamente mimetizan sus contactos cartográficos. En este caso las anomalías las causa el prácticamente exclusivo origen volcánico e ígneo de los materiales detriticos que constituyen esta formación en los que la magnetita causa anomalías que cartografián fielmente sus contactos.

6) Una respuesta similar da la Fm. Arroyo Blanco en el sinclinal de Los Güiros, también debido a que, puntualmente, en esta zona tiene un contenido elevado en materiales siliciclásticos de procedencia volcánica. Una anomalía negativa reproduce, en el flanco sur de este sinclinal, el tramo cartográfico correspondiente a la Fm. Quita Coraza.

7) En la parte más meridional de la sierra de Bahoruco, las acusadas anomalías denominadas BA1 y BA2 coinciden con los afloramientos de la formación volcánica La Ciénaga/Dumisseau del Cretácico Superior.

8) Los afloramientos de la Fm. Angostura dan una respuesta desigual puesto que el de la laguna del Rincón coincide con una anomalía negativa, mientras que los de Las Salinas se asocian a una anomalía positiva.

#### *Anomalías relacionadas con estructuras*

9) La sierra de Bahoruco produce una acusada alineación magnética que coincide con el contacto cartográfico fallado y rectilíneo entre las Fms. Neiba superior y Sombrerito.

10) En la hoja de Las Salinas una alineación magnética NE-SO que pasa por el límite sur de la laguna del Rincón, marca: el límite SE de la anomalía E1 en el interior de la cuenca; el límite SE de la escama de Fm. Angostura en el frente de sierra de Bahoruco; y el contacto entre las Fms Neiba superior y Sombrerito al sur de éste. Esta alineación es subparalela a las fallas NE-SO que afectan al frente de la sierra en la transversal de Las Salinas y se puede interpretar como una de ellas.

11) Inmediatamente al SE de la anterior, varias fallas de dirección NO-SE separan las anomalías E2 y E3 con un aparente movimiento dextral entre ambas, similar al que se deduce en superficie para fallas de igual orientación en otros puntos de la sierra de Bahoruco.

12) En esta misma zona una anomalía de gradiente magnético vertical parece conectar el cabalgamiento de la laguna de El Rincón con el doble cabalgamiento que en el subsuelo se ha cartografiado limitando la sierra de Martín García y ello sugiere su posible conexión.

13) Paralela a la alineación magnética de la sierra de Bahoruco, otra alineación muy marcada determina la terminación NE de la anomalía E1 en el subsuelo de la cuenca de Enriquillo. Esta alineación se superpone en

parte a la traza del cabalgamiento más oriental cartografiado en el subsuelo de la cuenca y se prolonga hacia el NO para marcar el límite meridional de la anomalía que se asocia al anticlinal de Las Cañitas.

14) Inmediatamente al NE de la anterior y paralela a ella, existe otra alineación magnética que ya se señaló en el informe preliminar. La alineación tiene dirección NO-SE y en su segmento norte viene a coincidir con las fallas o cabalgamientos que limitan el sinclinal de Apolinar Perdomo, si bien también parece que reproduce los materiales margosos poco magnéticos de la Fm. Sombrerito que ocupan el núcleo de este sinclinal. Esta alineación es todavía más espectacular en su segmento meridional donde produce el giro e inflexión en sentido dextral de la anomalía magnética asociada a las series que conforman el sinclinal de Los Güiros y la estructura de Quita Coraza

15) Quizá en continuidad con el anterior, el margen meridional cabalgante de la sierra de Martín García coincide con una alineación en la que el acusado contraste de anomalías (mínimo al sur y máximo al norte, es consistente con el fuerte salto en la vertical que se le deduce en la cartografía

16) Al norte de la sierra de Martín García, el mapa de gradiente vertical reproduce con gran fidelidad el sinclinal de Los Güiros.

17) El trazado rectilíneo del margen meridional de la sierra de Neiba produce una acusada alineación magnética que refuerza la hipótesis de su relación con la traza de la falla de Enriquillo

18) La anomalías relacionadas con el vulcanismo de la sierra de Neiba y sus anticlinales reflejan desplazamientos o interrupciones bruscas en sentido NE-SO o ENE-OSO que se deben asimilar a las fallas con esta misma dirección cartografiadas en superficie.

### 8.2.8. El modelo estructural

Está firmemente establecido que la zona de estudio está dominada por estructuras contractivas asociadas a fallas transcurrentes (Mann, 1983; Norconsult 1983; McLaughlin *et al.*, 1991; Mann *et al.* 1991c; Mann *et al.* 1995; Mann *et al.* 1999; entre otros). Para su análisis se ha elaborado un mapa estructural (Fig. 14) y una serie de cortes geológicos (Fig. 12). No son cortes “*plane strain*”, debido a la existencia de desplazamientos fuera del plano y por ello, solo informan del acortamiento medido perpendicularmente a la dirección de los pliegues.

La componente contractiva de las fallas transcurrentes está acomodada por cabalgamientos de alto ángulo y sentido opuesto que elevan las sierras de Bahoruco y Neiba sobre la cuenca de Enriquillo formando una estructura de *pop-up*, y por el perfil sinclinal de esta cuenca. Los cabalgamientos intracuenca pueden prolongarse por un despegue en las evaporitas de la Fm Angostura. La Sierra de Martín García emerge como un gran anticlinal (corte D-D') con flancos cabalgantes, el meridional con un salto vertical importante, y el septentrional dividido en varios cabalgamientos. Para el horizonte de la base o el techo de la Fm Sombrerito se ha calculado entre 7,5km (10%) en el corte C-C', a 11,75km (15%), en el corte D-D'.

En la Sierra de Neiba, los cortes geológicos muestran pliegues con flancos entre abiertos ( $120^\circ$ ) a algo cerrados ( $75^\circ$ ) y planos axiales subverticales o ligeramente vergentes al sur (Fig. 11). Una excepción a esta pauta general es el cabalgamiento del anticlinal de El Aguacate sobre el sinclinal de Apolinar Perdomo, donde la traslación horizontal superior a 2 km produce dos cabalgamientos con planos más tendidos y vergencia sur acusada. El perfil se asemeja a pliegues de propagación de falla. La estructura del margen norte de la Sierra de Neiba muestra así mismo pliegues limitados por cabalgamientos de alto ángulo, pero vergentes al norte (García y Harms, 1988) (cortes D-D', Fig. 12; y IX-IX', Fig. 11). Una línea sísmica realizada para la exploración petrolífera de la cuenca de San Juan (Nemec 1980) proporciona una buena imagen de la estructura del margen norte de la Sierra de Neiba. En ella, los principales reflectores de la cuenca son desplazados por cabalgamientos de alto ángulo que se verticalizan en profundidad, aunque las secuencias de relleno de la cuenca comprendidas entre estos reflectores apenas muestran acuñamiento hacia el margen.

En conclusión, el estilo estructural en la zona de estudio se caracteriza por:

1) Pliegues con doble inmersión en corto espacio y posible geometría cónica; 2) Pliegues en escalón con relevos acomodados por fallas, que los cortan o curvan asintóticamente hacia la falla; 3) Cabalgamientos con componente en dirección; y 4) Numerosas fallas menores en sistemas con direcciones y sentidos de movimiento consistentes, aunque las relaciones de corte no son fácilmente interpretables.

El modelo que se propone (Fig. 14) es una zona de cizalla izquierda, de dirección E-O, activa durante un amplio lapso de tiempo (Mioceno superior-Actualidad) de acuerdo con los sedimentos sintectónicos asociados. La dirección de acortamiento, NE-SO, es aproximadamente normal a la traza de los pliegues y cabalgamientos principales y coincide con la obtenida mediante el análisis de la fracturación (van den Berghe, 1983). La orientación de las fracturas y la posición de los pliegues y cabalgamientos, son consistentes con esta interpretación. De acuerdo con los modelos de Tchalenko (1968) y Rutter *et al.* (1986), los sistemas de fracturación se interpretan cinemáticamente respecto a la dirección de la cizalla principal representada por la falla de Enriquillo, en los siguientes términos (Fig. 14): Sistema ENE-OSO, fallas de tipo R o Riedel sintéticas de primer orden; sistema NNO-SSE, fallas de tipo R' antítéticas de primer orden; sistema NNE-SSO, fallas de tipo X, antítéticas de segundo orden; sistemas ONO-ESE a E-O, fallas sintéticas de segundo orden subparalelas (D) o ligeramente oblicuas (P) a la dirección de cizalla principal y con igual sentido de movimiento izquierdo que ella; también se identifican fallas normales de NE-SO subparalelas a la dirección de máximo esfuerzo.

## Bibliografía

- Butler, R.W.H., 1982. The terminology of structures in thrust belts. *Journal of Structural Geology*, 4, 239-245.
- Calmus, T., 1983. Décrochement senestre sud-haïtien: Analices et conséquences paléogéographiques
- CGG (Compagnie Generale de Geophysique), 1997. Informe final sobre la prospección magnética y radiométrica aerotransportada del territorio de la República Dominicana. Programa SYSMIN. Dirección General de Minería. Santo Domingo.
- Del Olmo Sanz, A., 2000. Mapa Geológico de la Hoja a E. 1:50.000 nº 6071-III (Pueblo Viejo) y Memoria correspondiente. Proyecto "C" de Cartografía Geotemática de la República Dominicana. Programa SYSMIN. Dirección General de Minería, Santo Domingo.
- Díaz de Neira, J.A., 2000. Mapa Geológico de la Hoja a E. 1:50.000 nº 6071-II (Azua) y Memoria correspondiente. Proyecto "C" de Cartografía Geotemática de la República Dominicana. Proyecto de Cartografía Geotemática de la República Dominicana. Programa SYSMIN. Dirección General de Minería, Santo Domingo.
- García Lobón, J. L., 2004. Interpretación de la Geofísica Aerotransportada del Proyecto "L" de Cartografía Geotemática de la República Dominicana. Programa SYSMIN. Dirección General de Minería, Santo Domingo.
- García Senz, J., 2004. Mapa Geológico de la Hoja a E. 1:50.000 nº 5871-III (Jimaní) y Memoria correspondiente. Proyecto "L" (Zona SO) de Cartografía Geotemática de la República Dominicana. Programa SYSMIN. Dirección General de Minería, Santo Domingo
- Gómez Sainz de Aja, J.A., 2000. Mapa Geológico de la Hoja a E. 1:50.000 nº 6071-IV (Yayas de Viajama) y Memoria correspondiente. Proyecto "C" de Cartografía Geotemática de la República Dominicana. Programa SYSMIN. Dirección General de Minería, Santo Domingo
- Hernaiz Huerta, P.P., 2000. Mapa Geológico de la Hoja a E. 1:50.000 nº 6071-I (San José de Ocoa) y Memoria correspondiente. Proyecto "C" de Cartografía Geotemática de la República Dominicana. Programa SYSMIN. Dirección General de Minería, Santo Domingo

- Hernaiz Huerta, P.P., 2004 a. Mapa Geológico de la Hoja a E. 1:50.000 n° 5971-IV (Galván) y Memoria correspondiente. Proyecto “L” (Zona SO) de Cartografía Geotemática de la República Dominicana. Programa SYSMIN. Dirección General de Minería, Santo Domingo
- Hernaiz Huerta, P.P., 2004 b. Mapa Geológico de la Hoja a E. 1:50.000 n° 5871-I (La Descubierta) y Memoria correspondiente. Proyecto “L” (Zona SO) de Cartografía Geotemática de la República Dominicana. Programa SYSMIN. Dirección General de Minería, Santo Domingo
- Hernaiz Huerta, P.P., 2006. La estructura del sector meridional de la República Dominicana. Una aproximación a su evolución geodinámica durante el Cenozoico. Tesis Doctoral. Universidad Complutense de Madrid, 287 p
- Hernaiz Huerta, P.P., Díaz de Neira, J.A., García Senz, J., Deschamps, I., Genna, A., Nicole, N., Lopera, E., Escuder Viruete, J., Ardévol Oró, Ll. y Pérez Estaún, A. 2006. La estructura del suroeste de la República Dominicana: un ejemplo de deformación en régimen transpresivo. Boletín Geológico y Minero, 118 (2): 337-358p
- Hernaiz Huerta, P.P., Pérez-Estaún, A., 2002. Estructura del cinturón de pliegues y cabalgamientos de Peralta, República Dominicana. En A. Pérez-Estaún, I. Tavares, A. García Cortes, P.P. Hernaiz Huerta (eds.). Evolución geológica del margen norte de la Placa del Caribe, República Dominicana. Acta Geológica Hispánica, 37, 183-205
- Heubeck, C., Mann, P., 1991. Structural Geology and Cenozoic Tectonic History of the Southeastern Termination of the Cordillera Central, Dominican Republic. En P. Mann, G. Draper, J.F. Lewis, (eds.), Geologic and tectonic development of the North America-Caribbean plate boundary in Hispaniola. Geological Society of America Special Paper 262, 315-336
- Llinas, R.A. 1971. Geología del área Polo-Duvergé, Cuenca de Enriquillo, República Dominicana. Tesis Doctoral. México City, México, Universidad Nacional Autónoma de México, Facultad de Ingeniería, 83 p
- Mann, P., 1983. Cenozoic tectonics of the Caribbean structural and stratigraphic studies in Jamaica and Hispaniola. Ph.D. Thesis. New York University, Albany, 688 p
- Mann, P., Draper, G., Lewis, J.F., 1991 b. An overview of the geologic and tectonic development of Hispaniola. En P. Mann, G. Draper, J.F. Lewis (eds.), Geologic and tectonic development of the North America-Caribbean plate boundary in Hispaniola. Geological Society of America Special Paper 262, 1-28
- Mann, P., Lebrón , M., Rodriguez, J., Heubeck, C., 1991 c. Geologic maps of the southern Dominican Republic. En P. Mann, G. Draper, J.F. Lewis (eds.), Geologic and tectonic development of the North America-Caribbean plate boundary in Hispaniola. Geological Society of America Special Paper 262, Plates 4a, 4b, and 4c, scale: 1:150.000
- Mann, P., McLaughlin, P.P., Cooper, C., 1991d. Geology of the Azua and Enriquillo basins, Dominican Republic; 2, Structure and tectonics. En P. Mann, G. Draper, J.F. Lewis (eds.), Geologic and tectonic development of the North America-Caribbean plate boundary in Hispaniola. Geological Society of America Special Paper 262, 367-390
- Mann, P., McLaughlin, P., Van den Bold, W.A., Lawrence, S.R., Lamar, M.E., 1999. Tectonic and Eustatic Controls on Neogene Evaporitic and Siliciclastic Deposition in the Enriquillo Basin, Dominican Republic. En P. Mann (ed.), Caribbean Basins. Sedimentary Basins of the World, 4 (Series Editor: K.J. Hsü), 3-31
- Mann, P., Taylor, F.W., Edwards, R.L., Ku, T.L., 1995. Actively evolving microplate formation by oblique collision and sideways motion along strike-slip faults: An example from the north-eastern Caribbean plate margin. Tectonophysics, 246, 1-69
- Mauffret, A., Leroy, S. 1997. Seismic stratigraphy and structure of the Caribbean igneous province. Tectonophysics, 283, 61-104
- McClay, K.R., 1992. Glossary of thrust tectonics terms. En McClay, K.R. (ed.), Thrust Tectonics. Chapman and Hall, 419-434.
- McLaughlin, P.P., Van Den Bold, W.A., Mann, P., 1991. Geology of the Azua and Enriquillo basins. Dominican Republic; 1, Neogene lithofacies, biostratigraphy, biofacies, and paleogeography. En P. Mann, G.

- Draper, J.F. Lewis (eds.), Geologic and tectonic development of the North America-Caribbean plate boundary in Hispaniola. Geological Society of America Special Paper 262, 337-366.
- Nemec, M.C., 1980. A two phase model for the tectonic evolution of the Caribbean. Transactions of the 9th Caribbean Geological Conference, 23-24.
- Norconsult, 1983. Dominican Republic. Petroleun Exploration Appraisal. Report for Dirección General de Minería. Santo Domingo, 81 p
- Ramírez, M.I., 1995. Neotectonic Structures and Paleostress in the Azua region, South-Central Hispaniola. MSc Thesis, Florida International University, 144 p
- Rutter, E.H., Haddock, R.H., Hall, S.H., White, S.H. 1986. Comparative microstructures of natural and experimentally produced clay-bearing fault gouges. *Palaeophysics*, 124
- Taylor, F.W., Mann, P., Valastro, S., and Burke, K., 1985. Stratigraphy and radiocarbon chronology of a subaerially exposed Holocene coral reef, Dominican Republic. *Journal of Geology*, 93, 311-332
- Tchalenko, J.S., 1968. The evolution of kink-bands and the development of compression textures in sheared clays. *Tectonophysics*, 6, 159-174
- van den Berghe, B. 1983. Evolution sedimentaire et structurale depuis le Paleocene de secteur “Massif de la Selle-Barouco-Nord de la Ride de Beata” dans l’orogenie nor Caraibe (Hispaniola Grandes Antilles). These de doctorat, Universidad Marie y Pierre Curie, Paris, 205 p

## RELACIÓN DE FIGURAS

Fig. 1. Esquema geológico del sector oriental - cinturón de Peralta y cuenca de Azua - (junto con el basamento de arco de islas), y leyenda correspondiente, con la localización de los cortes geológicos representados en este trabajo. Adaptada de Hernaiz Huerta (2006)

Fig. 1. Simplified geological map of eastern part – Peralta belt and Azua basin - (and the island arc basement), and respective legend, with the location of the geological cross sections represented in this work. Adapted from Hernaiz Huerta (2006)

Fig. 2. Esquema geológico del sector occidental - de la sierra de Neiba, vertiente norte de la sierra de Bahoruco, sierra de Martín García y cuenca de Enriquillo, y leyenda correspondiente -, con la localización de los cortes geológicos representados en este trabajo. Adaptada de Hernaiz Huerta (2004 a; 2004 b; 2006)

Fig. 2. Simplified geological map of sierra de Neiba, northern margin of sierra de Bahoruco and Enriquillo basin, with the location of the geological cross sections represented in this work. Adapted from Hernaiz Huerta (2004 a; 2004 b; 2006)

Fig. 3 (A). Corte VII-VII': transversal completa del cinturón de Peralta según Hernaiz Huerta (2000); Hernaiz y Perez-Estaún (2002); Hernaiz Huerta (2006) Ver localización en la figura 8.1.

Fig. 3 (A). Cross section VII-VII': Full geological transect of Peralta belt, alter Hernaiz Huerta (2000); Hernaiz and Perez-Estaún (2002); Hernaiz Huerta (2006). See location in figure 8.1

Fig. 3 (B). Corte VII-VII', restituido entre las líneas o marcas de referencia P y P', siguiendo un modelo de deformación “normal” o hacia el antepaís. El acortamiento medido perpendicularmente a las estructuras es, aproximadamente de 12 km (40%). Según Hernaiz Huerta (2006)

Fig. 3 (B). Cross section VII-VII' restored between reference lines P and P', following a normal or forward propagation deformation model. Shortening, measured normal to the direction of structures, is about 12 km (40%). After Hernaiz Huerta (2006)

Fig. 4. Zonación estructural del cinturón de Peralta (Hernaiz Huerta 2000; Hernaiz y Pérez-Estaún 2002). Ver explicación en el texto.

Fig. 4. Structural division of Peralta belt (Hernaiz Huerta 2000; Hernaiz y Pérez-Estaún 2002). See explanation in the text

Fig. 5. Proyección estereográfica de la estratificación, clivaje de plano axial y ejes de pliegues en el cinturón de Peralta (hoja de San José de Ocoa) (Hernaiz Huerta 2006)

Fig. 5. Stereographic projection of bedding, axial planar cleavage and Fol. Axes in the Peralta belt (San José de Ocoa sheet) (Hernaiz Huerta 2006)

Fig. 6. Cortes VIII-VIII' y IX-IX', del margen oriental del cinturón de Peralta y la cuenca de Azua. Ver localización en la figura 1. Modificados de Gómez Sainz de Aja (2002 b) en Hernaiz Huerta (2006)

Fig. 6. Geological cross sections VIII-VIII' and IX-IX' of eastern margin of Peralta belt and Azua basin. See location in Fig. 1. Modified from Gómez Sainz de Aja (2002) in Hernaiz Huerta (2006)

Fig. 7. Cortes X-X' y XI-XI', de la sierra de Martín García y la cuenca de Azua. Ver localización en la figura 1. Modificados de del Olmo (2000) en Hernaiz Huerta (2006)

Fig. 7. Geological cross sections X-X' and XI-XI' of sierra de Martín García and Azua basin. See location in Fig. 1. Modified from del Olmo (2000) in Hernaiz Huerta (2006)

Fig. 8. Diferentes interpretaciones de la estructura profunda de la cuenca de Azua y la sierra de Martín García (Hernaiz Huerta 2006). Ver explicación en el texto

Fig. 8. Different interpretations of Azua basin and sierra de Martín García deep structure (Hernaiz Huerta 2006). See explanation in the text

Fig. 9. Cortes XII-XII', XII-XIII' y XIV-XIV', de la cuenca de Azua al norte de la Bahía de Ocoa. Ver localización en la figura 1. Modificados de Díaz de Neira (2000) en Hernaiz Huerta (2006)

Fig. 9. Geological cross sections XII-XII', XII-XIII' and XIV-XIV', of Azua basin north of Ocoa bay. See location in Fig. 1. Modified from Díaz de Neira (2000) in Hernaiz Huerta (2006)

Fig. 10. Esquema-explicación del giro de escamas del cinturón de Peralta como consecuencia del empuje del *indenter* de Beata. Según Hernaiz Huerta (2000 a y b); Hernaiz y Pérez Estaún (2002) Ver explicación en el texto.

Fig. 10. Sketch for the explanation of thrust sheets rotation in the Peralta Belt due to the impingement of the Beata indenter. After Hernaiz Huerta (2000); Hernaiz y Pérez Estaún (2002). See explanation in the text

Fig. 11. Cortes geológicos de la sierra de Neiba (Hernaiz Huerta 2004 a; 2004 b; 2006; 2007). Ver localización en la Fig. 2

Fig. 11. Geological cross sections of sierra de Neiba (Hernaiz Huerta 2004 a; 2004 b; 2006; 2007). See location in Fig. 2

Fig. 11 (continuación)

Fig. 11 (continuation)

Fig. 12. Cortes geológicos regionales de la cuenca de Enriquillo y sierras limítrofes (Hernaiz Huerta 2004 a; 2004 b; 2006; 2007). Ver situación en la Fig. 8.2. La estructura profunda de la cuenca de Enriquillo, según Canadian Oil Superior Ltd. (en Norconsult, 1983)

Fig. 12. Regional geological cross sections of Enriquillo basin and surrounding sierras (Hernaiz Huerta 2004 a; 2004 b; 2006; 2007). See location in Fig. 8.2. Deep structure of the Enriquillo basin, deduced from the studies of Canadian Oil Superior Ltd. (in Norconsult, 1983)

Fig. 13. Representación de medidas de la estratificación, el clivaje de plano axial y las direcciones de la fallas en la Sierra de Neiba (Hojas de Galván y La Descubierta) (Hernaiz Huerta 2004 a; 2004 b). (A) Proyección estereográfica equiáreal de medidas de la estratificación: se representa el círculo máximo con mejor ajuste y su polo ( $\beta$ ), que indica la posición media estimada de los ejes de los pliegues. (B) Proyección estereográfica del clivaje de plano axial: el círculo máximo indica la posición media de las medidas. (C) Rosa de los vientos de direcciones de fallas ponderada arealmente para intervalos de  $10^\circ$ . (N: Nº de datos en cada proyección) (Hernaiz Huerta 2004 a; 2004 b)

Fig. 13. Representation of bedding, axial planar cleavage and fault direction measurements in sierra de Neiba (Galván and La Descubierta sheets) (Hernaiz Huerta 2004 a; 2004 b). (A) Equiáreal stereographic projection of bedding: best fit great circle and its pole indicates average position of fold axes. (B) Equiáreal stereographic projection of axial planar cleavage: great circle indicates average position of measurements. (C) Fault directions wind rose weighted for area intervals of  $10^\circ$ . (N: Number. of data in each projection)

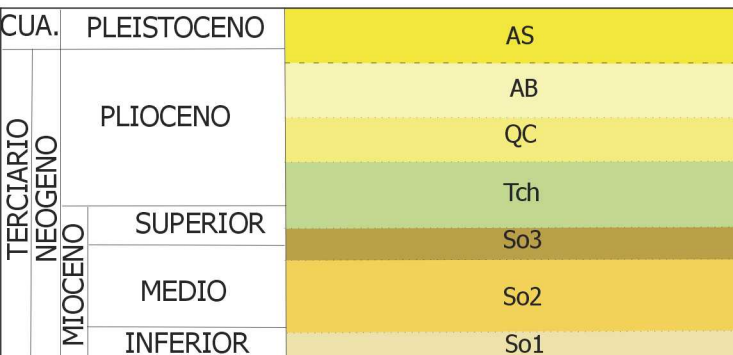
Fig. 14. Esquema estructural del sector occidental (cuenca de Enriquillo y sierras limítrofes). En el recuadro inferior, interpretación según un modelo teórico de cizalla izquierda (Hernaiz Huerta 2004 a; 2004 b; 2006; 2007). Ver explicación en el texto

Fig. 14. Schematic structural map of western part (Enriquillo basin and surrounding sierras). In the lower inset, interpretation as a theoretical model of left lateral shear zone (Hernaiz Huerta 2004 a; 2004 b; 2006; 2007). See text for explanation

Fig. 15. Correlación de la geología y la estructura del sector occidental (cuenca de Enriquillo y sierras limítrofes) con el mapa aeromagnético de gradiente vertical (Hernaiz Huerta 2004 a; 2004 b; 2006; 2007). Ver explicación en el texto

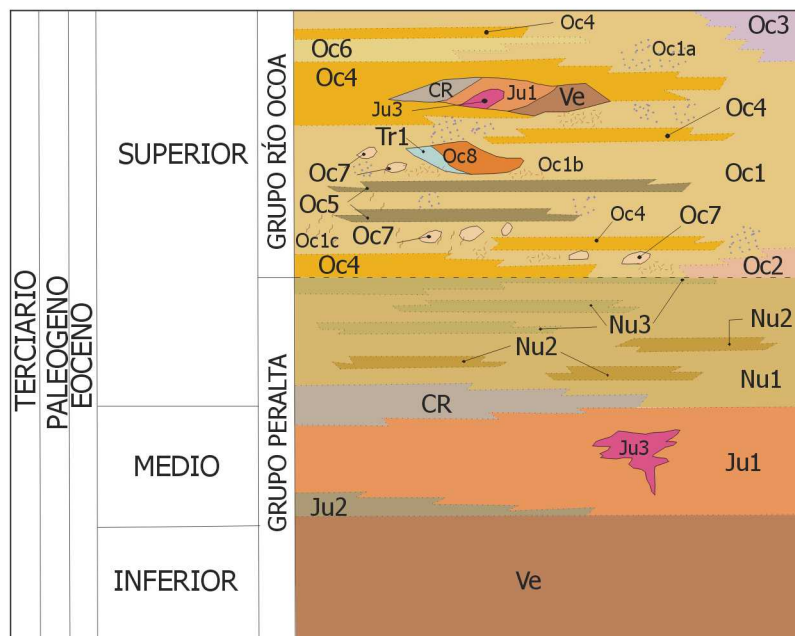
Fig. 15. Correlation of the geology and structure of western part (Enriquillo basin and surrounding sierras) with the aeromagnetic map (vertical gradient) (Hernaiz Huerta 2004 a; 2004 b; 2006; 2007) See explanation in the text

# CUENCA DE AZUA



- AS Fm. Arroyo Seco(= Fm. Vía). Conglomerados de tonos blancos y arcillas
- AB Fm. Arroyo Blanco. Conglomerados, areniscas y arcillas
- QC Fm. Quita Coraza. Margas y areniscas tableadas
- Tch Fm Trinchera. Areniscas tableadas con intercalaciones rítmicas de margas y tramos conglomeráticos
- So3 Fm. Sombrerito. Margas con intercalaciones de areniscas y calizas
- So2 Fm. Sombrerito. Calizas tableadas blancas y rosadas
- So1 Fm. Sombrerito. Margas grises con intercalaciones de areniscas

# CINTURÓN DE PERALTA



- Oc8 Fm. Ocoa. Olistolito de naturaleza desconocida en cuya base se reconoce la Fm. Tireo: calizas tableadas y masivas grises
- Oc7 Fm. Ocoa. Olistolitos de naturaleza desconocida ¿Capas rojas del Jura?: Alternancia de calizas, margocalizas, limolitas calcáreas y margas de tonos rojos y blancos
- Oc6 Fm. Ocoa. Calizas masivas o en bancos, con niveles de brechas y conglomerados calcáreos
- Oc5 Fm. Ocoa. Calizas tableadas y en bancos, blancas y grises
- Oc4 Fm. Ocoa. Conglomerados polimíticos masivos
- Oc3 Fm. Ocoa. Alternancia rítmica de margas y areniscas
- Oc2 Fm. Ocoa. Margas de tonos verdes
- Oc1 Fm. Ocoa indiferenciada. Margas y fangos, generalmente arenosos, con intercalaciones de areniscas turbidíticas, cantos polimíticos dispersos, bloques y olistolitos de origen diverso; frecuente aspecto caótico
- (a) Fm. Ocoa "facies organizada". Alternancia de margas y fangos ocres con niveles centimétricos y decimétricos de areniscas turbidíticas de grano fino. Frecuentes niveles canalizados de conglomerados
- Oc1 (b) Fm. Ocoa "facies desorganizada con bloques y olistolitos". Margas y fangos muy arenosos, de tonos oscuros y aspecto caótico que incluyen niveles

- discontinuos de areniscas turbidíticas, frecuentemente slumped, abundantes cantos polimíticos dispersos o formando niveles, y bloques y olistolitos de todos los tamaños y procedencias diversas
- (c) Fm. Ocoa "facies esquistosa". Idem al anterior pero con una intensa fábrica deformativa sin sedimentaria
- Nu3 Fm. El Número. Calizas masivas o estratificadas, frecuentemente fosilíferas, con intercalaciones de conglomerados y brechas
- Nu2 Fm. El Número. Calcarenitas y margas y calcarenitas de carácter turbidítico; frecuentemente megaturbiditidas
- Nu1 Fm. El Número. Alternancia de margas marrones y niveles decimétricos de turbiditas calcáreas y silicicísticas
- CR "Capas rojas" del Jura. Limolitas calcáreas, margas y margocalizas rojas con intercalaciones de calizas blancas
- Ju3 Fm. Jura. Coladas basálticas
- Ju2 Fm. Jura. Conglomerados polimíticos de color claro
- Ju1 Fm. Jura. Calizas tableadas blancas o gris claro
- Ve Fm. Ventura. Alternancia rítmica de areniscas turbidíticas silicicísticas. Localmente conglomerados y calizas. En la parte inferior, posibles intercalaciones de niveles volcánicos

	Basaltos		Areniscas masivas
	Pillow-lavas		Conglomerado
	Basaltos andesíticos y andesitas		Conglomerados poligénicos
	Diabasas y gabros		Conglomerados calcáreos
	Tonalitas no foliadas		Conglomerados poligénicos con matriz calcárea
	Tonalitas foliadas		Calizas laminadas
	Peridotitas		Calizas tableadas o en bancos
	Anfibolitas		Calizas arcillosas
	Traquiandesitas		Margas
	Riolitas		Margas arenosas
	Rocas volcánicas lávicas		Margas con intercalaciones de areniscas
	Rocas intrusivas		Arcillas
	Niveles volcanoclásticos		Arcillas englobando olistolitos
	Niveles volcanoclásticos de grano fino		Lutitas arenosas
	Brecha volcanoclástica		Calizas tableadas o en bancos
	Rocas volcanoclásticas estratificadas o laminadas		Calizas tableadas o en bancos con silex
	Cineritas		Grauwacas
	Ignimbritas		Limolitas
	Aglomerado		Niveles de chert
	Arenisca		Megaturbida
	Areniscas calcáreas/calcarenitas		Slumps
	Areniscas silíceas		Facies caóticas con fábrica deformativa sinsedimentaria. Sp = Fábrica o esquistosidad principal

So = Estratificación

Sp = Esquistosidad principal

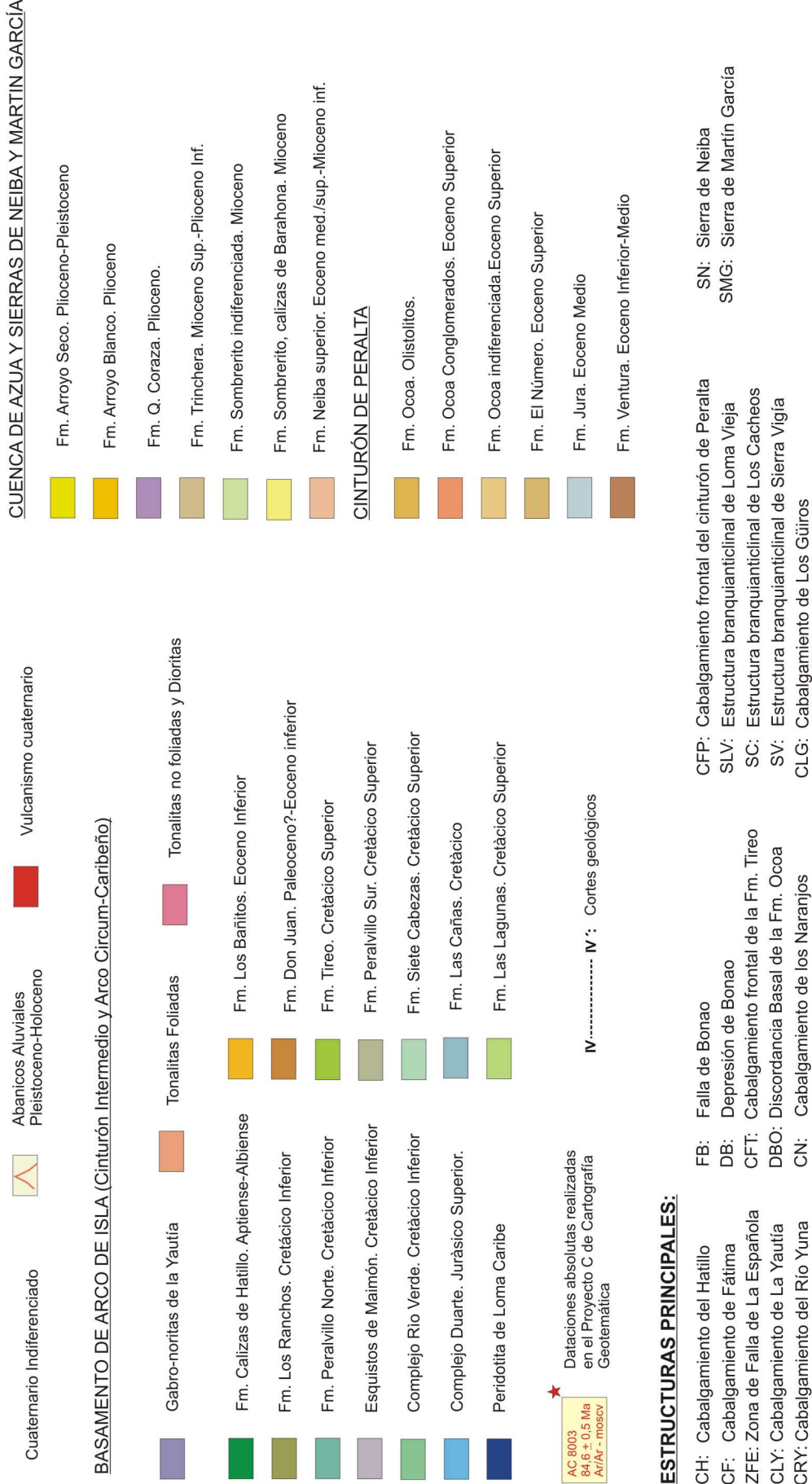
Sb = Bandeado magmático

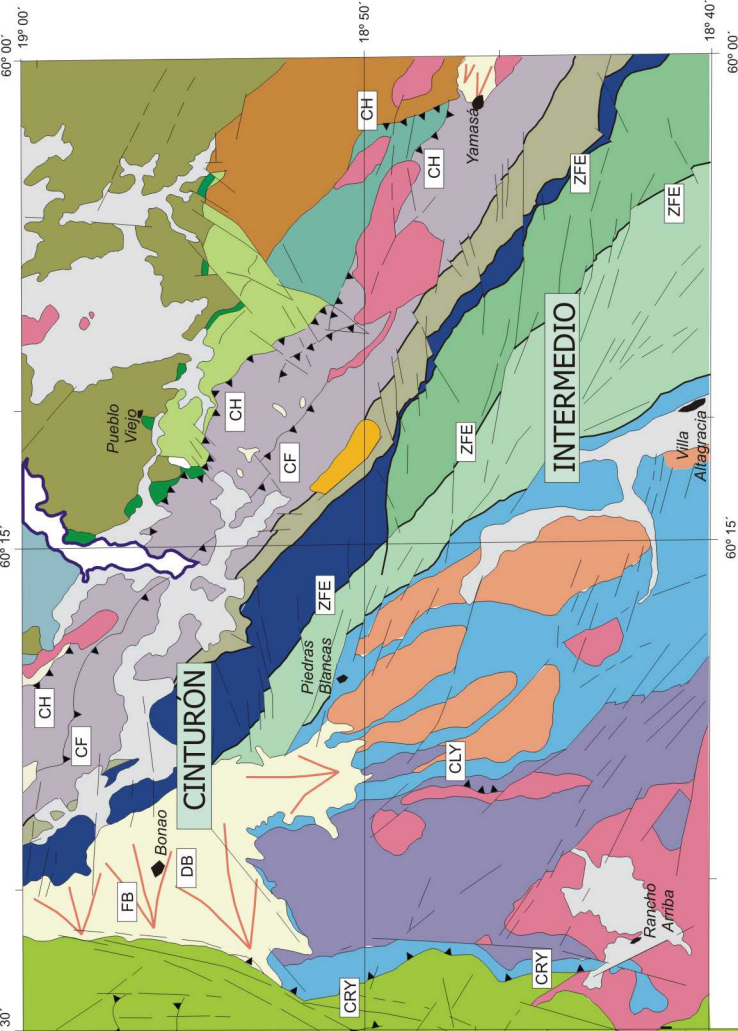
- / + Falla con movimiento en dirección.  
Bloque +, se aleja del observador

Cabalgamientos o despegues sinsedimentarios

# ESQUEMA GEOOLÓGICO DEL BASAMENTO DE ARCO DE ISLA, DEL CINTURÓN DE PERALTA Y DE LA CUENCA DE AZUÁ

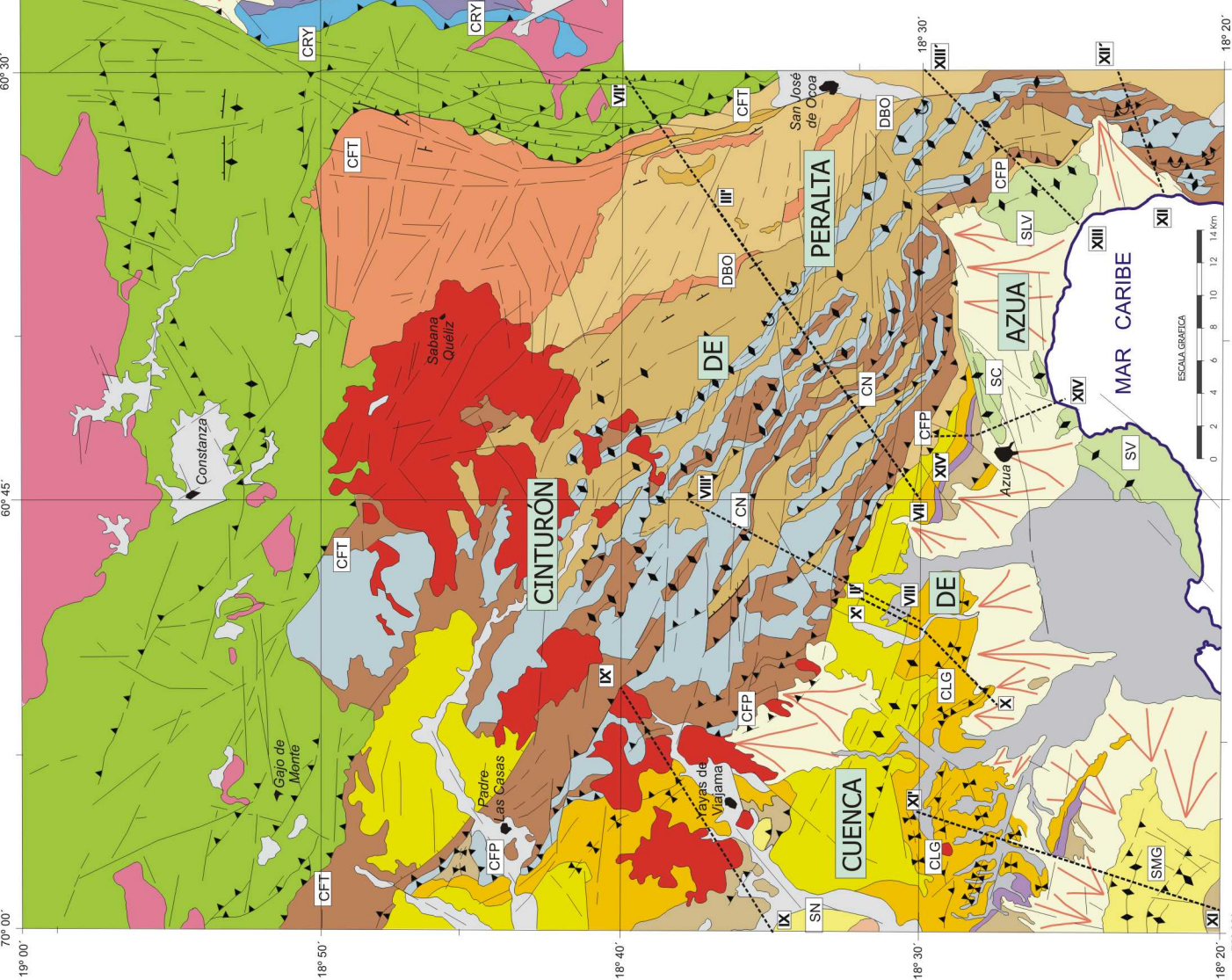
## LEYENDA





### ESQUEMA GEOLÓGICO DEL BASAMENTO DE ARCO DE ISLA, DEL CINTURÓN DE PERALTA Y DE LA CUENCA DE AZUA

IV	I	CONSTANZA	I	HATILLO
		6072		
SAJO DE MONTE		BONAO		VILLA ALTAGRACIA
III	II	SABANA QUELIZ	III	
PADRE LAS CASAS				
IV	I	YAYAS DE VIALAMA		SAN JOSE DE OCOA
		6071		
PUEBLO VIEJO				AZUA
III	II			



# ESQUEMA GEOLÓGICO DE LA SIERRA DE NEIBA, VERTIENTE NORTE DE LA SIERRA DE BAHORUCO, SIERRA DE MARTÍN GARCÍA Y CUENCA DE ENRIQUILLO

## LEYENDA

Cuaternario indiferenciado      Arrecifes costeros emergidos. Plio-Cuaternario

### Cuenca de Enriquillo y San Juan

Depósitos lacustres (y asociados) del lago Enriquillo. Holoceno

Arrecife subactual del Lago Enriquillo. Holoceno

Abanicos asociados al delta del Yaque. Pleistoceno-Holoceno

Abanicos aluviales y conos de deyeción. ¿Pleistoceno-Holoceno

Fm. Jimaní. Mbro. Superior. Pleistoceno

Fm. Jimaní. Mbro. inferior. Pleistoceno

Fm. Arroyo Seco. Plioceno sup.-¿Pleistoceno?

Fm. Arroyo Blanco-Las Salinas. Plioceno

Fm. Angostura. Plioceno inf.

Fm. Quita Coraza. Plioceno

Fm. Trinchera. Mioceno sup.-Plioceno inf.

Sondeo de exploración de hidrocarburos



### Cuencas de Enriquillo y San Juan

### Sierras de Neiba y de Bahoruco

Fm. Sombrerito margio-calcarea, Fm. Lemba y unidad del Majagua. Mioceno-Plioceno inferior

Fm. Sombrerito. Mbro. Gajo Largo. Mioceno sup.

Fm. Sombrerito calcárea (calizas de Barahona). Mioceno

Fm. Sombrerito indiferenciada. Mioceno

Fm. Neiba superior. Eoceno med./sup.-Mioceno inf.

Complejo Volcanosedimentario de El Aguacate de Neiba. Eoceno med.-sup.

Fm. Neiba brechoide. Eoceno

Fm. Neiba inferior. Eoceno inf.-med.

Und. El Manguito. Cretácico sup.

Isobatas y estructuras deducidas de la cartografía en el subsuelo de un nivel lutítico-margoso próximo al techo de la Fm. Sombrerito calcárea (según Canadian Superior Oil Ltd. 1979, en Norconsult 1983)

HH-9041  
★ 51,7 - 0,5 Ma  
U/Pb - RT  
50,1 - 3,4 Ma  
Ar/Ac en horn.



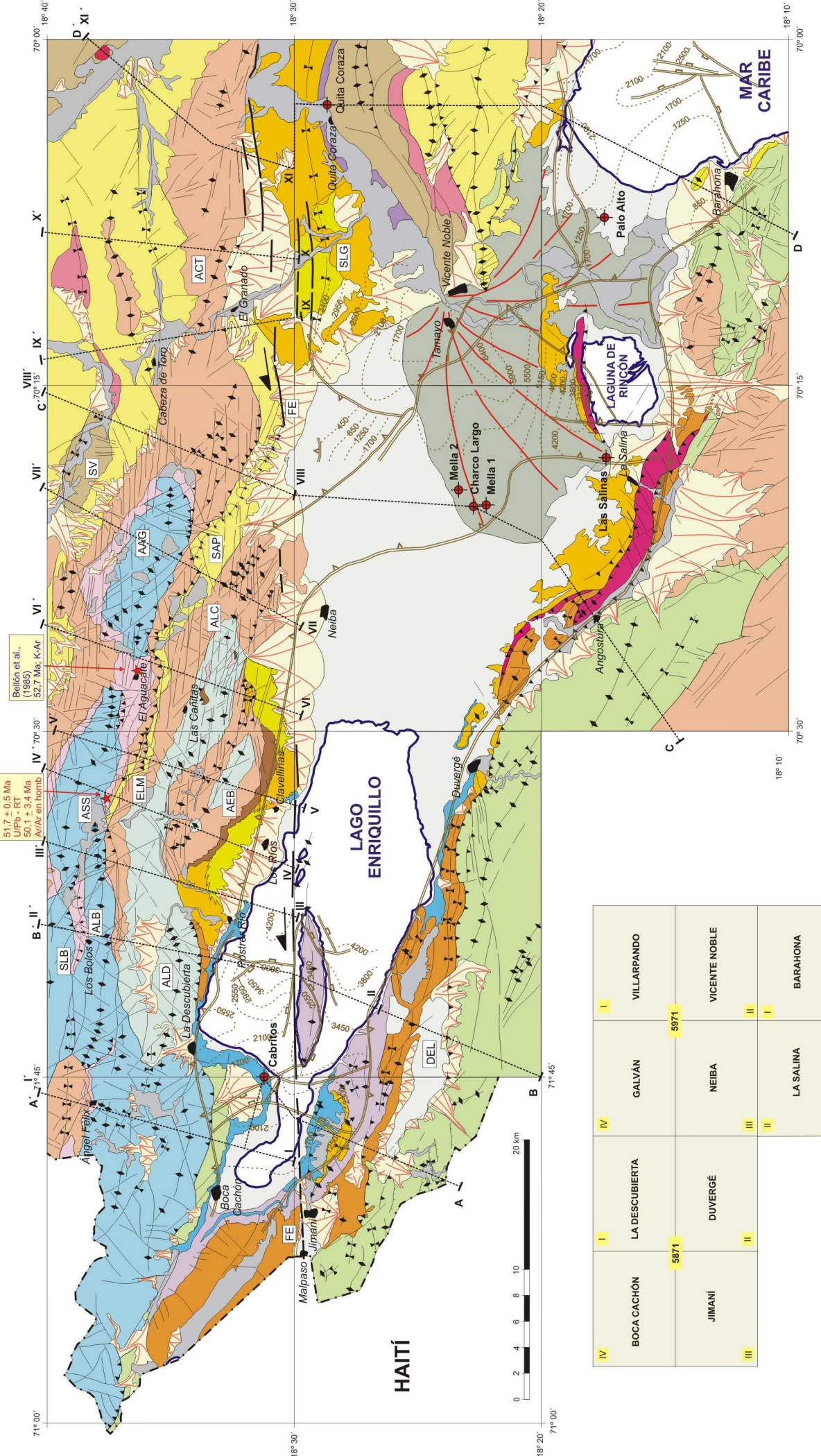
Dataciones absolutas realizadas en el Proyecto L de Cartografía Geométrica

IV : Cortes geológicos

### ESTRUCTURAS PRINCIPALES:

AAG:	Anticlinal de El Aguacate	ACT:	Anticlinal de Cabeza de Toro	ELM:	Escarma de Los Mosquitos	SLG:	Sinclinal de Los Güiros
ALC:	Anticlinal de Las Cañitas	ASS:	Anticlinal de Sabana del Silencio	ALD:	Anticlinal de La Descubierta	FE:	Falla de Enriquillo
SAP:	Sinclinal de Apolinar Perdomo	ALB:	Anticlinal de Los Bolos	AEB:	Anticlinal de El Barro		
SV:	Sinclinal de Vallejuelo	SLB:	Sinclinal de Los Bolos	DEL:	Depresión de El Limón		

**ESQUEMA GEOLÓGICO DE LA SIERRA DE NEIBA, VERTIENTE NORTE DE LA SIERRA DE BAHORUCO,  
SIERRA DE MARTÍN GARCÍA Y CUENCA DE ENRIQUILLO (PROYECTO L-ZONA SUROESTE)**



Cabalgamiento frontal de  
la Fm. Tireo  
(falla de San José-Restauración)

NE

Loma Monte Bonito

Pista de Carriona

Ctr. de San José de Ocoa a Constanza

Río Ocoa

Firme de Palos Mojados

Río El Cañal

Mogote Reparadero

Río Limón

Los Manaderos

Río Barrialjo

Lomas Los Tramojos

Río Agua Rica

Loma Naranjo

Ganáj

Las Yanivias

Fm. TRINCHERA

Fm. SOMBRERITO

AB

T1

N1

N2

N3

N4

T2

N5

N6

N7

N8

N9

N10

N11

N12

N13

N14

N15

N16

N17

N18

N19

N20

N21

N22

N23

N24

N25

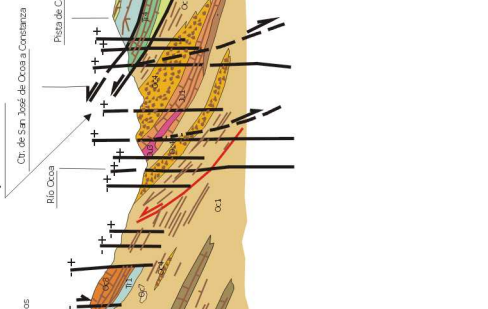
N26

N27

N28

N29

N30



**CORTE VII-VII'**

P' P'

Río El Cañal

Mogote Reparadero

Río Limón

Los Manaderos

Río Barrialjo

Lomas Los Tramojos

Río Agua Rica

Loma Naranjo

Ganáj

Las Yanivias

Fm. TRINCHERA

Fm. SOMBRERITO

AB

T1

N1

N2

N3

N4

N5

N6

N7

N8

N9

N10

N11

N12

N13

N14

N15

N16

N17

N18

N19

N20

N21

N22

N23

N24

N25

N26

N27

N28

N29

N30

N31

N32

N33

N34

N35

N36

N37

N38

N39

N40

N41

N42

N43

N44

N45

N46

N47

N48

N49

N50

N51

N52

N53

N54

N55

N56

N57

N58

N59

N60

N61

N62

N63

N64

N65

N66

N67

N68

N69

N70

N71

N72

N73

N74

N75

N76

N77

N78

N79

N80

N81

N82

N83

N84

N85

N86

N87

N88

N89

N90

N91

N92

N93

N94

N95

N96

N97

N98

N99

N100

N101

N102

N103

N104

N105

N106

N107

N108

N109

N110

N111

N112

N113

N114

N115

N116

N117

N118

N119

N110

N111

N112

N113

N114

N115

N116

N117

N118

N119

N110

N111

N112

N113

N114

N115

N116

N117

N118

N119

N110

N111

N112

N113

N114

N115

N116

N117

N118

N119

N110

N111

N112

N113

N114

N115

N116

N117

N118

N119

N110

N111

N112

N113

N114

N115

N116

N117

N118

N119

N110

N111

N112

N113

N114

N115

N116

N117

N118

N119

N110

N111

N112

N113

N114

N115

N116

N117

N118

N119

N110

N111

N112

N113

N114

N115

N116

N117

N118

N119

N110

N111

N112

N113

N114

N115

N116

N117

N118

N119

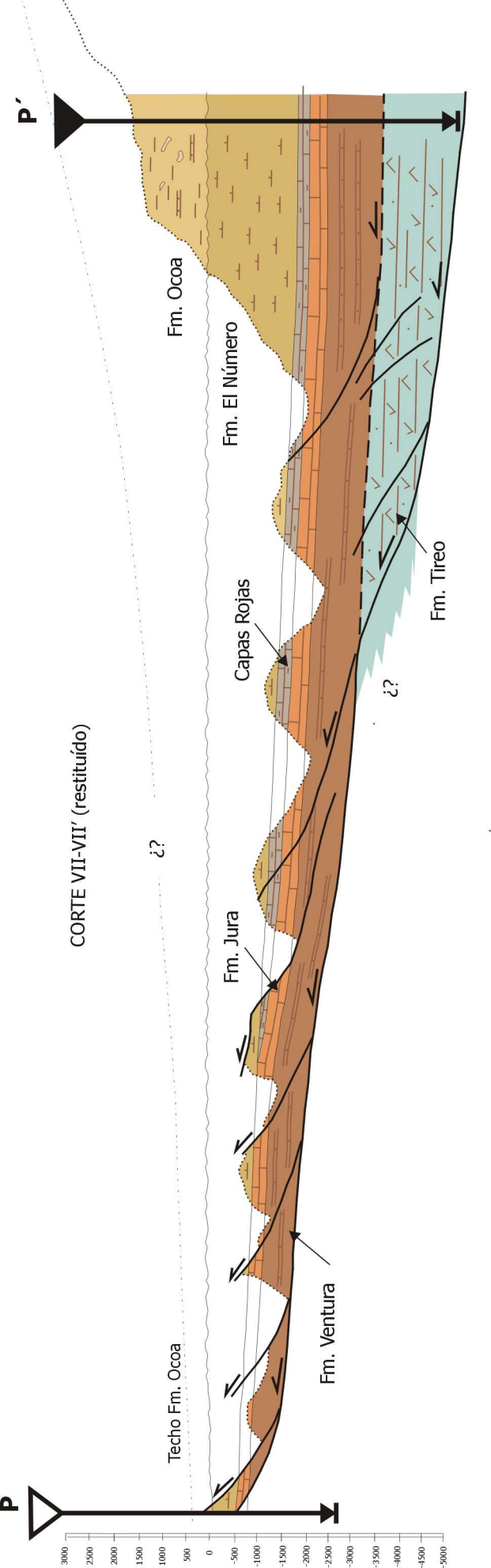
N110

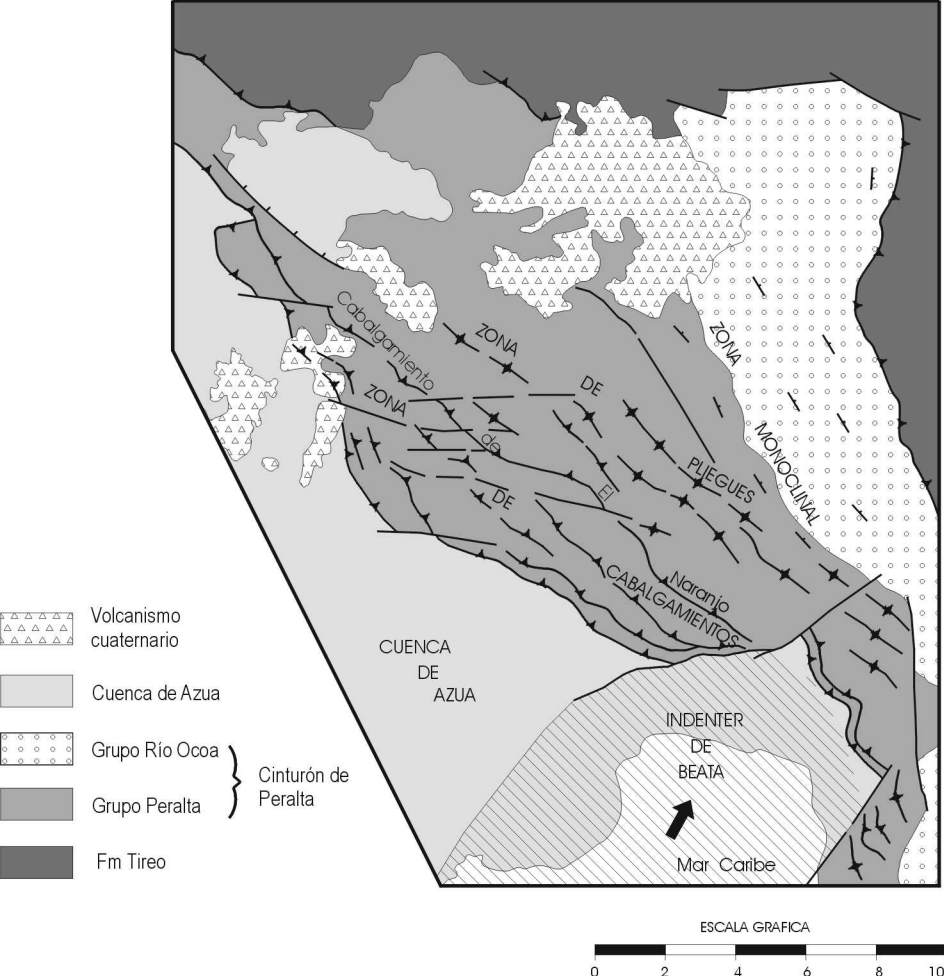
N111

N112

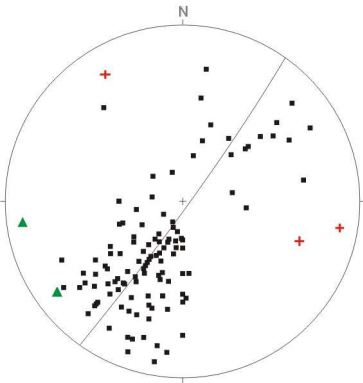
N113

N114





## Cinturón de Peralta (Grupo Peralta)



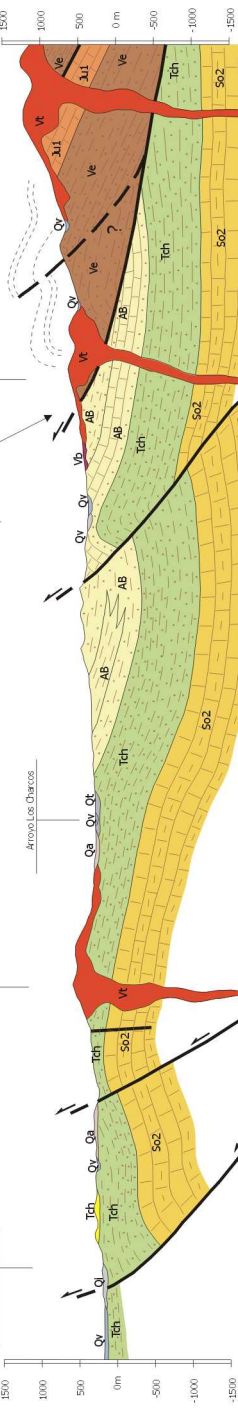
- Polos de la estratificación (So)
- ▲ Polos del clivaje de plano axial (Sax)
- ✚ Ejes de pliegues

SO

## CORTE IX-IX'

Cuenca de Azúa

Ctra. Atar-San Juan



Cabalgamiento frontal del  
Cinturón de Peralta  
(falla de San Juan-Los Pozos)

NE

## CORTE VIII-VIII'

Cuenca de Azúa

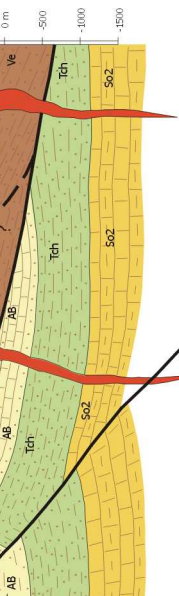
Loma de Las Mojetas

Arroyo Los Charcos

Ctra. de la Salsilla

Loma de los Chicos

Loma del Peralta



SSO

## CORTE VIII-VIII'

Cuenca de Azúa

Hoya de las Vinas

Arroyo Majano

Ctra. Atar-Peralta

Firme de Los Muños

Ctra. Atar-San Juan

Tch

So2

AB

Ve

Vt

Qv

Tch

So2

AB

Ve

Vt

Tch

So2

AB

Ve

Vt

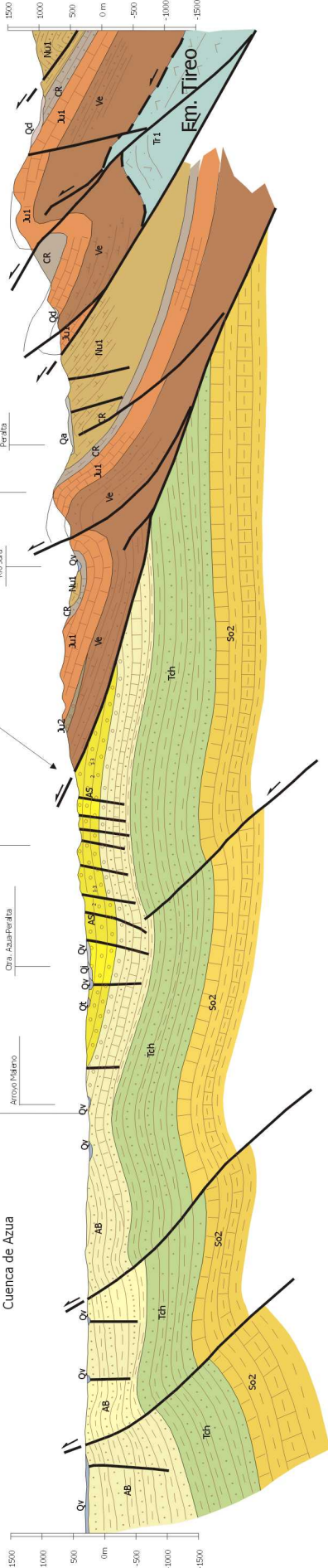
Qv

Tch

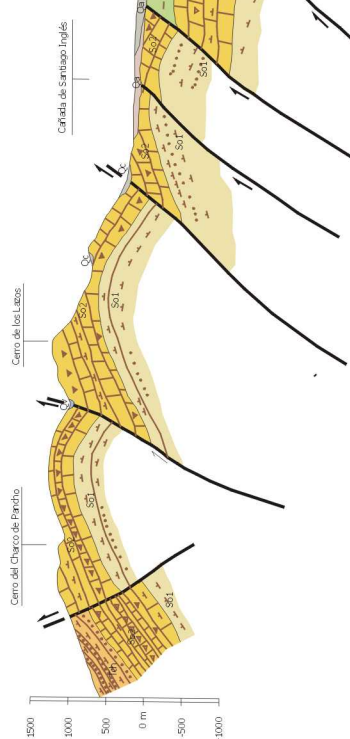
So2

Cabalgamiento frontal del  
Cinturón de Peralta  
(falla de San Juan-Los Pozos)

NNE

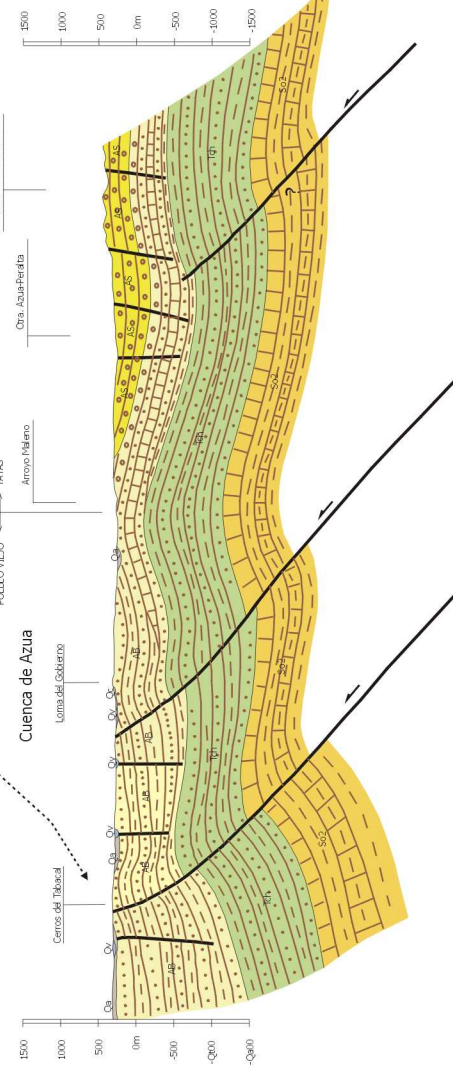


Sierra de Martín García



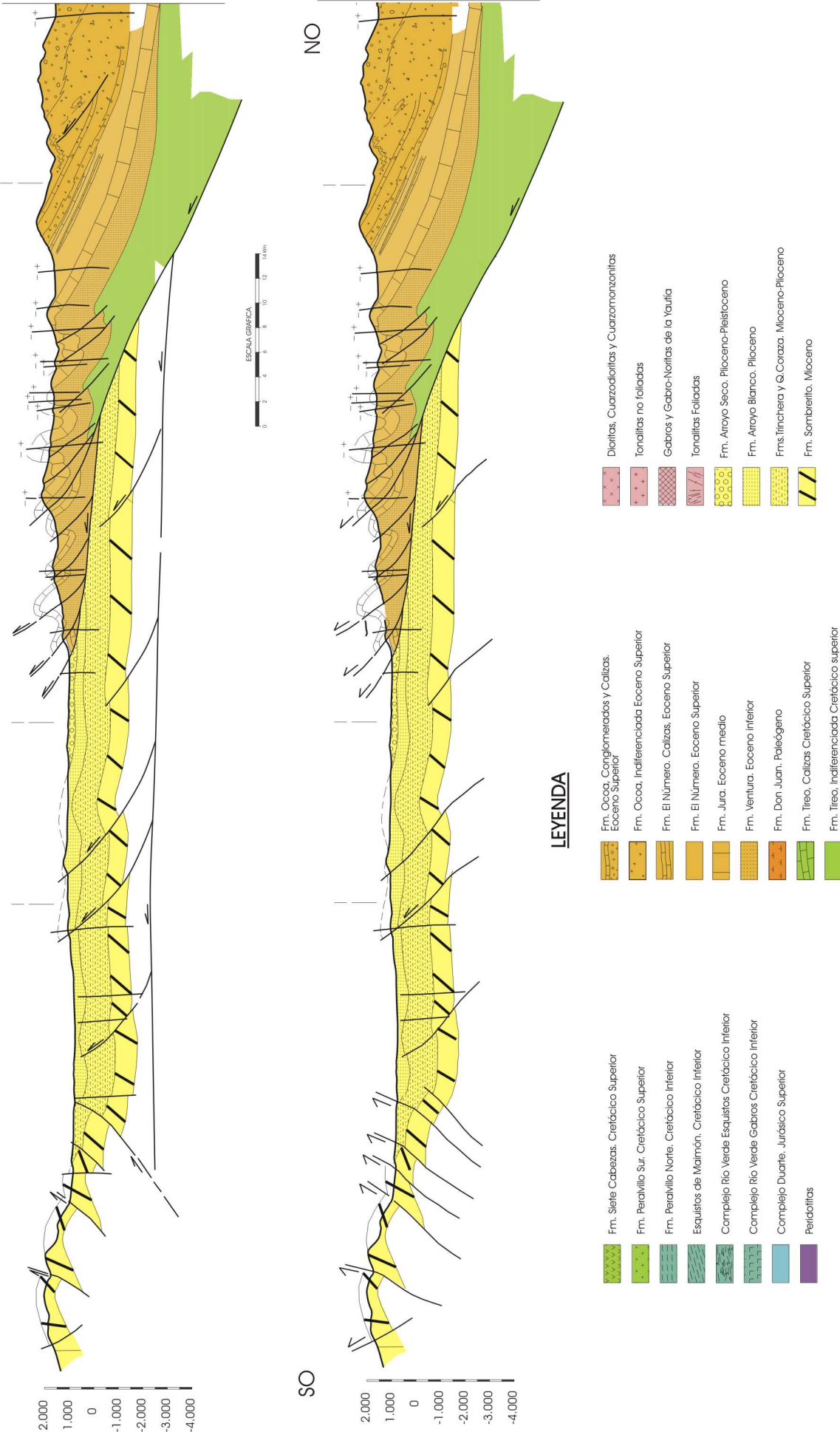
SSO

CORTE X-X'



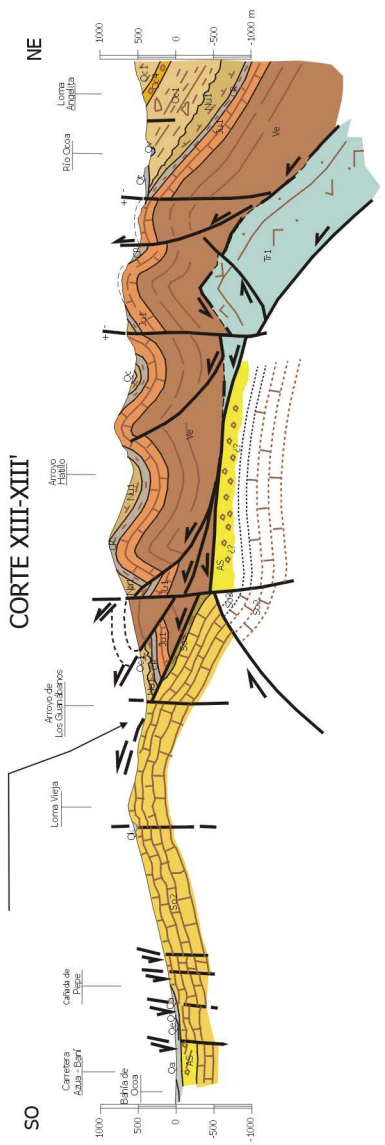
N

S

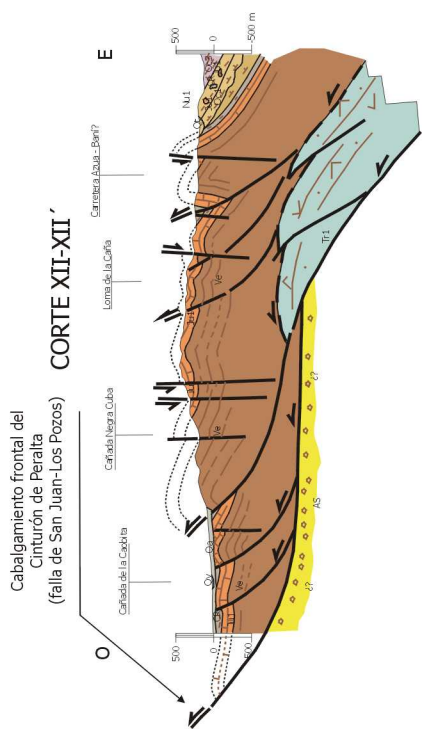


Cabalgamiento frontal del  
Cinturón de Peralta  
(falla de San Juan-Los Pozos)

**CORTE XIII-XIII'**

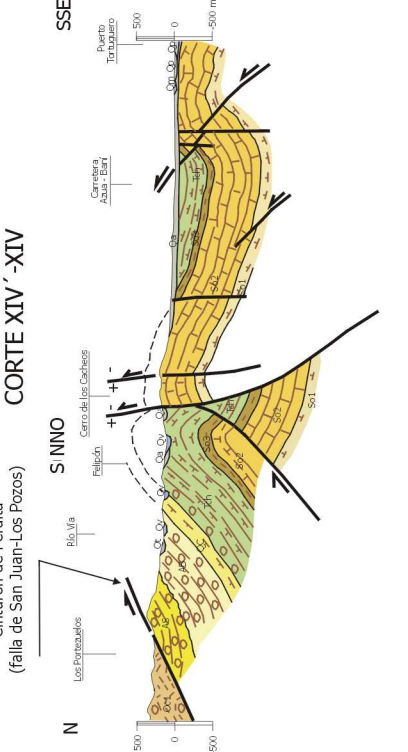


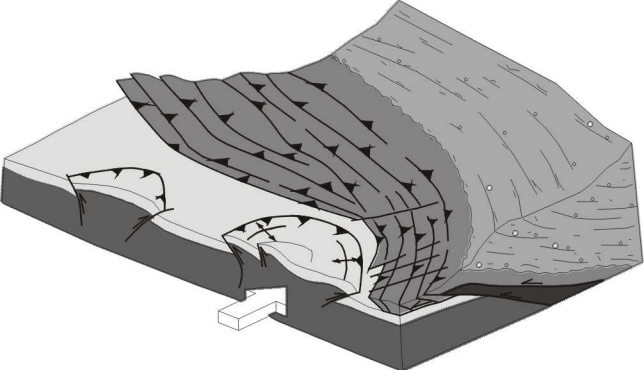
**CORTE XII-XII'**



Cabalgamiento frontal del  
Cinturón de Peralta  
(falla de San Juan-Los Pozos)

**CORTE XIV'-XIV**





Cuenca de Azua

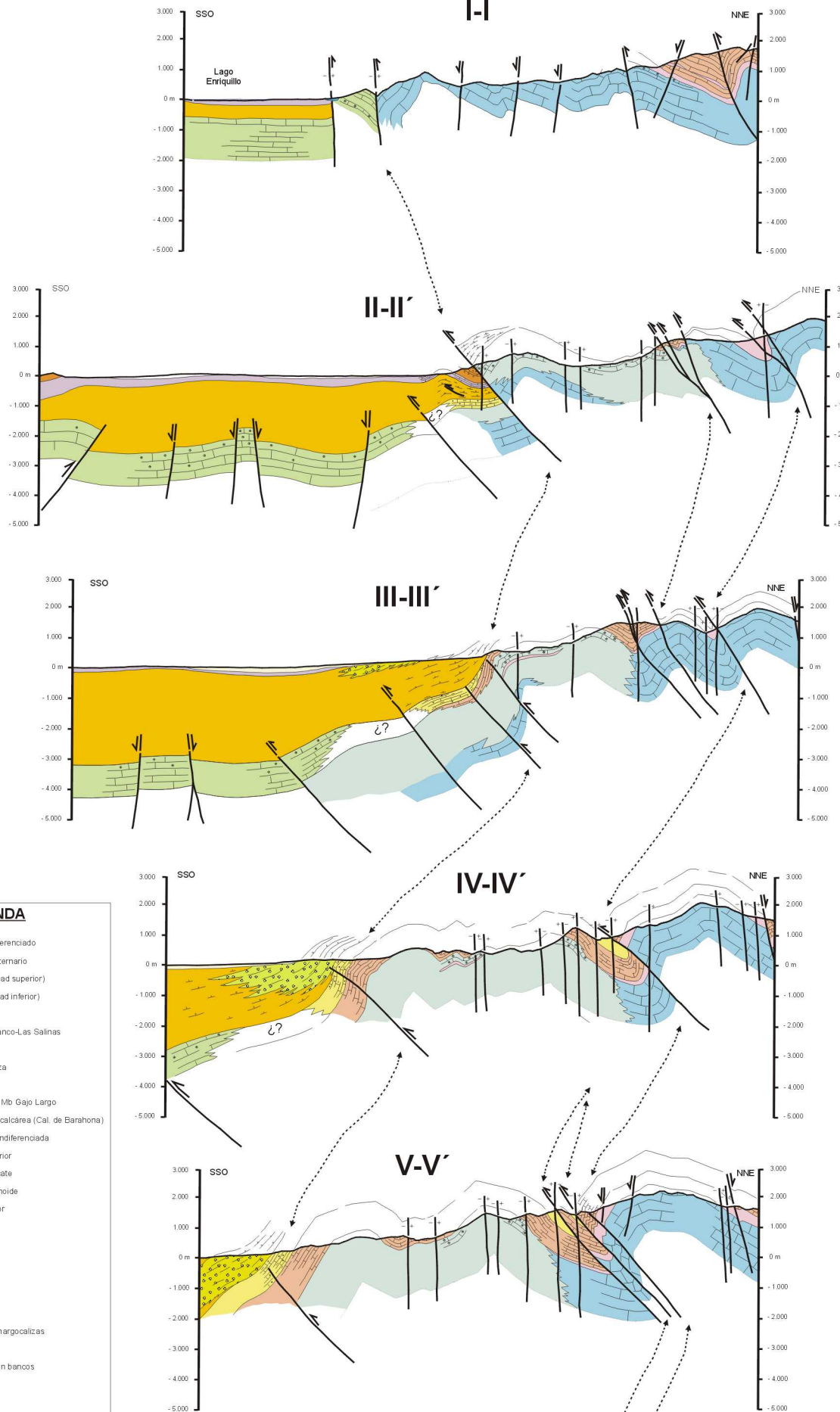
Basamento no determinado de la Cuenca de Azua

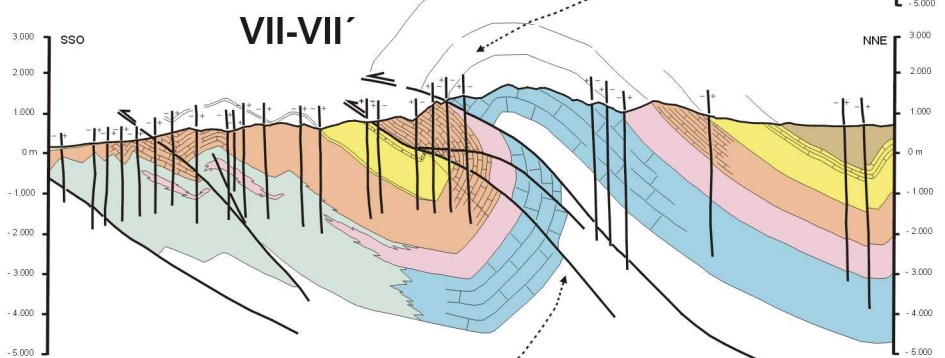
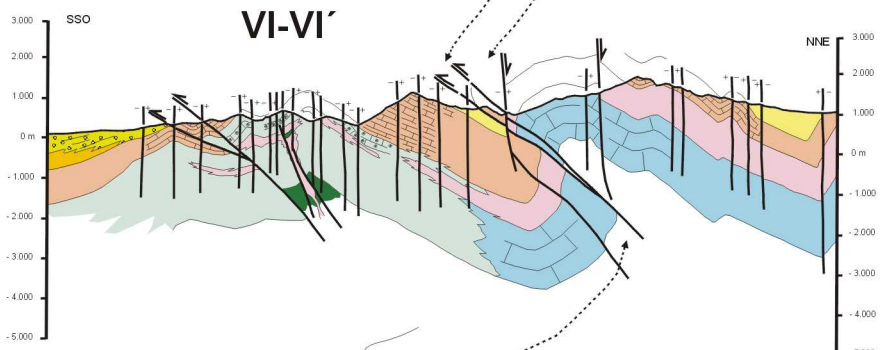
Grupo Río Ocoa

Grupo Peralta

Fm Tireo

} Cinturón de Peralta





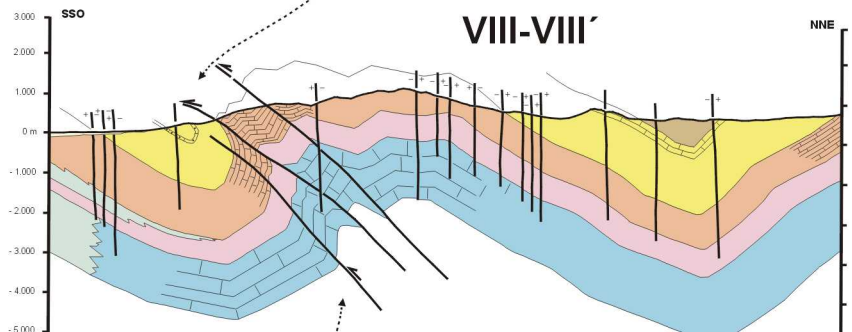
**LEYENDA**

[Light Green Box]	Qi. Cuaternario indiferenciado
[Red Box]	Vq. Vulcanismo cuaternario
[Orange Box]	Js. Fm. Jimani (unidad superior)
[Purple Box]	J. Fm. Jimani (Unidad inferior)
[Yellow Box]	As. Fm. Ayo. Seco
[Yellow Box]	AbLS. Fm. Ayo Blanco-Las Salinas
[Magenta Box]	An. Fm. Angostura
[Purple Box]	Qc. Fm. Guita Coraza
[Brown Box]	Tch. Fm. Trinchera
[Pink Box]	Gl. Fm. Sombrerito, Mb Gajo Largo
[Light Green Box]	Sc. Fm. Sombrerito calcárea (Cal. de Barahona)
[Yellow Box]	Si. Fm. Sombrerito indiferenciada
[Orange Box]	Ns. Fm. Neiba superior
[Pink Box]	CVA. C. V. El Aguacate
[Light Blue Box]	Nb. Fm. Neiba brechoide
[Dark Blue Box]	Ni. Fm. Neiba inferior

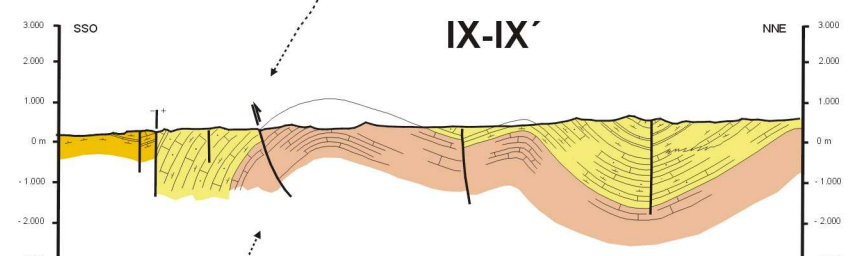
**Símbolos**

[Diamond with dot]	Sales y yesos
[Diamond with circle]	Conglomerados
[Diamond with dots]	Areniscas
[Diamond with horizontal line]	Margas
[Diamond with diagonal line]	Calizas margosas-margocalizadas
[Diamond with asterisk]	Calizas arrecifales
[Diamond with vertical lines]	Calizas masivas o en bancos
[Diamond with horizontal lines]	Calizas tableadas
[Diamond with diagonal lines]	Calcarenitas

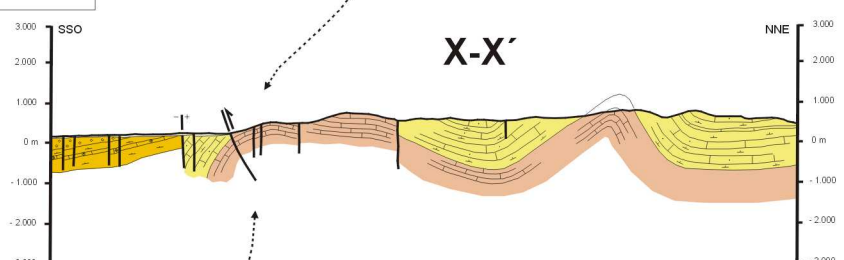
**VIII-VIII'**



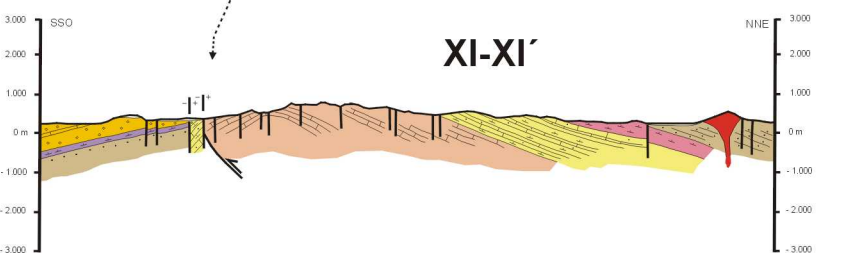
**IX-IX'**



**X-X'**



**XI-XI'**

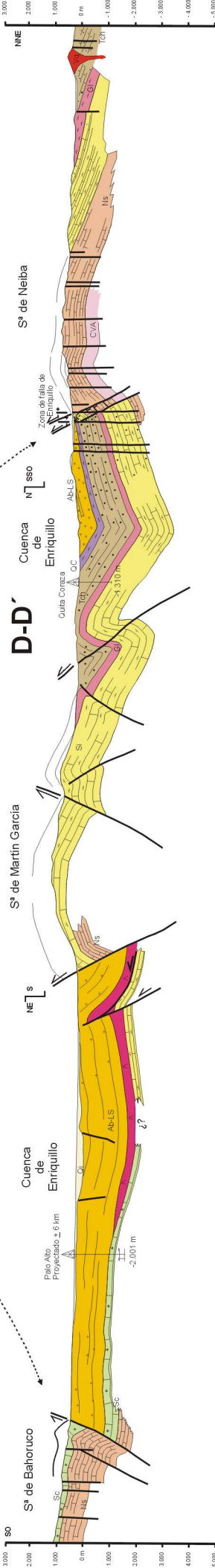
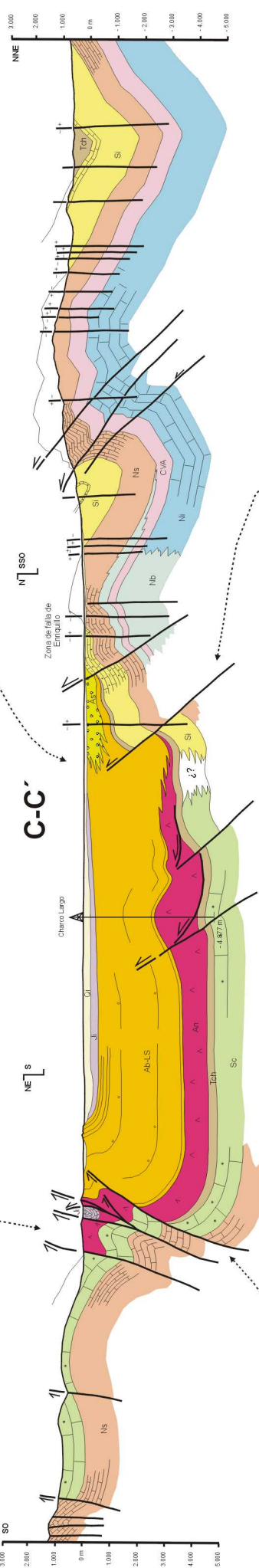
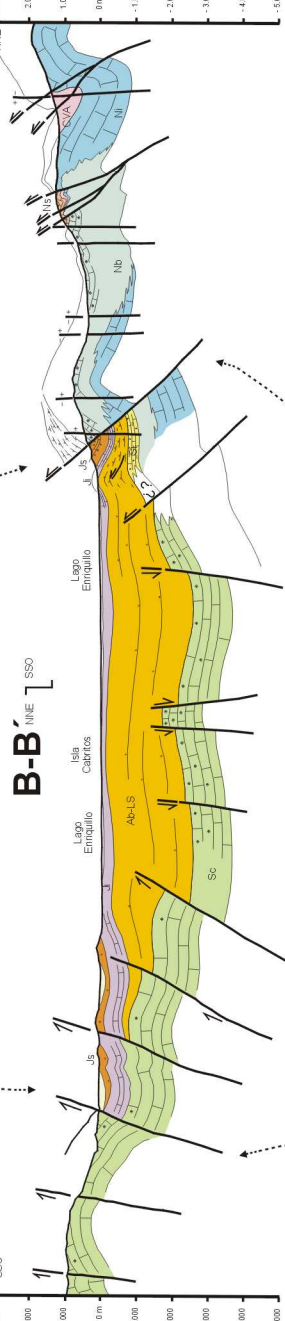
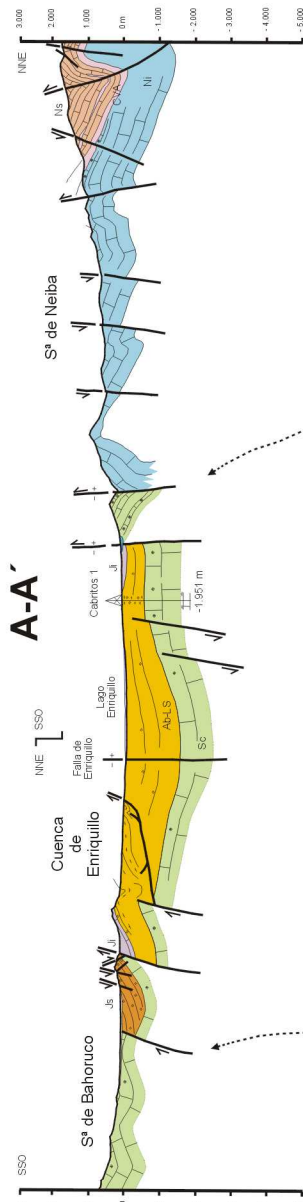


## LEYENDA

Qi. Cuaternario indiferenciado
Vq. Vulcanismo cuaternario
Js. Fm. Amaní (Unidad superior)
As. Fm. Ayo Seco
Ab-LS. Fm. Ayo Blanco-Las Salinas
An. Fm. Angostura
Qc. Fm. Guita Coraza
Tch. Fm. Timcheira
Gi. Fm. Sonibreno, Mts Gajío Largo
Sc. Fm. Sonibreno catárea (Cal. de Barahona)
Sl. Fm. Sonibreno Indiferenciada
Ns. Fm. Niebla superior
CVA. C. V. El Agujacate
Nb. Fm. Niebla bichotidae
Ni. Fm. Niebla inferior

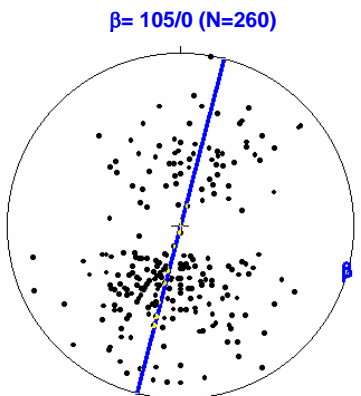
## Símbolos

Sales y yesos
Conglomerados
Areniscas
Margas
Caizas margosas-margocalizadas
Caizas arenicolas
Caizas masivas o en bancos
Caizas tabuladas
Calcareitas



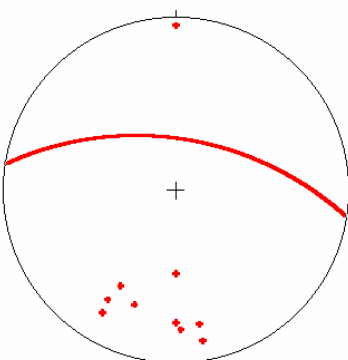
**(A)**

HOJA DE LA GALVÁN



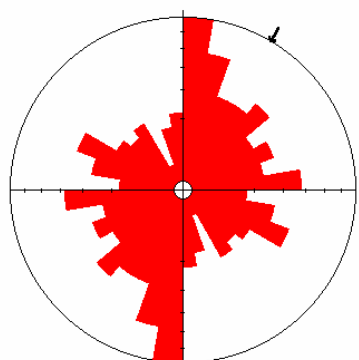
**(B)**

Sax media= 009/66 (N=10)

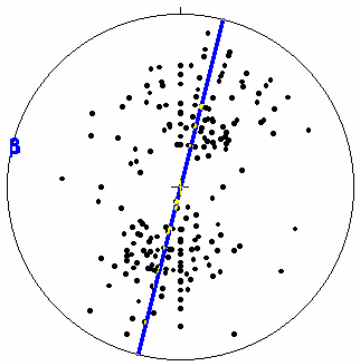


**(C)**

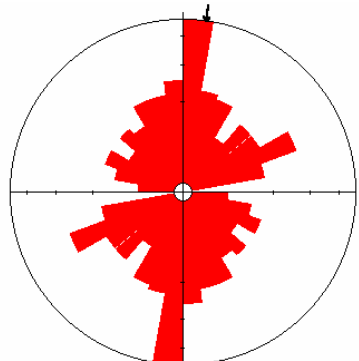
N-fallas: 252; N-max:45 (17,9%)



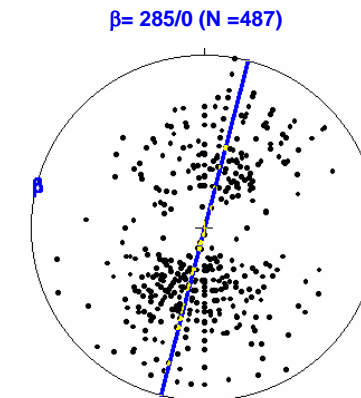
HOJA DE LA DESCUBIERTA



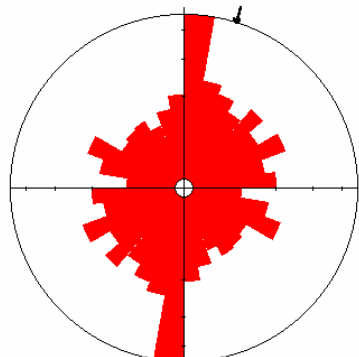
N-fallas=169; N max= 31 (18,3%)

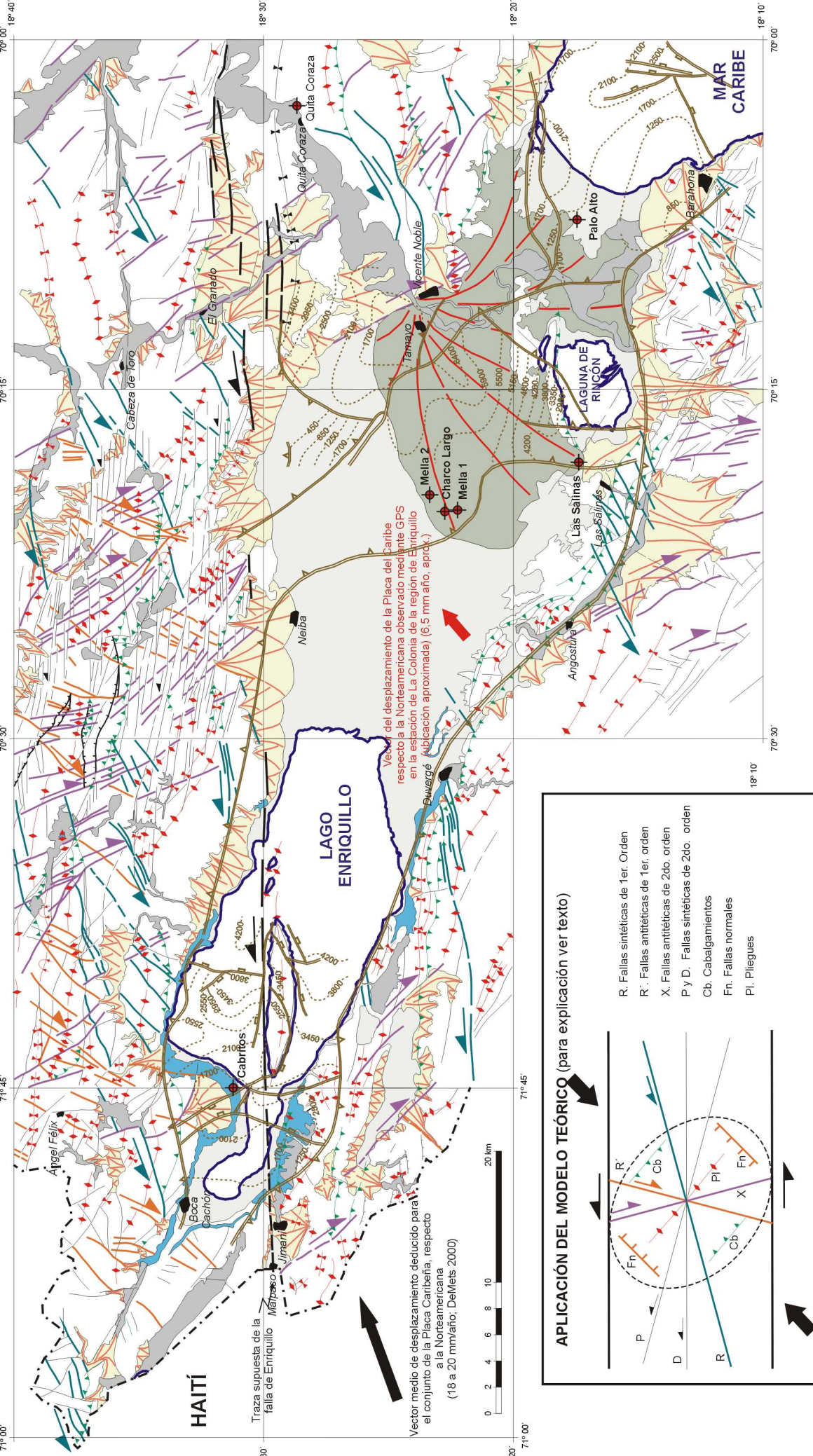


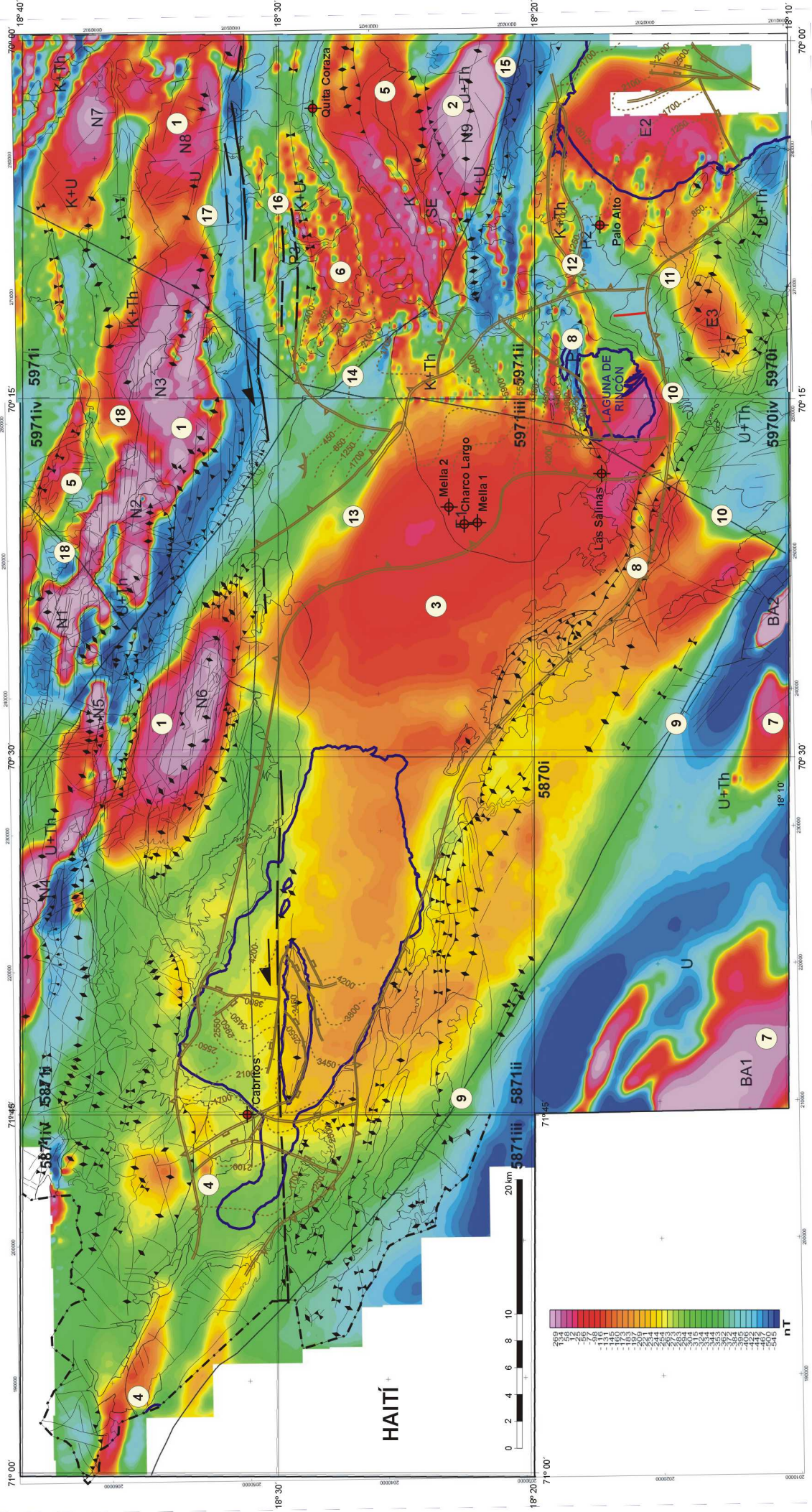
HOJAS DE GALVÁN Y LA DESCUBIERTA



N-fallas = 421; N max= 76 (18,1%)







## **Paradas de campo de la excursion de Enriquillo led by Pedro P. Hernaiz Enriquillo field stops led by Pedro P. Hernaiz**

### **Parada Nº 9:** Pendiente de determinar

**Título de la parada:** Terraza aluvial basculada por la falla de Enriquillo y abanico aluvial del Arroyo Blanco (García Senz 2004)

**Lugar de la parada:** Está situada al este del pueblo de Jimaní. Se accede por la carretera de Jimaní a la Descubierta, girando por una pista a la derecha antes de una curva fuerte de la carretera. La pista conduce al cauce seco del Arroyo Blanco y a la terraza deformada, que se puede recorrer a pie de este a oeste (UTM, X: 019982; Y: 204688). Otra posibilidad es descender caminando el cauce del Arroyo Blanco por 600 metros desde el puente sin terminar de la carretera Jimaní-Duvergé

**Tiempo estimado:** 45-60 minutes

#### **Descripción de la parada:**

##### **A) En relación con la falla de Enriquillo:**

La deformación en sedimentos aluviales recientes junto al pueblo de Jimaní se relaciona con la actividad de esta falla (ver Fig. 1, García Senz 2004). Estos sedimentos son conglomerados y areniscas que hacia el este gradan a depósitos subacuáticos de un antiguo nivel del lago Enriquillo. Se pueden considerar los siguientes aspectos más significativos:

- Un escarpe de unos 15 metros de alto y 750 m de largo formado por conglomerados basculados, deflecta y es paralelo al cauce principal del abanico del Arroyo Blanco. En la extremidad oriental del escarpe se observa un cambio lateral de facies hacia el este, de conglomerados aluviales a limos y arenas con cantos gasterópodos y foraminíferos. Corresponde a la entrada de un abanico aluvial en el margen del lago (o tal vez una bahía), y por tanto en un tiempo pre-actual un entrante del lago llegaba casi hasta el pueblo de Jimaní.
- En la extremidad occidental del escarpe la inclinación de las capas alcanza 17°, con una capa de arenisca que resalta por su color gris y que es erosionada pendiente arriba por pequeños canales. Esta capa y las inmediatas suprayacentes están cortadas por fallas inclinadas en sentidos opuestos definiendo una pequeña fosa (Fig. 1, B, C). El relleno de la fosa muestra una secuencia pre-cinemática (capas 3,4,5 en la figura) y una secuencia sin-cinemática (capa 6) que rellena el hueco creado por las fallas en la fosa. La capa 2 trunca así mismo pendiente arriba a sedimentos previos indicando que el basculamiento comenzó antes del depósito de la capa 2.
- Notoriamente los conglomerados están basculados con un eje paralelo a la falla de Enriquillo, situada sólo 500 metros al norte de este punto. Un tema de discusión es la existencia de una falla menor paralela a la de Enriquillo situada en la base del escarpe de conglomerados y el papel de ambas fallas en la elevación del área y la retirada del entrante del lago hasta su posición actual.

##### **B) En relación con el abanico aluvial del Arroyo Seco**

Los fondos de cañada torrencial son el principal testimonio de la actividad de la red fluvial actual. La intensidad de la erosión lineal ha formado barrancos, cañones, desfiladeros, cambios bruscos de pendiente y aristas divisorias. Destaca por su longitud, superficie de captación ( $139 \text{ km}^2$ ), pendiente y caudal permanente, la rivière Soliette-Arroyo Blanco, que tiene un eje de drenaje principal paralelo a la sierra (Fig. 2). En el cauce del Arroyo Blanco hay largos tramos con paredes verticales y anchuras de escasos metros.

Los abanicos aluviales están adosados al margen de la sierra de Bahoruco sobre la zona de cambio de pendiente a las depresiones de Jimaní y del Limón. Destaca por sus dimensiones (2.5 km desde el ápice a

la orla) el abanico del Arroyo Blanco, excavado por un canal principal amplio de 10 m de alto en algunos puntos, que desborda en crecidas excepcionales como la del 24 de mayo del 2004 que arrasó el pueblo de Jimaní.

Morfológicamente la terraza de conglomerados descrita en el apartado anterior forma un bloque elevado que corta el abanico del Arroyo Blanco y desvía sus aguas. Desde el punto de vista de avenidas catastróficas es seguro construir sobre el alto y evitar la zona del abanico al pie de escarpe susceptible de inundación

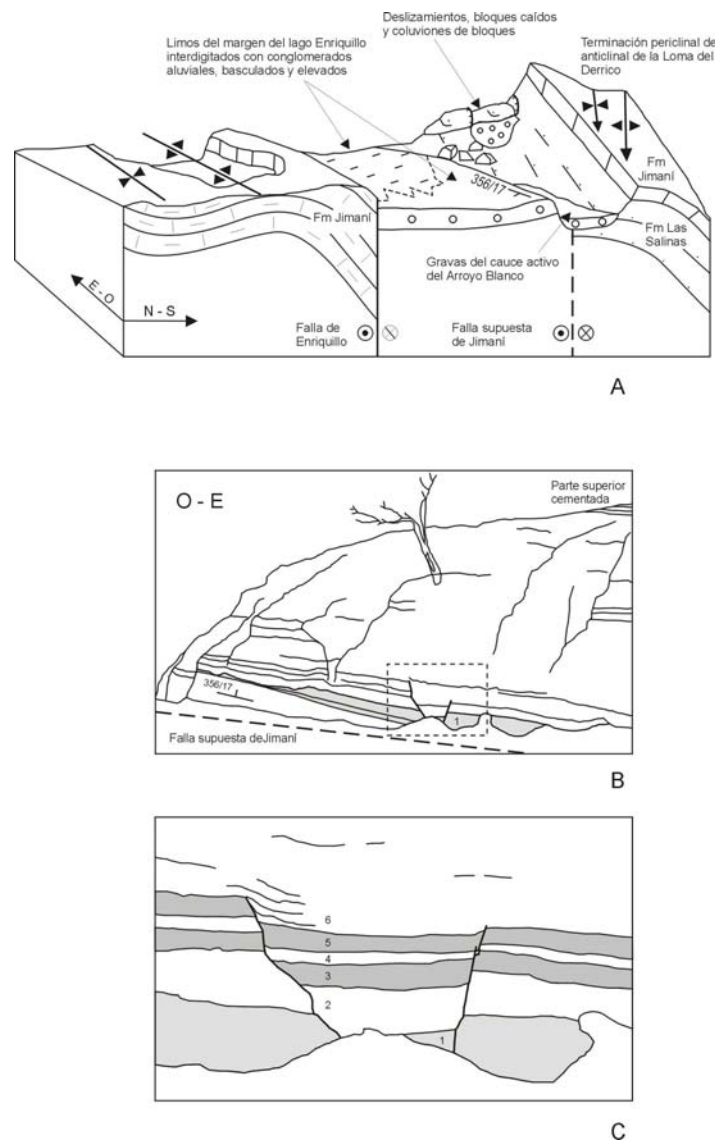


**Fig. 1.** Terraza aluvial basculada de edad holocena próxima a la falla de Enriquillo (según García Senz 2004)

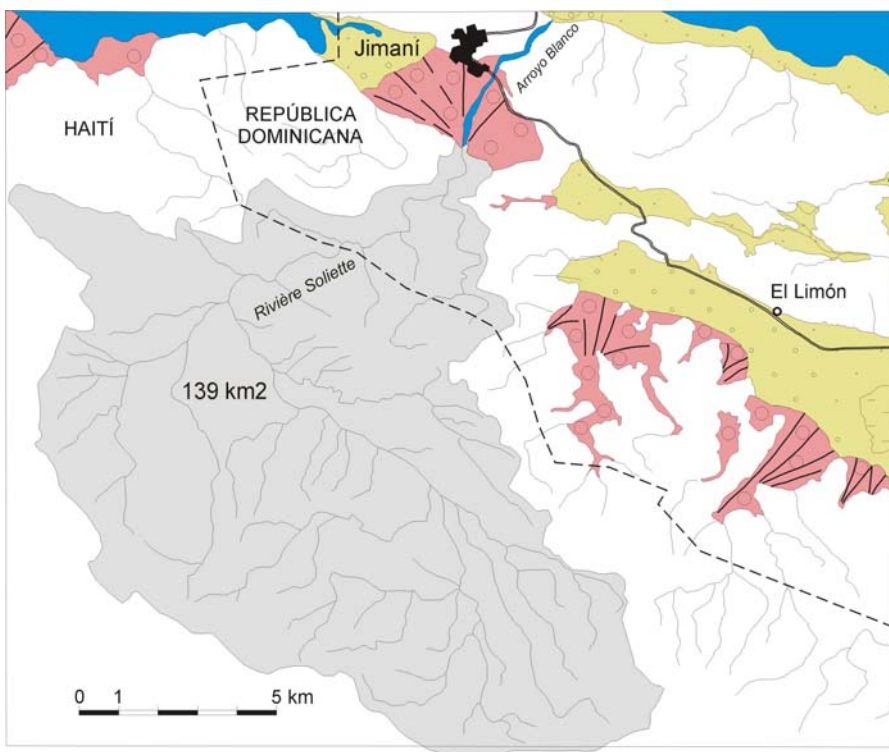


**Fig. 2.** La extensa red de drenaje de la Rivière Soliette-Arroyo Blanco y el abanico aluvial sobre el que se asienta el pueblo de Jimaní (según García Senz 2004)

#### Parada N° 11: Pendiente de determinar

**Título de la parada:** Corte de la Fm Arroyo Seco en el río Barreras

**Lugar de la parada:** Al lugar se accede desde la localidad de Los Ríos por el camino que lleva a la toma de agua desde el río Barreras. Desde allí, se coge el camino a pie que discurre paralelo a dicho río por la parte media de su margen derecha que conduce a la localidad con este nombre. El corte empieza en la misma toma de agua y se prolonga hacia el norte hasta el contacto con las calizas de Neiba, tras cruzar en la mitad de trayecto el río.

**Tiempo estimado:** 30-45 minutes

#### Descripción de la parada:

El corte, con un espesor mínimo de 800 m (Foto 1), muestra la disposición de los conglomerados calcáreos de la Fm Arroyo Seco en sucesivos ciclos granocrecientes (Fig. 1) que forman una discordancia progresiva, con acuñamiento de la serie hacia el norte. Internamente, en cada ciclo se distingue un término inferior en el que alternan lutitas, areniscas y conglomerados, y un término superior en el que los conglomerados son predominantes (Fig. 1). El ciclo basal, muy cubierto, descansa sobre la alternancia de margas, margocalizas y calcarenitas de la unidad de Cortadero, que aflora bien en el siguiente cruce del río, representada por una alternancia de margas y margocalizas blancas. En el trayecto citado se observa bien el progresivo aumento de

buzamiento de los conglomerados y una panorámica del ápice de los abanicos y de la discordancia progresiva que forman los distintos ciclos sobre el relieve de las calizas de la Unidad de Cortadero.



**Foto Y-1.** Panorámica de la discordancia progresiva de la serie conglomerática de la Fm Arroyo Seco en el río Barreras

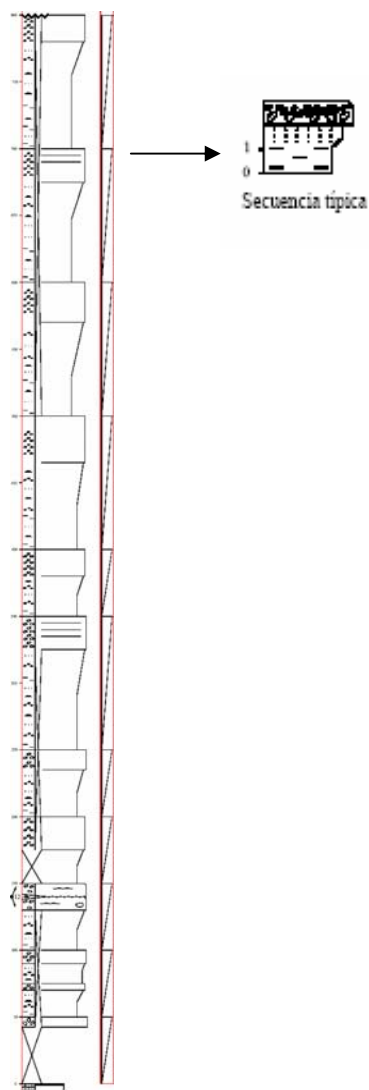


**Fig. 1. Columna estratigráfica sintética de la serie conglomerática de la Fm Arroyo Seco en el río Barreras (según Ardévol 2004)**

## **Parada N° 12:** Pendiente de determinar

**Título de la parada:** Descripción de la estructura de la sierra de Neiba

**Lugar de la parada:** La idea inicial es subir con el autobús por la carretera de El Aguacate unos 7-10 km, hasta pasado el desvío a El Copey, donde hay una buena panorámica del frente de la sierra. En este punto se explicará la estructura de la sierra con especial énfasis en las estructuras que se ven en el paisaje. Previamente, si el tiempo lo permite, se pueden hacer algunas paradas a lo largo del itinerario.

**Tiempo estimado: 1-1,5 h**

### **Descripción de la parada:**

#### **A) Observaciones a lo largo de la carretera:**

El itinerario comienza en las afueras de la localidad de Neiba coincidiendo con los primeros relieves calcáreos de la Fm Neiba superior. En los primeros 5 o 6 km se observa el aspecto tableado típico de esta formación y su estructura general anticlinal o anteclinorial, que se adivina en el paisaje. En los dos primeros kilómetros, correspondientes al flanco meridional de esta estructura, hay algunos buenos afloramientos de pliegues relativamente apretados y con vergencia sur que se asocian al bloque de muro de un cabalgamiento deducido en la cartografía. A la altura del paraje denominado Firme de Mauricio, hay un excelente ejemplo de un sinclinal (de dimensiones hectométricas) de plano axial subvertical que se situaría en el bloque de techo del citado cabalgamiento.

Nada más pasar el desvío a El Copey, en la misma cuneta de la carretera, se pueden observar las brechas volcánicas de la unidad basal de la Fm Sombrerito y de aquí en adelante hay varios afloramientos de las facies de alternancia de margas y calcarenitas típicas de esta formación. En este tramo de la carretera hay buenas vistas (hacia el norte) de los deslizamientos que afectan a la Fm Sombrerito, cuyas cicatrices se localizan en el contacto con la Fm Neiba superior que la cabalga hacia el sur. Precisamente en estas vistas, se aprecia bien el buzamiento hacia el norte de esta formación que, en posición invertida, es a su vez cabalgada por la Fm Neiba inferior que constituye los relieves principales del núcleo de la sierra.

#### **B) Descripción de la estructura de la sierra de Neiba**

Llegados al punto anterior se procede a la explicación de la estructura de detalle de la sierra de Neiba con ayuda del mapa, los cortes y el paisaje. La estructura general de la sierra, se describió en el apartado 8.2.1 de esta Guía de Campo.

En la sierra de Neiba se distinguen las siguientes estructuras principales (Fig. 2 de la guía de campo):

- El sinclinal de Vallejuelo. Es un sinclinal con una semi-longitud de onda de 5-6 km, que ocupa el área septentrional de las hojas de Villarpando y Galván, donde aflora ampliamente la Fm Sombrerito y en menor grado la Fm Trinchera. Su traza axial presenta una inflexión de ENE-OSO a ONO-ESE (Fig. 2). La superficie axial es subvertical o ligeramente vergente al sur en la hoja de Galván, cambiando a ligeramente vergente al norte en la hoja de Villarpando (Fig. 11-cortes VII-VII' a X-X').
- La alineación anticlinal de Cabeza de Toro-El Aguacate-Sabana del Silencio discurre desde el sector meridional de la hoja de Villarpando hasta el norte de La Descubierta y Boca Cachón (Fig. 2). Es la estructura que se observa en esta parada. Consiste en una sucesión escalonada y en relevo de anticlinales en cuyo núcleo aflora al Fm Neiba superior y la Fm Neiba Inferior y el Conjunto Volcanosedimentario de El Aguacate. El flanco meridional de esta alineación es cabalgante sobre el sinclinal de Apolinario Perdomo con un desplazamiento importante en la hoja de Galván que se va amortiguando hacia el SE y el NO. En este sector, la zona de mayor complejidad corresponde al flanco meridional del anticlinal de El Aguacate con un doble cabalgamiento: la falla más septentrional superpone la Fm Neiba Inferior sobre la superior y omite completamente el tramo

volcanosedimentario y la falla meridional superpone una escama invertida de la Fm Neiba superior sobre la Fm Sombrerito del sinclinal contiguo (Figs. 2 y 11-cortes VII-VII' y VIII-VIII'). La traslación mínima hacia el sur de cada uno de los cabalgamientos es de 1 y 2km, respectivamente. Desde esta zona hacia el SE, la traslación se consume con rapidez y la alineación anticlinal recupera una geometría más simple, definida en el sector SE de la hoja de Galván por un anticlinorio vergente al sur y ligeramente cabalgante sobre el sinclinal de Apolinar Perdomo, y más al este por una disposición escalonada izquierda de los pliegues, que se sumergen bajo la cuenca de San Juan-Azua (Fig. 2).

Hacia el NO, sin embargo, se mantienen las fallas de flanco, con la Fm Neiba superior invertida cabalgando hacia el S/SSO el anticlinal de la Sabana del Silencio. En el sector central de la hoja de La Descubierta, la traslación del cabalgamiento es relevada por un nuevo anticlinal (anticlinal de Los Bolos), situado al sur de la alineación principal. Entre este anticlinal y el contiguo situado al norte de la Sabana del Silencio, el valle intermedio de Los Bolos está modelado en un sinclinal volcado al sur (sinclinal de Los Bolos), cuyo flanco septentrional está cortado por una falla inversa. El núcleo de este sinclinal volcado lo ocupa el Conjunto Volcanosedimentario de El Aguacate (Fig. 2).

- El sinclinal de Apolinar Perdomo es contiguo al sur con la alineación anticlinal de Cabeza de Toro-El Aguacate-Sabana del Silencio. En el sector SE de la hoja de Galván presenta un perfil sinclinal volcado al sur, aunque con un plano axial relativamente erguido (Fig. 11-cortes VIII-VIII'). Hacia el NO es cabalgado por el anticlinal de El Aguacate y reduce sus dimensiones en planta (Fig. 11-cortes VI-VI' y VII-VII'). Más al NO, ya en la hoja de La Descubierta, a la altura de Los Mosquitos incluye una escama de la Fm Neiba superior con poca continuidad lateral (escama de Los Mosquitos, Fig. 11-cortes IV-IV' y V-V').
- La alineación anticlinal de Las Cañitas-La Descubierta define el sector meridional de la Sierra de Neiba entre las hojas de Galván y La Descubierta (Fig. 11) y a ella se asocian los principales afloramientos de la Fm Neiba brechoide. La estructura en la parte central de la hoja de La Descubierta presenta una marcada inflexión inducida por el movimiento sinistro de fallas transversas NNE-SSO a ENE-OSO que producen la rotación de los ejes desde direcciones E-O y NE-SO, al oeste, a direcciones ONO-ESE al este. En el límite entre las hojas de Galván y La Descubierta adquiere su máxima anchura cartográfica al añadirse un anticlinal (anticlinal de El Barro) al sur del anticlinal principal de las Cañitas. El perfil resultante es un anticlinorio formado por dos anticlinales y un sinclinal de superficies axiales subverticales a ligeramente vergentes tanto al norte como al sur (Fig. 11-cortes IV-IV' a VI-VI'). Al norte de los pueblos de La Descubierta y Postrer Río, el anticlinal de Las Cañitas se prolonga o es relevado por el anticlinal de La Descubierta.

### **Part III: Holocene coral reef exposure at Cañada Honda, Lake Enriquillo (Stop 10)**

Wilson R. Ramírez-Martínez

Viviana Díaz-Díaz

Department of Geology, University of Puerto Rico at Mayagüez, Mayagüez, Puerto Rico

Dennis K. Hubbard

Department of Geology, Oberlin College, Oberlin, Ohio, USA

Clark E. Sherman

David Cuevas-Miranda

Department of Marine Sciences, University of Puerto Rico at Mayagüez, Mayagüez, Puerto Rico

The Enriquillo Valley in the western Dominican Republic is a fault-bounded, east-west trending feature resulting from subsidence following north-south compression (Mann et al. 1984; Taylor et al., 1985) (Figs. 1, 2, 3). Rapid sea level rise around 10 k.y. ago flooded the valley where initial transgressive deposits (varying from brackish, fresh-water deposits to open-marine) gave way to a shallowing upward sequence as rising sea level slowed (Taylor et al. 1985) (Figs. 3, 4). Around 5.0 to 4.0 k.y. ago fluvial deposits from Río Yaque Del Sur gradually isolated the marine embayment until it became completely separated from the Caribbean Sea forming Lake Enriquillo (Taylor et al. 1985). Today the lake is approximately 40 m below sea level (Mann et al., 1984). Although alluvium has covered much of the reef upper surface, deeply incised streams flowing into the lake have created spectacular exposures of the reef. To our knowledge, this is the best exposed Holocene coral reef in the world.

Previous studies by Mann et al. (1984), Taylor et al. (1985), Stemann and Johnson (1992) and Hubbard et al. (2004) state the importance of high sediment influx in the development of these reefs. First, the ancient “Enriquillo Bay” occurred in a restricted environment (85-km long and 12-km wide) resulting in limited wave action (Mann et al. 1984) and may well explain the large volumes of the stag-horn coral *Acropora cervicornis* which is characteristic of protected environments (Geister, 1977) and the complete absence of the elk-horn coral *Acropora palmata* which depends on the action of the waves to remove sediment (Hubbard and Pocock, 1972). Secondly, the bay is bounded to the north and south by elevated mountain ranges of abrupt topographic relief which allowed large amounts of sediment originated from the mountains to be accumulated within the embayment affecting any developing coral reef. Thirdly, Stemann and Johnson (1992) documented low-diversity assemblages of large colonies of coral species like *Siderastrea siderea* and *Stephanocoenia interseptae* in the Enriquillo fossil reefs. This particular assemblage is characteristic of reefs under siltation stress (Cortés and Risk 1985). In the latter study, Stemann and Johnson (1992) described three statistically discrete biofacies which included an *Acropora cervicornis* facies, the low-diversity assemblage of *Siderastrea siderea* and *Stephanocoenia interseptae*, and a higher diversity assemblage (or mix zone) consisting of *Montastraea* spp., *Colpophyllia* spp. and *Agaricia* spp. According to Stemann and Johnson (1992) the coral species richness and diversity are comparable to that found in recent reef assemblages of the Caribbean.

#### *Community structure and sediment distribution*

The Cañada Honda fossil coral reef in the Enriquillo Valley of western Dominican Republic consists of six coral facies (Hubbard et al. 2004). These are the platy coral zone, three massive coral

zones (M1, M2 and M3), a mixed coral zone, and a branching coral zone (Hubbard et al. 2004). The latter is largely dominated by thick accumulations of the stag-horn coral *Acropora cervicornis*, but also present are *Montastraea annularis* and *Undaria tenuifolia*. The other five coral zones are dominated by the massive coral *Siderastrea siderea* followed by *Montastraea faveolata* and the plate-like coral *Undaria agaricites* (Figure 6 and Table 1). As the name itself suggests, the mixed coral zone is the most diverse yielding at least 21 coral species. Although *Siderastrea siderea* is a major component, together *Eusmilia fastigiana*, *Porites porites*, *Colpophyllia natans*, and *Undaria agaricites* comprise the majority of the mixed zone coral assemblage (Table 1). This contrasts with the massive coral zones 1 and 2 which are characterized by low species richness (5-6 coral species) and are largely dominated by large ( $\geq 0.3$  m) colonies of *Siderastrea siderea* (Table 1). The latter coral species is also evident in the platy coral zone and in this case displays a semi-platy morphology (personal observation, 2004). Most of the plate-like corals in the platy zone consist of *Helioceris cucullata*, *Undaria agaricites*, *Agaricia lamarcki* and other *Agaricia* species. *Montastraea cavernosa* is also an important coral species in the platy coral zone (Table 1). The massive coral zone 3 is widely distributed across the uppermost portion of the reef (Figure 6) and consists mostly of the coral species *Montastraea franksi*, *Montastraea cavernosa*, and *Colpophyllia natans* which in typical Caribbean coral reefs can be found in the deep foreef (Acevedo et al. 1989; Morelock et al. 2001).

Sediment distribution along the reef exposure ranges from approximately 5% to 73%. Nonetheless, the amount of sediment present does not vary substantially between coral zones with an average value of 20.8% (Table 1). The branching coral zone show the largest amount of sediment counts followed by the platy coral zone, mixed coral zone, massive coral zone 2, massive coral zone 1, and massive zone 3 (Table 1). Although it seems that the most diverse coral zones contain more sediment, no clear correlation between amount of sediment and species richness is observed (Figure 7).

#### *Sediment character*

Most of the sediment in the reef has a similar distribution of grain size showing a mixture between sand to fine sand (Figure 8). Observable differences can be found mostly within the branching coral zone and the mixed coral zone. In the branching coral zone the sediment is characterized by a larger amount of coarse grains (-4 phi to -2 phi) compared to the sediment in other reef facies (Figure 8) whereas the sediment in the mixed coral zone show larger percentage of fine-grained material. At least for the branching coral zone, this grain size distribution is expected due to the higher degree of branching coral fragmentation, therefore, providing large skeletal fragments to the sediment.

In terms of composition, the Cañada Honda fossil reef sediment is characterized by the large percentage of carbonate material (Figure 9). Insoluble residue varied from 2% to 9 %. The sediment with the greater amount of insoluble material was detected in the massive coral zones 1 and 3, followed by the platy coral zone, the branching coral zone, massive coral zone 2 and finally the mixed coral zone (Figure 9). Although not very conspicuous, a relation between the amount of insoluble material and the species richness within zones is observed, being the mixed coral zone the one with the least amount of insoluble material present (Figure 9).

#### *Coral growth rates*

The massive coral *Montastraea faveolata*, annual growth rate is highly variable ranging from 0.13 to 0.45 cm/yr. The lowest growth rates are observed in samples from the M3 zone and the M2 zone (Figure 10). The highest growth rates were recorded in coral samples from the M2 zone and the mixed

coral zone (Figure 10). In coral colonies of *Siderastrea siderea*, annual growth rate varied from 0.22 to 0.41 cm/yr. The lowest growth rate value was recorded in a sample from the mixed coral zone, while the highest growth rate value was recorded in the M2 zone (Figure 10). Compared with *Montastraea faveolata*, *Siderastrea siderea* showed less variability in the annual growth rate values (Figure 10). For both coral species, no particular correlation between coral growth rate, coral zone, quantity of sediment, species richness, and amount of insoluble material exists.

## Overview

The Cañada Honda fossil reef in Southwestern Dominican Republic can be considered as a reef under the influence of high sedimentation as evidenced by the remarkable abundance of *Siderastrea siderea* throughout most of the reef sequence (Cortés and Risk, 1985). This is especially obvious in the deeper massive zones M1 and M2. In fact, these two zones can be regrouped in one single, low diversity massive zone due to their similarities in coral community (Table 1). The Cañada Honda fossil reef shows lower coral species richness compared to some modern coral reefs where sedimentation is an important controlling factor. For example, in the coral reef at Parque Nacional Cahuita in the Caribbean coast of Costa Rica, 34 coral species were described by Cortés and Risk (1985), while approximately 21 coral species were described in the present study. This contrasts with approximately 16 coral species found at Parque Nacional del Este in the Dominican Republic by Torres et al. (2001). It is important to point out that differences in the number of species could also be related to the survey method used for each particular study and not necessarily the actual number of species in the localities described above. Nevertheless, the Cañada Honda fossil reef share more similarities with the Río Bueno reefs in Jamaica (Mallela et al. 2004) and the Cahuita reefs in Costa Rica (Cortés and Risk, 1985) in terms of morphology (i.e. fringing reefs), coral species distribution with depth, and the dominant coral species which are largely controlled by large colonies of sediment tolerant corals (e.g. *Undaria agaricites*, *Siderastrea siderea*, *Montastraea* spp., *Colpophyllia natans*, *Stephanocoenia interseptis*) and by a tendency to form monospecific stands (Cortés and Risk, 1985). Contrasting differences between these reef systems are the complete absence of brain corals (*Diploria* spp.) and the remarkable occurrence of thick accumulations of the stag-horn coral *Acropora cervicornis* in Cañada Honda and elsewhere in the Holocene fossil reefs of the Enriquillo Valley.

The M3 massive zone is a particularly interesting feature (Hubbard et al. 2004). As mentioned, the coral assemblage of the M3 zone is similar to that found in the deep foreef of typical Caribbean coral reefs (Acevedo et al. 1989; Morelock et al. 2001). The fact that the M3 zone is widely distributed across the Cañada Honda fossil reef from the shallow branching coral zone to the deeper platy coral zone (Figure 6) suggests it formed late in the development of the coral reef. Perhaps, the M3 zone is the result of increasingly stressful conditions as the water quality of the former “Enriquillo Bay” deteriorated as the latter became more isolated from the Caribbean Sea at approximately 5.0 to 4.0 k.y. ago.

The fraction of non-carbonate material in the reef sediment is relatively low (<10 wt %) for all the samples analyzed. This concentration of non-carbonate sediment is comparable to reef sediment in sites far from terrigenous sediment influence like the reef tract off La Parguera in southwestern Puerto Rico (Morelock et al. 1994). However, these low concentrations of non-carbonate, insoluble material should not be interpreted as a lack of terrigenous sediment influx to the Cañada Honda fossil reef. The mountains north and south of the Enriquillo Lake consist of Tertiary and Pleistocene carbonate rocks (Mann et al. 1984). In such a setting, it is no surprise that the reef sediment in Cañada Honda consists of more than 90% carbonate material. The non-carbonate portion of the sediment could be made of clays,

some siliciclastic rocks (diagenetic chert) found on the mountainside (personal observation, 2004), and from sponge spicules.

Although more information is needed to make a definite conclusion, it seems that the sediment from the coral reef facies located in the deeper portions of the reef (i.e. M1 zone, Platy zone and M3 zone) contain more non-carbonate sediment (Figure 9) than the shallower reef facies (i.e. mixed zone, M2 zone and branching coral zone). This distribution pattern is unexpected given the fact that those areas of the reef closer to the shore should contain more insoluble sediment due their proximity to the terrigenous sediment source. Nonetheless, it is possible that the non-carbonate fraction of the reef sediment consists of fine-grained material and therefore was transported easily by the relatively higher energy that prevailed in the branching and mixed coral zone towards deeper water environments were energy is lower and eventually the insoluble sediment settled.

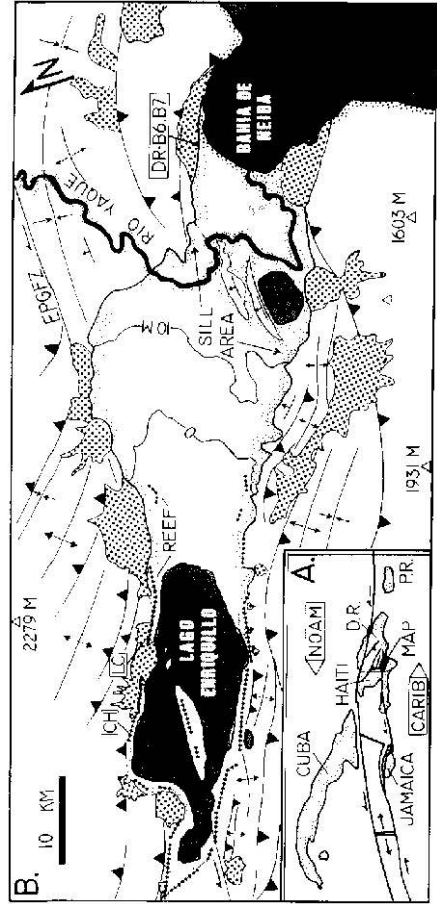
Measured growth rates in the corals from Cañada Honda are relatively lower compared with corals from other studies. At least for the species *Siderastrea siderea*, in the study by Cortés and Risk (1985) they obtained growth rate values of approximately 0.5 cm/yr, compared to approximately 0.4 cm/yr in Cañada Honda (Figure 10). However, these values are similar to coral growth rate values in *Siderastrea siderea* (0.26-0.4 cm/yr) from the heavily impacted Mayagüez reefs in western Puerto Rico (unpublished data by J. Morelock and W. Ramírez). The *Montastraea faveolata* growth rate values are also very low, compared to the estimates obtained by Cortés and Risk (1985) in a *Montastraea annularis* from the Cahuita reef (~0.63 cm/yr). However these values have to be considered with caution given the fact that it was not until recently that the *Montastraea annularis* complex was divided into three sibling species (Knowlton et al. 1992). Therefore, these values can not be compared properly. Even so, coral growth rate values for these two coral species in sites of very low terrigenous influence are close to 1.0 cm/yr for *Siderastrea siderea* and 2.0 cm/yr for the *Montastraea annularis* complex (Cortés and Risk, 1985). Comparison between the coral growth rates values of these two species in Cañada Honda show more variation in growth for *Montastraea faveolata* than *Siderastrea siderea* (Figure 10). It is possible that the latter is more adapted to varying stress conditions than the former. Also *Montastraea faveolata* could probably reflect more accurate the conditions of sedimentation. However, no definite conclusion can be reached until more data is gathered and an analysis of the insoluble material within coral skeleton is made following the methods by Cortés and Risk (1985). If this pattern of measured growth rates is consistent, it will imply that the Cañada Honda fossil reef reflect sediment stress conditions more severe than previously thought. Yet, this reef system managed to continue for thousands of years (Taylor et al. 1985).

Some questions arise after looking at these preliminary results from the Cañada Honda fossil reef. First, how constant (or episodic) and how much was the sedimentation on the reef? It could be possible that even though sedimentation was high, this occurred sporadically allowing time for the reef corals to respond and grow back, in such a way that they were able to “keep-up” with sedimentation. Second, could it be possible that the high carbonate content of the terrigenous sediment have had a less “disturbing” effect? This could also explain the excellent preservation of the reef. Answers to these and other questions will come after comparisons with modern coral reefs within similar sedimentary conditions.

## REFERENCES CITED

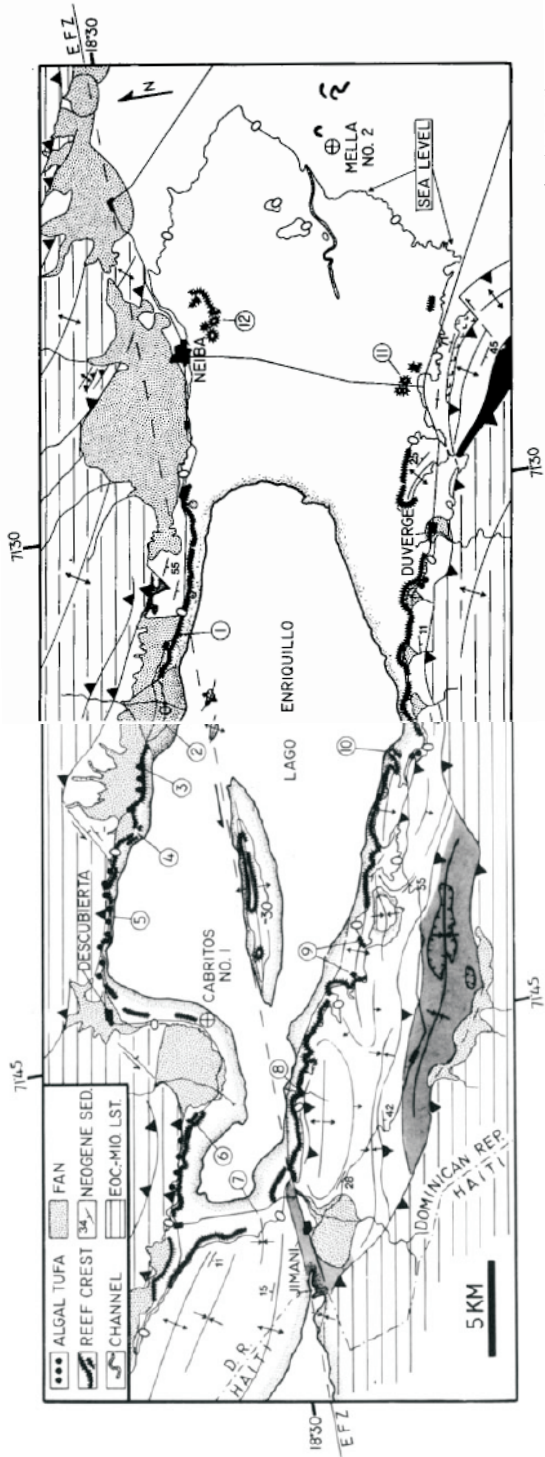
- Acevedo, R., Morelock, J. and Olivieri, R.A., 1989, Modification of coral reef zonation by terrigenous sediment stress: *Palaios*, v. 4, p. 92-100.

- Cortés, J. and Risk, M.J., 1985, A reef under siltation stress: Cahuita, Costa Rica: Bulletin of Marine Science, v. 36, no. 2, p. 339-356.
- Geister, J., 1977, The influence of wave exposure on the ecological zonation of Caribbean coral reefs: Proceedings of the 3<sup>rd</sup> International Coral Reef Symposium, v. 1, p. 23-29.
- Hubbard, D.K., Ramírez, W., Davis, A., Lawson, G., Oram, J., Parsons, K., Cuevas, D. and Del Coro, M., 2004, A preliminary model of Holocene coral-reef development in the Enriquillo Valley, SW Dominican Republic: Geological Society of America, Abstracts with Programs, v. 36, no. 5, p. 313.
- Hubbard, J.A.E.B., and Pocock, Y.P., 1972, Sediment rejection by recent scleractinian corals: A key to paleo-environmental reconstruction Geologische Rundschau, v. 61, p. 598-626.
- Knowlton, N., Weil, E., Weight, L.A., and Guzmán, H.M., 1992, Sibling species in *Montastraea annularis*, coral bleaching, and the coral climate record: Science, v. 255, p. 330-333.
- Mallela, J., Perry, C.T., and Haley, M.P., 2004, Reef morphology and community structure along a fluvial gradient, Río Bueno, Jamaica: Caribbean Journal of Science, v. 40, no. 3, p. 299-311.
- Mann, P., Taylor, F. W., Burke, K. and Kulstad, R., 1984, Subaerially exposed Holocene coral reef, Enriquillo Valley, Dominican Republic: Geological Society of America Bulletin, v. 95, p. 1084-1092.
- Morelock, J., Ramírez, W., Bruckner, A., and Carlo, M., 2001, Status of coral reefs, southwest Puerto Rico: Caribbean Journal of Science Special Publication No. 4, 57 p.
- Morelock, J., Winget, E., and Goenaga, C., 1994, Marine geology of the Parguera-Guánica quadrangles, Puerto Rico: United States Geological Survey Miscellaneous Map Series, Washington, D.C.
- Stemann, T.A. and Johnson, K.G., 1992, Coral assemblages, biofacies and ecological zones in the Mid-Holocene reef deposits of the Enriquillo Valley, Dominican Republic: Lethaia, v. 25, p. 231-241.
- Taylor, F.W., Mann, P., Valastro Jr., S., and Burke, K., 1985, Stratigraphy and radiocarbon chronology of a subaerially exposed Holocene coral reef, Dominican Republic: Journal of Geology, v. 3, p. 311-332.
- Torres, R., Chiappone, M., Geraldès, F., Rodríguez, Y., and Vega, M., 2001, Sedimentation as an important environmental influence on Dominican Republic Reefs: Bulletin of Marine Science, v. 69, no. 2, p. 805-818.



From Taylor et al. (1985)

FIG. 1.—*A.*, Plate tectonic setting of Hispaniola straddling the NOAM-CARB plate boundary zone. The Enriquillo-Plantain Garden fault zone (EPGFZ) extends westward through southwestern Haiti, Jamaica, and along the southern side of the Cayman trough to the mid-Cayman spreading center. Estimates for total relative rates of movement between the NOAM and CARB plates range up to nearly 4 cm/yr (Sykes et al., 1982). *B.*, Geology of the Enriquillo Gardens fault zone where it crosses the valley. Exposures of the Holocene reef are indicated by strings of diamonds. The location of an exposure of a last interfacial age reef is indicated by sample numbers DR-B-6 and DR-B-7 at the eastern end of the valley (table 1B). Heavily stippled areas indicate alluvial fans. Lightly stippled areas indicate the boundary between the valley floor and higher areas or bodies of water. The 0 m contour line, which crosses the middle of the valley, and the 10 m contour outline the sill area of the Rio Yaque del Sur on the valley floor. The sill separates the subsea level interior part of the valley from the sea. On the north side of the Lake Enriquillo "CH" indicates Cañada Honda and "L.C." the gully east of Las Clavellinas.



From Mann et al. (1984)

Figure 2. Geology of the central and western Enriquillo Valley, Dominican Republic. Map area includes all of Lago Enriquillo (elevation -40 m) and the eastern extremity of Etang Saumatre (elevation +14 m) in Haiti. The Holocene coral reef is found only in the sub-sea-level depression around Lago Enriquillo and occurs at an average elevation of -10 m. Reef substrates include anticlinal axes of post-Miocene sediments, Eocene to Miocene limestones, and basin-floor sand and mud. Gray areas indicate structural sediment traps that restrict the amount of sediment that can reach Lago Enriquillo. The reef trend is buried by only one alluvial fan north of the lake. Localities of radiometrically dated coral samples are noted.

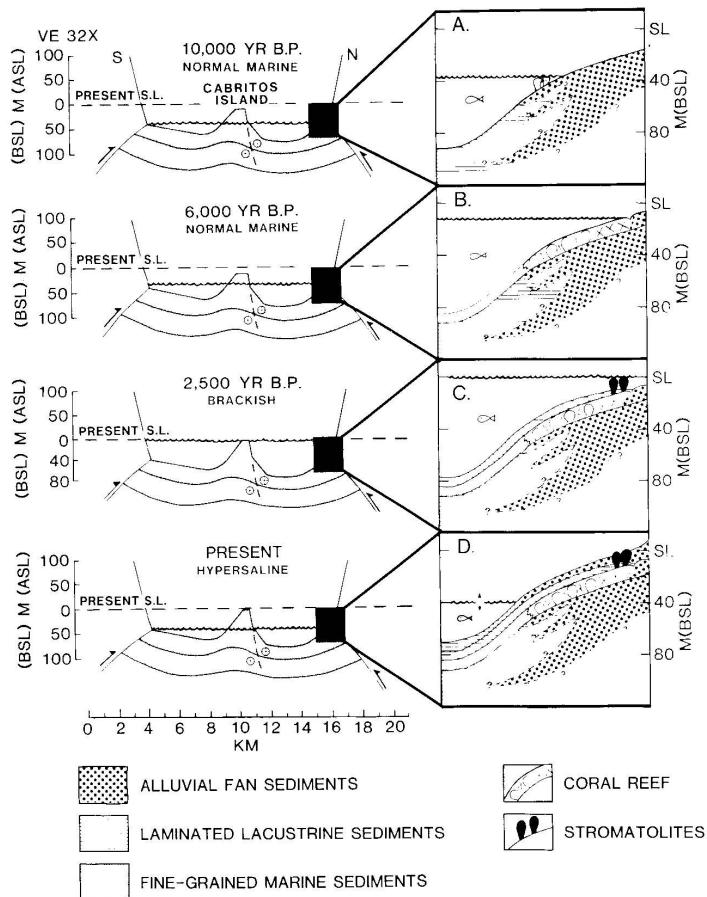


Figure 3. Summary of Holocene depositional environments and sea level history in the Enriquillo Valley: A. At approximately 10,000 yr B.P. rising post-glacial sea level flooded the Enriquillo Valley. Intertidal mollusks grew on drowned alluvial fan deposits along the lake shore by  $9760 \pm 100$  yr B.P. By  $8990 \pm 60$  yr B.P. reef corals had colonized the shell deposits. B. Sea level rose rapidly until about 6000 yr B.P. From 6000 yr B.P. until the reef died sometime after  $4760 \pm 90$  yr B.P. (Mann et al. 1984a) sea level rose much more slowly than before and a morphologic reef crest developed near sea level. C. By 2500 yr B.P. salinities had been reduced by addition of river water from the Rio Yaque del Sur and the reef had died. A shallow inlet to the Caribbean Sea may have existed and stabilized water levels and shorelines in the valley. Large stromatolites grew at two distinct levels along the valley shore and on Cabritos Island at this time. D. Isolation of the valley from the sea allowed evaporation to lower the lake to its present level of about 41.5 m BSL and salinity of approximately 50 parts per mil. Alluvial fans prograded over the reef as the lake level fell and gullies incised the upper parts of the alluvial fans and reef as drainage adjusted to lowered base levels. Infrequent additions of large volumes of rain water from storms separated by years of net evaporation of the lake have caused the lake level to fluctuate between 34 and 44.3 m since 1900 A.D. (Garcia 1976, p. 266).

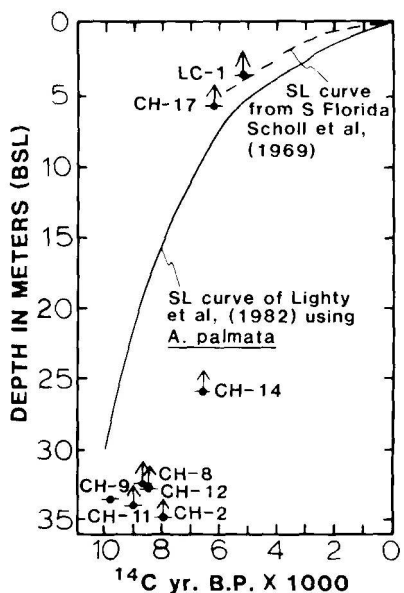


Figure 4. Minimum sea level curve based on  $^{14}\text{C}$  ages of western Atlantic and Caribbean *A. palmata* samples (after Lighty et al. 1982). The dashed line represents a south Florida sea level curve based on  $^{14}\text{C}$  ages of peat samples (Scholl et al. 1969). Our samples are represented by dots with short horizontal error bars showing the standard error on the age determination. There is virtually no vertical error because we leveled the samples and there is very little age error relative to the scale of this figure. Arrows on samples indicate those which could have lived well below sea level. However, sea level could not have been lower than any sample when it was living. The sample plotted with no arrow (CH-9) represents the intertidal *I. alatus* oysters which we consider to be reliable sea level indicators for  $9760 \pm 100$  yr B.P.

From Taylor et al. (1985)

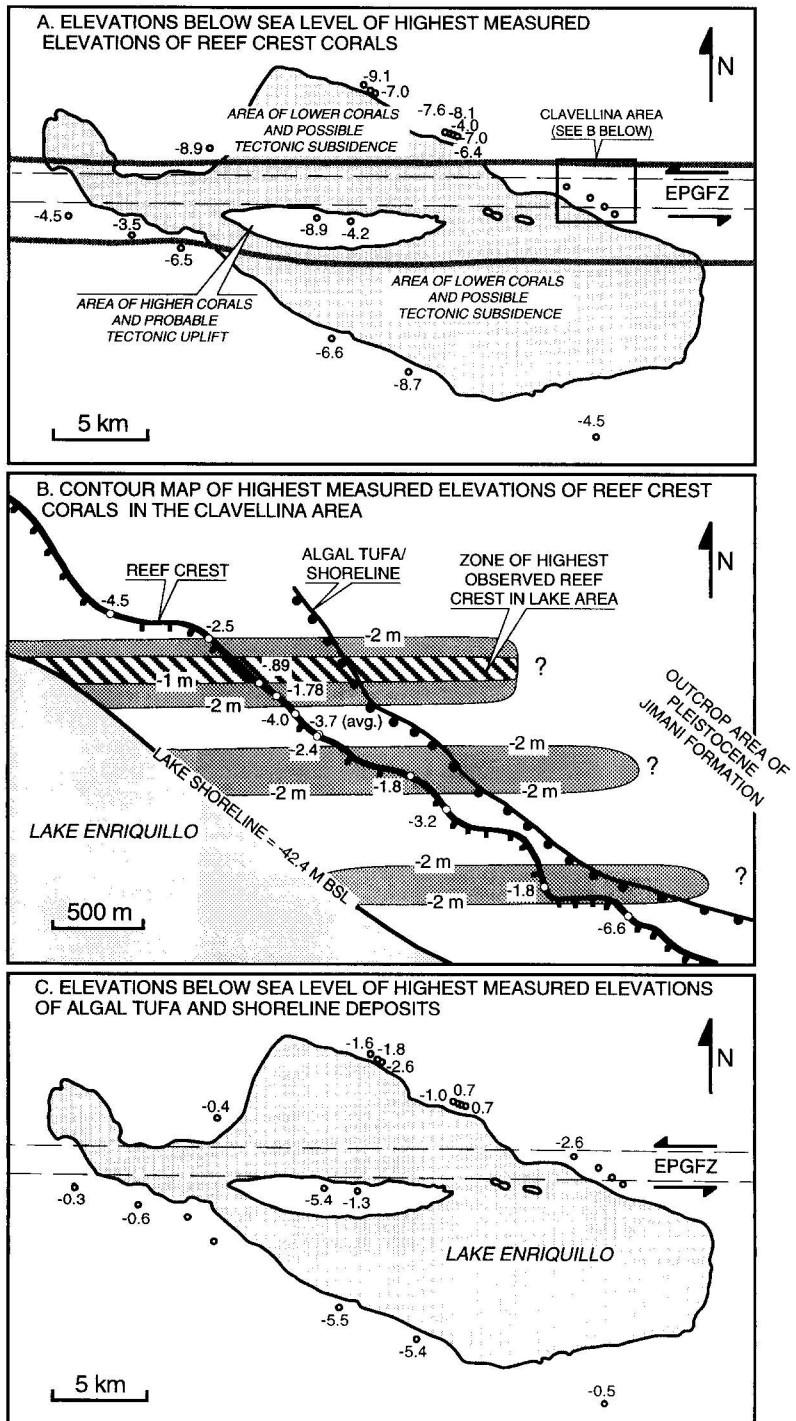


Figure 5. A. Summary map of elevations in meters below sea level of highest measured reef crest corals ranging in age from about 9000 to 3300 yr. BP. These data distinguish an area of relatively uplifted corals in a band parallel to the Enriquillo-Plantain Garden fault zone (EPGFZ). Variations in the highest reef crest coral is also a function of not being able to identify and measure the highest reef crest coral in some areas. B. Summary contour map of highest measured elevations in meter of reef crest corals in the Clavellina area ranging in age from about 4800 to 3800 yr. BP. We interpret that the highest corals in the shaded areas have been tectonically uplifted along the EPGFZ. C. Summary map of elevations below sea level of highest measured algal tufa and shoreline deposits ranging in age from about 2000-1000 yr. BP. Variations in the highest algal tufa and shoreline deposits is also a function of not being able to identify and measure the highest tufa and shoreline deposits in some areas. No clear uplift trend is present in this tufa datum probably because the tufa is younger than the coral and may have not had time to deform significantly. From Mann et al. (1995)



Figure 2. Stratigraphy of a portion of the Canada Honda fossil reef. Columns are based on vertical transect data. Location of each vertical transect is shown at the bottom of each column where each number represents the distance relative to the southern end of the outcrop. Vertical scale in columns represent elevation in meters.

TABLE 1. DISTRIBUTION (% COUNTS) OF CORAL SPECIES AND SEDIMENT FOR EACH CORAL ZONE

Coral species	M1 zone	M2 zone	M3 zone	Platy zone	Mixed zone	Branching zone
<i>Siderastrea siderea</i>	51.5	56.3	14.7	27.1	38.1	3.9
<i>Montastraea faveolata</i>	14.0	10.1	5.1	10.3	5.0	0.0
<i>Stephanocoenia intersepts</i>	7.3	1.0	0.0	2.1	0.1	0.0
<i>Madracis spp.</i>	0.0	0.6	0.1	0.1	0.7	1.3
<i>Dichocoenia stokesi</i>	1.7	0.9	0.1	0.4	0.9	1.4
<i>Colpophyllia natans</i>	1.7	3.3	10.7	1.9	4.1	2.6
<i>Agaricia lamarckii</i>	0.0	0.0	0.0	2.6	2.1	0.0
<i>Undaria agaricites</i>	0.5	0.6	8.4	18.8	7.8	4.1
<i>Acropora cervicornis</i>	0.0	0.0	0.0	0.0	1.1	28.1
<i>Oculina diffusa</i>	0.3	0.3	0.0	0.0	0.2	0.3
<i>Porites porites</i>	0.0	0.2	8.1	0.8	7.6	3.3
<i>Siderastrea radians</i>	0.0	0.4	0.1	0.5	0.3	0.0
<i>Helioceris cucullata</i>	0.5	0.3	0.1	2.5	0.2	0.1
<i>Mussa angulosa</i>	0.0	0.0	0.1	0.5	0.2	0.0
<i>Manicina aerolata</i>	0.0	0.2	0.0	0.4	0.3	0.0
<i>Eusmilia fastigiana</i>	0.0	1.5	1.1	1.1	5.8	0.3
<i>Montastraea annularis</i>	0.0	0.0	0.0	0.0	0.0	13.6
<i>Montastraea franksi</i>	0.0	0.0	26.7	0.0	0.0	2.0
<i>Montastraea cavernosa</i>	0.0	0.0	8.3	4.6	3.8	0.0
<i>Porites astreoides</i>	0.0	0.1	0.1	0.0	0.4	1.0
<i>Undaria tenuifolia</i>	0.0	0.0	0.0	0.0	1.1	7.0
<i>Scolymia spp.</i>	0.2	0.0	0.0	0.0	0.0	0.6
Other*	0.3	0.8	0.1	0.9	0.8	1.1
sediment	16.2	18.5	15.7	25.5	19.5	29.3
Mad layer	5.8	5.2	0.0	0.0	0.0	0.0
Total %	100.0	100.0	100.0	100.0	100.0	100.0

\*Refers to unrecognizable, highly damaged coral colonies.

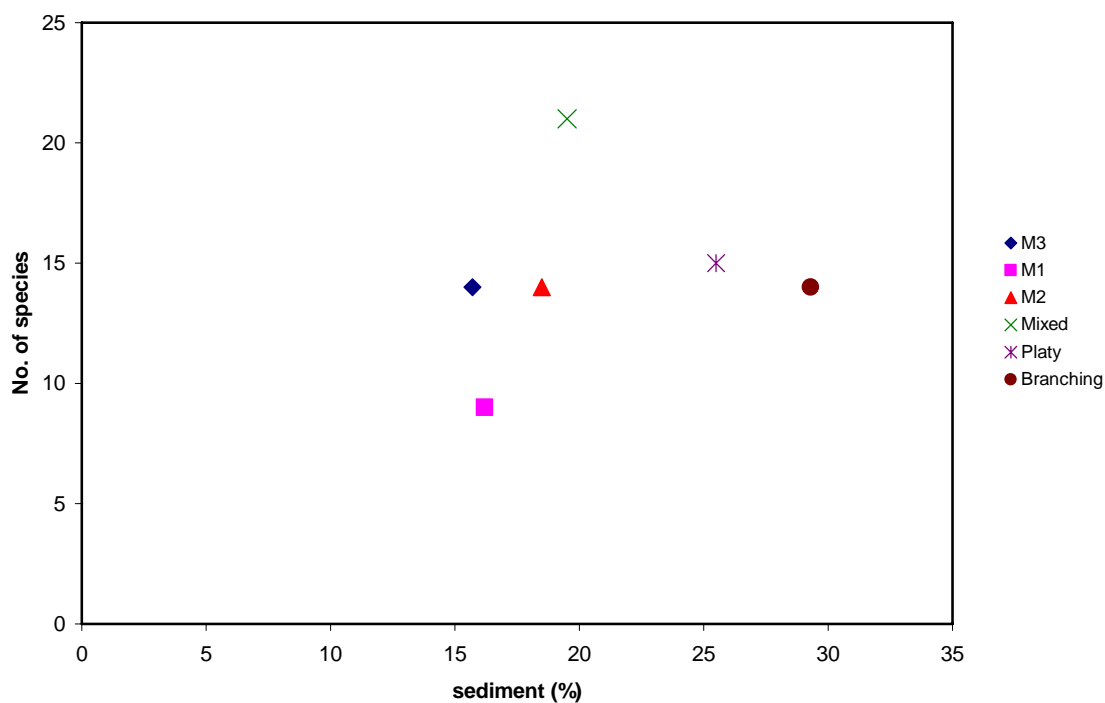


Figure 7. The number of coral species present in each coral zone as a function of the amount (%) of sediment for each facies in the Cañada Honda fossil reef.

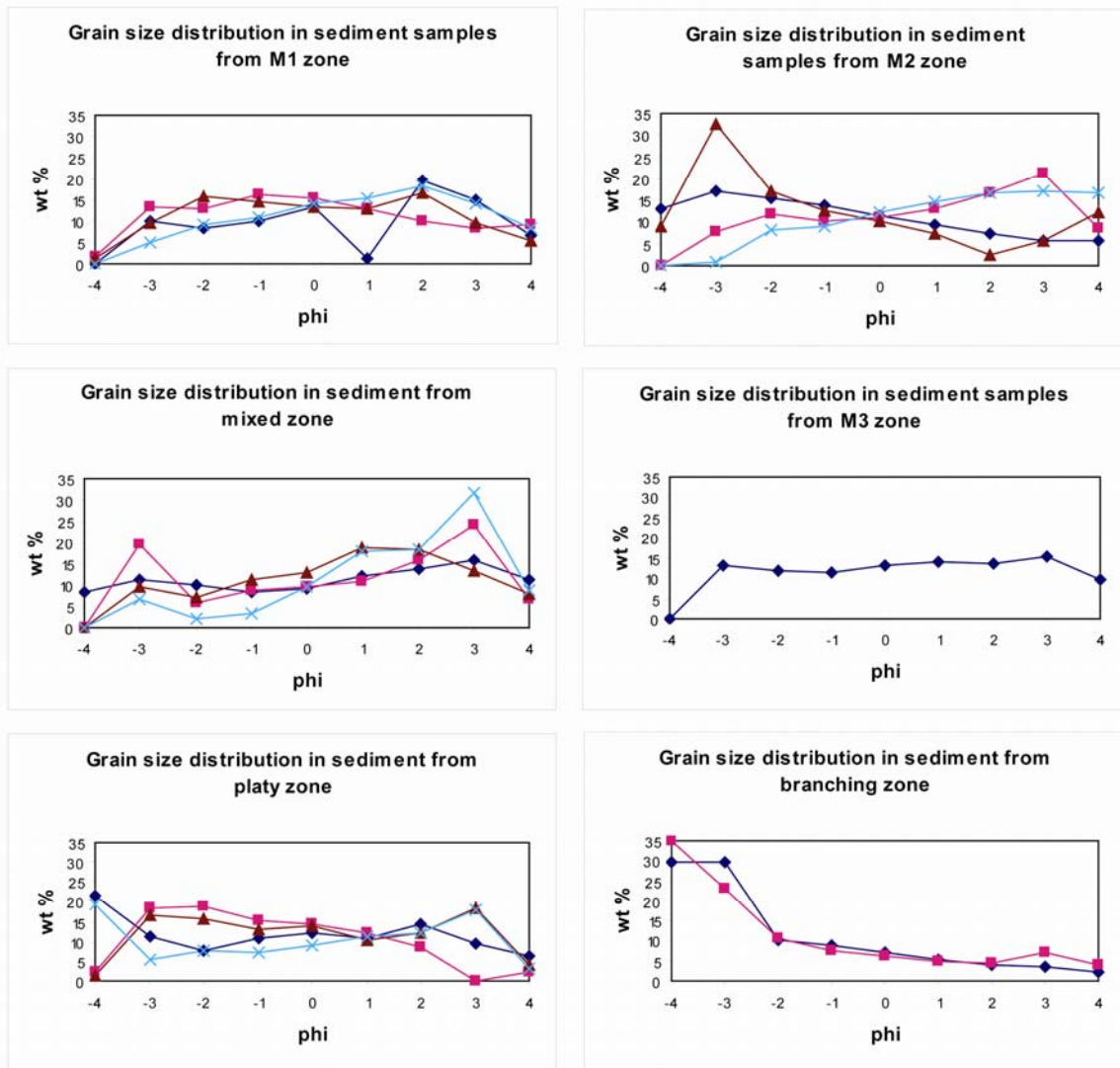
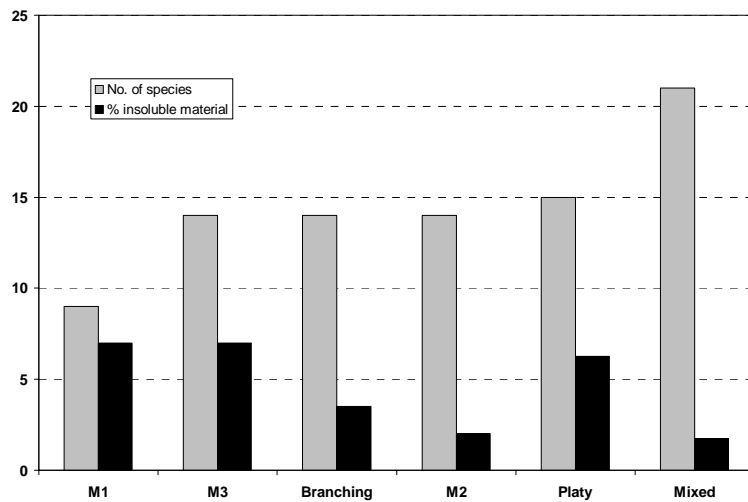
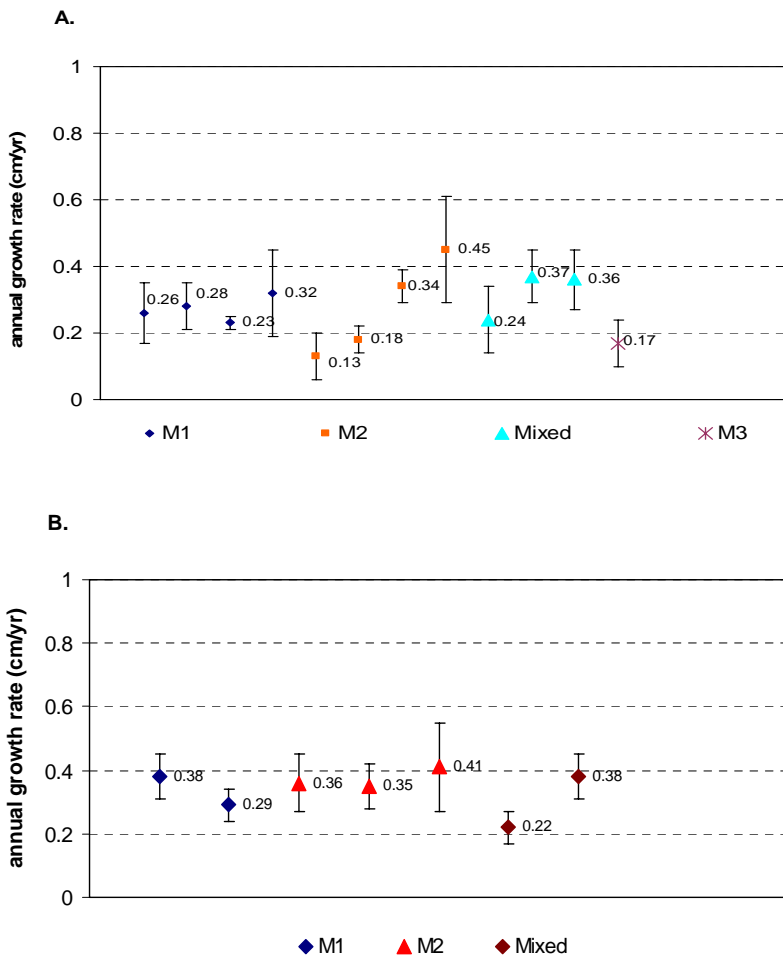


Figure 8. Grain size distribution in sediment samples from the Cañada Honda fossil reef.



**Figure 9. Number of species and amount of insoluble sediment (%) within the different coral zones in the Cañada Honda reef**



**Figure 10. Annual growth rate values for the coral *Montastraea faveolata* (A) and *Siderastrea siderea* (B) in the Cañada Honda fossil coral reef**